5-2012

LMW-E MEDIATES MAMMARY TUMORIGENESIS BY DEREGULATING ACINAR MORPHOGENESIS & GENERATING CANCER STEM CELLS

MyLinh T. Duong

LMW-E MEDIATES MAMMARY TUMORIGENESIS BY DEREGULATING ACINAR MORPHOGENESIS & GENERATING CANCER STEM CELLS

by

MyLinh Thi Duong, B.S.

APPROVED:

_____
Khandan Keyomarsi, Ph.D.
Supervisory Professor

_____
Michelle Barton, Ph.D.

_____
Mong-Hong Lee, Ph.D.

_____
Sendurai Mani, Ph.D.

_____
Frank Marini, Ph.D.

APPROVED:

_____
Dean, The University of Texas
Health Science Center Houston
Graduate School of Biomedical Sciences

LMW-E MEDIATES MAMMARY TUMORIGENESIS BY DEREGULATING ACINAR MORPHOGENESIS & GENERATING CANCER STEM CELLS

A DISSERTATION

Presented to the Faculty of
The University of Texas
Health Science Center at Houston
and
The University of Texas
M.D. Anderson Cancer Center
Graduate School of Biomedical Sciences
in Partial Fulfillment

of the Requirements

for the degree of

DOCTOR OF PHILOSOPHY

By
MyLinh Thi Duong, B.S.
Houston, Texas

May, 2012

DEDICATION

This dissertation is dedicated to my loved ones who have encouraged and supported me for the pursuance of this degree. I especially want to thank my parents for instilling the importance of education in me and for their relentless love and encouragement that have helped made me become a resilient person during the pursuit of my educational ambition. In the memory of my aunt and uncle who both passed away last year due to cancer, I promise you that I will continue to labor my knowledge to contribute to the fight against this disease. And most of all I dedicate this dissertation to my husband who I shared all the ups and downs of this journey with and provided rational encouragements when I am overcome with emotions.

ACKNOWLEDGEMENTS

I would like to first acknowledge my thesis mentor, Dr. Khandan Keyomarsi, for the opportunity to pursue my research interest in her laboratory. As a mentor, she has provided guidance to maintain my focus during my research and given invaluable advices and tools to help shape and develop me into an able scientist. I am thankful for her continual encouragement to develop independent thinking and her patience to see me through this process. As a friend, her genuine cheerfulness and understanding has made this journey special and memorable in my heart.

I also would like to thank Dr. Kelly Hunt, who has served as a co-mentor during my research in Dr. Keyomarsi's lab. She has provided significant advices and ideas to help lead my research project in the direction where it is today. I would like to thank all of the faculty members, Drs. Michelle Barton, Mong-Hong Lee, Sendurai Mani, Frank Marini, Kelly Hunt, Janet Price, Guillermina Lozano, and Lei Li who have served in my committees and provided critical advices and ideas to better my research. I would like to acknowledge Dr. Thomas Goka for his academic and career advices throughout my graduate study and for enthusiastically agreeing last minute to serve in my thesis defense committee. I would also like to thank the Department of Defense Breast Cancer Research foundation, the American Legion Auxiliary Fellowship and the Andrew Sowell-Wade Huggins Graduate Fellowship for their generous contribution to fund this research study.

I thank Dr. Said Akli for his professional and personal advices on my project as well as on being a well-respected scientist. I enjoyed and learned a lot from my collaboration work with him on the microarray project. I'd like to thank Tony Caruso, Liem Phan, and Dr. Bisrat Debeb for sharing their ideas and technical skills that have greatly improved my research and sharpened my scientific knowledge. Finally, I'd like to give many thanks to the members of the Keyomarsi/Hunt lab, both past and present, for their friendship and encouragement. Each and every one of them have helped contributed to this thesis dissertation as well as influenced my experience here at MD Anderson.

LMW-E MEDIATES MAMMARY TUMORIGENESIS BY DEREGULATING ACINAR MORPHOGENESIS & GENERATING CANCER STEM CELLS

Publication No. _____

MyLinh Thi Duong, B.S.

Supervisory Professor: Khandan Keyomarsi, Ph.D.

Cyclin E is the regulatory subunit of the cyclin E/CDK2 complex that mediates the G1-S phase transition. N-terminal cleavage of cyclin E by elastase in breast cancer generates two low molecular weight (LMW) isoforms that exhibit both enhanced kinase activity and resistance to p21 and p27 inhibition compared to full-length cyclin E. Clinically, approximately 27% of breast cancer patients overexpress LMW-E and associate with poor survival. Therefore, we ***hypothesize*** that *LMW-E disrupts normal mammary acinar morphogenesis and serves as the initial route into breast tumor development.* We first demonstrate that LMW-E overexpression in non-tumorigenic hMECs is sufficient to induce tumor formation in athymic mice significantly more than overexpression of full-length cyclin E and requires CDK2-associated kinase activity. Further *in vivo* passaging of these tumors augments LMW-E expression and tumorigenic potential. When subjected to acinar morphogenesis *in vitro*, LMW-E mediates significant morphological disruption by generating hyperproliferative and multi-acinar complexes. Proteomic analysis of patient tissues and tumor cells with high LMW-E expression reveals that the activation of the b-Raf-ERK1/2-mTOR pathway in concert with high LMW-E expression predicts poor patient survival. Combination treatment using roscovitine (CDK inhibitor) plus either rapamycin (mTOR inhibitor) or sorafenib (b-raf inhibitor) effectively prevented aberrant acinar formation in LMW-E-expressing cells by inducing the G1/S cell cycle arrest. In addition, the LMW-E-expressing tumor cells exhibit phenotypes characteristic of the EMT and enhanced cellular invasiveness.

These tumor cells also enrich for cells with CSC phenotypes such as increased $CD44^{hi}/CD24^{lo}$ population, enhanced mammosphere formation, and upregulation of ALDH expression and enzymatic activity. Furthermore, the $CD44^{hi}/CD24^{lo}$ population also shows positive correlation with LMW-E expression in both the tumor cell line model and breast cancer patient samples ($p<0.0001$ & $p=0.0435$, respectively). Combination treatment using doxorubicin and salinomycin demonstrates synergistic cytotoxic effects in cells with LMW-E expression but not in those with full-length cyclin E expression. Finally, ProtoArray microarray identifies Hbo1 as a novel substrate of the cyclin E/CDK2 complex and its overexpression results in enrichment for CSCs. Collectively, these data emphasize the strong oncogenic potential of LMW-E in mammary tumorigenesis and suggest possible therapeutic strategies to treat breast cancer patients with high LMW-E expression.

TABLE OF CONTENTS

LIST OF ILLUSTRATIONS

LIST OF TABLES

ABBREVIATIONS

HER2	human epidermal growth factor receptor 2
ER	estrogen receptor
PR	progesterone receptor
SERMs	selective estrogen receptor modules
LHRH	luteinizing hormone-releasing hormone
EGFR	epidermal growth factor receptor
CSCs	cancer stem cells
ALDH	aldehyde dehydrogenase
CDK	cyclin dependent kinase
CAK	CDK-activating kinase
CKI	CDK inhibitor
HPV	human papillomavirus
ORC	origin replication complex
MCM	minichromosome maintenance complex
NPM/B23	nucleophosmin B23
bHLH	basic-helix-loop-helix
Id	inhibitor of DNA binding
hMECs	human mammary epithelial cells
MEF	mouse embryonic fibroblast
LMW	low molecular weight
EL	full-length cyclin E
T1	trunk 1
T2	trunk 2
I3C	indole-3-carbinol
2D	2-dimensional
3D	3-dimensional
ACUF	Animal Care and Use Committee
DSS	disease-specific survival
EHS	Engelbreth-Holm-Swarm

FACS	fluorescence activated cell sorting
TDCs	tumor-derived cells
RPPA	reverse phase protein array
EMT	epithelial-mesenchymal transition
MET	mesenchymal-epithelial transition
TN	triple negative
ABC	ATP-binding cassette
DAPI	4’,6-diamidino-2-phenylindole
DAB	diaminobenzidene
HTSA	high-throughput survival assay
MTT	3-(4,5-Dimethylthiazol-2-yl)-2,5-diphenyltetrazolium bromide
BAAA	Bodipy-aminoacetaldehyde
BAA	Bodipy-aminoacetate
DEAB	diethylamino-benzaldehyde
HAT	histone acetyltransferase
Hbo1	HAT binding to ORC
RAD51AP1	RAD51 associated protein 1
NME1/E2	non-metastatic cells 1/2
PRC1	protein regulator of cytokinesis 1
CINP	cyclin-dependent kinase 2-interacting protein
LIG3	ligase III
MTG1	mitochondrial GTPase 1
MRPL40	mitochondrial ribosomal protein L40
TEKT2	tektin 2
IRAK3	interleukin-1 receptor-associated kinase 3
FOXRED1	FAD-dependent oxidoreductase domain containing 1
CDC2	cell division cycle 2
MYST	MOZ, Ybf2/Sas3, Sas2, TIP60
pre-RC	pre-replication complex
Plk1	polo-like kinase 1

CHAPTER 1: INTRODUCTION TO THE ROLE OF CELL CYCLE IN BREAST CANCER

1.1. THE MAMMARY GLAND AND BREAST CANCER DEVELOPMENT

1.1a. Breast cancer statistics

The mammary gland is highly susceptible to tumor-initiating mutations and oncogenic modulations since the gland itself develops after birth and undergoes repeated cycles of remodeling and regression involving proliferation, differentiation, and apoptosis (1). Consequently, breast cancer is currently the second most common type of cancer in the United States with approximately 200,000 new cases and over 40,000 expected deaths in 2010. Although breast cancer incidence has been rising steadily mainly due to increased awareness, innovative treatment and disease management has dramatically improved patient outcome. Estimates from the National Cancer Institute suggested that approximately 2.5 million women who had a history of breast cancer were still survivors in 2006. However, despite development of better therapeutic practices that greatly improved patient survival, breast cancer still remains the leading cause of cancer death in women worldwide. This is due to our incomplete understanding of the biology and evolution of breast cancer, which results in the high rate of tumor relapse and metastatic dissemination. To improve breast cancer treatment, we must clearly elucidate the mechanism of mammary oncogenesis in order to develop targeted therapy that can specifically and completely eradicate tumor growth.

1.1b. The physiology of the mammary gland

The mammary gland is an exocrine gland that produces and secretes milk during lactation. Alveoli are the most basic components of the mammary gland; they are hollow cavities that contain luminal cells, which produce and secrete milk into the lumen (Figure 1). These luminal cells are highly differentiated and the cells organize to form polarized acinar structure. Myoepithelial cells surround the luminal cells and provide basement support as well as to contract in response to oxytocin stimulation to excrete milk. Multiple alveoli combine to form mammary lobules,

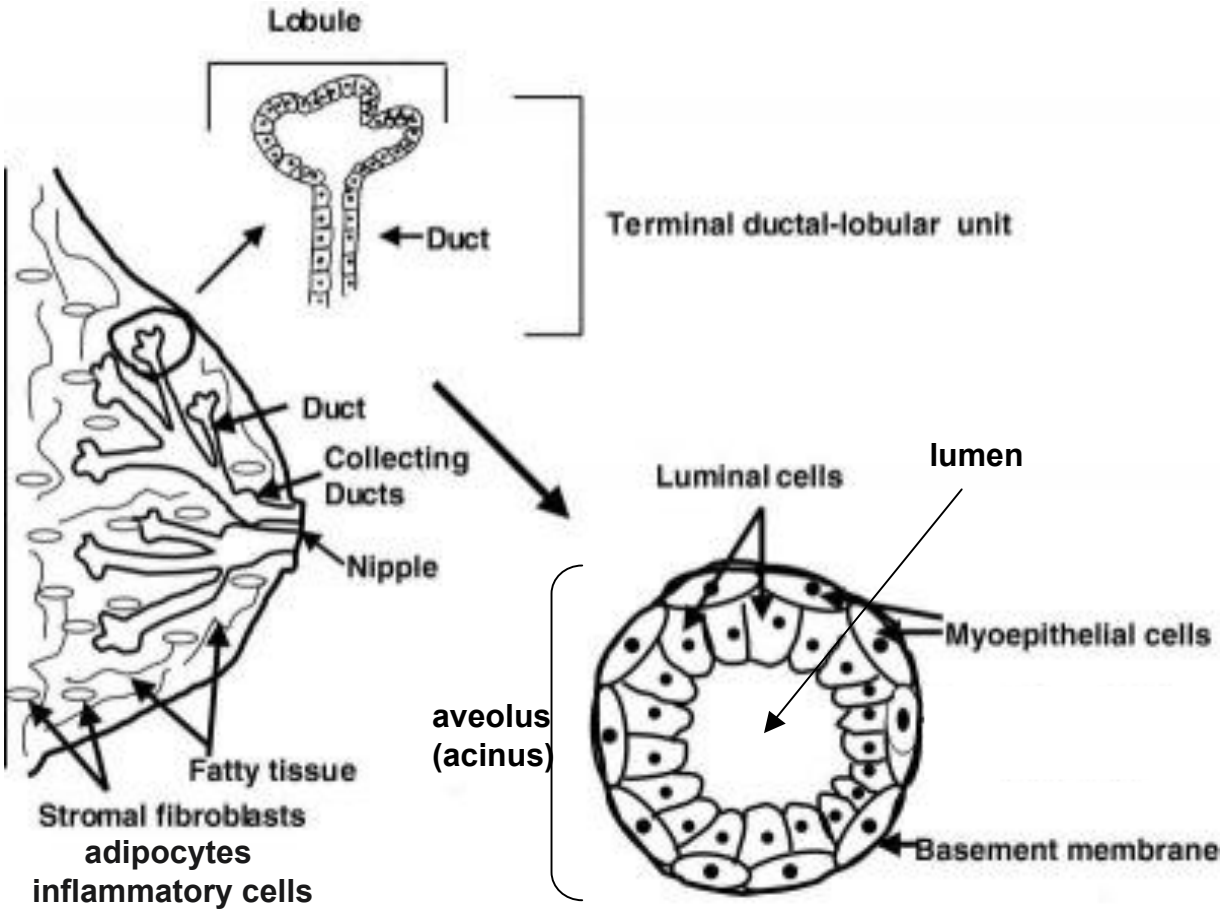

Figure 1: The structure of the mammary gland. The mammary gland is composed of multiple lobules that are connected by ducts to form a hollow network for milk production and secretion through the nipple during lactation. The lobule consists of multiple aveoli (acini) which are the basic unit of the mammary gland. Each aveolus is made up of luminal cells, which produce and secrete milk into to the lumen. The myoepithelial cells surround the luminal cells and the aveolus is enclosed by a basement membrane. Image obtained and modified from Tutorvista.com.

which are connected by lactiferous duct to allow milk to flow to the nipple. The mammary extracellular matrix, which is composed of myoepithelial basement membrane and connective tissues, along with fibroblasts, adipocytes, and inflammatory cells, functions to maintain the morphology of the mammary gland and to provide signaling between mammary epithelial cells as well as signaling from other organs and tissues. The structure of the mammary gland is organized intricately to achieve efficient function. Therefore, tissue organization or morphogenesis in the mammary gland is critical to maintain the integrity of the tissue and prevent pathogenesis. Breast cancer most commonly arises from luminal cells, which are the cells that produce milk, and a smaller percentage of breast cancer arise from the lactiferous duct (Figure 1).

1.1c. Treatment options for breast cancer

After a patient is diagnosed with breast cancer, treatment options include surgery, chemotherapy, radiation therapy, and systemic therapy. Most patients will undergo surgery (lumpectomy or mastectomy) to remove the cancer from the breast tissue, and this tumor mass is also used to assess the stage of the disease. Surgery is typically combined with other treatment options to enhance the chance of complete remission. In cases when the tumors are in excess of 1 cm, radiation or neoadjuvant therapy are performed to reduce the tumor size prior to surgery. Once all detectable tumor tissue has been removed by surgery, additional adjuvant therapy is given to women with breast tumors larger than 1 cm or have node positive disease. Adjuvant therapy administered systemically, is defined as the use of anti-cancer agents administered orally or intravenously and includes immunotherapy, endocrine therapy and chemotherapy.

Immunotherapy involves the manipulation of the patient's immune system to fight cancer cells and thus renders less toxic side effects compared to traditional chemotherapy. The most commonly recognized agents used in immunotherapy are trastuzumab (Herceptin), lapatinib (Tykerb), and bevacizumab (Avastin). Trastuzumab, a monoclonal antibody to human epidermal growth factor receptor 2 (HER2), has gained tremendous recognition due to the results of clinical trials

demonstrating that trastuzumab synergizes with standard chemotherapy to effectively lower the risk of recurrence and death (2). As a result, trastuzumab has been approved by the Food and Drug Administration to treat breast cancer patients with HER2 overexpression (3).

On the other hand, breast tumors with positive expression for estrogen receptor (ER) and/or progesterone receptor (PR) receive endocrine therapy. There are 3 major types of endocrine therapy: ovarian ablation, selective estrogen receptor modules (SERMs), and aromatase inhibitors. The ovaries are the main source of estrogen production in pre-menopausal women, and estrogen is mitogenic because it promotes growth of breast cancer cells that express ER. As a result, women with hormone receptor positive disease are given luteinizing hormone-releasing hormone (LHRH) to shut down estrogen production or subjected to ovarian removal by surgery. There are a total of 3 SERMs available in the clinic: tamoxifen, raloxifene, and toremifene, and they function by competitively inhibit the binding of estrogen to ER. While tamoxifen is the standard treatment for both pre- and postmenopausal patients positive for ER expression, aromatase inhibitors prove to be more effective in postmenopausal women (4, 5). Aromatase is an enzyme that is responsible for the aromatization of androgen to estrogen in the final step of estrogen synthesis. Irreversible steroidal aromatase inhibitor such as exemestane permanently binds to and inhibits aromatase activity while nonsteroidal inhibitors such as anastrozole and letrozole reversibly compete with the enzyme (6-8). The major side effects of endocrine therapy include menopausal symptoms and increased risk of endometrial cancer.

Given that cancerous cells possess uncontrolled proliferation, chemotherapeutic agents are designed to target rapidly dividing cells. By doing so, chemotherapy tend to render toxic side effects because the cells in the bone marrow, digestive tracts and hair follicles are normal cells that also undergo rapid cell division. The mechanism of most chemotherapeutic agents is to inhibit cell cycle progression, particularly by inducing DNA damage. These drugs include alkylating agents, anthracyclines, topoisomerase inhibitors, antimetabolites, and plant alkaloids. Many studies have shown that the effectiveness of chemotherapy

improves greatly when the agents are administered in combination regimen as opposed to single drug treatment (9).

1.2. THE FIVE MOLECULAR SUBTYPES OF BREAST CANCER

Cancer is a heterogenous disease giving rise to dissimilar biology in different patients. Therefore, to achieve improved patient outcome, a better understanding of the molecular patterns of the tumors is necessary to identify clinical markers and design effective therapeutic agents. Using DNA microarray, Perou and colleagues first examined the gene expression signature of breast cancer tissues and applied hierarchical clustering analysis to divide the tumors into 5 groups based on the expression pattern of 8,102 human genes (Table 1) (10). The 5 molecular subtypes are: basal, luminal A, luminal B, ErbB2, and normal-like, and they all differ in clinical outcome but surprisingly not in lymph-node metastasis status (11). Significantly, the results from this and subsequent studies changed the way we study and treat breast cancer.

Based on its name, basal-like tumors are classified by high expression of cytokeratins, which are basal epithelial markers, and growth factor receptors, such as epidermal growth factor receptor (EGFR) and c-kit (12, 13). Indeed, cell culture studies demonstrate that the basal-like breast cancer cell lines are sensitive to EGFR inhibitors (14). The majority of basal-like tumor lacks ER, PR, and HER2 expression and therefore is frequently associated with triple negative tumors. Consequently, patients diagnosed with basal-like tumors face with limited choices in molecular treatment and thereby explain their association with short overall- and disease-free survival. The genes represented in the luminal A subtype are mainly associated with steroid hormone-mediated signaling pathways and fatty acid metabolism. As a result, most luminal A tumors express high levels of ER and PR, display low Ki67 index, are histologically low-grade, and associate with favorable clinical outcome. Consequently, treatment for luminal A patients relies on endocrine therapy such as SERMs and aromatase inhibitors. Despite being positive for ER and PR expression, luminal B tumors are not sensitive to endocrine therapy and as a result, patients with luminal B tumors have high genomic grade and their

Table 1. The six molecular subtypes of breast cancer

SUBTYPE	EXPRESSION PROFILE	THERAPEUTIC AGENTS	PROGNOSIS	PREVALENCE (%)	12YR SURVIVAL (%)
Basal-like	ER-, PR-, HER2-, cytokeratin 5/6+, EGFR+, c-kit+	EGFR inhibitors	poor	11-23	35
Luminal A	ER+, PR+, HER2-, cytokeratin 8/18+. Ki67+	Hormonal therapy	good	28-31	80
Luminal B	ER+, PR+, HER2+, cytokeratin 8/18+, Ki67+	Chemotherapy, not responsive to hormonal therapy	poor	19-23	50
HER2+	HER2+, ER-, PR-	Trastuzumab, Lapatinib	poor	12-21	60
Normal-like	undefined		good	3-10	
Claudin-low	E-cadherin-, occludin-, claudin 3, 4, 7-, HER2-, ER-, PR-, Ki67-, ALDH+, $CD44^{hi}/CD24^{lo}$+	Chemotherapy	poor	7-14	25

(+): high

(-): low/undetectable

Adapted from these publications:

1. Perou CM, Sorlie T, Eisen MB, *et al. Nature* 2000, 406:747-52.
2. Carey LA, Perou CM, Livasy CA, *et al*. *JAMA* 2006, 295(21):2492-502.
3. Fan C, Oh DS, Wessels L, *et al*. *N Engl J Med* 2006, 355(6):560-9.
4. Potemski P, Kusinska R, Watala C, *et al*. *Oncology* 2005, 69(6):478-85.
5. Herschkowitz JI, Simin K, Weigman V J, *et al. Genome Biol* 2007, **8**:R76.
6. Prat, A., Parker, J. S., Karginova, O., *et al*. *Breast Cancer Res* 2010, **12**:R68.
7. Prat A, Parker JS, Karginova O, *et al*. *Breast Cancer Res.* 2010, 12(5):R68.

prognosis is poor.

Additionally, luminal B tumors display high Ki67 index, which is a marker for proliferation. Since gene expression of luminal B tumors is less strictly defined, the best treatment strategy for luminal B tumors appear to rely on chemotherapy to target the cell cycle. Tumors with HER2 amplification are categorized in the HER2+ subtype, and patients with this subtype present poor prognosis. Given the high HER2 protein levels, these patients are generally given trastuzumab or lapatinib. Interestingly, most of these tumors are negative for ER and PR making them poor candidates for endocrine therapy. Finally, normal-like tumors resemble normal breast tissues, contain less genomic alterations, and associate with good outcome.

Seven years after the five molecular subtypes were first described, Perou and colleagues identified an additional subtype of breast cancer termed claudin-low from analysis of 13 breast cancer samples (Table 1) (15). These tumors exhibit low expression for tight junction proteins such as E-cadherin, occludin, claudin 3, 4, and 7 and this subtype was also observed mouse breast tumor samples. Furthermore, this gene expression profile is found in breast cancer stem cells (CSCs) that are enriched for the $CD44^{hi}/CD24^{lo}$ cell surface marker as well as high aldehyde dehydrogenase (ALDH) expression, and these cells are insensitive to chemotherapy and hormone therapy (15-17). Compared to the other subtypes, claudin-low tumors express low levels of HER2, ER, and PR and are characterized by relatively slow proliferation as shown by low Ki67 transcription (15). Similar to the basal-like subtype, the prognosis of patients with claudin-low tumors is poor with a hazard ratio of 17.98 for overall survival (15). Although claudin-low tumors demonstrate response to chemotherapy, they are predicted to experience high probability of relapse due to the fact that the tumor is composed of CSCs that can reinitiate tumor growth once therapy is withdrawn and thus explain the poor clinical outcome (17). In conclusion, the vast difference in the genomic and transcriptional aberrations between the 6 subtypes of breast cancer suggests that perhaps each tumor subtype originated from different neoplastic cell type (18, 19). Undoubtedly, better understanding on the origin of tumor initiation will allow researchers to develop targeted therapeutic strategies to prevent and treat breast cancer.

1.3. THE CELL CYCLE AND CANCER

1.3a. Overview of the cell cycle

The cell cycle chronicles the events during which the cell undergoes DNA duplication followed by segregation of the copies of chromosomes to create two identical daughter cells (Figure 2). The cell cycle consists of two major stages: 1) interphase is the period of time to allow the cells to grow in size and duplicate DNA and 2) mitosis represents the division of the nuclei. Interphase includes G1, S and G2 phases. Cellular growth and preparation for DNA replication occurs during G1 phase, which is followed by S phase when DNA synthesis occurs, and the cell again prepares for mitosis during G2 phase. The two gap phases are essential to provide the cell more time to grow in size and sufficiently prepare for the commitment to DNA synthesis during S phase and mitosis in M phase. Cells in G1 phase can enter G0, a quiescent state, if external conditions are not ideal for cell division such as lack of nutrients, contact inhibition, and loss of adhesion (20). However, once the cell has passed the G1 checkpoint, DNA replication is committed.

The engine of the cell cycle clock machinery is driven by different cyclins and cyclin dependent kinases (CDKs) (Table 2). There are 16 cyclins (A, B1, B2, C, D1, D2, D3, E1, E2, F, G1, G2, H, I, K, L) and 9 CDKs (CDK1-9) identified thus far; however, not all cyclins and CDKs carry out cell cycle-related functions (21-24). All cyclin proteins contain a “cyclin box,” a sequence of homology that binds to a conserved region, PSTAIRE, on CDKs to activate their kinase activity (25). As indicated by their name, the protein levels of most cyclins fluctuate at different phases of the cell cycle to ensure the correct spatial and temporal scheduling of cell proliferation. In contrast, CDKs belong to a family of serine/threonine protein kinases and their protein levels remain constant throughout the cell cycle. To achieve specific control of cell cycle progression, cyclins interact with their specific CDK partner and thus the cyclin protein level dictates the cell cycle activity of different cyclin/CDK complexes. To achieve full activation of the cyclin/CDK complexes, CDK-activating kinase (CAK) composed of cyclin H and CDK7 phosphorylates CDKs at the T160 site that is adjacent to their active site (26). There

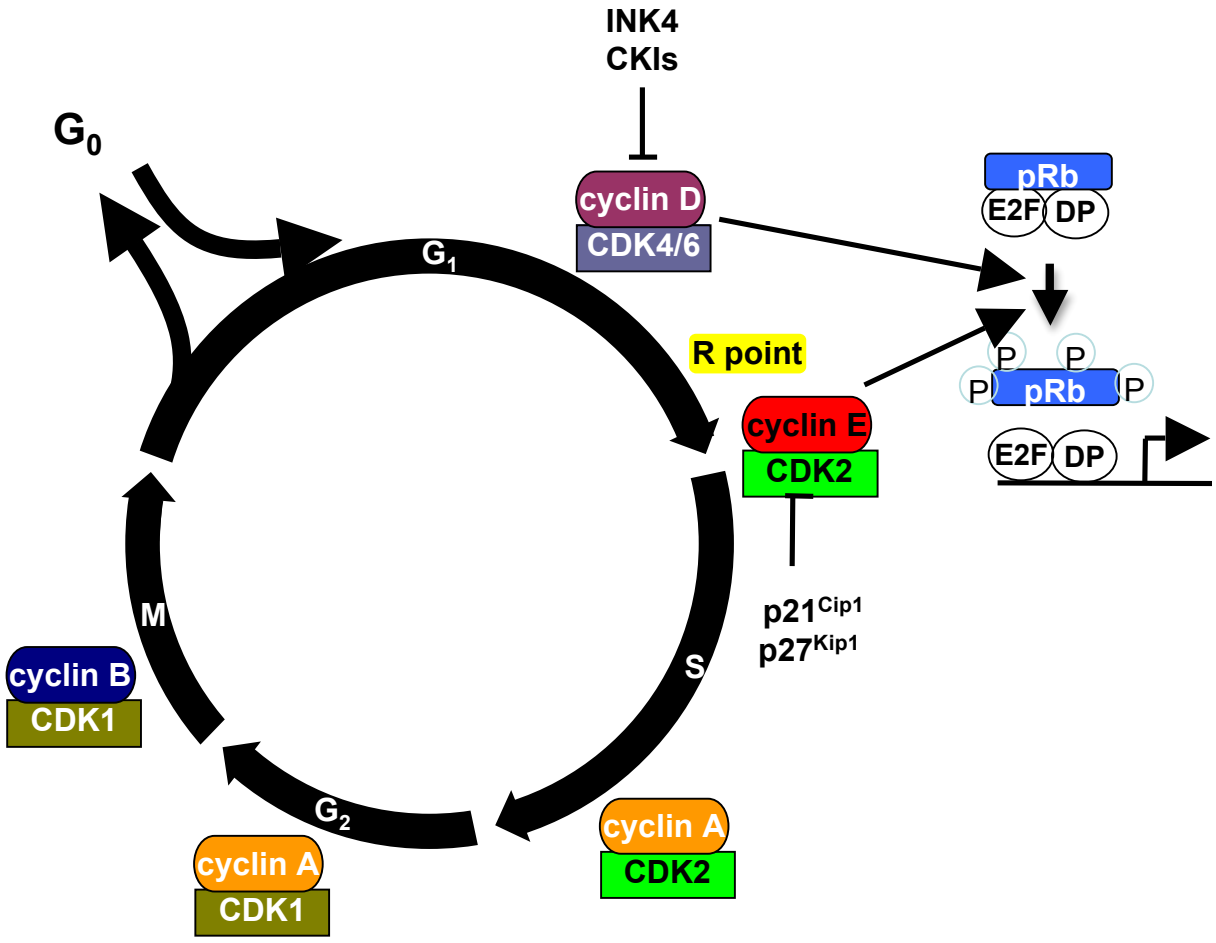

Figure 2: Regulation of the cell cycle by cyclin/CDK complexes. The cell cycle is defined by 5 major phases, which are G0, G1, S, G2, and M, and is designed to achieve faithful cellular duplication to create 2 daughter cells. The progression of a cell through the cell cycle is guided by the kinase activity of different cyclin/CDK complexes, which function to prepare the cell for progression into the next stage of the cell cycle.

Table 2. Cyclins and CDKs' biological functions and knockout consequences		
CYCLINS & CDKs	**FUNCTIONS & INTERACTING PARTNERS**	**KNOCKOUT CONSEQUENCES**
A	- binds to S phase CDK2 to allow the cell to progress through the S-phase - binds to CDK1 at the G2-M transition to prepare for entry into mitosis - cyclin A1 is expressed mainly in the early zygotes and testis and function in the meiotic cell cycle - cyclin A2 is widely expressed in most somatic cells	**Cyclin A1:** Viable, no abnormalities [25] **Cyclin A2:** Embryonic lethality before E6.5 [26]
B	- binds to CDK1 to regulate mitosis by phosphorylating cytoskeleton proteins such as histone H1, lamins, and components of the mitotic spindle - cyclin B1 co-localizes with microtubules - cyclin B2 is primarily associated with the Golgi region	**Cyclin B1:** Embryonic lethality by E10.5 [27] **Cyclin B2:** Viable, no abnormalities [27]
D	- binds to CDK4 and CDK6 to phosphorylate and inhibit members of the pRb protein family to control the G_1/S transition	**Cyclin D1:** Viable, reduced body size, hypoplastic retina, neurological abnormalities, mammary gland defects [28,29] **Cyclin D2:** Viable, defects in B-lymphocyte proliferation, pancreatic b-cell proliferation, cerebellar development, adult neurogenesis and hypoplastic thymus [30,31,32,33] **Cyclin D3:** Viable, defects in T-lymphocyte development [34]

		Cyclin D1 & D2: Viable until P30, reduced body size, hypoplastic cerebella [35] **Cyclin D1 & D3:** Die at P1, neurological abnormalities [35] **Cyclin D2 & D3:** Embryonic lethality before E16.5, megaloblastic anemia [35] **Cyclin D1, D2 & D3:** Embryonic lethality before E16.5, proliferation defects in hematopoietic cells and cardiac myocytes [36]
E	- binds to CDK2 to regulate the G1/S transition.	**Cyclin E1:** Viable, no abnormalities [37] **Cyclin E2:** Viable, no abnormalities [38] **Cyclin E1 & E2:** Embryonic lethality before E14.5, severe defects in extraembryonic tissues [38]
F	- orphan cyclin that is essential for G_2/M transition	Embryonic lethality by E10.5 [39]
CDK1	- required for entry into S-phase and mitosis	Embryonic lethality by E2.5 [40]
CDK2	- essential for G1/S phase transition - associates with and regulated by cyclin A or E, CDK inhibitor $p21^{Cip1}$ and $p27^{Kip1}$	**CDK2:** Viable, reduced body size, impaired neural progenitor cell proliferation [41] **CDK2 & 4:** Embryonic lethality by E14.5, heart defects [42] **CDK2, 4 & 6:** Embryonic lethality before E14.5, heart defects, hematopoietic defects [40]
CDK4/6	- activity is restricted to the G1-S phase with phosphorylation of pRb	**CDK4:** Viable, reduced body size, insulin deficient diabetes

	- binds to D-type cyclins and CDK inhibitor $p16^{INK4a}$	due to decreased pancreatic b-cells [43,44] **CDK6:** Viable, hypoplasia of thymus and spleen and defects in hematopoiesis [45] **CDK4 & 6:** Embryonic lethality by E16.5, severe anemia [45]
CDK11	- CDK11(p110) is involved in transcription and RNA processing - CDK11(p58) is involved in centrosome maturation and spindle morphogenesis	Embryonic lethality before E6.5, mitotic defects [46]
Adapted from Satyanarayana A. and Kaldis P. *Oncogene* 2009, 28:2925-39 [47].		

are 3 types of cyclin D proteins (D1, D2, and D3), and they associate with either CDK4 or CDK6 to promote G1 entry and progression (27). D-type cyclins carry out redundant functions as knockout of each individual cyclin D gene does not cause embryonic lethality while mice with loss of cyclin D2 and D3 and mice with all 3 D-type cyclins knockout are not viable at birth (Table 2) (28-36). (Cyclin D1 will be discussed primarily in this thesis and referred to as cyclin D.) Cyclin D expression is predominately controlled by the presence of growth factor stimulation (37). Unphosphorylated retinoblastoma (pRb) tumor suppressor protein forms a complex with E2F and DP. When present in this complex, E2F and DP, which are transcription factors for genes necessary for S phase progression (including cyclin A, cyclin E and CDK1), cannot activate gene transcription (38-40). The cyclin D/CDK4/6 complex phosphorylates pRb, which contains multiple phosphorylation sites. Increasing phosphorylation of pRb displaces E2F and DP interaction, thereby resulting in increased transcription of cyclin E. There are 2 cyclin E genes (cyclin E1 and cyclin E2) and they share approximately 47% sequence homology and functional activity (41-43). Similar to D-type cyclins, cyclin E1 and E2 also exhibit redundant functions since mice with loss of each cyclin E gene are viable but double knockout mice die before birth (Table 2) (44, 45). (Cyclin E1 will be discussed primarily in this thesis and referred to as cyclin E.) At the G1-S phase boundary when cyclin E protein level is highest, cyclin E associates with CDK2 and further phosphorylates pRb to completion thus creating a positive feedback loop on its own transcription. In cells lacking pRb, cyclin E/CDK2, but not cyclin D/CDK4/6, kinase activity is necessary for cell cycle progression suggesting that cyclin E/CDK2 activity is critical to phosphorylate other key substrates in the cell cycle (46).

During S phase, cyclin A protein accumulates and replaces cyclin E as the partner of CDK2 to promote S phase progression (47, 48). Mice with cyclin A1 knockout are viable while those with loss of cyclin A2 show embryonic lethality possibly due to the fact that cyclin A2 is expressed in most somatic cells and cyclin A1 is only expressed in zygotes and testis (Table 2) (49, 50). At the G2-M transition, cyclin A now interacts with CDK1 to prepare for entry into mitosis. Cyclin A negatively regulates E2F transcriptional activity by phosphorylating DP and

preventing E2F to bind to DNA and therefore shutting down S phase-related gene transcription. At this stage, CDK1 switches partner by associating with cyclin B to regulate mitosis by phosphorylating cytoskeleton proteins such as histone H1, lamins, and components of the mitotic spindle (24, 51). In fact, cyclin B1 colocalizes with microtubules and loss of this gene causes embryonic lethality in mice (Table 2) (52). In contrast, cyclin B2 is associated with the Golgi and mice lacking this gene are viable with no apparent abnormalities (52). Cyclin B/CDK1 kinase activity is negatively regulated via phosphorylation by the Wee1 and Myt1 protein kinases (53-56). This inhibitory phosphorylation serves to prevent premature exposure of nuclear contents to the mitotic kinase in case the cell is not ready to enter mitosis. These phosphorylation sites are removed by the protein phosphatase cdc25C to activate the cyclin B/CDK1 complex when the cell is ready to divide (57, 58). During mitosis, which consists of prophase, metaphase, anaphase, and telophase, the duplicated chromosomes are segregated into opposing nuclei and cytokinesis follows to generate two identical daughter cells. The cell cycle now begins again at the entrance of G1 phase when the cell must make the decision to undergo another round of cell division or enter quiescence in G0 phase.

In addition to regulation by the cyclic trancription of cyclin proteins, the cyclin/CDK kinase activities are also controlled by 2 families of CDK inhibitors (CKIs), the INK4 (**in**hibitors of CD**K4**) and Cip/Kip families (59). The INK4 family includes $p16^{INKa}$, $p15^{INKb}$, $p18^{INKc}$, and $p19^{INKd}$ whose function is to bind to CDK4 and CDK6 to prevent cyclin D association and thereby suppress their kinase activity (60). The 4 members of the INK4 family share approximately 40% homology through the tandem ankyrin motifs. On the other hand, the Cip/Kip family includes $p21^{Cip1}$, $p27^{Kip1}$, and $p57^{Kip2}$ and they are able to bind to and inhibit cyclin E/CDK2, cyclin A/CDK1, and cyclin B/CDK1 complexes (61). In addition to its inhibitory function on the cyclin/CDK complexes, $p21^{Cip1}$ also binds to and inhibits proliferating cell nuclear antigen (PCNA) to halt DNA synthesis (62). The *$p21^{Cip1}$* gene is a transcriptional target of the tumor suppressor protein p53 (63). Upon detection of DNA damage, p53 protein is stabilized and upregulates $p21^{Cip1}$ transcription causing cell cycle arrest to repair the damaged DNA. Paradoxically, $p21^{Cip1}$ and

$p27^{Kip1}$ have been reported to stabilize and thereby stimulating the activity of the cyclin D/CDK4/6 complex (64). In response to TGFß treatment, upregulated $p15^{INKb}$ proteins bind to CDK4/6 and as a result displace $p27^{Kip1}$ from the cyclin D/CDK4/6 complex (65, 66). The protein level of $p27^{Kip1}$ accumulates leading to increased binding and inhibition of cyclin E/CDK2 kinase activity (67). Thus, arrest of cell cycle progression mediated by cyclin E/CDK2 is downstream of the growth inhibitory effect of TGFß.

To ensure that cell division results in a faithful duplication of the cell's genetic information, there are a few checkpoints throughout the cell cycle in which cell cycle progression can be halted if the previous stages have not been completed. First, the restriction point (R) at the G1-S phase boundary is known as "the point of no return" because it marks the commitment of the progress through the cell cycle by initiating DNA synthesis. Prior to R, serum starvation causes the cell to enter G0 phase; however, once the cell has passed R, the cell cycle continues to mitosis even in the absence of serum (68). The G2 checkpoint occurs at the G2-M phase boundary when the cell checks for completion of DNA replication before entry into mitosis. During mitosis, detection of impaired chromosome alignment activates the spindle checkpoint and arrests the cells in metaphase. Additionally, DNA damage checkpoints are activated if the cell senses chromosome damage by radiation or chemicals, and this represents the major mechanism of action of most chemotherapeutic agents, which will be discussed in greater details in the last section of this chapter. The cell cycle resumes once these damages are successfully repaired.

1.3b. Deregulation of the cell cycle in cancer

By definition, cancer results from uncontrolled proliferation of transformed cells. Therefore, in all aspects, deregulation of the cell cycle is the gateway to oncogenesis. Nearly all regulators of the cell cycle such as cyclins, CDKs, and CKIs have been demonstrated to participate in cancer development by altering their expression, function, and/or localization (Table 3). Tight regulation of cyclin expression leaves the cell cycle prone to oncogenic aberrations. Cyclin D

Table 3. Deregulation of the cell cycle in cancer		
PROTEIN	**ONCOGENIC ABERRATION**	**TYPE OF CANCER**
Cyclin D1	Overexpression	Parathyroid adenoma, lymphoma, breast, lung, bladder (78-80)
Cyclin E1	Overexpression	Breast, lung, colorectal, lymphoma, leukemia, gastric, osteosarcoma (152-161)
Cyclin A	Overexpression	Lung carcinoma [81]
CDK1	Overexpression	Colon [84]
CDK2	Overexpression	Colon [83]
CDK4	Overexpression	Glioma, melanoma, sarcoma (82)
CDK4	Mutation	Neuroblastoma (85)
CDK6	Mutation	Neuroblastoma (85)
$p16^{INKa}$	Deletion, mutation, hypermethylation	Melanoma, pancreatic adenocarcinoma, esophageal cancer, gastric cancer (80, 86, 87)
$p27^{Kip1}$	Reduced expression	Lung, breast, bladder (88, 89)
$p21^{Cip1}$	Deletion	Thyroid papillary carcinoma (90)
pRb	Deletion, mutation	Retinoblastoma, lung (91)
E2F	Overexpression	Skin (96-98)

transcription is mainly controlled by mitogenic stimuli and its overexpression is reported in numerous types of human cancers, such as parathyroid adenoma, lymphoma, breast, lung and bladder cancer to name a few (Table 3) (69-71). The role of cyclin E in human cancer has been well documented and will be discussed in greater details in section 1.4. Meanwhile, cyclin A has been shown to be aberrantly high in lung carcinoma and correlate with poor survival (Table 3) (72). Since the expression of CDKs is unchanged and thus not tightly regulated throughout the cell cycle, deregulation of CDKs is not commonly observed in cancer. However, CDK4 overexpression has been observed in glioma, melanoma, and sarcoma (73), while overexpression of CDK1 and 2 was reported in colon cancer (Table 3) (74, 75). Additionally, loss of CKI binding mutations in *CDK4* and *CDK6* have also been identified in neuroblastoma cell lines (76).

CKIs provide the braking mechanism in the progression of the cell cycle by inhibiting the kinase activity of cyclin/CDK complexes. Consequently, CKI deregulation is commonly documented in tumor development. As described previously, $p16^{INKa}$, $p15^{INKb}$, $p18^{INKc}$, and $p19^{INKd}$ are CKIs that inhibit the cyclin D/CDK4/6 and their genes are encoded by the ARF-INK4 locus. This locus is deleted frequently resulting in downregulation of the transcription of these CKIs (Table 3) (77, 78). Particularly, inactivation or loss of $p16^{INKa}$ due to deletion, mutation, and hypermethylation occurs in most tumors (71). In the Cip/Kip family, $p27^{Kip1}$ has been shown to be downregulated in lung, breast, and bladder due to elevated proteolysis by the proteasome, and low $p27^{Kip1}$ is associated with increased tumor aggressiveness and poor outcome (79, 80). In addition, $p21^{Cip1}$ is a gene target of p53 and given that *p53* is the most frequently mutated gene in human cancer, $p21^{Cip1}$ expression is downregulated in a number of human cancers (81).

Deregulated pRb function by gene deletion, inactivating mutations, viral inactivation, or overexpression of cyclin D and cyclin E is frequently observed in human cancer (Table 3). The pRb gene is mutated in retinoblastoma and lung cancer (82). Tumor virus proteins such as the human papillomavirus (HPV) E7, the adenovirus E1A, and the simian virus 40 (SV40) large T (tumor) antigen bind to and sequester pRb from its inhibitory, tumor suppressive, function in the cell cycle (83-

85). In the absence of pRb, E2F is relieved from inhibition and is now able to activate transcription of S phase genes resulting in uncontrolled cellular proliferation (86). The pRb pathway is an important mechanism of the cell to suppress tumor growth since it is estimated that approximately 90% of human cancers possess abnormalities in the components of this pathway (71). Although the involvement of E2F gene alteration in human oncogenesis has not been observed, E2F overexpression has been reported to induce transformation and skin tumor development in cell culture and transgenic mouse models, respectively (Table 3) (87-89).

1.4. THE ROLE OF CYCLIN E IN ONCOGENESIS

1.4a. Cyclin E functions

Results from knockout animal studies further advanced our knowledge on the role of cyclin E and CDK2 in the cell cycle. Single cyclin E1 and cyclin E2 knockout mice are viable and develop normally with normal rates of proliferation in fibroblasts (Table 2) (44, 45). However, cyclin E1/E2 double knockout mice died during midgestation due to endoreduplication impairment. The giant trophoblast cells and megakaryocytes display defective endoreduplication in the cyclin E-*null* mice, which could be due to defects in MCM loading (90, 91). Cyclin E-*null* cells fail to enter S phase following serum stimulation and are resistant to oncogenic transformation by Ras (45, 92, 93). Given that cyclin E and CDK2 depend heavily on their interaction to exert their functions, one would expect CDK2-*null* mice to exhibit similar phenotypes to the cyclin E-*null* mice. Contrary to expectation, CDK2-*null* mice actually do not develop the phenotypes observed in cyclin E-*null* mice. That is, the CDK2-*null* mice carry out normal endoreduplication, are able to enter S phase upon serum stimulation and are susceptible to oncogenic transformation (94, 95). These findings suggest two possible scenarios to explain for the fact that lack of *CDK2* does not compromise the cell cycle functions of cyclin E. First, cyclin E is able to form active complex with another CDK that can compensate for CDK2 absence since cyclin E has been shown to interact with CDK1, 2, and 3 (96). The second, more intriguing theory is that perhaps cyclin E does not require association with

another kinase to exert its function. Indeed, evidences supporting this possibility include the fact that CDK2-kinase dead cyclin E mutants exhibit transforming capability *in vitro* and are still capable of entering S phase as long as the centrosomal localization signal is intact (97, 98). All in all, these results suggest that cyclin E does not require CDK2 to perform normal cell cycle activity as well as to mediate cellular transformation.

Cyclin E protein level and, consequently, its CDK2-associated kinase activity peak at the G1-S phase boundary making this complex the rate-limiting regulator of this checkpoint. Indeed, constitutive overexpression of cyclin E shortens G1 phase (46, 99, 100) and inhibition of the cyclin E/CDK2 activity prevents S phase entry (101, 102). Geng and colleagues demonstrated that cyclin E/CDK2 activity is sufficient to support S phase entry in the absence of cyclin D (103). That is, replacement of the cyclin D coding sequence with cyclin E cDNA in mice rescues the phenotypes associated with cyclin D knockout (103). Cyclin E is inactive unbound and requires interaction with its regulatory subunit, CDK2, to exert its kinase function. The cyclin E protein contains 2 motifs that regulate substrate binding. In the N-terminus, MRAIL at residues 130 to 134 mediates binding of substrates containing RXL motifs (104-106) while VDCLE at residues 274 to 278 in the C-terminus regulates binding of pocket proteins such as pRb, p107, and p130 (107).

One critical function of cyclin E/CDK2 complex is to further phosphorylate and inactivate pRb to allow E2F-mediated transcription of S phase genes (Table 4) (91, 93). As mentioned previously, $p27^{Kip1}$ is a CDK inhibitor that binds and inhibits the cyclin E/CDK2 complex. However, during S phase, cyclin E/CDK2 phosphorylates $p27^{Kip1}$ to mark it for ubiquitin-mediated proteasomal degradation by the Skp2 ubiquitin ligase (Table 4) (108, 109). At the G1-S phase checkpoint, cyclin E/CDK2 also phosphorylates p220NPAT (nuclear protein mapped to the ATM locus) to stimulate synthesis of 3 histone genes (H2B, H4, and H3) (Table 4) (110, 111). Particularly, the cyclin E/CDK2 complex colocalizes with p220NPAT at Cajal bodies, which are subcellular structures associated with histone gene clusters. CBP/p300, a histone acetyltransferase, is also a substrate of the cyclin E/CDK2 complex and

Table 4. Substrates of the cyclin E/CDK2 complex	
SUBSTRATES	**FUNCTIONS**
pRb	Relief pRb inhibition of E2F to activate transcription of S phase genes (91,93)
$p27^{Kip1}$	Mark $p27^{Kip1}$ for ubiquitin-mediated proteasomal degradation by Skp2 (116,117)
p220NPAT	Stimulate histone synthesis (118,119)
CBP/p300	Cofactor for multiple transcription factors (120)
Histone H1	Chromatin rearrangement required for DNA synthesis (121)
Cdc6	Initiation of DNA replication (123,124)
NPM/B23	Dissociate NPM/B23 from the centrosome to allow centriole orientation and splitting (126)
CP110	Regulates centrosomal duplication (125)
Mps1p-like kinase	Regulates centrosomal duplication (127)
Id2, 3	Release inhibitory effect on bHLH-mediated gene transcription (133)
Smad2, 3	Inactivate Smad's transcriptional activity; reduce $p15^{INKb}$ and $p21^{Cip1}$ expression and enhance c-myc expression (140)

acts as a cofactor for multiple transcription factors (Table 4) (112). Additionally, histone H1 is a substrate for the cyclin E/CDK2 complex and phosphorylation of histone H1 is important for chromatin rearrangement, which is required for DNA synthesis (Table 4) (113).

Additionally, the role of cyclin E in facilitating the assembly of the pre-replicative complex is important for proper DNA synthesis. At the origins of replication, origin replication complex (ORC) recruits Cdc6 and minichromosome maintenance complex (MCM) to the chromatin to prepare for DNA synthesis (114). DNA replication begins once cdc6 is removed from the origin of replication. Interestingly, cyclin E/CDK2 has been shown to bind to the chromatin via its interaction with cdc6 through and RXL motif, and these events are necessary for DNA replication to begin (Table 4) (115, 116). Cyclin E/CDK2 continues to bind to the chromatin as DNA replication progresses, and this interaction is critical to prevent re-replication of the DNA. *In vitro* studies demonstrated that once the cell is in mitosis and DNA synthesis is completed, cyclin E is phosphorylated by mitogen activated protein kinase (MAPK) and cyclin B/CDK1 causing its dissociation from the chromatin (115).

Another function of cyclin E is in its interaction with the components of the centrosome machinery. The centrosome is copied once per cell cycle and interacts with chromosomes to create the mitotic spindle. During mitosis, the centrosomes migrate to opposite poles of the cell and as a result segregate the duplicated chromosomes. The process of centrosomal duplication must be tightly controlled since aberrations of this event result in polyploidy and aneuploidy, which are known to cause genomic instability. Cyclin E plays a critical role during centrosomal duplication by phosphorylating nucleophosmin B23 (NPM/B23), CP110, and Mps1p-like kinase (Table 4) (117-119). Specifically, phosphorylation of NPM/B23 by cyclin E/CDK2 causes NPM/B23 to dissociate from the centrosome to allow centriole orientation and splitting (118). Furthermore, Matsumoto and colleagues discovered a centrosomal localization signal in the cyclin E gene that facilitates cyclin E's function during centrosomal duplication to support S phase entry (98). Tumor cells with *p53* loss and cyclin E overexpression were observed to have elevated

frequency of centrosomal hyperamplification (120). Thus, hyperactive cyclin E/CDK2 complexes play a major role in inducing genomic instability that ultimately contribute to oncogenesis.

The kinase activity of the cyclin E/CDK2 complex is also important in regulating the function of the basic-helix-loop-helix (bHLH) transcription factors. The Id (Inhibitor of DNA binding) proteins, whose family consists of 4 members (Id1-4), are HLH proteins that form heterodimers with the bHLH transcription factors and prevent their binding to DNA to promote gene transcription (121). These bHLH factors regulate the gene transcription important for G1 progression, such as $p21^{Cip1}$, as well as the differentiation pathway (122-124). The protein sequence of the Id2, 3, and 4 members contains a consensus CDK2 phosphorylation motif and is shown to be phosphorylated by cyclin E/CDK2 (Table 4) (125). This phosphorylation event alters the interaction of the heterodimer between Ids and the bHLH transcription factors thus releasing the inhibitory effect on bHLH-mediated gene transcription. Cells expressing mutant Id2 and Id3 that lack the CDK2 phosphorylation site arrest in S phase possibly due to the repressed transcription of $p21^{Cip1}$ (126). Thus, the function of cyclin E is involved in the intricate network of gene transcription regulation to promote a smooth G1 to S phase transition.

Cyclin E/CDK2 activity is also important in signal transduction pathways involving TGFß. The TGFß signaling is known to induce paradoxical cellular effects and the participation of cyclin E in this pathway may explain this phenomenon. Under physiological condition, TGFß promotes anti-proliferative signaling by inducing G1 arrest and promoting differentiation and apoptosis. In contrast, TGFß promotes cancer progression and metastasis in malignant condition (127). At the cell surface, TGFß binds to its transmembrane receptor and activates the intracellular Smad signaling cascade (128). Upon phosphorylation by the receptor, Smad proteins translocate to the nucleus to activate $p15^{INKb}$ and $p21^{Cip1}$ expression while repressing c-myc, Id1, Id2 and Id3 gene transcription (65, 129-131). In the nucleus, Smad2 and Smad3 are phosphorylated by cyclin D/CDK4, cyclin E/CDK2, and cyclin A/CDK2 complexes (Table 4) (132). This phosphorylation of the Smad proteins inactivates their transcriptional activity as mutations to the CDK

phosphorylation sites of Smads result in elevated $p15^{INKb}$ and $p21^{Cip1}$ expression and c-myc repression leading to enhanced G1-S progression (132, 133). These findings are similarly observed with knockdown of CDK2 by siRNA or treatment of the cells with CDK2 inhibitor II (compound 3) (133). Therefore, the tumor-promoting role of TGFß is activated in cells with high CDK2 and CDK4 kinase activity, which can suppress the growth inhibitory signal mediated by Smad proteins while simultaneously upregulating the protein level of the oncoprotein c-myc.

1.4b. Controlling the fluctuation of cyclin E protein levels

The G1-S phase checkpoint is vital for maintaining cellular differentiation and tissue integrity since it occurs prior to DNA synthesis. Cyclin E is a critical regulator of cell proliferation because it positively controls the transition of cells into S phase to signal the initiation of DNA replication. Cyclin E expression varies at different phases of the cell cycle and is highest at the G1-S phase boundary (134). The periodicity of cyclin E protein levels depends on transcriptional and post-translational controls. Upregulation of cyclin E transcription during late G1 phase is due to hyper-phosphorylation of the pRb/E2F/DP complex by cyclin D/CDK4/6 complex while removal of cyclin E proteins during S phase is achieved by ubiquitin-mediated proteasomal degradation by Fbw7.

During G1 phase, cyclin D/CDK4/6 complex progressively phosphorylates pRb to release free E2F and DP to activate S phase genes, including cyclin E (38-40). Since CDK2 expression is constant throughout the cell cycle, upregulation of cyclin E transcription results in elevated levels of active cyclin E/CDK2 complexes. Cyclin E/CDK2 complex continues to phosphorylate and completely inactivate pRb, thereby creating a positive feedback loop for cyclin E transcription. Cyclin E level gradually diminishes during S phase due to reduced gene transcription and increased proteasomal degradation.

The half-life of cyclin E in a normally cycling cell is less than 30 minutes, and inhibition of the proteasome can extend this to more than 2 hours. Unbound cyclin E proteins are susceptible to ubiquitin-mediated proteasomal degradation by Cul-3 during early embryogenesis (135, 136). When cyclin E is bound to CDK2, auto-

phosphorylation of cyclin E at the T380 site is recognized by the F-box protein Skp2 to mark it for ubiquitin-mediated degradation (137). Complete knockout of *Skp2* leads to the accumulation of cyclin E and $p27^{Kip1}$, which is also a substrate of Skp2 (137-139). Inhibition of the cyclin E/CDK2 kinase activity by $p27^{Kip1}$ prevents auto-phosphorylation at T380 and thus allowing cyclin E to avoid degradation. In addition, the Fbw7 ubiquitin ligase also targets cyclin E bound to CDK2, and this degradation is dependent of the phosphorylation status of several sites on the cyclin E protein (140-142). In particular, T380 and T62 are the two auto-phosphorylation sites on cyclin E critical for Fbw7 binding to cyclin E to mediate ubiquitination. Cyclin E/CDK2 complexes that are bound to either $p21^{Cip1}$ or $p27^{Kip1}$ are inactive and thus cannot be degraded by Fbw7 because they lack the required phosphorylation (135, 143). Taken together, the periodic rise and fall of cyclin E protein levels are fine-tuned by tight regulation of the pRb pathway and redundant degradation mechanisms by the proteasome to ensure timely removal of this G1 cyclin.

1.4c. Deregulation of cyclin E in human cancers

The function of cyclin E is to ensure proper progression of the cell into S phase; therefore, it is not surprising that deregulation of cyclin E contributes to oncogenesis. Indeed, cyclin E proves to be an important oncogene since its overexpression via gene amplification, upregulation of protein expression, or post-translational deregulation occurs in multiple cancers, including breast, lung, colorectal, lymphoma, leukemia, gastric, and osteosarcoma to name a few (144-153). Since repression of pRb from cyclin D/CDK4/6 phosphorylation positively controls cyclin E transcription through E2F activity, inactivation of pRb by the oncogene HPV16-E7 causes cyclin E overexpression in human foreskin fibroblasts (154). Additionally, multiple lines of evidence indicate Fbw7 is an important tumor suppressor and its loss of function mutations is thought to result in high cyclin E protein levels (141, 155, 156). Particularly, analysis of breast cancer cell lines reveals that the cyclin E gene is amplified and gene transcription is upregulated to as high as 64 folds resulting in elevated cyclin E activity throughout the cell cycle (144, 157, 158). In breast cancer patients, cyclin E gene amplification is rarely

observed in which only 14 of 1082 breast tumors were detected to show amplification (159). In contrast, the level of cyclin E protein expression is more frequently upregulated and our clinical study previously found that 127 of 268 breast tumor tissues demonstrated high cyclin E protein level (160). In fact, cyclin E overexpression was shown to be a stronger marker for predicting patient outcome than other traditionally used markers such as lymph node, ER and PR status or levels of HER2 (160). More specifically, high cyclin E expression was estimated with a hazard ratio of 13.3 for death from breast cancer, which is almost 8 folds higher than other established predictive factors such as positive nodes, late stage, and ER negative status. In the laboratory, approximately 10% of transgenic mice with human cyclin E overexpression in the mammary gland develop mammary gland hyperplasia and carcinomas at 8-13 months of age (161).

One mechanism of cyclin E-mediated oncogenesis is through inducing genomic instability (162-164). Initiation of DNA synthesis and centrosome duplication occurs almost concomitantly and cyclin E is intimately involved in these events. Indeed, constitutive overexpression of cyclin E, but not cyclin D or cyclin A, in rat embryo fibroblasts and human mammary epithelial cells (hMECs) leads to chromosome instability (163). Given the critical role of cyclin E during DNA pre-replication complex formation, high cyclin E activity may cause defects in MCM loading resulting in breakage of DNA at the replication forks, impaired chromosomal duplication, or incomplete chromosomal replication due to premature entrance into mitosis. Ensuring proper centrosome duplication is another cell cycle event that requires cyclin E function. Consequently, persistent cyclin E/CDK2 activity has been observed to lead to centrosome amplification, which predisposes the cell to genomic instability (120). More specifically, *Skp2null* mouse embryonic fibroblasts (MEFs) accumulate cyclin E and $p27^{Kip1}$ proteins and exhibit chromosomal defects such as polyploidy and centrosome amplification (137). As a result, elevated cyclin E expression and activity leave the cell vulnerable to neoplastic transformation brought about by genetic aberrations.

1.5. LMW-E IN BREAST CANCER

1.5a. The isoforms of cyclin E and their subcellular localization

The transcriptional regulation of cyclin E is complex and results in multiple cyclin E isoforms due to mainly post-translational modification as well as some splicing and alternative start site changes. In normal cells, the predominant cyclin E isoform is 50kD and is termed EL1, and the start codon is 15 amino acids upstream from the originally discovered cyclin E cDNA (46, 165). Although rare, an alternative translation site at methionine 46 gives rise to EL4. In addition to genomic and transcriptional amplification of the cyclin E gene in breast cancer cell lines, another mechanism of oncogenic transformation of cyclin E is post-translational modification of the protein. Full-length cyclin E is subjected to elastase-mediated cleavage (but not due to genomic rearrangements of the cyclin E gene) to generate 2 low molecular weight (LMW) isoforms in breast cancer (144, 165). This alteration of cyclin E occurs at 2 cleavage sites on the N-terminus of the full-length cyclin E (EL) giving rise to trunk 1 (T1) and trunk 2 (T2) isoforms. T1 and its phosphorylated isoform are named EL3 and EL2, respectively, while T2 and its phosphorylated isoform are called EL6 and EL5, respectively (166).

Similar to most nuclear proteins, cyclin E is translated in the cytoplasm where it forms a complex with CDK2, and then transported to the nucleus via the importin-dependent pathway (167). The nuclear localization signal sequence is found at the N-terminus of the cyclin E gene, which is cleaved off in the LMW-E isoforms (168). In fact, fractionation and protein complementation assays demonstrate that the LMW-E/CDK2 complexes preferentially accumulate in the cytoplasm (169). Since the Fbw7 ubiquitin ligase is located in the nucleus, the altered subcellular localization of LMW-E renders it less susceptible to proteasomal degradation. This finding implicates many possibilities that can explain the particular oncogenic characteristics of LMW-E that is distinct from full-length cyclin E, and that these effects could be independent from cell cycle regulation.

1.5b. LMW-E causes genomic instability

Since the function of cyclin E is critical during centrosome duplication and DNA replication, the presence of hyperactive LMW-E in the cell cycle undoubtedly results

in abnormal genetic content. Accordingly, LMW-E expression induces genomic instability by increasing the percentage of cells with polyploid and tetraploid DNA, subtelomeric chromatid breaks and multiple chromosomal fragments (170). Since cyclin E participates in MCM loading during DNA pre-replication complex assembly, elevated cyclin E activity exerted by LMW-E results in deregulation of DNA replication. In addition to deregulation of LMW-E during S-phase, LMW-E has been recently implicated in deregulating mitosis (171). As described previously, cdc25C is the phosphatase that removes the inhibitory phosphorylation sites on cyclin B to activate the cyclin B/CDK1 complex when the cell is ready for mitosis. In cells expressing LMW-E however, LMW-E phosphorylates and prematurely activates cdc25C causing faster mitotic exit and consequently cytokinesis failure and chromosomal instability (171). Furthermore, LMW-E expression in breast cancer patient samples also correlates with centrosome amplification, a process that leads to chromosome missegration and genetic instability (171). Examination of 331 breast cancer patients revealed a significant correlation between high LMW-E expression and polyploidy ($p = 0.0003$) and these patients demonstrate significantly lower disease specific survival ($p = 0.02$).

1.5c. LMW-E is oncogenic by adopting the 6 hallmarks of cancer

In 2000, Hanahan and Weinberg proposed that malignant growth requires 6 specific alterations in cellular physiology collectively known as the 6 hallmarks of cancer: 1) self-sufficiency in growth signals, 2) insensitivity to anti-growth signals, 3) limitless replicative potential, 4) evading apoptosis, 5) sustained angiogenesis and 6) tissue invasion and metastasis (172). That is, in order for a normal cell to successfully undergo neoplastic transformation, it must acquire most if not all of these capabilities. These hallmarks were argued to be present in all types of human cancer and thus explaining the relatively rare occurrence of cancer as well as the complexity and difficulty of developing effective anti-tumor therapy. Here we present research evidence accumulated from the last decade demonstrating that LMW-E does indeed drive malignant transformation by adopting these 6 hallmarks of cancer (Table 5).

Table 5. LMW-E induces the 6 hallmarks of cancer	
THE HALLMARKS OF CANCER	**ONCOGENIC ROLE OF LMW-E IN BREAST CANCER**
1) self-sufficiency in growth signals	• Breast cancer patients with high HER2 and LMW-E levels associate with poor survival (181)
2) insensitivity to anti-growth signals	• Increases resistance to $p21^{Cip1}$/$p27^{Kip1}$ inhibition (178, 182) • Reduces sensitivity to fulvestrant (178) • Reduces sensitivity to letrozole (183)
3) limitless replicative potential	• Tighter affinity to CDK2 causing increased S and G2/M phase entry and cellular proliferation (182, 184)
4) evading apoptosis	• Reduced apoptotic cells in melanoma xenografts (185)
5) sustained angiogenesis	• Higher tumor microvessel density in melanoma xenografts (185)
6) tissue invasion and metastasis	• Increased melanoma metastatic potential in experimental lung metastasis assay (185) • Higher frequency of mammary tumor and metastasis development in transgenic mice (186)

The decision to enter G1 phase is controlled by cyclin D, which requires the presence of growth factors. One mechanism acquired by cancer cells is to amplify growth factor signaling by upregulating the expression of growth factor receptors such as EGFR. Indeed, the oncogenic role of LMW-E is implicated in breast tumors with high HER2 expression. Retrospective study found that approximately 25% of 395 breast cancer patient tissues examined had high LMW-E expression, which is associated with poor survival ($p < 0.001$) (160). Moreover, patients with overexpression of both HER2 and cyclin E, particularly LMW-E, were found to experience reduced 5-year disease-specific survival compared to patients with low cyclin E expression (173). Interestingly, knockdown of HER2 by siRNA reduces LMW-E expression and associated kinase activity and induces G1 arrest and apoptosis. Similarly, trastuzumab-treated xenografts created by MCF7-HER18 cells injection into nude mice showed reduced HER2 phosphorylation and LMW-E expression (173). Furthermore, cyclin E overexpression and amplification has been shown to play a direct role in mediating trastuzumab resistance in breast cancer, and treatment of these resistant cells with CDK2 inhibitor (CYC065), which is a 2,6,9-trisubstituted purine derivative of roscovitine, induces apoptosis and inhibits xenograft tumor growth (174). Perhaps in tumors with high HER2 and LMW-E expression, constitutive growth signaling mediated by HER2 collaborates with the oncogenic functions of LMW-E to increase tumor aggressiveness and thus leads to poor patient outcome.

As described previously, cyclin/CDK complexes are the accelerators of the cell cycle while CKIs represent the brakes. Cyclin E/CDK2 kinase activity is critical for S phase entry and is subsequently inhibited by $p21^{Cip1}$ and $p27^{Kip1}$. *In vitro* studies revealed that compared to EL, the LMW-E isoforms exhibit increased resistance to inhibition by $p21^{Cip1}$ and $p27^{Kip1}$ even though these CKIs demonstrated equal binding stoichiometry (175). These results suggest that the LMW-E isoforms are sequestering the CKIs from the full-length isoform and thereby causing an aberrant and prolonged cyclin E/CDK2 kinase activity beyond the G1-S phase boundary. Moreover, proteolytic processing of cyclin E into LMW-E renders tighter association with CDK2 resulting in elevated CDK2-associated kinase activity (175, 176).

Exogenous LMW-E expression in immortalized human mammary epithelial cells (hMECs) enhances S and G2/M phase entry thus increasing the rate of cellular proliferation (176).

In addition to insensitivity to CKI inhibition, LMW-E also mediates acquired resistance to pharmacological agents such as antiestrogen and aromatase inhibitor. MCF7 cells expressing exogenous LMW-E are less sensitive to growth inhibitory activity induced by fulvestrant treatment compared to EL-expressing cells, and this reduced sensitivity was demonstrated to be due to increased resistance of LMW-E to inhibition by $p21^{Cip1}$ and $p27^{Kip1}$ (170). These results were further confirmed using breast cancer patient data. More specifically, patients whose tumors are ER positive and express high cyclin E demonstrate no significant improvement in disease specific survival compared to patients not receiving antiestrogen ($p = 0.083$). Indeed, Pan and colleagues previously reported that cyclin E expression in breast cancer is a strong predictor of endocrine therapy failure (177). Additionally, aromatase inhibitors represent another form of endocrine therapy and have been reported to be more effective in the treatment of postmenopausal breast cancer patients compared to tamoxifen. Similar to fulvestrant, LMW-E expression also renders MCF7 cells resistant to inhibition by letrozole, an aromatase inhibitor, and breast cancer patients with LMW-E expression are predicted to be insensitive to aromatase inhibitor treatment (178). Interestingly, roscovitine, a CDK inhibitor, can reverse the letrozole-induced resistance mediated by LMW-E in breast cancer cells suggesting a potential therapeutic value of using roscovitine to treat postmenopausal breast cancer patients with high LMW-E levels.

Programmed cell death or apoptosis is a cellular event critical for the maintenance of tissue homeostasis and prevention of accumulation of damaged cells. Examination of xenografts generated from orthotopic injection of primary melanoma cells revealed that the LMW-E-expressing tumors showed reduced apoptotic cells visualized by TUNNEL staining compared to tumors with EL expression (179). More importantly, the LMW-E-induced melanoma tumors demonstrate higher microvessel density than tumors with EL expression indicating enhanced angiogenic potential, which is one of the hallmarks of cancer. Further

analysis of these melanoma cells using an experimental lung metastasis assay revealed that LMW-E expression induced greater metastasis potential than EL. Increased tumor and metastasis incidence due to LMW-E has been previously reported in breast cancer. Transgenic mice expressing LMW-E isoforms are themselves malignant since approximately 27% of LMW-E transgenic mice develop mammary adenocarcinomas compared to 10% of transgenic mice with EL expression (180). The frequency of tumor development in transgenic mice with full-length cyclin E expression reported by Akli *et al* is similar to results reported previously by Bortner *et al* (161, 180). Furthermore, approximately 25% of the LMW-E tumors develop metastasis compared to 8% in the EL tumors (180). Taken together, the LMW-E isoforms are strong oncogenes that can successfully initiate and sustain tumor development through promotion of the 6 hallmarks of cancer.

1.6. TARGETING THE CELL CYCLE

1.6a. DNA damage-inducing agents

Given the idea that tumors arise from uncontrolled proliferation by altering the cell cycle, traditional chemotherapeutic agents were designed to target tumor cells by inducing DNA damage to arrest the cell cycle mainly in S or G2/M phases and subsequently induce apoptosis. Depending on the chemotherapeutic agent, tumor cells can be targeted in one of three ways: 1) chemically alter the DNA structure, 2) inhibit DNA synthesis, or 3) inhibit the mitotic process. For instance, cisplatin and nitrogen mustard function by cross-linking DNA resulting in chromosome breakage and causing the cell cycle to halt (181). As described previously, DNA damage induces p53 stabilization, $p21^{Cip1}$ transcription, cell cycle arrest and/or apoptosis (182, 183). Topoisomerase is an enzyme that unwinds the DNA strands to aid during DNA replication, and inhibitors to this enzyme have been shown to be effective anti-tumor agents. More specifically, both camptothecin and etoposide are chemicals derived from natural compounds found in plants that inhibit topoisomerase activity by forming a ternary complex with the enzyme and DNA. As a result, the induced DNA damage causes the cell to arrest in G1 phase, upregulate $p16^{INKa}$ level and thereby inhibit the cyclin D/CDK4/6 kinase activity (184).

Doxorubicin is another potent topoisomerase inhibitor that has been used in the clinic, albeit dangerous heart toxicity at high dose. Doxorubicin is an anthracycline antibiotic that functions by intercalation into DNA helices and preventing topoisomerase from re-annealing the cut DNA during DNA replication (185). Microtubule inhibitors, on the other hand, disrupt mitotic spindle formation and arrest cells at the mitotic spindle assembly checkpoint, which is a radiosensitive period in the cell cycle (186). Similar to other agents mentioned, radiation therapy uses ionizing radiation to also inflict DNA damage, and is often combined with other chemotherapeutic agents to enhance tumor toxicity. Consequently, taxol and vinca alkyloids are two prominent microtubule inhibitors proven to be effective radiosensitizers in the clinic (187, 188).

1.6b. CDK inhibitors

In the cell cycle, countless proteins are known to be involved in oncogenesis such as cyclin D, cyclin E, pRb, and $p16^{INKa}$ to name a few. Particularly, CDKs are the regulatory subunits of the cyclin/CDK complexes that exert kinase activity to control cell cycle progression. Consequently, CDKs proved to be ideal targets to halt cell cycle progression of tumor cells. To date, more than 50 CDK inhibitors have been reported, and most inhibitors are small molecule inhibitors that act by competitively binding to the ATP binding pockets of CDKs. For instance, olomoucine and its analog roscovitine are purine analogues that were shown to inhibit the kinase activity of CDK1 and CDK2 causing G1 and G2 cell cycle arrest and apoptosis (189, 190). Roscovitine demonstrates stronger anti-tumor effects compared to olomoucine and is currently under testing in clinical trials (191, 192). Further discussion on the use of roscovitine in cancer research will be discussed in more details below. Staurosporine and its analogue UCN-01 (7-hydroxystaurosporine) are microbial alkaloids and were found to be non-specific inhibitors of CDK1 and PKC (193, 194). When combined with camptothecin and cisplatin, treatment of *p53*-deficient cells with UCN-01 induce DNA damage and apoptosis (195). Since most of these inhibitors rely on functional *pRb* and *p53* to mediate cell cycle arrest and apoptosis, the status of these genes must be identified

prior to therapy to avoid unresponsiveness or resistance of the tumor to the therapeutic agents.

1.6c. Targeting LMW-E/CDK2 kinase activity

Cyclin E is the regulatory subunit whose function requires interaction with CDK2 to phosphorylate target genes to allow transition from G1 to S phase of the cell cycle. In tumor cells, high cyclin E/CDK2 kinase activity persists throughout the cell cycle (157). Retrospective clinical evaluation of high-grade ovarian tumors identified cyclin E/CDK2 kinase activity as a significant predictive marker for response to platinum-based therapy (196). Moreover, CDK2 was recently reported to be required for LMW-E-mediated mammary oncogenesis in transgenic mice (197). Consequently, CDK2, which is a serine/threonine kinase, is and ideal anti-tumor target to disrupt the cyclin E/CDK2 kinase activity. Indeed, roscovitine (Seliciclib) is a purine derivative that preferentially inhibits the kinase activity of CDK1 and 2 over other CDKs (191, 192). Recent study showed that roscovitine can reverse LMW-E-induced resistance to letrozole treatment in breast cancer cells (178). Moreover, when combined with doxorubicin or trastuzumab, roscovitine exerts synergistic effects in the combination treatment on sarcoma and breast cancer cells, respectively (173, 198). Roscovitine has entered phase I clinical trial where it demonstrated response in metastatic ovarian cancer and nasopharyngeal carcinoma while phase II trial which involves the combination of roscovitine with either gemcitabine/cisplatin or docetaxel showed partial response in patients (199, 200). Perhaps the efficacy of roscovitine in these clinical studies can be improved if these patients were selected based on their LMW-E expression status given that CDK2-associated kinase activity is critical in inducing LMW-E-mediated tumor development.

1.6d. Inhibition of LMW-E generation

Research in the last decade has moved towards a more mechanistic approach utilizing information from molecular profiling to achieve personalized treatment. Given the strong prognostic and predictive role of LMW-E in breast

cancer, the regulation of cyclin E expression and post-translational processing is a unique target for anti-cancer therapy. The generation of LMW-E isoforms is proposed to be a result of high elastase proteolytic activity, which is expected to result in enhanced cleavage of cyclin E into LMW isoforms and ultimately lead to tumor development (165). Indeed, treatment of a breast cancer cell line (MDA-MB-157) with a neutrophil elastase inhibitor CE-2072 reduced the production of some LMW-E isoforms and also arrested the cells in G1 phase (201). In contrast, this inhibitor showed no effect in an immortalized hMEC line MCF-10A. Another potent and promising elastase inhibitor is ONO-5046, which has been demonstrated to inhibit the proliferation and metastatic development of non-small cell lung cancer cell line and tumor xenografts, respectively (202, 203). In addition, a recent study discovered the phytochemical indole-3-carbinol (I3C) found in most leafy vegetables as a neutrophil elastase inhibitor (204). Analysis of the proteolytic activity of elastase by zymography revealed that I3C effectively disrupts the cleavage of cyclin E into LMW isoforms and arrests MDA-MB-231 cells in G1 phase. These effects are similarly observed with knockdown of elastase protein expression by siRNA. Elastase expression is high in breast cancer and this is associated with poor patient outcome and high frequency of metastatic progression (205-209). Combined with the established oncogenic role of LMW-E in cancer, targeting elastase represents a unique therapy for cancers with high LMW-E expression and elastase activity.

Another mechanism of targeting the proteolytic processing of cyclin E is through the use of elafin, which is an endogenous elastase inhibitor that prevents the cleavage of cyclin E into LMW isoforms by elastase. C/EBPβ is a transcription factor that regulates elafin gene expression (210). In breast cancer cell lines and patient tissues, C/EBPβ is downregulated resulting in reduced elafin transcription. More specifically, elafin exerts its tumor suppressive role by inducing pRb-dependent cell cycle arrest in breast cancer cells while triggering caspase-3-dependent apoptosis in pRb-deficient cells (211). In immortalized hMECs with an intact G1-S checkpoint, elafin does not exert cytotoxic effect suggesting a valuable therapeutic utility of elafin in targeting tumor cells.

1.7. GAP IN KNOWLEDGE

Cyclin E and more specifically, LMW-E, play critical role in the initiation, progression, and metastasis in human cancer. Clinical and molecular studies clearly identify the LMW-E isoforms as novel oncogenes and powerful predictors of patient survival. Consequently, mechanistic examination of the oncogenic functions elicited by LMW-E is necessary to better understand and target tumors with high LMW-E levels. Biological and molecular studies accumulated from the last decade lead us to the following questions:

- Is LMW-E capable of initiating and maintaining tumor development?
- What effect does LMW-E have on the proliferation and architecture of the mammary acini, and if so, can inhibition of LMW-E by pharmacological agents rectify these defects?
- What signaling pathway(s) is/are deregulated in breast tumors with high LMW-E expression?
- Does LMW-E induce tumor initiation, progression, and metastasis by altering gene expression to enhance invasiveness and self-renewal capability?
- Are these phenotypes driven by previously unidentified substrate(s) of the LMW-E/CDK2 complex?

These are the main objectives of this dissertation, and the research data to address them are described in the following chapters. The overall hypothesis of this dissertation is that **LMW-E initiate and maintain mammary tumor via deregulation of mammary acinar morphogenesis, induction of the EMT, and generation of cells with CSC properties**. By examining these aspects of LMW-E in respect to the mammary gland and human pathophysiology, the results obtained will indeed move us closer to achieving personalized and molecularly targeted therapy for cancer treatment.

CHAPTER 2: **LMW-E REQUIRES CDK2-ASSOCIATED KINASE ACTIVITY TO INDUCE ABERRANT ACINAR MORPHOGENESIS AND MAMMARY TUMORIGENESIS**

2.1. INTRODUCTION

2.1a. LMW-E in breast cancer

Prior to the G1-S phase boundary, cyclin E associates with CDK2 to further phosphorylate and inactivate the pRb-E2F complex to promote S phase entry (212-214). Cyclin E overexpression by genomic and transcriptional amplification has been reported in multiple cancers, particularly in breast cancer (157, 161, 215-219). Additionally, posttranslational proteolytic cleavage of cyclin E mediated by serine protease generates two LMW-E isoforms in cancer cells (165, 220). Compared to full-length cyclin E, the LMW-E isoforms are hyperactive by forming tighter interaction with CDK2 and are more resistant to CKI inhibition resulting in higher rate of proliferation (175, 221). When subjected to antiestrogen treatment with fulvestrant and aromatase inhibitor with letrozole, LMW-E mediates resistance to the growth inhibitory effect of these agents (178, 201). Finally, retrospective examination of 395 breast cancer patient tissues identifies LMW-E as an independent and powerful prognostic and predictive marker of patient outcome (160).

2.1b. The functional relationship between LMW-E and CDK2

There are a total of 16 cyclins and 9 CDKs identified to date, and most of them participate in regulating the cell cycle (Figure 2) (21-24). Although the primary structures of cyclins are different from each other, the tertiary structures are similar consisting of 2 compact domains of 5 alpha helices. Additionally, all cyclins share a homologous sequence of approximately 100 amino acids known as the cyclin box, which mediates their interaction with CDKs (25). Interestingly, results from knockout animal studies unveiled considerable functional redundancy and compensatory mechanisms between the different cyclin/CDK complexes in normal tissues. Since there are two cyclin E proteins (E1 and E2), mice with single cyclin E gene knockout

carry out normal development (44, 45). However, double cyclin E knockout mice die during gestation due to defects in endoreduplication of the giant trophoblast cells and megakaryocytes. Surprisingly, CDK2-*null* mice are viable and show no proliferation defects (94, 95).

In contrast to findings regarding cyclin E and CDK2 in normal development, the inter-dependency between LMW-E and CDK2 is different in malignant transformation. Transgenic mice expressing the LMW-E isoforms develop mammary adenocarcinomas at higher frequency (27%) compared to mice expressing full-length cyclin E (10%) (180). Furthermore, LMW-E overexpression does not induce mammary tumor development in $CDK2^{-/-}$ transgenic mice, and treatment of the mice with LMW-E-induced tumor using two different CDK inhibitors, meriolin and roscovitine, significantly delayed mammary tumor formation by approximately 6 weeks suggesting that the oncogenic potential of LMW-E requires CDK2-associated kinase activity (197). Interestingly, these mice succumb to salivary gland tumors indicating that perhaps LMW-E interacts with novel partner(s) specifically expressed in this tissue to cause neoplastic transformation. These findings suggest the tissue-specific requirement of CDK2 by LMW-E to induce tumor development.

2.1c. Mammary acinar morphogenesis

The role of LMW-E in breast cancer is well established due to extensive molecular examination of this oncogene in the last decade. Biological processes are governed by the intimate relationship between form and function, which also helps explain how alteration of gene expression drives the development of malignant tumors. Perhaps by understanding the role of LMW-E in the context of the mammary acinus and how its expression affects form, then we will gain insights into its oncogenic function. Therefore, one of the objectives of this study is to examine the role of the LMW-E isoforms during acinar morphogenesis, which is an *in vitro* assay that closely recapitulates the mammary tissue.

Numerous studies have demonstrated that extracellular matrix interaction is very important for proper structure and function of normal tissues (222-224). When

cultured on 2-dimensional (2D) plates, both non-tumorigenic and tumorigenic epithelial cells form spindle-shaped structures. However, in 3-dimensional (3D) culture provided by a layer of laminin-rich basement membrane, non-tumorigenic hMECs arrest proliferation and undergo structural differentiation to form highly polarized acinar structures (Figure 1 & 3) (224). Meanwhile, tumorigenic cell lines grown in 3D culture do not arrest growth or polarize but instead form disorganized masses of cells. The acinus, or more commonly referred to as the alveolus, is the basic structure of the mammary gland. The basement membrane containing myoepithelial cells surrounds the single layer of luminal epithelial cells, which are highly differentiated and polarized, to provide structural and molecular support for the acinus (1, 225, 226). Towards the late stage of acinar morphogenesis, the cells in the center of the structure undergo apoptosis that results in luminal clearance and formation of a hollow lumen that serves to contain milk secretion during lactation (227, 228). Acinar morphogenesis involves 4 distinct stages of development: proliferation, polarization, luminal cell death, and continued proliferation along with luminal cell death (Figure 3). In essence, the mammary acinus can serve as an experimental “organism” to investigate mechanisms involved in tissue development and derailment in malignancy (1). In fact, recent studies have shown that the morphology of the acini is an accurate predictor for patient outcome. That is, human breast tumors that share a gene expression signature to the nontumorigenic HMECs in 3D culture are predicted to show significantly better prognosis (229). The morphological and functional relevance of this 3D culture system provides proof that this is a method of choice for studying form and function of the mammary gland *in vitro*.

2.1d. Hypothesis and Specific Aims

Normal acinar morphogenesis is critical for maintaining homeostasis of the mammary gland, and cell cycle regulation plays a pivotal role in this process. Aberration from this control will undoubtedly result in uncontrollable proliferation and genomic instability. Therefore, we ***hypothesize*** that *LMW-E disrupts normal mammary acinar development and serves as the initial route into breast tumor*

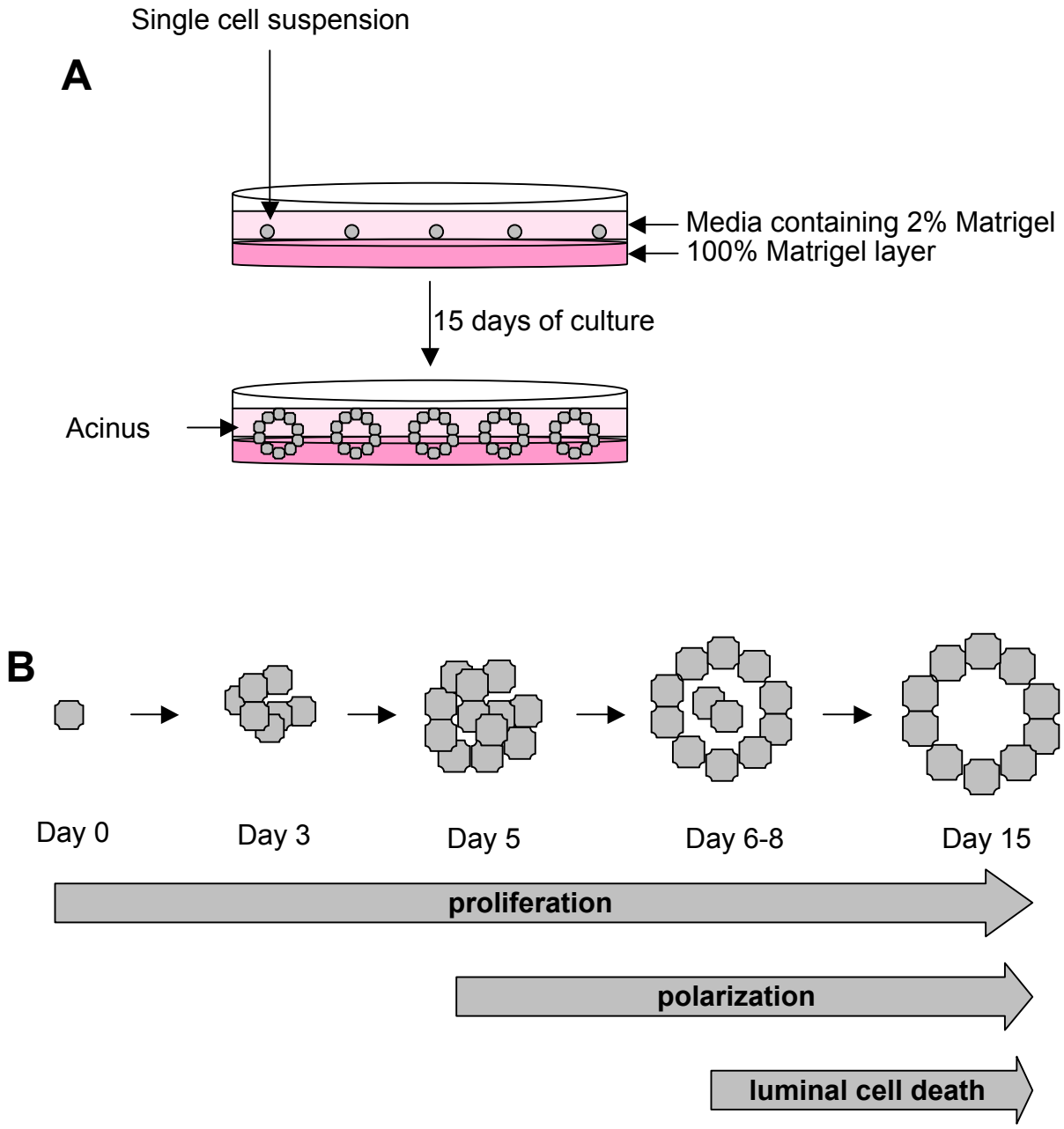

Adapted from *Methods* 2003;30(3):256-68

Figure 3: ***In vitro*** **acinar morphogenesis assay.** (A) On day 0, cells in single suspension are seeded on top of a 1 mm layer of solidified Matrigel. The cells are covered with a layer of culture media containing 2% Matrigel and fresh media is replaced every 4 days to provide continuous nourishment. After 15 days of culture, these cells undergo proliferation and organization to form spherical acinar structures. (B) Schematic of the progression of one cell seeded at day 0 into a fully-formed acinus on day 15.

development. The oncogenicity of LMW-E depends on CDK2-associated kinase activity and thus represents an ideal target for developing therapy to treat breast cancer patients with high LMW-E expression. To address the hypothesis, we will closely examine the following specific aims:

- Investigate the role of LMW-E in regulating acinar development
- Examine the tumorigenicity of overexpression of LMW-E *in vivo*
- Determine whether the deregulation by LMW-E is dependent on the CDK2-associated kinase activity.
- Elucidate a common signaling pathway present in 3D cultures and patient tissues that is deregulated by LMW-E

Briefly, the results presented in this chapter demonstrate that overexpression of LMW-E disrupts normal acinar morphogenesis in 3D *in vitro* culture and promotes tumorigenesis when expressed in non-transformed hMECs *in vivo*. CDK2-associated kinase activity is necessary to induce these phenotypes, and roscovitine (a CDK inhibitor) treatment can rescue the aberrant morphologies induced by LMW-E expression. Reverse-phase protein array assay of 276 breast tumor patient samples and cells cultured on monolayer and in 3D Matrigel demonstrated that in terms of protein expression profile, mammary epithelial cells cultured in Matrigel more closely resembled patient tissues than did cells cultured on monolayer. Additionally, the b-Raf-ERK1/2-mTOR pathway was activated in LMW-E expressing patient samples and activation of this pathway was associated with poor disease-specific survival. Combination treatment with roscovitine plus either rapamycin (mTOR inhibitor) or sorafenib (b-Raf inhibitor) effectively prevented aberrant acinar formation in LMW-E-expressing cells by inducing G1/S cell cycle arrest.

2.2. MATERIALS and METHODS

2.2a. Constructs and cell culture

All immortalized cell lines were cultured in DFCI-1 medium as described previously (230). FLAG-tagged cyclin E gene constructs EL and LMW-E were cloned into the pcDNA 4.0 vector (Clontech, Mountain View, CA) and transfected

into 76NE6 hMECs. Transfected cells were selected with 80 μg/mL zeocin (Invitrogen, Carlsbad, CA), and stable transfectants were maintained in culture with 10 μg/mL zeocin.

To generate 76NE6 cells with tetracycline-inducible cyclin E expression the cyclin E gene constructs were cloned into the pRetro-CMV/TO vector and transfected into 293T cells to produce retroviruses carrying the cyclin E constructs, and the pBMN-BSR-TetR vector to produce retroviruses carrying the Tet repressor. The 76NE6 cells were infected first with the retroviruses carrying the Tet repressor (TetR) gene fused with blasticidin-S resistance gene and then with the retroviruses carrying the cyclin E constructs. 76NE6 cells inducibly expressing TetR-vector, EL, LMW-E, EL^{R130A}, and LMW-E^{R130A}, were maintained in DFCI-1 medium with 20 μg/ml blasticidin-S and 1 μg/ml puromycin (InvivoGen, San Diego, CA). Other cell lines used in this study (i.e. Hs578T and MDA-MB-231) were obtained from American Type Tissue Collection and cultured as described previously (231).

2.2b. Tumorigenic assay and *in vivo* passaging

Nude mice were purchased from Charles River Laboratories (Wilmington, MA) and maintained in the Department of Veterinary Medicine at The University of Texas MD Anderson Cancer Center. The mice were injected subcutaneously in the mammary fat pad with $1x10^6$ cells suspended in 100 μL of a 1:1 Matrigel:media mix (Matrigel from BD Biosciences, San Diego, CA). Doxycycline was added to drinking water containing 1% sucrose, and water was replaced twice weekly. Mice were sacrificed under an Animal Care and Use Committee (ACUF)-approved protocol when tumors reached approximately 12 mm in diameter or 10 weeks after injection, whichever came first. The tumors were harvested for histopathological analysis or for expansion of tumor cells in tissue culture for reinjection into mice for *in vivo* passaging. Tumors submitted for histopathology were fixed in 10% neutral buffered formalin, paraffin embedded, and serially sectioned at 5 μm thickness.

2.2c. Staining of tumor sections

Paraffin-embedded tumor sections were stained with hematoxylin and eosin and for cyclin E using a polyclonal anti-cyclin E antibody (Santa Cruz Biotechnology, Santa Cruz, CA). The immunostaining was done as previously described (180) using a Vectastain ABC kit (per manufacturer's web site) and a BCIP/NBT chromogen detection system (Vector Laboratories, Burlingame, CA). Briefly, the sections were incubated in 1% H_2O_2 to block endogenous peroxidase activity and then incubated for 20 min in 10 mmol/L sodium citrate buffer (pH 6.0) at 90°C to retrieve nuclear antigens. Both primary and secondary antibody incubations were performed for 1 hr in blocking buffer (5% bovine serum albumin and 0.5% Tween-20 in 1x phosphate-buffered saline [PBS]) at room temperature. Nuclei were counterstained with hematoxylin.

2.2d. Morphogenesis assay and drug treatment

3D culture on basement membrane was performed as described previously (232). Assay medium (DFCI-1 medium with 2% growth factor-reduced Matrigel) with or without drugs was replaced every 4 days, and cells were cultured for 15 days.

2.2e. Indirect immunofluorescence analysis

Indirect immunofluorescence analysis of 3D cultures was performed as previously described with minor modifications (233). Cells cultured in 8-well chamber slides were fixed with 2% paraformaldehyde at room temperature for 20 min, permeabilized with 1% Triton X-100 in PBS for 20 min, washed thrice with PBS/glycine buffer (130 mM NaCl, 7 mM Na_2HPO_4, 3.5 mM NaH_2PO_4, and 100 mM glycine), and blocked with IF buffer (130 mM NaCl, 7 mM Na_2HPO_4, 3.5 mM NaH_2PO_4, 7.7 mM NaN_3, 0.1% bovine serum albumin, 0.2% Triton X-100, and 0.05% Tween-20) plus 10% goat serum for 1 hr at room temperature. Primary antibodies (laminin V and α6-integrin [Chemicon, Billerica, MA], GM-130 & E-cadherin [BD Pharmingen, San Diego, CA], and Ki67 [Abcam, Cambridge, MA]) were incubated in IF buffer at 1:200 dilution overnight at 4°C. The cells were incubated with Alexa fluor-conjugated rabbit (488), mouse (594), or rat (680) secondary antibodies (Molecular Probes, Carlsbad, CA), counterstained with 4,6-

diamidino-2-phenylindole (DAPI) (Sigma, St. Louis, MO) for 15 min at room temperature, and mounted with antifade solution (Molecular Probes, Carlsbad, CA). Confocal microscopy was performed at room temperature using an Olympus FV300 laser scanning confocal microscope (Olympus America, Inc., Center Valley, PA) at 40x magnification, and images were processed using Adobe Photoshop (Version 11.0.2). For quantification, the diameter of each acinus was measured, and unpaired Student *t* test was used for statistical analysis.

2.2f. Protein isolation for Western blot and kinase assay

Cell lysates were prepared and subjected to Western blot analysis as described previously (220). To obtain lysates from acini, acini were washed once with cold PBS, scraped, collected, and washed twice with cold PBS. Cell recovery solution (BD Biosciences) was added to the Matrigel/acini mixture at 1:1 volume, and cells were incubated on ice for 1 hr, washed with PBS, and lysed as described previously (165) The protein blots were incubated with primary antibodies (cyclin E, vinculin [Santa Cruz Biotechnology, Santa Cruz, CA], β-actin [Chemicon, Billerica, MA], BIM [Epitomics, Burlingame, CA], FAK, b-Raf, ERK1/2, pERK1/2 (T202/Y204), pMEK1/2 (S217/221), pS6 (S235/236), mTOR, eIF4E, Akt, pAkt(T308), and pRb(S807/811) [Cell Signaling Technology, Danvers, MA]) at 4°C with gentle shaking overnight. Kinase assay with histone H1 and GST-Rb as cyclin E substrates was performed as described previously (165).

2.2g. Reverse-phase protein array (RPPA) analysis

The RPPA approach was performed as previously described (234). Cellular proteins were prepared as described for western blotting were denatured by boiling in 1% SDS (with beta-mercaptoethanol) and diluted in five 2-fold serial dilutions in dilution buffer (lysis buffer containing 1% SDS). Serial diluted lysates were arrayed on nitrocellulose-coated slides (Grace Biolab) using Aushon 2470 Arrayer (Aushon BioSystems). Each sample was robotically printed in 5 fold serial dilutions on multiple slide including positive and negative controls prepared from mixed cell lysates or dilution buffer, respectively as well as multiple cell lines incubated with

and without growth factors to provide dynamic range.

Each slide was probed with a validated primary antibody plus a biotin-conjugated secondary antibody. Antibody targets were selected as being relevant to breast cancer through a literature review. Antibodies where then obtained and validated against each potential target. Only antibodies with a Pearson correlation coefficient between RPPA and western blotting of greater than 0.7 were used in reverse phase protein array study. Antibodies with a single or dominant band on western blotting were further assessed by direct comparison to RPPA using cell lines with differential protein expression or modulated with ligands/inhibitors or siRNA for phospho- or structural proteins, respectively.

The signal obtained was amplified using a Dako Cytomation–catalyzed system (Dako) and visualized by DAB colorimetric reaction. The slides were scanned, analyzed, and quantified using a customerized-software Microvigene (VigeneTech Inc.) to generate spot intensity.

Each dilution curve was fitted with a logistic model ("Supercurve Fitting" developed by the Department of Bioinformatics and Computational Biology in MD Anderson Cancer Center, "http://bioinformatics.mdanderson.org/OOMPA"). This fits a single curve using all the samples (i.e., dilution series) on a slide with the signal intensity as the response variable and the dilution steps are independent variable. The fitted curve is plotted with the signal intensities – both observed and fitted - on the y-axis and the log2-concentration of proteins on the x-axis for diagnostic purposes. The protein concentrations of each set of slides were then normalized by median polish, which was corrected across samples by the linear expression values using the median expression levels of all antibody experiments to calculate a loading correction factor for each sample.

2.2h. Breast cancer patient samples and clinical data

The clinical data from 267 breast cancer patients used in this study were reported previously (160). Each patient had received a diagnosis of breast cancer between 1990 and 1995 at 1 of 12 hospitals in the Chicago area. The study was approved by the institutional review board of the Wadsworth Center (Albany, NY). In

the study reported herein, we used tissue samples from a portion of these for RPPA analysis to investigate large-scale protein expression pattern.

2.2i. Statistical analysis

Each cell culture experiment was performed at least three times. Continuous outcomes were summarized with means and standard deviations. Comparisons among groups were analyzed by two-sided *t* test and Wilcoxon rank-sum test. Analyses were performed using SPSS software, version 12.0. For analysis of the RPPA results**,** the data for each protein were median-centered, and then the medians of each sample were subtracted from the raw data for the sample. For the 71 proteins common between the 2D culture, 3D culture and patient data sets, the data for each protein in each data set were standardized (subtraction of mean then divided by standard deviation), and then the standardized data were combined. The combined data set contains 93 cell line samples from 2D and 3D each, with three technical replicates for each of the 31 unique samples, and 276 breast tumor patient samples.

Disease-specific survival (DSS) was calculated from the date of surgical resection of the primary tumor to the date of death or last follow-up. Data for patients who died from causes other than breast cancer were censored at the time of death. DSS curves were computed by the Kaplan-Meier method (235). Bivariate analyses of DSS in patients with high LMW-E expression according to levels of FAK, BIM, total Akt, and pAkt(T308) were performed with the use of a two-sided log-rank test (236).

2.3. RESULTS

2.3a. Breast cancer cells fail to undergo acinar morphogenesis in 3D culture

Cellular context provided by the extracellular matrix plays a critical role in defining the morphological development of the cell. Therefore, the acinar morphogenesis assay was performed to determine if the 3D culture system can distinguish acinar morphology between normal and breast cancer cells. This assay involves culturing cells on top of a layer of Matrigel, a laminin-rich basement

membrane, and a single cell seeded on day 0 is capable of forming a highly polarized acinus that is fully differentiated by day 15 in culture (224, 233) (Figure 4A). The 76N cell line is a mortal hMEC line isolated from a reduction mammoplasty specimen, and these cells senesce at passages 18-20 in tissue culture (230). The 76NE6 cell line was generated by infection of the 76N cells with the HPV E6 virus, which binds and degrades p53 (237). As a result, the 76NE6 cells lack functional p53, are immortalized, but remain nontumorigenic. MCF-10A is also a nontumorigenic hMEC line that was immortalized spontaneously by extended culture (238). The 2 breast cancer cell lines used were Hs 578T and MDA-MB-231, which are $p53^{+/mut}$ and express endogenous LMW-E. These cells were cultured on Matrigel surface for 15 days and then subjected to immunofluorescence (IF) staining. The staining markers were GM-130 and α6-integrin, which stain the apical and basal surfaces of the acinus, respectively (239). Figure 4A clearly shows that the immortalized hMECs arrested proliferation and formed differentiated, polarized acinar structures. More specifically, these acini were spherical in structure and showed distinct α6-integrin staining on the outer surface (basal) and GM-130 staining on the inner surface (apical) of the acini. In contrast, the 2 breast cancer cell lines maintained single-cell morphology in 3D culture. That is, these cells failed to form coherent, round structures with unorganized α6-integrin and GM-130 staining.

To examine the effect of Matrigel culture on proliferation, a growth curve assay was performed on these cells cultured on 2D and 3D culture conditions for a total of 20 days. Both hMECs exhibited faster proliferation in 2D culture than in 3D culture with the 76NE6 cells growing much faster than the MCF-10A cells in both culture contexts (Figure 4B and C). Additionally, both hMECs demonstrated growth arrest on day 20 with a total of approximately 300,000 cells. On the contrary, both breast cancer cell lines displayed faster proliferation in 3D cultures as compared to normal cells. (Figure 4D & E). Particularly, the breast cancer cells cultured on 2D culture appeared to plateau at day 10 whereas those cultured in 3D culture seemed to continue to proliferate until day 20. Perhaps in addition to having aberrant cell cycle arrest machinery, the 3D culture environment provides more nutrients for the

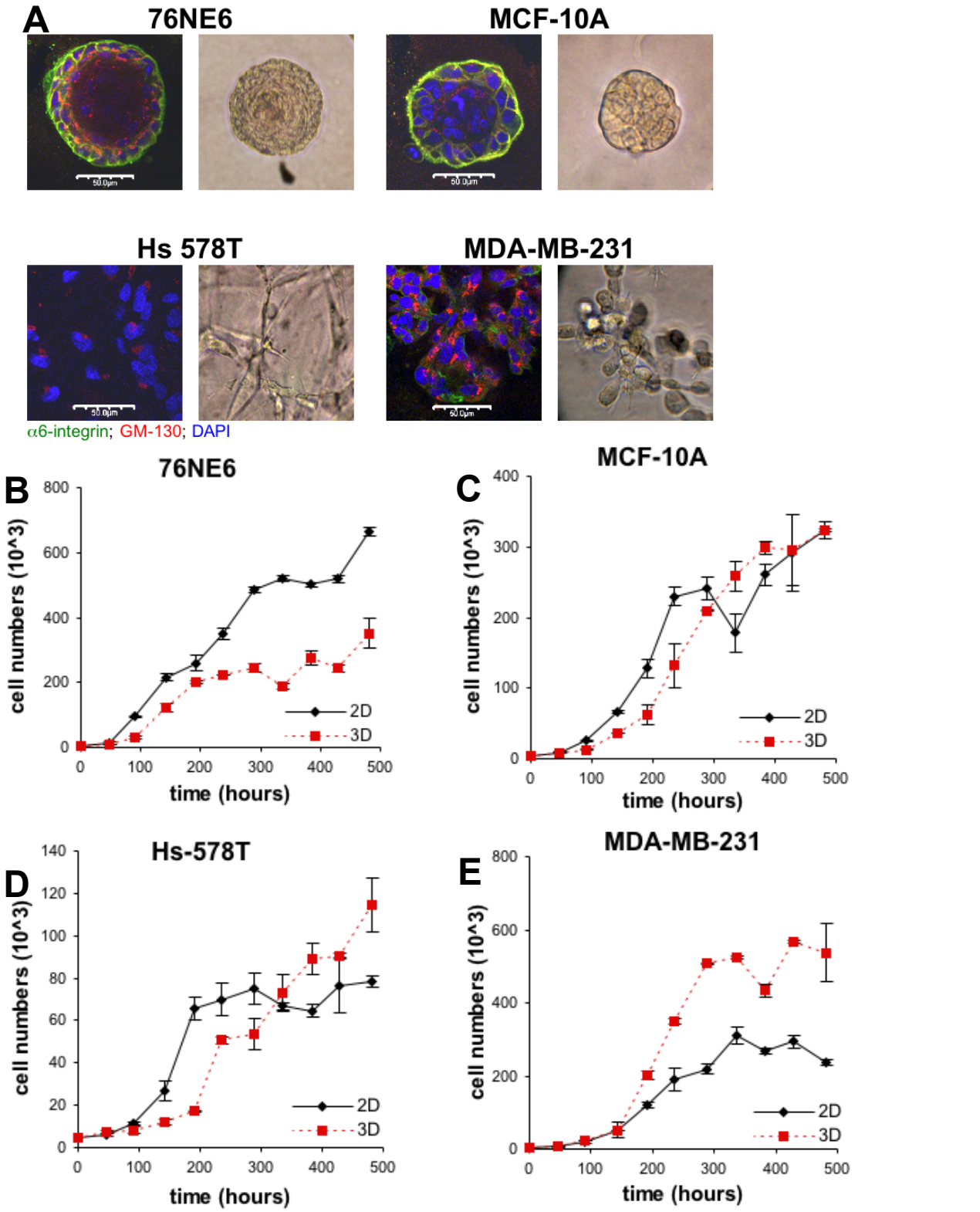

<u>Figure 4:</u> Breast cancer cells fail to undergo acinar morphogenesis in 3D culture. (A) MCF-10A, 76NE6, Hs 578T and MDA-MB-231 cells were seeded at 70 cells/mm^2 density on 1 mm Matrigel thickness. After 15 days in 3D culture, the cells were fixed and immuno-stained with anti-GM-130 and anti-a6-integrin antibodies. Nuclei were counter-stained with DAPI. Scale bar = 50 um. (B-E) On day 0, 5000 cells were seeded on 8 chamber slides for monolayer or coated with Matrigel as in A and harvested every 2 days until day 20 for cell count using the automatic cell culture counter.

Hs 578T and MDA-MB-231 cells to continue to proliferate. Taken together, these observations suggest that breast cancer cells lose the ability to respond to environmental cues provided by the basement membrane to undergo morphogenetic differentiation and growth arrest. Additionally, these results further confirm the unique ability of this 3D culture system to morphologically distinguish normal from cancer cells.

2.3b. hMECs but not breast cancer cells demonstrate cell cycle arrest in 3D culture

Since the initial stage of acinar morphogenesis involves extensive cell division, is cell cycle regulation responsible for the aberrant phenotypes observed? To address this question, cell lysates of MCF-10A, 76NE6, Hs 578T, and MDA-MB-231 cells from day 0 (2D) and day 15 of morphogenesis (3D) were subjected to Western blot analysis for proteins that regulate cell cycle progression. Overall, the protein expression profiles of the 4 cell lines examined were largely different from 2D to 3D culture condition. Both hMEC lines demonstrate cell cycle arrest by reducing the expression levels of cyclin B, D, E, CDK1, 2 and upregulating $p27^{Kip1}$. In contrast, the breast cancer cells express high levels of cyclin D and CDK4 suggesting that perhaps G1 phase progression is active (Figure 5A). Matrigel is composed of a protein mixture secreted from the Engelbreth-Holm-Swarm (EHS) mouse sarcoma cells that also contains high growth factor level thus explaining the elevated cyclin D and CDK4 proteins. In addition, all 4 cell lines express high levels of pAkt (S473) in 3D culture, and phosphorylation of Akt activates both $p21^{Cip1}$ and $p27^{Kip1}$, which in turn inhibit cyclin E/CDK2 activity. Cyclin E protein level is lower in 3D culture suggesting reduced G1-S phase transition. Moreover, a previous study has shown that Akt is selectively activated in the matrix-attached cells and not in the centrally located cells in the luminal space (239). Perhaps the presence of extracellular matrix signaling enables these matrix-attached cells to survive by activating the Akt pathway. This finding also explains the high levels of pAkt (S473) in both the Hs 578T and MDA-MB-231 cell lines in 3D culture since these breast cancer cells maintain single cell morphology and thus every cell is in contact with

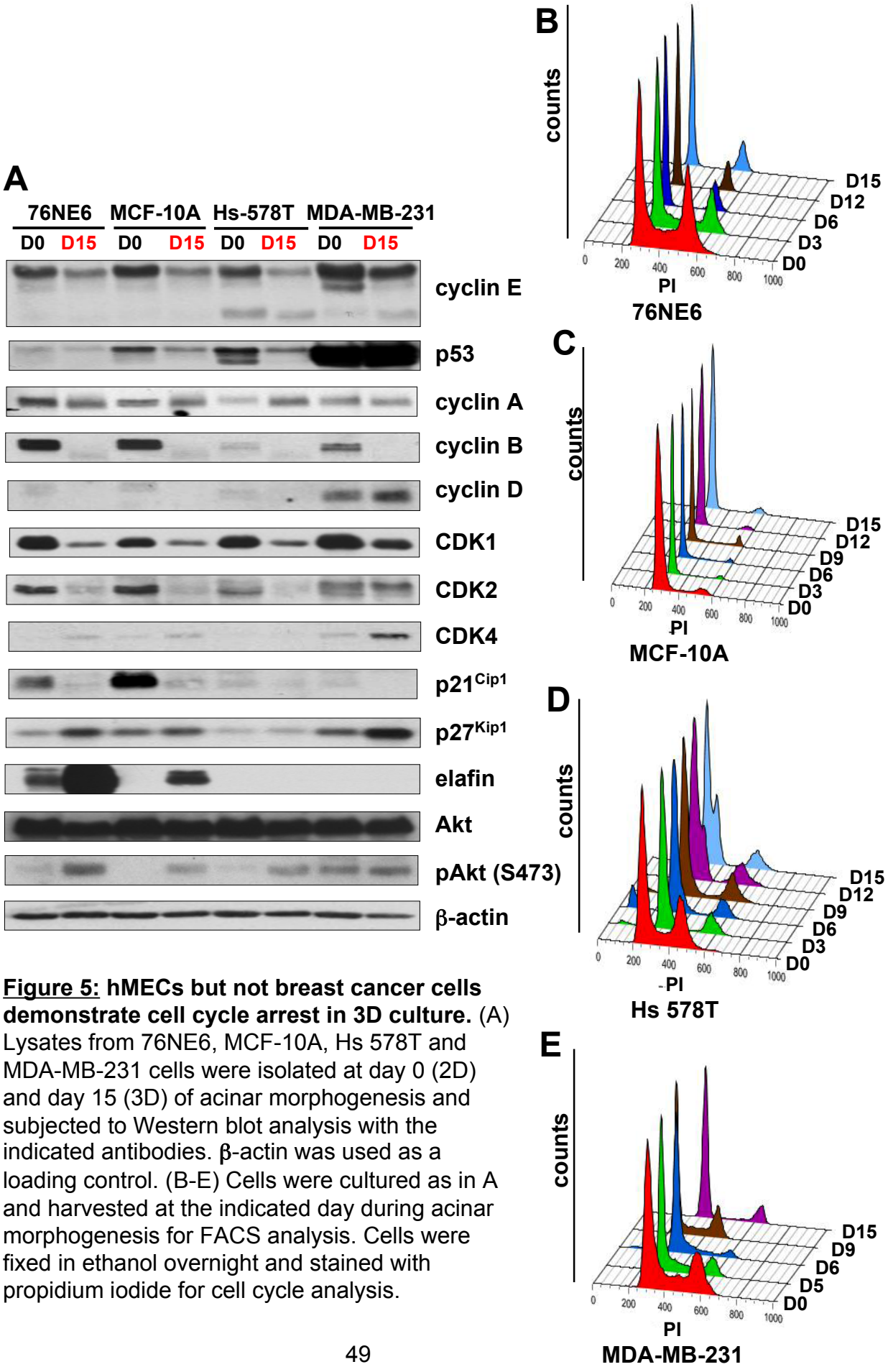

Figure 5: hMECs but not breast cancer cells demonstrate cell cycle arrest in 3D culture. (A) Lysates from 76NE6, MCF-10A, Hs 578T and MDA-MB-231 cells were isolated at day 0 (2D) and day 15 (3D) of acinar morphogenesis and subjected to Western blot analysis with the indicated antibodies. β-actin was used as a loading control. (B-E) Cells were cultured as in A and harvested at the indicated day during acinar morphogenesis for FACS analysis. Cells were fixed in ethanol overnight and stained with propidium iodide for cell cycle analysis.

the basement membrane. In addition, elafin is an endogenous inhibitor of elastase, which is responsible for LMW-E cleavage. Elafin has been reported to be downregulated in many breast cancer cell lines, and both the Hs 578T and MDA-MB-231 cell lines completely lack elafin protein expression. Meanwhile, the hMECs dramatically upregulate elafin expression in 3D culture suggesting that these cells are entering cellular quiescence since elafin upregulation has been demonstrated to induce cell cycle exit.

Fluorescence activated cell sorting (FACS) analysis with propidium iodide (PI) staining was used to directly assess the cell cycle distribution of normal and cancer cells grown on 3D culture from day 0 to day 15. As expected, the control MCF-10A cells were mostly in G1 phase during the entire morphogenetic process (Figure 5C). The 76NE6 cells also became G1 arrested and showed very low S phase population (<5%) after 6 days in 3D culture (Figure 5B). Interestingly, the 2 breast cancer cell lines also showed decreasing S phase (but not until day 15 in the MDA-MB-231 cells) and a slight increase in G1 phase from day 0 to day 15 in 3D culture (Figure 5D & E). Collectively, the 76NE6 and MCF-10A cell lines showed growth arrest and polarity organization in 3D culture, whereas the Hs 578T and MDA-MB-231 cells, to some extent, failed to show these behaviors. These findings suggest that cell cycle regulation is important for proper acinar morphogenesis, but does not entirely account for the aberrant morphologies observed in the breast cancer cells.

2.3c. LMW-E expression leads to aberrant acinar morphogenesis

We speculate that LMW-E is a critical initiator of oncogenesis and one of its early roles during this process is to deregulate mammary acinar morphogenesis. Similar to the parental 76NE6 cells, the 76NE6-vector cells formed perfectly spherical acinar structures (Figure 6A). Interestingly, the acini developed from the 76NE6-EL cells are larger compared to those of vector control cells, but the structures remained spherical in shape. In contrast, the 76NE6-LMW-E cells formed very large, irregularly shaped structures with a few multi-acinar complexes. We quantified the size of the acini by measuring the longest diameter of the structures

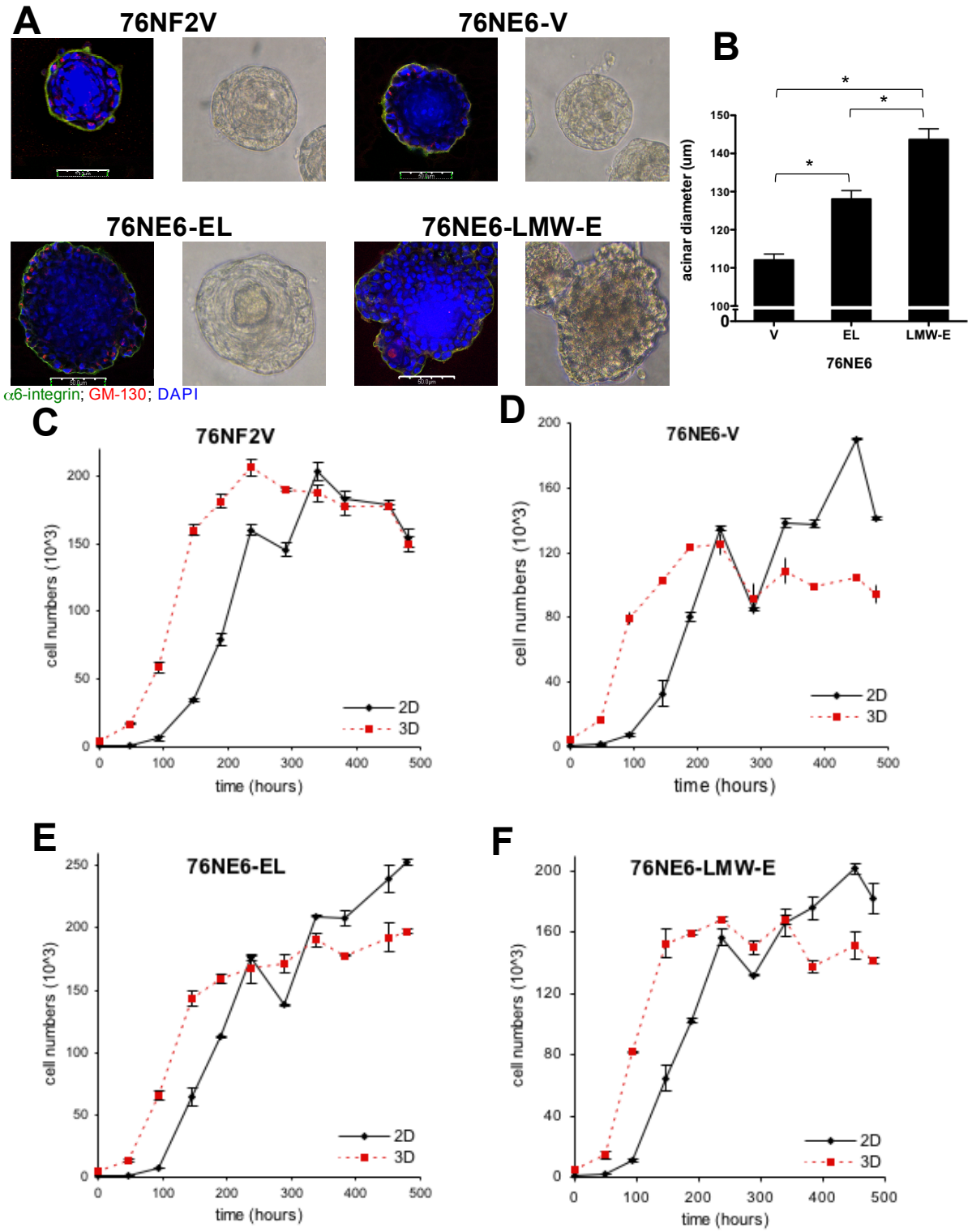

Figure 6: LMW-E expression leads to aberrant acinar morphogenesis. (A) 76NF2V, and 76NE6 cells with stable expression of V, EL, and LMW-E(T1) were seeded at 70 cells/mm2 density on 1 mm Matrigel thickness. After 15 days in 3D culture, the cells were fixed and immuno-stained with anti-GM-130 and anti-a6-integrin. Nuclei were counter-stained with DAPI. Scale bar = 50 um. (B) The diameter of the acini were measured and averaged from 3 independent experiments. Error bars = SEM (Student's *t* test, *p<0.05). (C-F) On day 0, 5000 cells were seeded on 8 chamber slides for monolayer or coated with Matrigel as in A and harvested every 2 days until day 20 for cell count.

and found that ectopic LMW-E expression in the 76NE6 cells does lead to approximately 28% larger acini compared to vector control cells ($p < 0.0001$) (Figure 6B). These results signify that, in the mammary gland, LMW-E is an important regulator of the early onset of oncogenesis by perhaps causing enlargement of mammary lobules.

As established previously, the morphology and growth patterns of human mammary epithelial cells are dramatically different from 2D to 3D culture. Normal hMECs grown in 3D culture provided by laminin rich basement membrane arrest proliferation and form fully differentiated acinar structures. The 76NE6-vector, 76NE6-EL, LMW-E, and 76NF2V cells had almost identical doubling times in 2D culture at approximately 45 hours (Figure 6C-F). In contrast, when cultured in 3D medium, these cells exhibited fast rate of proliferation up to day 5 and begin to plateau at day 10, which is consistent with previous observations (239). The difference in growth behavior between the EL and LMW-E clone was not apparent in 3D culture except that the total cell number of the EL clone was larger than the LMW-E clone after 20 days of culture. Furthermore, the 76NF2V cell line showed growth arrest at the latest time point, but the cell number declined noticeably after reaching the peak. This is due to the control of the cell cycle by an intact *p53*. In addition, these results also suggest that the 3D culture system is more sensitive at distinguishing the differences between EL and LMW-E in the cells than the 2D counterpart.

2.3d. Deregulation of the cell cycle progression by LMW-E during acinar morphogenesis

Protein expression relies on different cellular context, depending what environment the cell is in contact with. Since expression of key cell cycle regulators could be modulated by signals received from the 3D environment, we questioned if the addition of Matrigel was sufficient to mediate changes in expression levels of these proteins. To address this question we subjected cells cultured in 2D and 3D conditions to western blot analysis). The results from this experiment demonstrated that in all cell lines examined (76NF2V, 76NE6-V, EL, and LMW-E), the activity of

the cell cycle is greatly repressed in 3D context as evidenced by reduced expression of many of the cyclins and CDK expression (Figure 7A). This suggests that cells cultured on monolayer plates do not experience growth-inhibiting effects from the extracellular matrix and exhibit high cell cycle activity continuously. However, the cells in 3D culture showed dramatic proliferation arrest behavior after 15 days in culture with the protein levels of cyclin A, B, D, CDK1, 2, 4, and pAkt (S473) significantly downregulated. In contrast, both the 76NE6-EL and 76NE6-LMW-E cells upregulate cyclin E expression in 3D culture. Contrary to our expectation, overexpression of LMW-E did not affect the expression of these cell cycle proteins in 3D culture as the expression profile of the LMW-E cells is similar to that of the vector control cells. Interestingly, the 76NE6-LMW-E cells express much higher elafin proteins in 3D culture compared to the 76NE6-EL cells. Elafin is an endogenous inhibitor of elastase and therefore can prevent the cleavage of cyclin E into LMW isoforms (240). Maybe this induction of elafin expression can compensate for the oncogenic effects of LMW-E in these cells by preventing further LMW-E generation.

To determine the effect of overexpression of EL and LMW-E on the cell cycle profile of hMECs during acinar morphogenesis, the cells were cultured on Matrigel and subjected to FACS analysis with PI staining every 3 days post seeding on matrigel. As observed previously with the 76NE6 cell cycle profile (Figure 5B), the 76NE6-V, EL and 76NF2V cells arrest in G1 phase by reducing the S and G2/M population from day 6 to day 15 of acinar development (Figure 7B-D). In contrast, the 76NE6- LMW-E cells demonstrate a dramatically different cell cycle distribution during acinar morphogenesis (Figure 7E). On day 0, the cell cycle distribution of the 76NE6- LMW-E cells is similar to the parental cells with approximately 60% in G1, 15% in S, and 25% G2/M phase. After 6 days in 3D culture, these cells appear to lack S and G2/M population as the DNA content represents mainly G1 phase. This population then shifts gradually to S and then G2/M population from days 9 to 15 of acinar morphogenesis. On day 15, approximately 90% of the population is in G2/M phase while about 10% are in G1 phase. This unusual pattern of cell cycle distribution suggests that the LMW-E overexpressing cells are able to traverse the

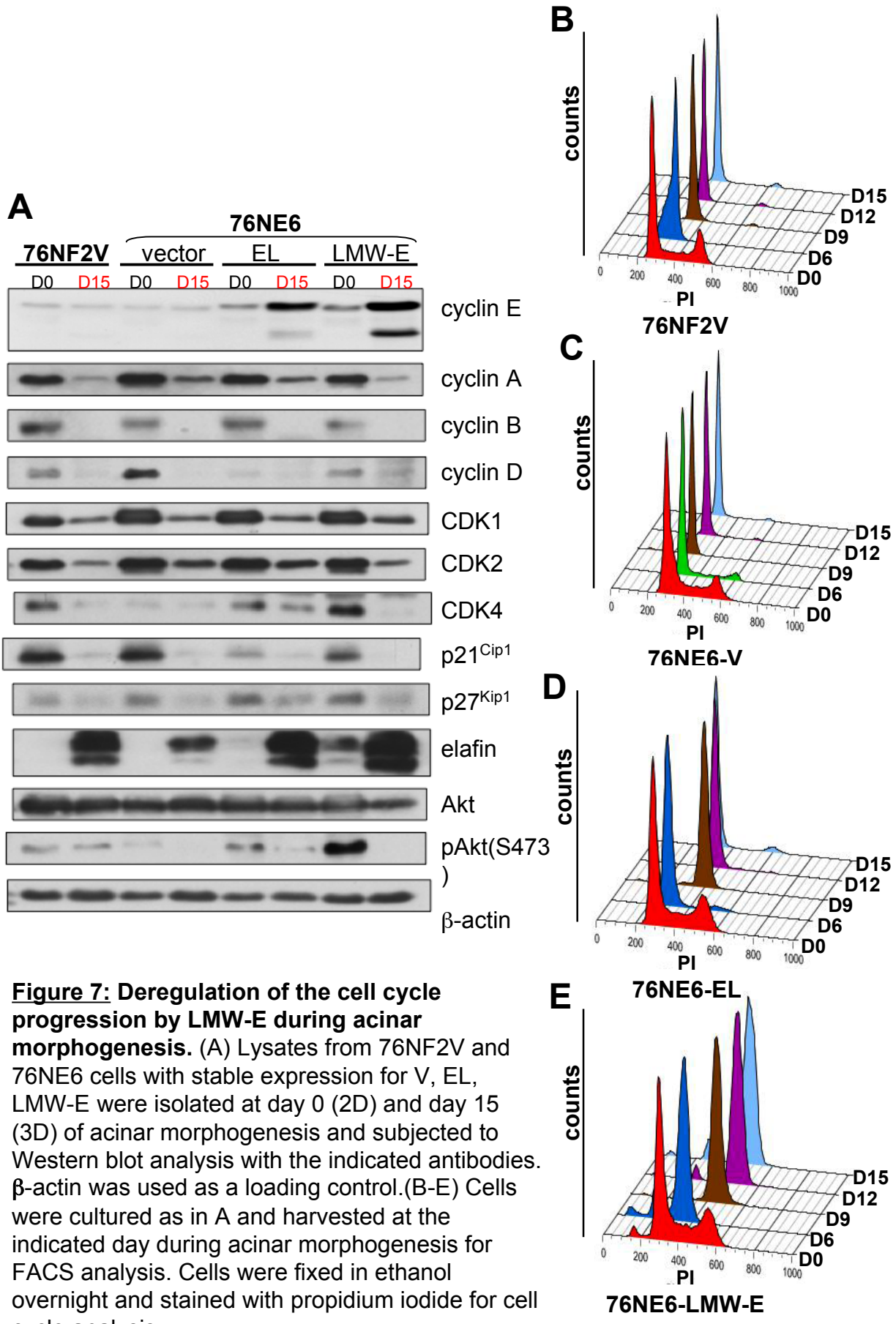

Figure 7: Deregulation of the cell cycle progression by LMW-E during acinar morphogenesis. (A) Lysates from 76NF2V and 76NE6 cells with stable expression for V, EL, LMW-E were isolated at day 0 (2D) and day 15 (3D) of acinar morphogenesis and subjected to Western blot analysis with the indicated antibodies. β-actin was used as a loading control.(B-E) Cells were cultured as in A and harvested at the indicated day during acinar morphogenesis for FACS analysis. Cells were fixed in ethanol overnight and stained with propidium iodide for cell cycle analysis.

G1-S phase transition but arrest in S and G2/M phase due to increasing DNA damage that LMW-E overexpression can induce in these cells (176). Taken together, these results suggest that LMW-E expression induces formation of large and irregular acini, which could be explained by the aberrant cell cycle machinery during the progression through the different developmental stages of acinar morphogenesis.

2.3e. Elafin overexpression fails to completely revert breast cancer cells during acinar morphogenesis

LMW-E expression is unique in cancer cells due to the action of elastase, and their expression leads to more aggressive proliferative phenotype (165). Elafin is a potent endogenous inhibitor specific for elastase and proteinase-3 (241). We recently reported that elafin is transcriptionally down regulated in most tumor cell lines and thus explaining the generation of LMW-E in tumor but not in normal cells (210). Previous studies have shown that exogenous elafin expression can inhibit the proliferation of MDA-MB-468, which express high levels of LMW-E, *in vitro* and in xenograft mouse model suggesting that perhaps elafin is an effective candidate to negate the growth advantage given by LMW-E expression. Therefore, we aim to determine whether inhibition of elastase by overexpression of elafin in breast cancer cells would cause reversion of these cells into highly organized acinar structures. Adenovirus containing elafin DNA were infected into the 76NE6, MCF-10A, Hs 578T, and MDA-MB-231 cell lines and then cultured on Matrigel (Figure 8A). On day 15 of morphogenesis, the cells were fixed and stained with GM-130 and a6-integrin antibodies. The results obtained indicated that overexpression of elafin was not toxic to immortalized cells (Figure 8B). That is, the 76NE6 and MCF-10A cells still formed correct acinar structures in the presence of high levels of elafin. However, the Ad-luciferase and Ad-elafin conditions generated larger acini perhaps due to the presence of adenovirus in general. As for the breast cancer cells, the Hs 578T cells remained single-cell phenotype in contrast to the MDA-MB-231 cells, which formed adherent round structures in the presence of both Ad-luciferase and Ad-elafin. Western blot analysis confirmed that overexpression of elafin reduced

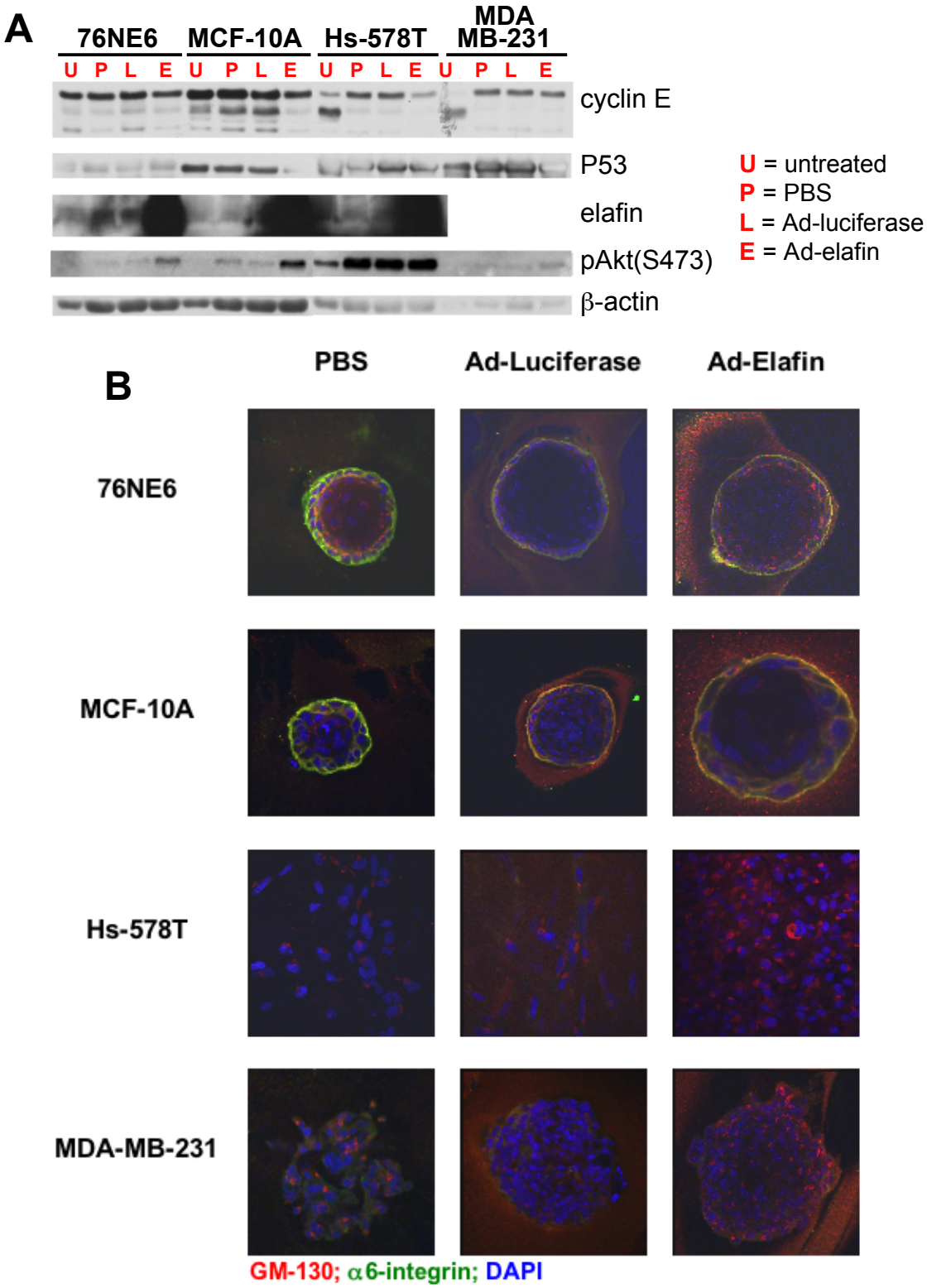

Figure 8: Elafin overexpression fails to completely revert breast cancer cells during acinar morphogenesis. Cells were treated with PBS and adenovirus carrying luciferase and elafin DNA on 2D plates. Three days later, the cells were extracted for (A) Western blot analysis with the indicated antibodies and (B) acinar morphogenesis assay. On day 15 of morphogenesis, all cells were fixed and immunostained with GM-130 and a6-integrin antibodies, and nuclei were counterstained with DAPI.

LMW-E expression and this is correlated with increased pAkt (S473) expression. The pAkt pathway leads to many different downstream effects, one of which is activation of $p27^{Kip1}$, which then can act to inhibit the cyclinE/CDK2 complex. Perhaps this pathway is activated to keep the cell cycle in check when elafin is expressed.

2.3f. Loss of p53 control cooperates with LMW-E to drive aberrant acinar formation

Cyclin E and p53 are both critical regulators of the cell cycle. Numerous studies have shown that overexpression of cyclin E and its LMW isoforms lead to high proliferation, aberrant expression of other cell cycle regulators, and chromosomal instability. Furthermore, *p53* is a tumor suppressor and was found to have high frequency of mutation in breast tumors with high cyclin E protein content (242). The association between cyclin E expression and *p53* gene status plays important role in maintaining the integrity of the cell cycle machinery in normal mammary cells. Since previous experiments demonstrated that stable LMW-E expression leads to formation of larger and irregularly shaped acini compared to the 76NE6 parental cells, we next aim to investigate whether p53 collaborates with LMW-E to induce these phenotypes. Adenovirus containing the LMW-E DNA was infected into the 76NE6 (degraded *p53*) and 76NF2V (wt *p53*) cells, and these cells were cultured on Matrigel for 15 days to analyze acinar formation (Figure 9A). The 76NF2V cells infected with the LMW-E construct still maintain the spherical acinar structure with the size of the acini slightly larger than those of the PBS and Ad-luciferase control cells (Figure 9B). However, the size of these acini is in similar range to those of the 76NE6 parental cells. Meanwhile, the 76NE6 cells induced with LMW-E expression via adenoviral infection lead to formation of acini with misshapen structures that are about 2 times larger than the parental control cells. The results obtained suggest that loss of p53 control cooperates with LMW-E expression to drive aberrant acinar formation. This deregulation by p53 and LMW-E appears to affect the size and shape of the acini only but not on the polarity and lumen formation as even parental 76NF2V acini contain filled lumen.

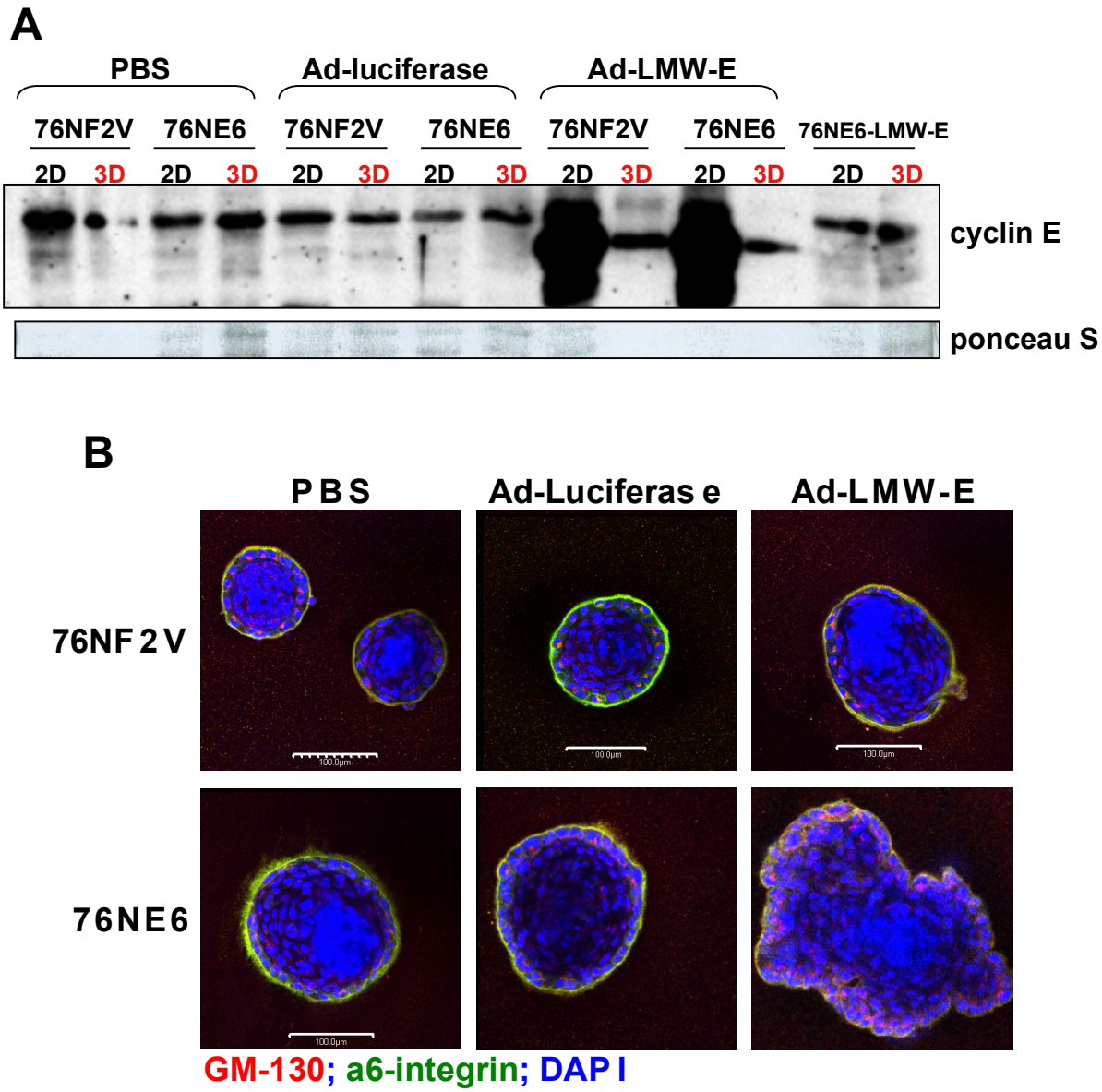

Figure 9: Loss of p53 control cooperates with LMW-E to drive aberrant acinar formation. Cells were treated with PBS and adenovirus carrying luciferase and LMW-E DNA on 2D plates. Three days later, the cells were extracted for (A) Western blot analysis and (B) acinar morphogenesis assay. On day 15 of morphogenesis, all cells were fixed and immunostained with GM-130 and a6-integrin antibodies, and nuclei were counterstained with DAPI.

2.3g. Coculture with breast cancer cells cause formation of larger hMEC acini

The microenvironment provides physical support as well as molecular crosstalk to nearby cells and thus creating a niche for these cells to grow and differentiate into specific tissue. This experiment was designed to address the question of whether signals released from normal cells can overcome those of tumor cells or can tumor cells recruit normal cells to become more abnormal? The cell lines examined were: 76NE6, MCF-10A, 76NF2V, Hs 578T, and MDA-MB-231. These cells were cultured on Matrigel and brightfield images were taken at days 6, 10 and 15 of acinar morphogenesis. Figure 10A shows that the breast cancer cells do not form coherent acinar structures but instead their morphologies are similar to those observed on monolayer culture, which are single-celled and spindle-shaped phenotypes. The MCF-10A, 76NF2V and 76NE6 cells were grown in 3 different 3D culture conditions: 1) alone, 2) mixed with Hs 578T or MDA-MB-231 cells at 1:1 ratio, and 3) on the top layer (insert) of a transwell plate with the Hs 578T or MDA-MB-231 cells on the bottom well (Figure 10B-D). Contrary to our expectation that coculture could rescue the morphology of breast cancer cells, the results revealed that it actually causes increase in acinar size of all 3 immortalized hMEC lines. The results demonstrated that the morphology of breast cancer cells did not change when cultured together with normal breast cells in 3D culture. However, the acinar structures of the normal cells are slightly larger when cultured with breast cancer cells. It is possible that breast cancer cells release certain growth factors or cytokines to stimulate enhanced proliferation of the normal cells thus implicating that tumor cells can recruit normal cells to become abnormal.

2.3h. LMW-E is tumorigenic

Previous experiments using cultured cells have demonstrated that the LMW-E isoforms are both biochemically and biologically hyperactive and exhibit strong oncogenic potentials (175). In addition, LMW-E is found in breast cancer cell lines and patient samples but not in normal tissues suggesting that perhaps LMW-E partakes unique oncogenic role in malignancy. To investigate whether ectopic

Figure 10

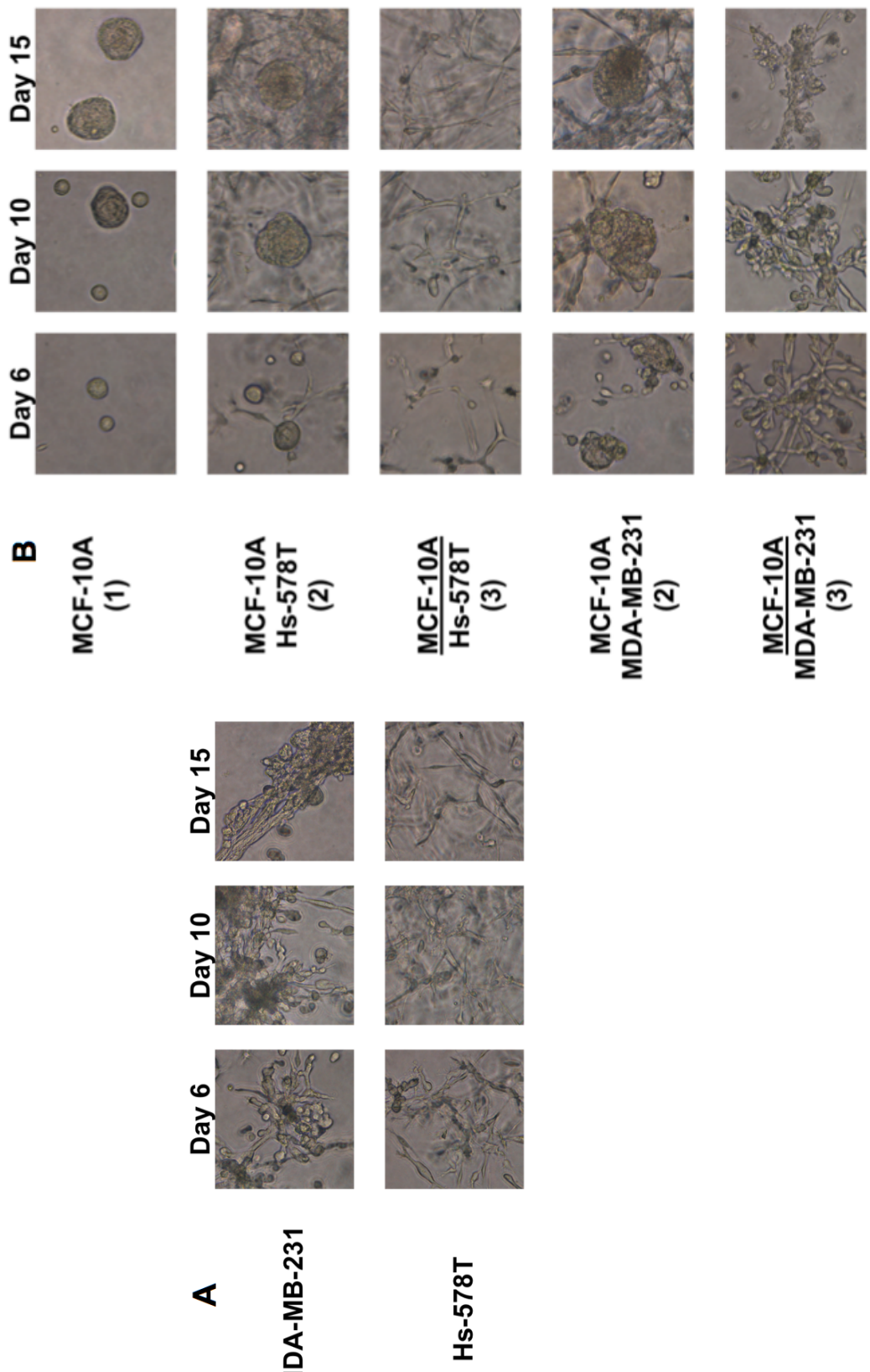
A
MDA-MB-231
Hs-578T
Day 6
Day 10
Day 15
B
MCF-10A (1)
MCF-10A Hs-578T (2)
MCF-10A Hs-578T (3)
MCF-10A MDA-MB-231 (2)
MCF-10A MDA-MB-231 (3)
Day 6
Day 10
Day 15

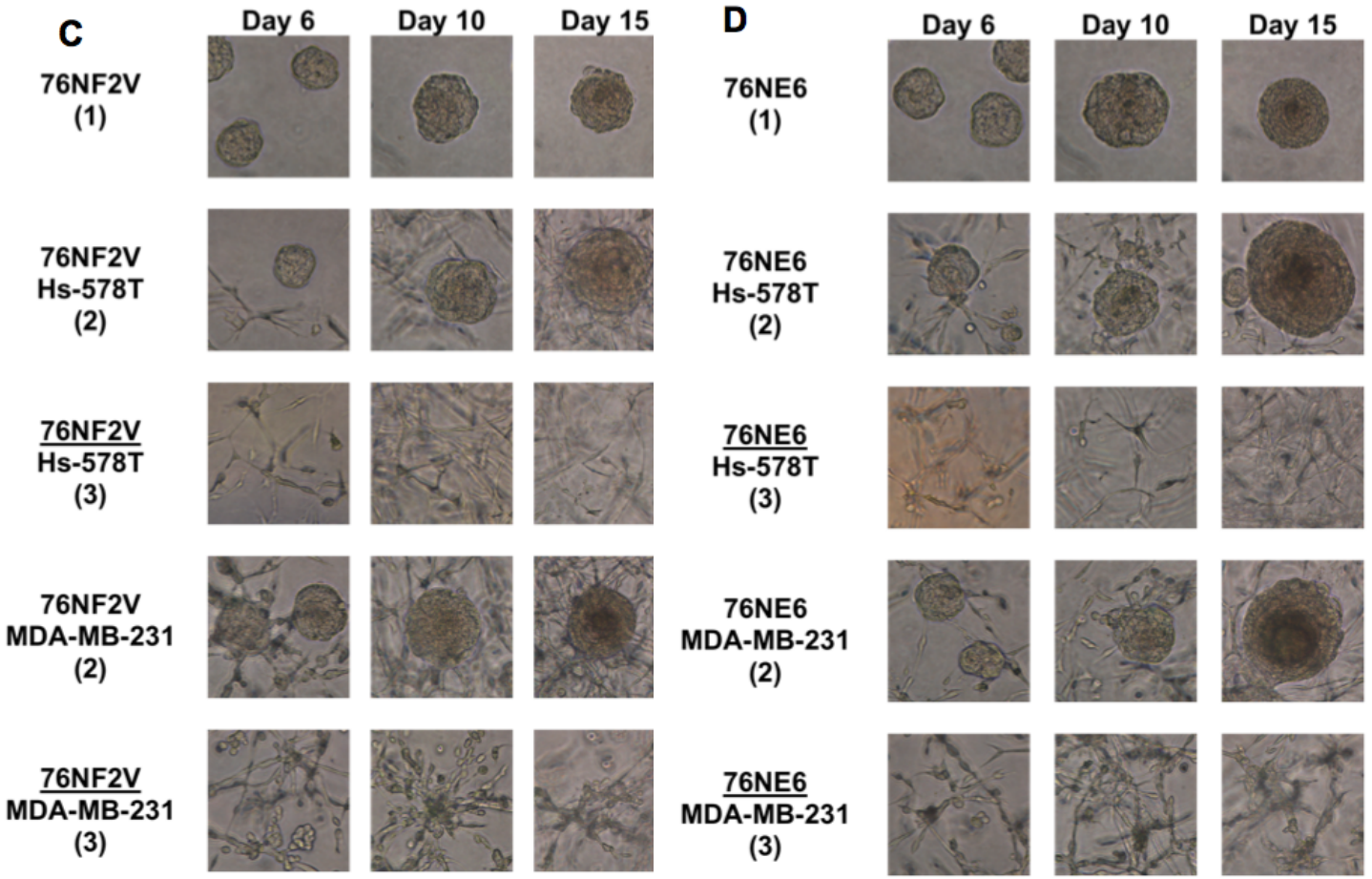

Figure 10: Coculture with breast cancer cells cause formation of larger hMEC acini. (A) MDA-MB-231 and Hs578T cells were seeded at 70 cells/mm2 density on 1 mm Matrigel thickness. Brightfield images were taken on days 6, 10, and 15 of acinar morphogenesis. (B-D) MCF-10A, 76NF2V, and 76NE6 cells were cultured on Matrigel in 3 different 3D culture conditions: 1) alone, 2) mixed with Hs 578T or MDA-MB-231 cells at 1:1 ratio, and 3) on the top layer (insert) of a transwell plate with the Hs 578T or MDA-MB-231 cells on the bottom well. Brightfield images were taken on days 6, 10, and 15 of acinar morphogenesis.

LMW-E expression in a non-tumorigenic hMEC line, 76NE6, induces cellular transformation *in vivo*, we injected these cells stably expressing vector, EL, and LMW-E subcutaneously into nude mice and observe for xenograft development (Table 6). The MDA-MB-468 breast cancer cell line was injected as a positive control. While injection of the vector control cell did not yield tumor development, 7% of the injection of the 76NE6-EL cells formed tumors. More importantly, the 76NE6-LMW-E is significantly more tumorigenic as their injection led to 74% tumor incidence ($p<0.0001$). The significant difference in the tumorigenic potential between EL and LMW-E led us to believe that the proteolytic cleavage of cyclin E into LMW-E renders novel physical and molecular interactions with other proteins to support tumor growth in mice.

Now that we have established that LMW-E is tumorigenic, the next question to address is: does LMW-E function to sustain tumor maintenance and reinitiate tumor development? Consequently, we subjected the LMW-E-expressing tumor cells to serial *in vivo* passaging in the mouse mammary fat pad. The 76NE6-LMW-E tumors were removed and prepared for culture *in vitro* (T1G2 clones) (see Figure 11A for schematic of *in vivo* passaging). Two clones from this generation were injected back into the mice (T1G2.2 and T1G2.7) and all 10 of the injections rendered tumor growth (Table 6). We repeated the passaging for two additional rounds generating the T1G3 and T1G4 clones, and the injections also resulted in 100% tumor formation. We selected 3 clones from each generation for further studies *in vitro* (T1G2.2, 5, 7; T1G3.1, 5, 8; and T1G4.2, 7, 8), and they are collectively named tumor-derived cells (TDCs). Taken together, these results strongly indicate that LMW-E expression by itself is capable of promoting tumor development and enhancing tumorigenicity with *in vivo* passaging.

2.3i. *In vivo* passaging selects for increasing LMW-E and decreasing elafin expression

To further investigate the mechanism of LMW-E-mediated tumorigenesis, the TDCs were subjected to western blot analysis for cyclin E and elafin expression. Most of the TDC clones show dramatic increase in LMW-E protein levels compared

Table 6: LMW-E is tumorigenic

	Tumors/ Injections (%)
76NE6-vector	0/12 (0%)
76NE6-EL	1/15 (7%)
76NE6-LMW-E	23/31 (74%)
T1G2.2	5/5 (100%)
T1G2.7	5/5 (100%)
T1G3.7	5/5 (100%)
T1G3.8	5/5 (100%)
MDA-MB-468	11/11 (100%)

Athymic mice were injected subcutaneously with $1x10^7$ 76NE6 cells stably transfected with empty vector, EL, LMW-E and MDA-MB-468 cells. After 10 weeks, the tumors were removed for expansion in culture for further *in vivo* passaging and also for IHC analysis. Tumor incidence rate was estimated with exact 95% confidence intervals and Fisher's exact tests were used to compare tumor incidence rate between/among groups (*$p<0.0001$).

Figure 11

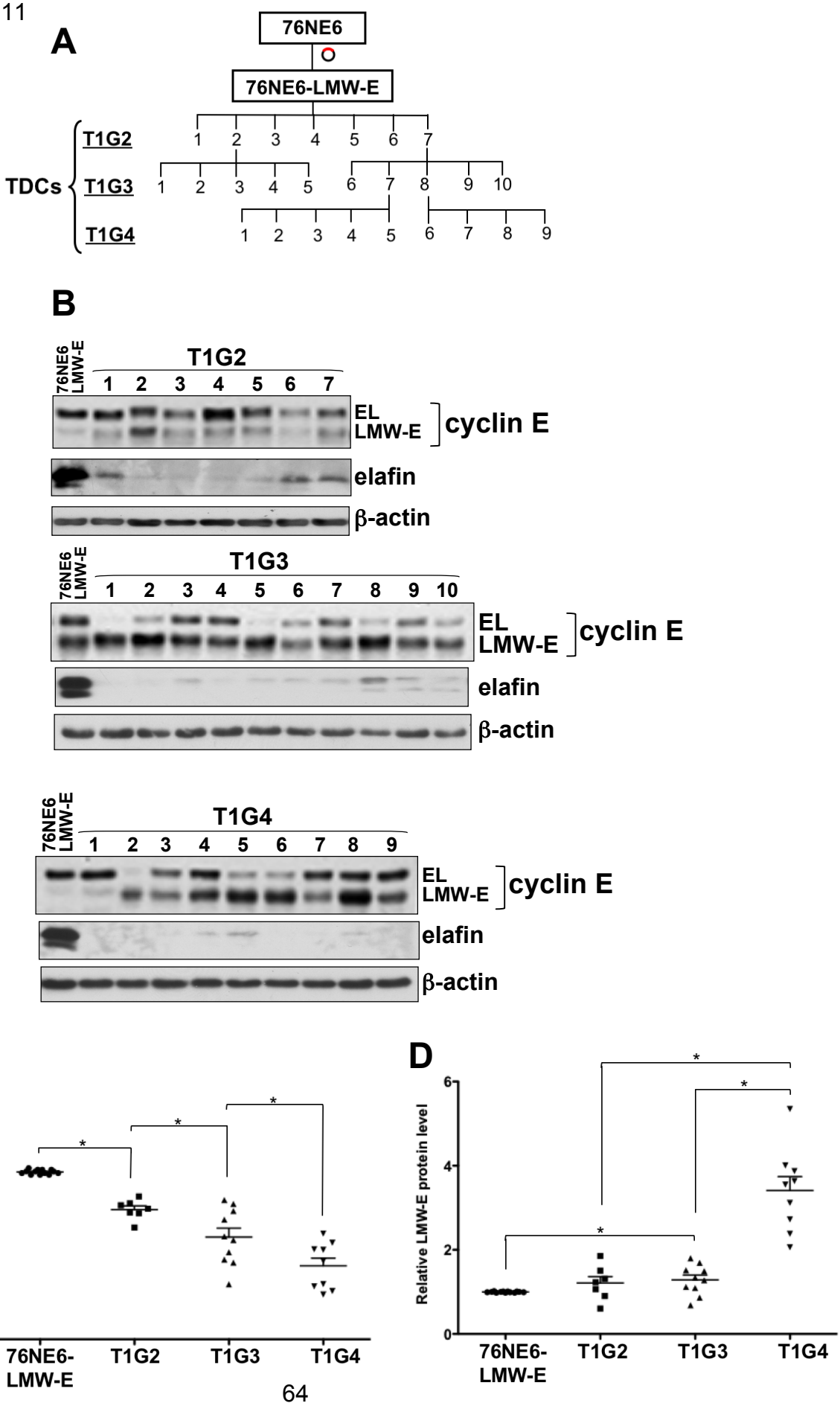
A
76NE6
76NE6-LMW-E
TDCs
T1G2
T1G3
T1G4
B
76NE6 LMW-E
T1G2
T1G3
T1G4
EL
LMW-E
cyclin E
elafin
β-actin
C
Relative EL protein level
76NE6-LMW-E
T1G2
T1G3
T1G4
D
Relative LMW-E protein level
76NE6-LMW-E
T1G2
T1G3
T1G4

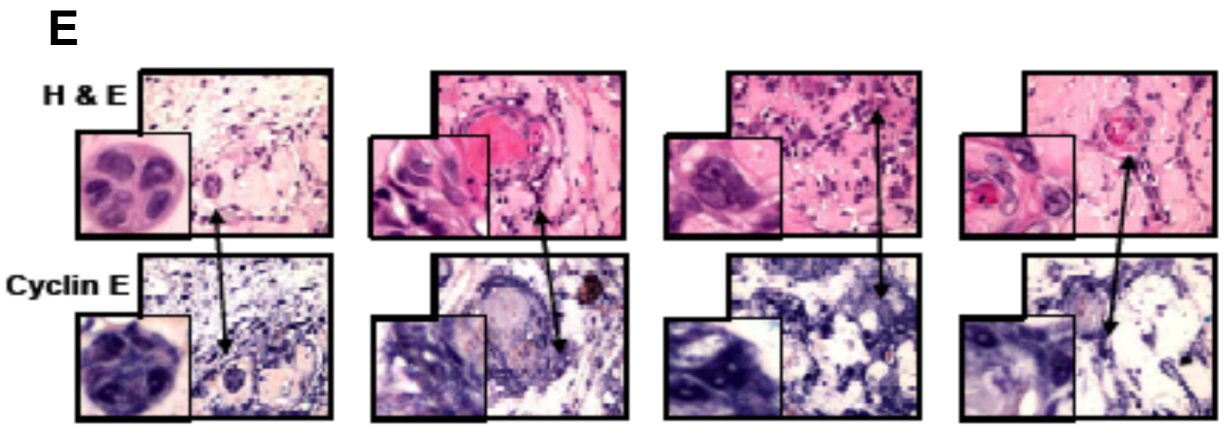

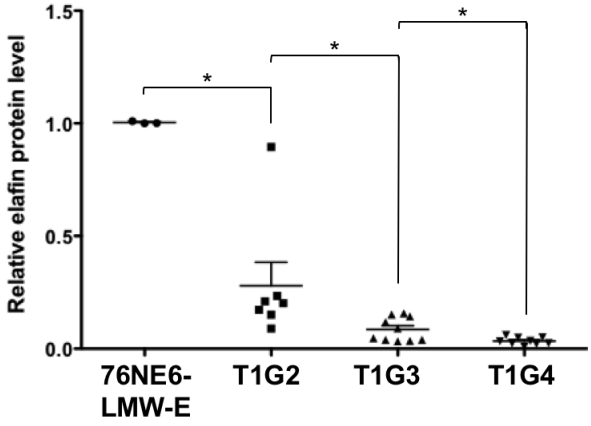

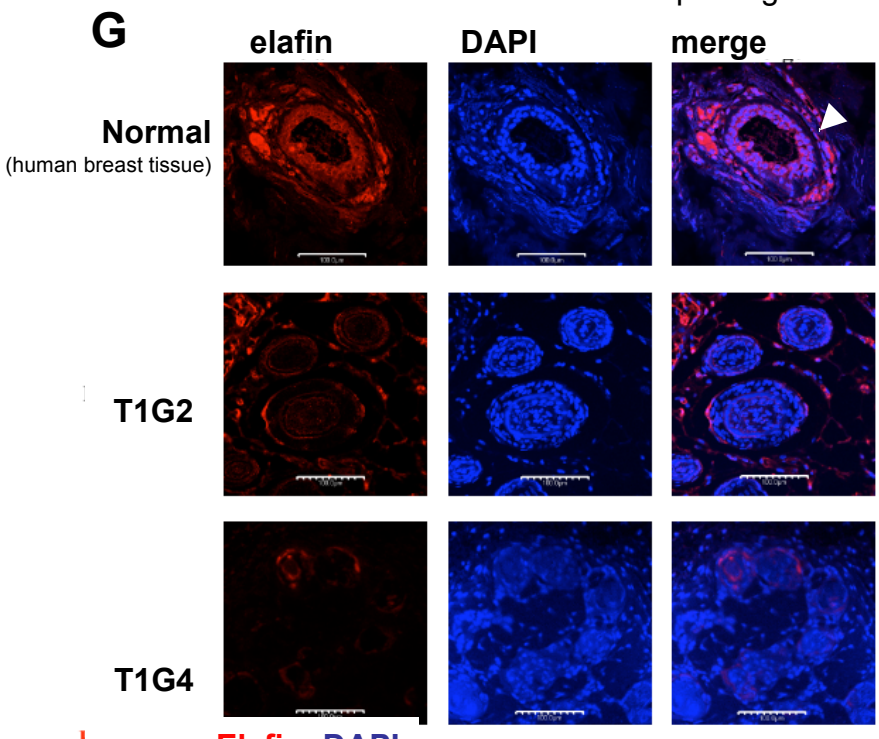

Figure 11: ***In vivo*** **passaging selects for increasing LMW-E and decreasing elafin expression.** (A) Schematic of the generation of *in vivo* passaged clones with 3 successive injections (T1G2-G4). (B) Tumors were removed from the fat pad of 76NE6-LMW-E mice, minced, and cultured on monolayer plates. Lysates were extracted and subjected to Western blot analysis with antibodies against cyclin E, elafin and β-actin. EL (C), LMW-E(D), and elafin (F) protein levels were quantified by densitometry and compared between different generations of *in vivo* passaged cells (Student *t* test, *p<0.05). (E) Paraffin-embedded slides of the 4 representative tumors were stained with hematoxylin and eosin (top panel) and cyclin E antibody (bottom panel). (G) Parafin-embedded tumor sections from normal human breast tissue, T1G2, and T1G4 tumors were subjected to immunofluorescent staining with elafin antibody and nuclei were counterstained with DAPI. Scale bar = 100um.

to the 76NE6-LMW-E cells (Figure 11B). Furthermore, quantification of the cyclin E protein levels by densitometric analysis suggested that *in vivo* passaging resulted in the reduction of the full-length (EL) cyclin E level (Figure 11C) while the LMW-E isoform level was increasing with each generation of passaging (Figure 11D). Analysis of the tumor tissues by immunohistochemistry staining revealed strong cyclin E expression (Figure 11E). Pathological analysis was performed by Dr. Caroline Van Pelt and the results suggested that the tumors formed by the 76NE6-LMW-E were characterized as adenosquamous carcinoma, adenocarcinoma with pillar differentiation, and squamous cell carcinoma. The morphology of the tumors also appear less organized, diffuse and lack obvious glandular structures.

In contrast to cyclin E, elafin is thought to play anti-tumor promoting role since elafin prevents the cleavage of cyclin E by inhibiting elastase and its expression is downregulated in most breast cancer cell lines (210). We speculate that since the levels of LMW-E is augmented with in vivo passaging, this phenomenon could be due to loss of elafin expression during growth selection in the mouse fat pad. Most of the *in vivo* passaged clones demonstrated near complete loss of elafin expression while the 76NE6-LMW-E parental cells express very high elafin (Figure 11B). Densitometric analysis also showed that the expression level of elafin (an endogenous inhibitor of serine protease (210) diminished with increasing passaging *in vivo* indicated that cyclin E was subjected to elevated proteolytic processing in the mouse microenvironment (Figure 11F). In addition, immunofluorescence staining was performed using paraffin section of normal human mammary tissue and the xenograft tumors from the T1G2 and T1G4 generations to examine elafin expression pattern in these tissues. The normal human breast tissues contain numerous acini with a clear hollow lumen and contain 1 to 2 layers of luminal cells (Figure 11G, top panel white arrow). These luminal cells and the cells in the interstitial region express relatively high elafin. In contrast, the T1G2 tumor contains acini with filled lumen with noticeably reduced elafin expression, especially in the cells that make up the acinar structures. More convincingly, the T1G4 tumor shows even more disorganized acinar structures that are less defined and elafin expression is almost completely lost. These observations

suggest that with *in vivo* passaging, the LMW-E-expressing cells lose control of the regulation of acinar morphogenesis, and elafin downregulation could be either the cause or effect of this deregulation. These findings suggest that not only LMW-E is tumorigenic, but also the fact that LMW-E expression was enhanced in most of the TDCs implies that perhaps LMW-E expression is advantageous and selects for growth and survival of these cells in the mice.

2.3j. The tumorigenicity of LMW-E requires CDK2-associated kinase activity

To eliminate potential false positive and effects from clonal variation, we generated a more stringent model system in the 76NE6 cell line in which the expression of FLAG-tagged vector, EL, and LMW-E can be induced with varying doxycycline concentrations (Figure 12A). At the G1-S phase boundary, cyclin E binds to CDK2 to form an active complex that phosphorylates multiple proteins to induce S-phase entry. Immunoprecipitation using FLAG antibody followed by incubation with ^{32}P-γ-ATP and histone H1 confirms that inducible EL and LMW-E have functional cyclin E-associated kinase activity (Figure 12A). The inducible 76NE6 cells expressing V, EL, and LMW-E and were injected subcutaneously into the mammary fat pad of nude mice and cyclin E expression was induced by doxycycline administration in drinking water 24 hours after the injection. Induction of LMW-E expression with 500 μg/ml doxycycline led to significantly more tumor formation at 95% for LMW-E and 90% for compared to uninduced cells at 11% as assessed by the Fisher's Exact test ($p<0.0001$) (Table 7). Similar to our previous observation, induction of EL expression with doxycycline led to tumor formation at 17% compared to 11% uninduced cells.

Given that cyclin E requires interaction with CDK2 to exert its kinase activity, we next aimed to investigate whether the oncogenicity of LMW-E requires CDK2-associated kinase activity. Previous study reported that the R130 site on the cyclin E protein is important for mediating the interaction between cyclin E and CDK2 (135). As a result, the point mutation R130A was introduced into the different isoforms of cyclin E. Results shown in Figure 12A confirm that the cyclin E/CDK2 kinase activity of these cyclin E mutants is abolished by immunoprecipitating cyclin

Figure 12

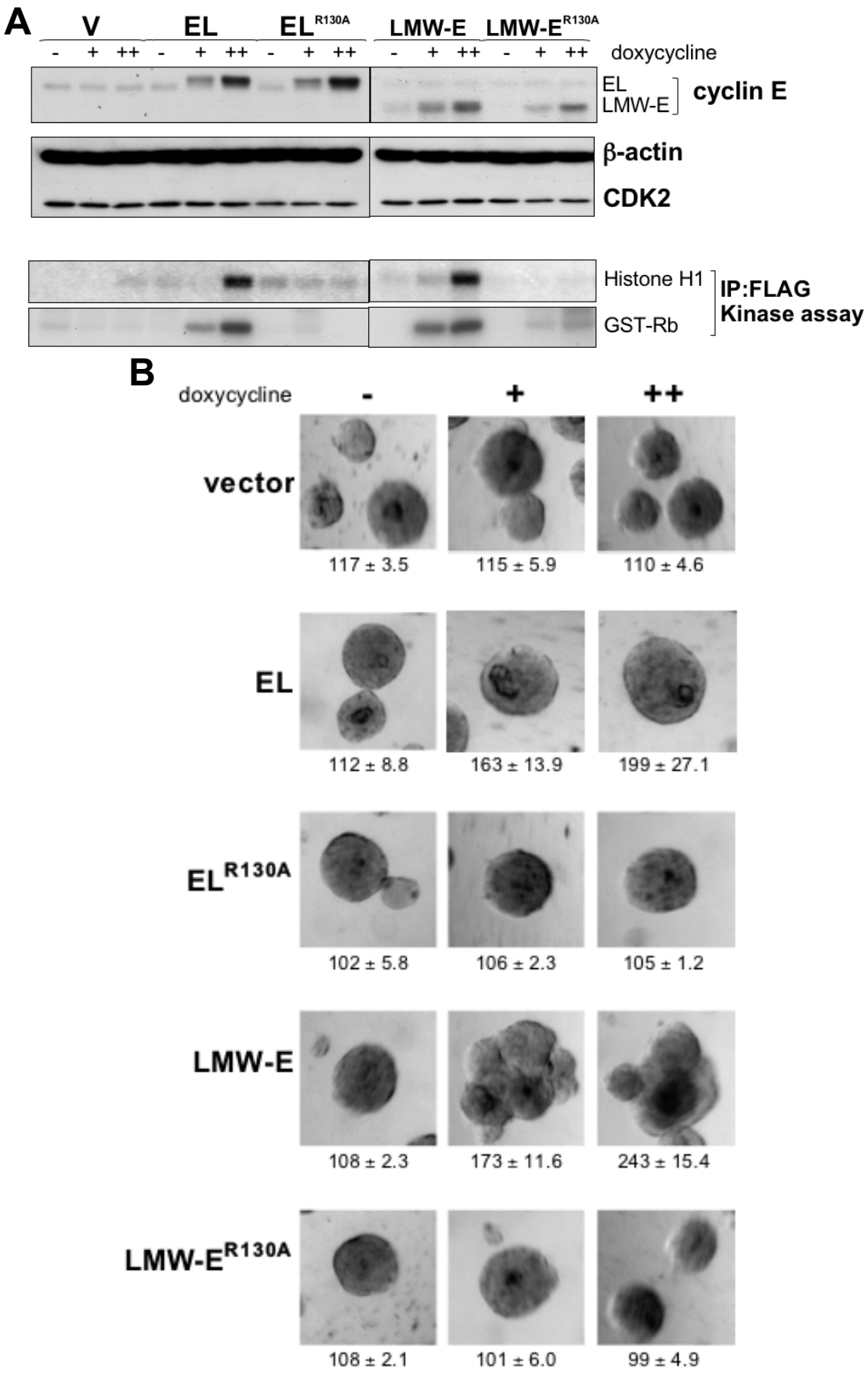
A
V
EL
EL R130A
LMW-E
LMW-E R130A
- + ++ - + ++ - + ++ - + ++ - + ++
doxycycline
EL
LMW-E
cyclin E
β-actin
CDK2
Histone H1
GST-Rb
IP:FLAG
Kinase assay
B
doxycycline
-
+
++
vector
117 ± 3.5
115 ± 5.9
110 ± 4.6
EL
112 ± 8.8
163 ± 13.9
199 ± 27.1
EL R130A
102 ± 5.8
106 ± 2.3
105 ± 1.2
LMW-E
108 ± 2.3
173 ± 11.6
243 ± 15.4
LMW-E R130A
108 ± 2.1
101 ± 6.0
99 ± 4.9

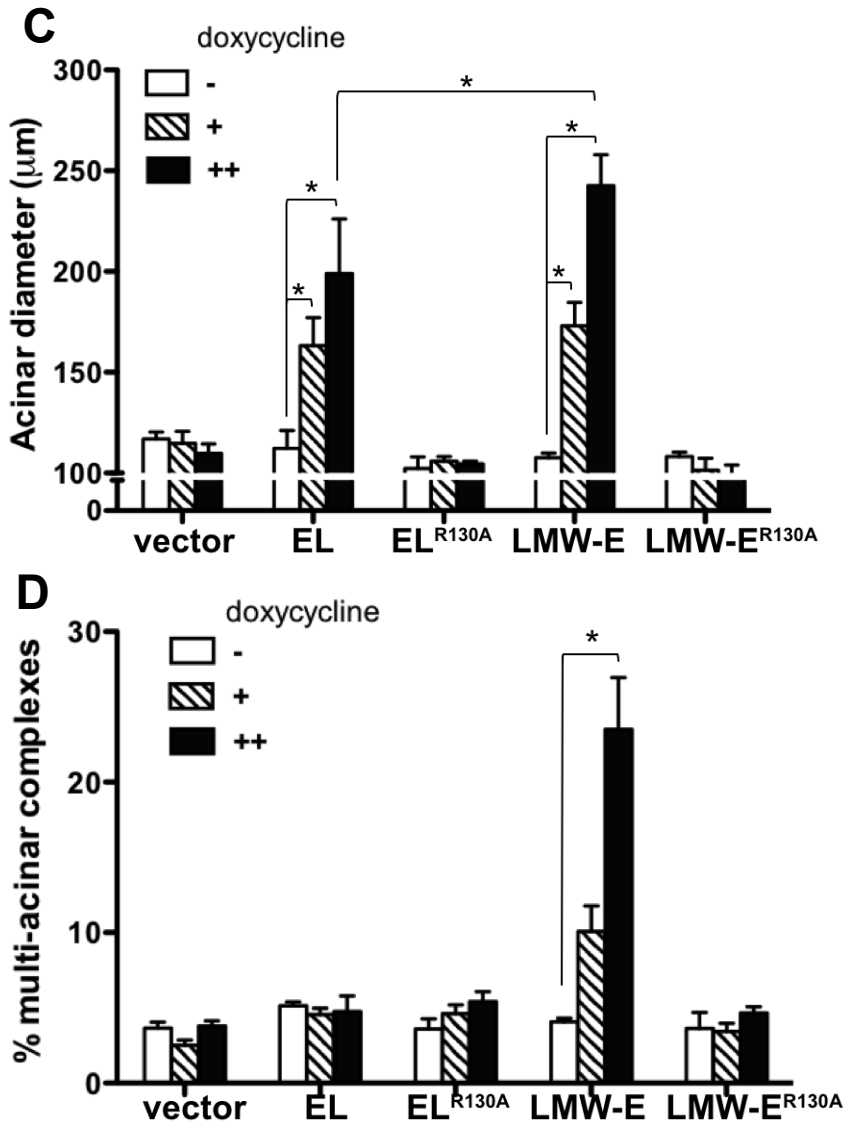

Figure 12: LMW-E deregulation of acinar morphogenesis is dependent on CDK2-associated kinase activity. (A) 76NE6-TetR cells were cultured with or without doxycycline induction, and the lysates were extracted and subjected to Western blot analysis with antibodies against cyclin E and β-actin. *In vitro* kinase assay was performed by immunoprecipitation with FLAG antibody and histone H1 and GST-Rb were added as substrates. Doxycycline was administered to achieve approximately 1x and 2x cyclin E protein levels. (The doxycycline concentrations for the 76NE6-TetR-V and wild-type EL and LMW-E cells were 0, 0.2, and 0.4 ng/ml, and the doxycycline concentrations for the $EL^{R130A}$and LMW-E^{R130A}cells were 0, 1, and 2 ng/ml.) (B) 76NE6-TetR cells were cultured on Matrigel for 15 days with or without doxycycline induction. Bright-field images were taken at day 15. Values underneath each figure represent mean diameter (μm) ± SEM. (C) The diameters of at least 100 acini from 3 different experiments were measured. Error bars = SEM (Wilcoxon rank-sum test, *$p<0.05$). (D) Multi-acinar complexes were counted. Error bars = SEM (Wilcoxon rank-sum test, *$p<0.05$). Multi-acinar complexes were defined as complexes with more than 2 acini growing on top of each other. Logistic regression models were used to compare the rate of formation of multi-acinar complexes between/among groups (*$p<0.05$).

Table 7: The tumorigenicity of LMW-E requires CDK2-associated kinase activity

Dox (μg/ml)	0	500
	Tumors/ Injections (%)	**Tumors/ Injections (%)**
vector	1/18 (6)	2/18 (11)
EL	2/18 (11)	3/18 (17)
LMW-E	2/18 (11)	19/20 (95)
EL^{R130A}	0/8 (0)	1/12 (8)
$LMW\text{-}E^{R130A}$	0/8 (0)	2/12 (17)

Athymic mice were injected with $1x10^7$ 76NE6-TetR cells with inducible expression for empty vector, EL, LMW-E, EL^{R130A}, and $LMW\text{-}E^{R130A}$. Doxycycline was added to to drinking water containing 1% sucrose 24 hours after injection and replaced twice weekly. The diameter of the tumors were measured and recorded weekly. Tumor incidence rate was estimated with exact 95% confidence intervals and Fisher's exact tests were used to compare tumor incidence rate between/among groups (*$p<0.0001$).

E FLAG-tagged proteins and measure the extent of histone H1 phosphorylation (Figure 12A). Injection of the 76NE6 cells with inducible expression for EL^{R130A} and LMW-E^{R130A} and into the mammary fat pad of nude mice revealed that LMW-E does require CDK2-associated kinase activity to induce tumor formation (Table 7). In other words, the tumor incidence caused by EL^{R130A} and LMW-E^{R130A} and compared with vector control is not statistically significant. These data suggest that LMW-E demonstrates stronger tumorigenic potential than EL, and this ability to induce tumor formation requires the kinase activity exerted from interaction with CDK2.

2.3k. LMW-E deregulation of acinar morphogenesis is dependent on CDK2-associated kinase activity

As CDK2-associated kinase activity is required for mammary tumor development, we speculate that this same requirement is critical for LMW-E-mediated acinar deregulation. Bright field images of 76NE6 cells with inducible expression for different cyclin E constructs during acinar morphogenesis confirm previous data that induction of EL led to generation of larger acini with the structures remaining spherical (Figure 12B). In contrast, induction of the LMW-E isoforms generated acini with very irregular shapes and multi-acinar aggregations. The diameter of at least 100 acini were measured and the quantification revealed that cyclin E expression lead to large acini formation in a dose dependent manner (Figure 12C). On the contrary, we observed that induction of EL^{R130A} and LMW-E^{R130A} did not result in enlargement of acinar size (Figure 12C). In addition, LMW-E expression tend to form multiacinar complexes in which at least 2 acini are overlapping or fused into one aggregate (Figure 12B). Quantification revealed that this phenotype was only observed in wild type LMW-E-expressing cells but not in the cells expressing EL or the R130A mutant cyclin E variants (Figure 12D). These results suggest that the LMW-E/CDK2-associated kinase activity is responsible for driving mammary tumorigenesis by generating deregulated acinar structures in the mammary gland. Previous clinical examination of breast cancer patient samples revealed that high LMW-E protein levels significantly correlate with poor patient

survival, and the data presented here further confirms that the level of LMW-E expression positively correlates with aberrant acinar development.

2.3I. LMW-E generates enlarged acini by reducing apoptosis and enhancing proliferation

To determine the mechanism of LMW-E-mediated tumorigenesis, the 9 TDC clones were also subjected to acinar morphogenesis. Similar to our observation with the stable and inducible model systems, all TDCs form large and non-spherical acini that are approximately 28% larger than the 76NE6 parental acini ($p < 0.05$) (Figure 13A and B). The acinar morphogenesis process includes several distinctive stages. During the first 8 days of culture on Matrigel, the cells undergo high rates of proliferation, which continues to occur while the cells in the interior of the structure undergo apoptosis due to anoikis or detachment from the basement membrane to generate a hollow lumen (239). The luminal cell layer is highly polarized which is important for milk secretion into the luminal space. Cell proliferation subsides towards the late stage of morphogenesis from day 10 to day 15 to form a mature acinus that is approximately 120 um in diameter. As expected, the levels of cyclin E protein in the parental 76NE6 cells is lower in 3D culture compared to 2D culture since these cells have arrested proliferation by downregulating the G1-S phase cyclin (Figure 5A). However, the 76NE6-LMW-E and TDCs express dramatically high cyclin E protein levels during acinar morphogenesis compared to the parental, vector and 76NE6-EL cells (Figure 13C). *In vitro* kinase assay demonstrates that the TDCs exhibit high cyclin E/CDK2 kinase activity indicating that these cells are not arresting cell cycle progression but instead are actively traversing through the G1-S phase transition (Figure 13C). Perhaps LMW-E expression generates an aberrant positive feedback loop during acinar morphogenesis that leads to further upregulation of cyclin E expression in the acini.

BIM is a Bcl2 pro-apoptotic protein that is upregulated during acinar morphogenesis to induce cell death in the matrix-detached cells to create a hollow lumen (243). Interestingly, the acini expressing cyclin E downregulate BIM expression suggesting that there is reduced apoptosis in these acini (Figure 13C).

Figure 13

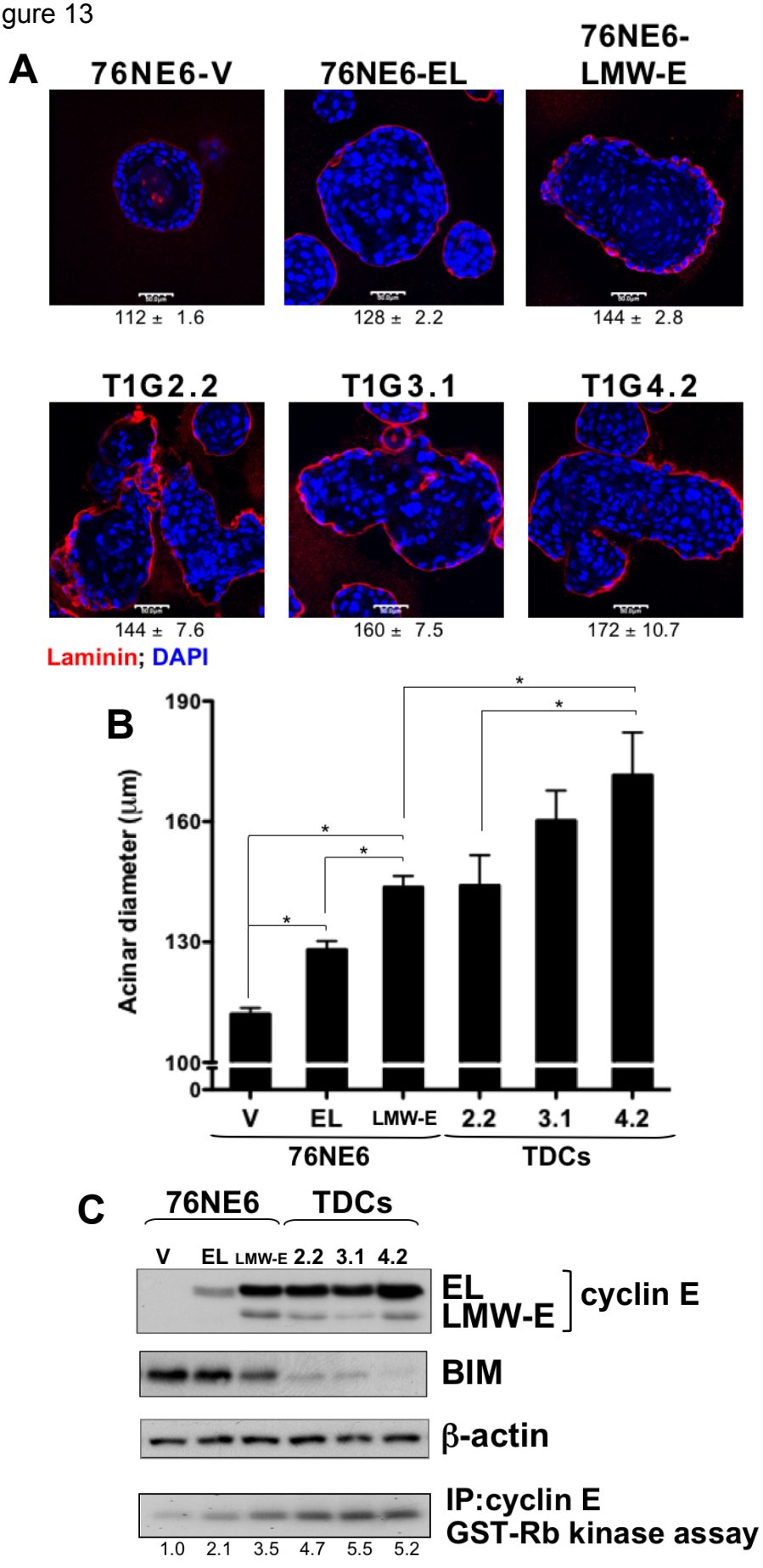
A
76NE6-V
76NE6-EL
76NE6-LMW-E
112 ± 1.6
128 ± 2.2
144 ± 2.8
T1G2.2
T1G3.1
T1G4.2
144 ± 7.6
160 ± 7.5
172 ± 10.7
Laminin; DAPI
B
Acinar diameter (μm)
190
160
130
100
0
V
EL
LMW-E
2.2
3.1
4.2
76NE6
TDCs
C
76NE6
TDCs
V EL LMW-E 2.2 3.1 4.2
EL
LMW-E
cyclin E
BIM
β-actin
IP:cyclin E
GST-Rb kinase assay
1.0 2.1 3.5 4.7 5.5 5.2

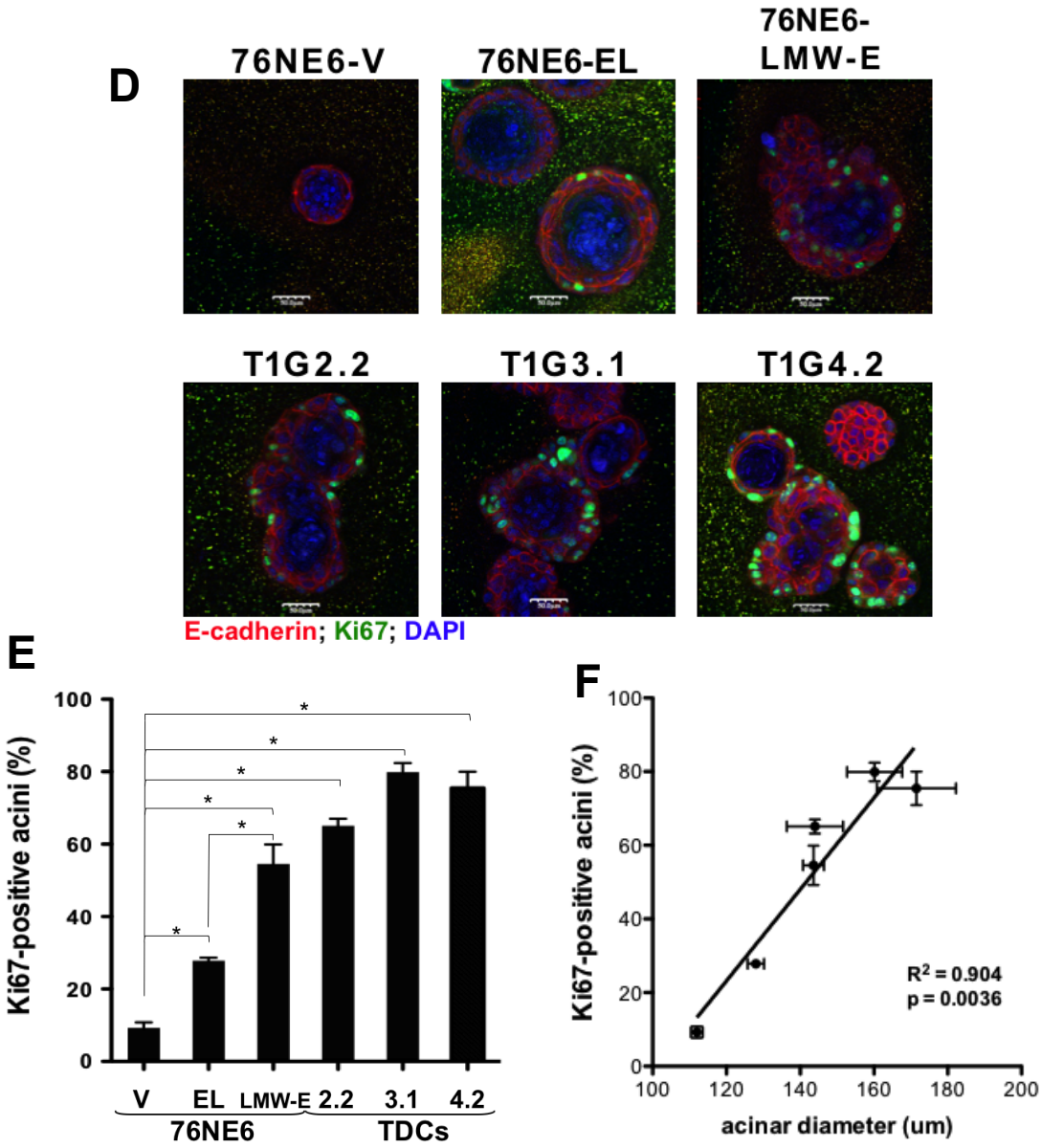

Figure 13: LMW-E generates enlarged acini by reducing apoptosis and enhancing proliferation. (A&B) 76NE6 cells stably transfected with vector, EL, and LMW-E and tumor-derived cells (TDCs) were seeded at a density of 70 cells/mm^2 on 1-mm-thick Matrigel. After 15 days in 3D culture, cells were fixed and immunostained with GM-130 and α6-integrin antibodies. Nuclei were counterstained with DAPI. Scale bar = 50 μm. The diameters of the acini were measured and averaged from 3 independent experiments. Values underneath each figure represents mean (μm) ± SEM. Error bars = SEM (Student *t* test, *p<0.05). (C) Lysates from these cells were isolated at day 15 and subjected to Western blot analysis with the indicated antibodies. *In vitro* kinase assay was performed by immunoprecipitation of lysates from 3D culture using polyclonal cyclin E antibody and incubation with (γP32)ATP and GST-Rb. (D&E) Cells cultured on Matrigel for 15 days were fixed and immunostained with E-cadherin and Ki67 antibodies. Nuclei were counterstained with DAPI. Scale bar = 50 μm. The number of Ki67-positive cells per acinus was counted and averaged from 3 independent experiments. Error bars = SEM (Student *t* test, *p<0.05). (F) Linear regression of the correlation between acinar diameter and percentage of Ki67-positive cells.

To determine whether LMW-E expression was sufficient to prevent growth arrest of cells in mature acini, we fixed acini at 15 days and stained them for Ki67. While Ki67 expression was not detectable in the 76NE6-vector acini, LMW-E-expressing acini displayed high Ki67 staining, particularly in cells that were in contact with the basement membrane (Figure 13D & E). Furthermore, we determined a strong positive correlation between the acinar diameter and the percentage of Ki67-positive acini, indicating that the formation of large acini may be due to increased proliferation (Figure 13F). Taken together, we demonstrate here that LMW-E causes generation of large and misshapen acini by enhancing cell proliferation and inhibiting apoptosis. These phenotypes share similarity with early-staged tumors and those with HER2 overexpression (232). Therefore, we believe that this deregulation of the mammary acinar morphogenesis by LMW-E occurs *in vivo* thus explaining the tumorigenicity of LMW-E and its advantageous selection with increasing *in vivo* passaging.

2.3m. Roscovitine rescues LMW-E-induced aberrant acinar development

Given that LMW-E-mediated tumorigenesis and aberrant acinar morphologies depend on intact CDK2-associated kinase activity, we next aim to determine whether inhibition of this kinase activity can reverse these phenotypes. Roscovitine was the pharmacological agent of choice since it has demonstrated high CDK1 and 2 specificity and potent anti-tumor effectiveness. The 76NE6 and T1G2.2 cells were seeded on Matrigel culture and treated with roscovitine 24 hours after seeding every 4 days until day 15 in culture. The results showed that the treatment of the T1G2.2 cells during acinar morphogenesis with roscovitine led to formation of smaller and spherical acini while showing no effects on the 76NE6 parental cells (Figure 14A & B). These data suggest that roscovitine is effective in reversing the aberrant acinar phenotypes caused by LMW-E expression and is non-toxic to normal cells.

Further treatment of the TDCs with 3 different roscovitine concentrations demonstrated significant reduction of acinar diameter (Figure 14C). Similar to the 76NE6 parental cells, the 76NE6-vector and EL acini show no significant effects in

Figure 14

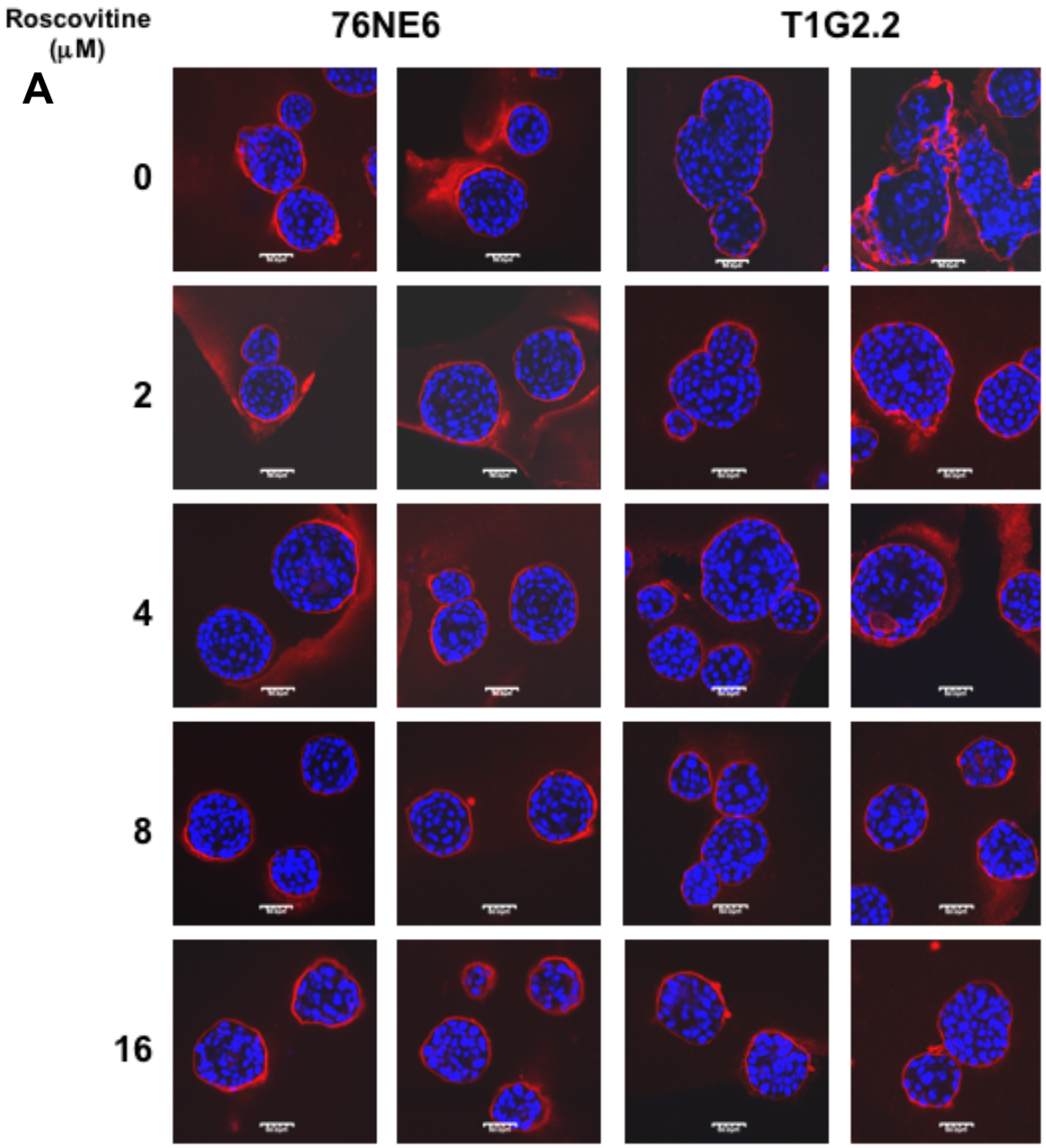
Roscovitine (μM)
76NE6
T1G2.2
A
0
2
4
8
16
Laminin V; DAPI

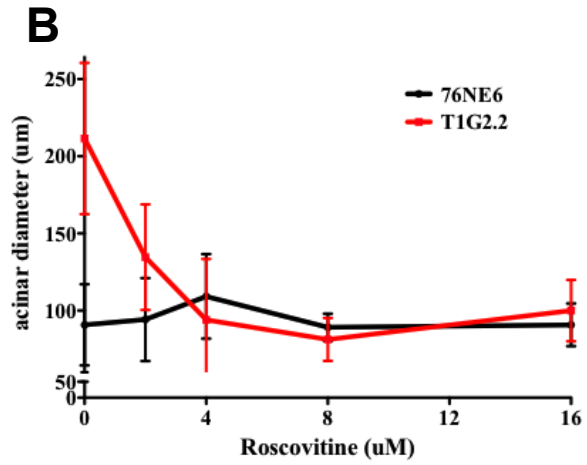
B
acinar diameter (um)
250
200
150
100
50
0
0
4
8
12
16
Roscovitine (uM)
76NE6
T1G2.2

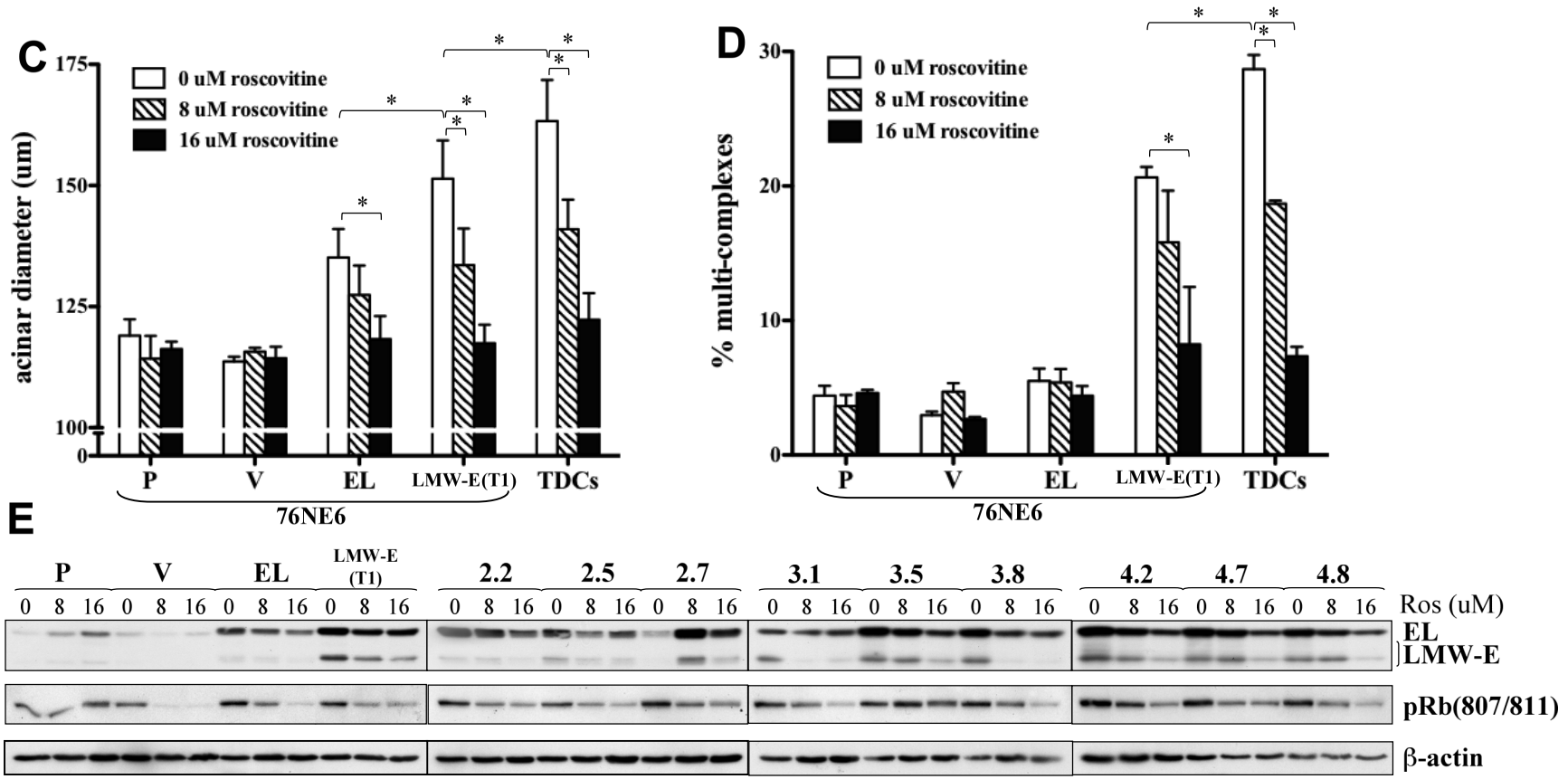

Figure 14: Roscovitine rescues LMW-E-induced aberrant acinar development. A) 76NE6 and T1G2.2 cells were cultured on Matrigel for 15 days and treated with roscovitine from 0 to 16 uM on days 1, 5, 9, and 13. Cells were fixed and immunostained with laminin V antibody and nuclei were counter-stained with DAPI. Scale bar = 50um. (B) The diameter of at least 100 acini from 3 different experiments was measured. Error bars = SEM. (C) 76NE6 parental (P), vector (V), EL, LMW-E and TDC cells were cultured on Matrigel for 15 days and treated with roscovitine at 0, 8 and 16 uM on days 1, 5, 9, and 13. The diameter of at least 100 acini from 3 different experiments was measured. TDCs represent average of all 9 tumor clones. Error bars = SEM (Student's *t* test, *p<0.05). (D) The number of multi-complexes were counted and averaged from 3 experiments. Error bars = SEM (Student's *t* test, *p<0.05). (E) Lysates from 3D culture were extracted and subjected to Western blot analysis with antibodies against cyclin E, pRb (S807/811) and β-actin.

response to roscovitine treatment. We also observed that roscovitine treatment significantly reduces the multi-acinar complex formation by the LMW-E-expressing cells ($p < 0.05$) (Figure 14D). Perhaps roscovitine induces a G1 arrest since cyclin E and pRb protein levels are downregulated in the roscovitine-treated acini (Figure 14E). We speculate that inhibition of LMW-E/CDK2 complex by roscovitine allows the acini to arrest proliferation and thereby suppressing the aberrant positive loop that drives cyclin E protein overexpression. Growth arrest towards the end of morphogenesis (days 12-15) also allows cells to properly organize into correct and spherical acinar structures. Thus, our data suggest that roscovitine is an effective pharmacological agent that can reverse the phenotypes mediated by LMW-E/CDK2 complex and sheds light into our effort to develop therapeutic strategy for breast cancer patients with high LMW-E expression levels.

2.3n. High LMW-E expression is associated with activated b-Raf-ERK1/2-mTOR pathway *in vitro* and in human tumor tissues

While it is widely accepted that the 3D culture system serves as a more physiologically relevant model for the investigation of cell behavior compared to 2D plastic surface (223, 228), no direct comparison between cells cultured on this 3D model and human samples has been performed. To provide such a comparison, we analyzed the protein expression of the TDCs grown on monolayer and Matrigel cultures as well as 276 breast cancer patient tissues by performing Reverse Phase Protein Array (RPPA) analysis (234). The RPPA method is a proteomic protein expression analysis that has been shown to be highly reproducible in analyzing the expression patterns of proteins involved in cell signaling (16, 234, 244). Hierarchical clustering was performed using Euclidean distance and Ward's minimum variance for agglomeration (Figure 15A). The resulting heat map demonstrated that the cells from 2D and 3D cultures had strikingly different protein expression patterns and that the protein expression pattern of the cells from 3D cultures (mammary epithelial cells cultured in Matrigel) more closely resembled that of patient tissues than did the protein expression pattern of cells grown on monolayer. These results were expected since it is has been established that the 3D culture system is a more

Figure 15

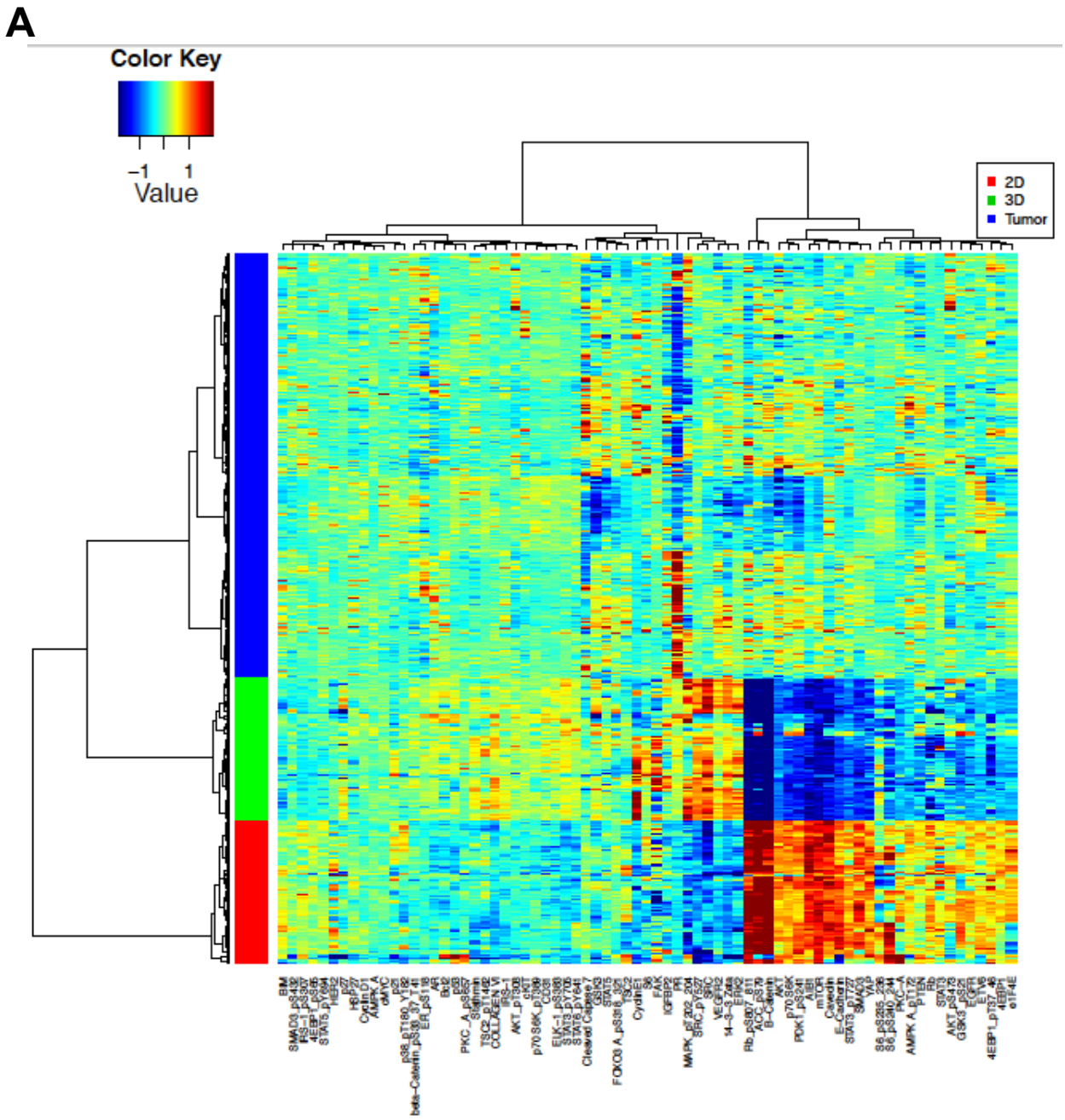

Figure 15

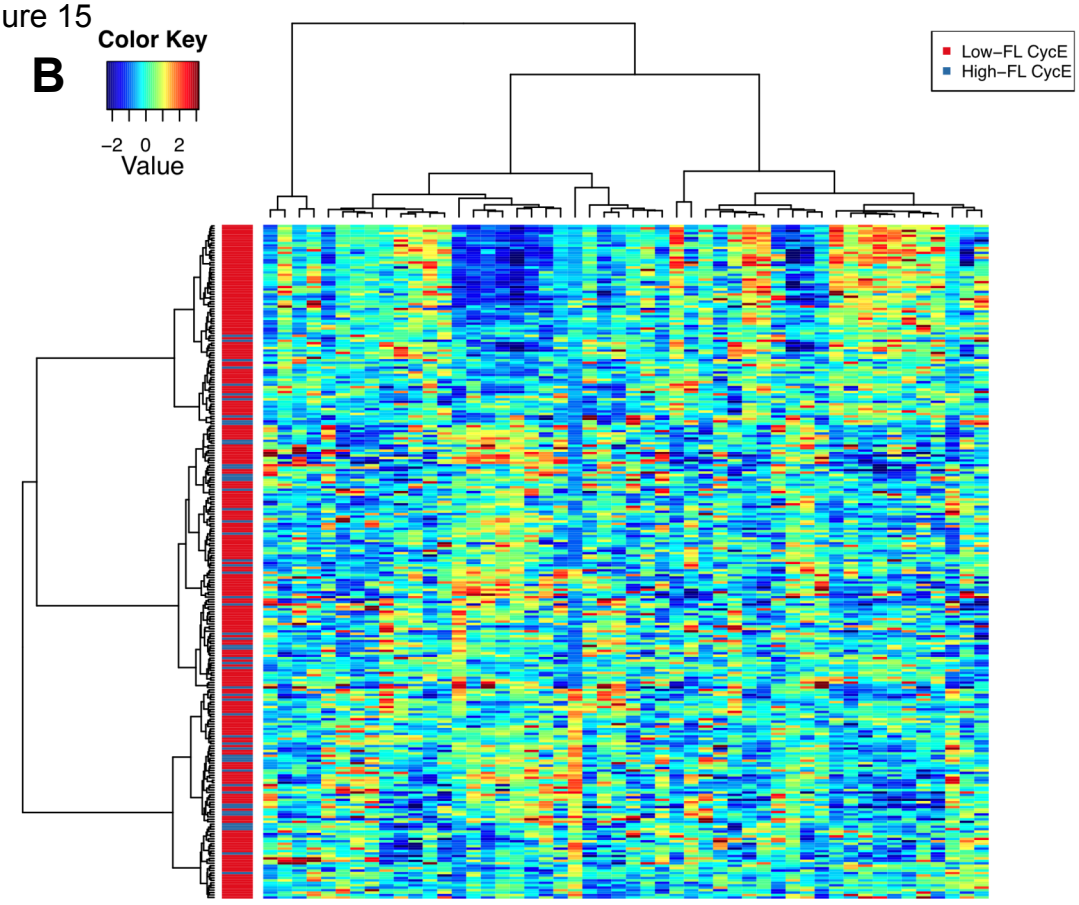
B
Color Key
−2 0 2
Value
Low−FL CycE
High−FL CycE

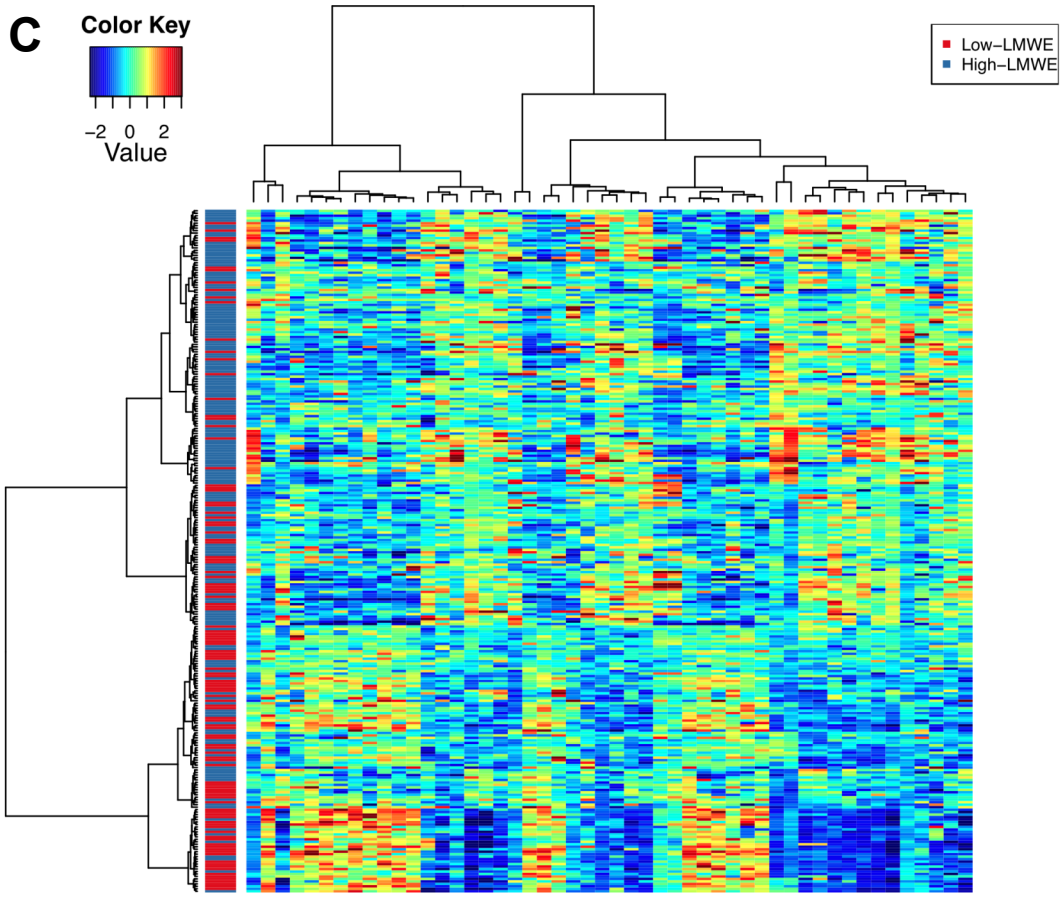
C
Color Key
−2 0 2
Value
Low−LMWE
High−LMWE

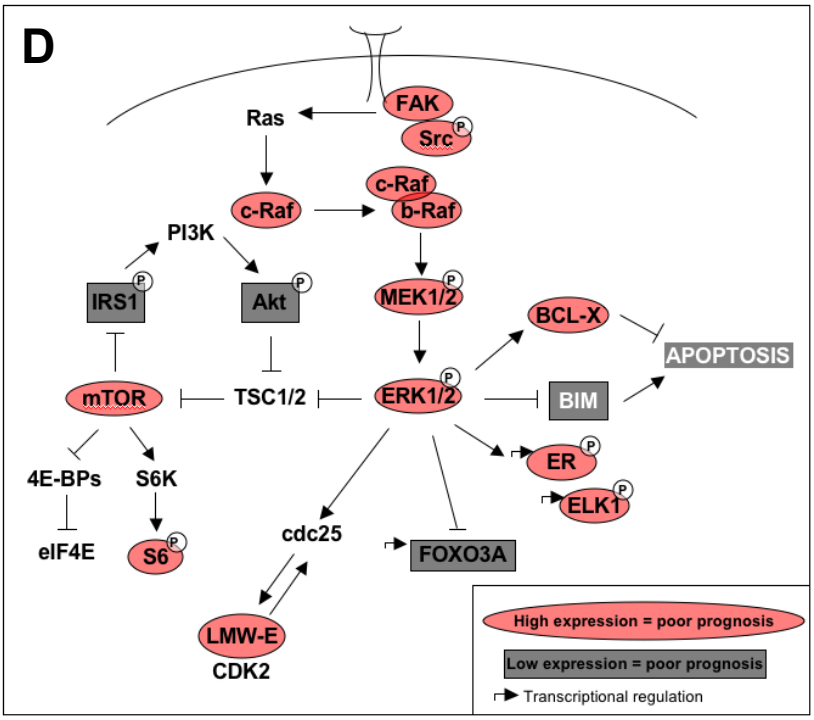

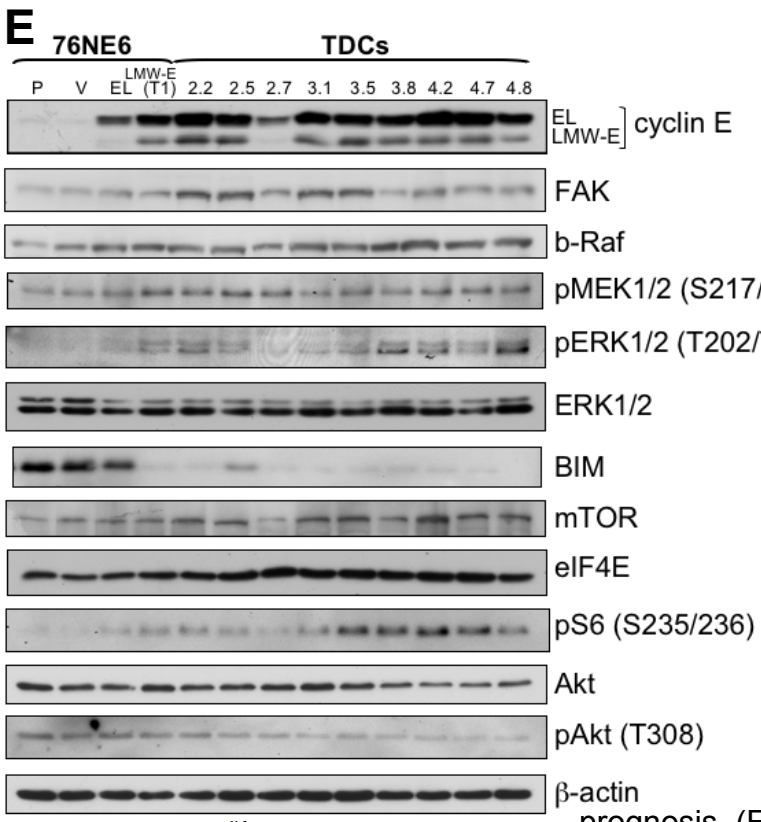

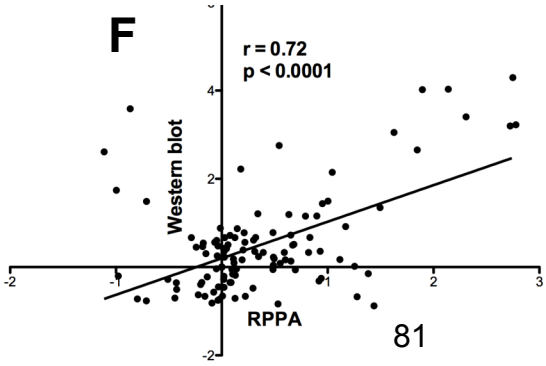

Figure 15: High LMW-E expression is associated with activated b-Raf-ERK1/2-mTOR pathway *in vitro* and in patient tissues. (A) Hierarchal cluster analysis of protein expression in 76NE6, 76NE6-LMW-E and all of the TDC clones grown on 2D (red) and 3D (green) cultures and 276 breast cancer patient samples (blue). Unsupervised clustering of the top 50 proteins separated by low versus high EL (B) and LMW-E (C) expression. (Red: patients with low cyclin E expression; blue: patients with high cyclin E expression.) (D) Proteins whose expression was associated with high LMW-E levels. Red indicates that high LMW-E along with high protein expression was associated with poor prognosis; grey indicates that high LMW-E along with low protein expression was associated with poor prognosis. (E) The lysates from 3D culture were subjected to Western blot analysis to validate the RPPA data. The cell lines are 76NE6-parental (P) and with stable expression of vector (V), EL, and LMW-E and the tumor-derived cells (TDCs). (F) Linear regression analysis between the RPPA data and the densitometry values from Western blot analysis of the proteins from (E).

physiologically relevant model than cell culture on a 2D plastic surface for the investigation of cell behavior (223, 228). Furthermore, in an unsupervised analysis of the patient RPPA data, we observed separate clustering between the low and high LMW-E-expressing breast tumors but not between low and high full-length cyclin E (Figure 15B & C).

We next identified the proteins whose expression was significantly associated with LMW-E levels as well as patient survival in the tumor database. Our analysis revealed that in the breast cancer patient samples with high LMW-E expression, the b-Raf-ERK1/2-mTOR pathway was also activated (Figure 15D). Furthermore, Western blot analysis of the lysates from the TDCs grown on Matrigel showed high concordance with the RPPA data and also validated the activation of this signaling axis *in vitro*: (Figure 15E & F). Additionally, breast cancer patient tumors with high LMW-E expression also expressed high levels of b-Raf, pMEK1/2 (S217), ERK2, mTOR, and eIF4E and a low level of pAkt (T308) while those with high EL expression only showed significant difference in the expression of b-Raf, mTOR, and eIF4E (Table 8). Collectively, these data suggested that in terms of proteomic expression patterns, breast cancer cells grown in 3D culture more closely resemble human tumors than do breast cancer cells grown in 2D culture and that 3D culture thereby facilitates the identification of signaling events that correlate with LMW-E levels.

2.3o. Combination drug treatment prevents induction of aberrant acinar development by LMW-E

Having established the importance of CDK2-associated kinase activity in aberrant acinar morphogenesis in 3D culture and given that the b-Raf-ERK1/2-mTOR signaling axis was deregulated in tumor cells and patient samples with high LMW-E expression, we hypothesized that combination treatment with roscovitine (a CDK inhibitor) plus either rapamycin (an mTOR inhibitor) or sorafenib (a pan kinase inhibitor that has activity against b-Raf) normalizes acinar morphology. Combination treatments of cells cultured in Matrigel using these agents resulted in a larger reduction of the levels of pS6 (S235/236), pERK1/2 (T202/Y204), and pRb

Table 8. Patient protein expression based on low and high LMW-E and EL levels by RPPA analysis

	Relative protein levels		
Proteins	**Low LMW-E**	**High LMW-E**	**P value***
ERK2			2.27E-07
Median	0.47	0.542	
Mean (range)	0.459 (0.134 - 1.02)	0.581 (0.134 - 1.88)	
pMEK1/2 (S217)			4.85E-06
Median	0.2	0.223	
Mean (range)	0.203 (0.111 - 0.348)	0.235 (0.112 - 0.806)	
b-Raf			2.05E-04
Median	0.159	0.209	
Mean (range)	0.198 (0.0549 - 0.756)	0.264 (0.069 - 1.505)	
mTOR			5.45E-04
Median	0.099	0.127	
Mean (range)	0.112 (0.043 - 0.297)	0.135 (0.0424 - 0.423)	
eIF4E			7.06E-02
Median	0.356	0.392	
Mean (range)	0.381 (0.143 - 0.777)	0.405 (0.093 - 0.795)	
pAkt (T308)			4.67E-02
Median	0.145	0.123	
Mean (range)	0.164 (0.071 - 0.841)	0.168 (0.068 - 1.362)	
	Low EL	**High EL**	
ERK2			0.2
Median	0.516	0.53	
Mean (range)	0.521 (0.134 - 1.344)	0.568 (0.284 - 1.88)	
pMEK1/2 (S217)			0.5
Median	0.212	0.216	
Mean (range)	0.222 (0.111 - 0.806)	0.22 (0.143 - 0.352)	
b-Raf			2.09E-05
Median	0.163	0.246	
Mean (range)	0.223 (0.055 - 1.505)	0.292 (0.089 - 0.752)	
mTOR			1.29E-02
Median	0.111	0.13	
Mean (range)	0.121 (0.042 - 0.423)	0.142 (0.047 - 0.297)	
eIF4E			5.65E-03
Median	0.362	0.416	
Mean (range)	0.384 (0.093 - 0.795)	0.44 (0.143 - 0.703)	
pAkt (T308)			0.9
Median	0.131	0.134	
Mean (range)	0.162 (0.071 - 1.227)	0.184 (0.068 - 1.362)	

* Wilcoxon ranksum test

(S807/811) than no treatment or treatment with single agents (Figure 16A). Moreover, the combination treatments upregulated the expression of the CDK inhibitors p21 and p27, consistent with a cell cycle arrest at the G1/S phase (data not shown). Examination of the acinar formation as a result of the combination drug treatments revealed that the TDCs displayed a significant reduction in acinar size and Ki67 levels compared to the untreated cells and cells treated with single agents ($p < 0.05$) (Figure 16B-D). More specifically, both combination drug treatment conditions led to a 2-fold reduction in both acinar size and the number of Ki67-positive acini compared to the single agent conditions (Figure 16C & D). In contrast, the 76NE6-vector and 76NE6-EL cells displayed no change in these phenotypes in response to the drug treatments, suggesting that the absence of LMW-E expression may protect these cells from the toxic effects of the drugs. Thus, roscovitine in combination with either rapamycin or sorafenib can prevent the development of the aberrant acinar phenotypes caused by LMW-E expression, confirming a role for LMW-E/CDK2 kinase activity in causing formation of large, multilobular acini and demonstrating a potential therapeutic approach to treat cancer patients with high LMW-E expression.

2.3p. Activated b-Raf-ERK1/2-mTOR signaling pathway and high LMW-E expression predict poor survival

In a large retrospective clinical study, we previously found that breast cancer patients whose tumors had high levels of LMW-E expression, as determined by Western blot analysis, have significantly worse DSS than patients whose tumors had low LMW-E expression (160). In the study reported herein, we used tissue samples from a portion of this patient cohort for RPPA analysis to investigate large-scale protein expression pattern. Similar to our previous observation, we found that patients with high LMW-E protein levels had significantly worse DSS than patients with low LMW-E expression ($p<0.0001$) (Figure 17A). More specifically, patients with high LMW-E and low full-length cyclin E expression demonstrated significantly worse DSS compared to patients with high LMW-E and also high full-length cyclin E ($p=0.004$). Bivariate analysis of LMW-E along with key nodes in the b-Raf-ERK1/2-

Figure 16

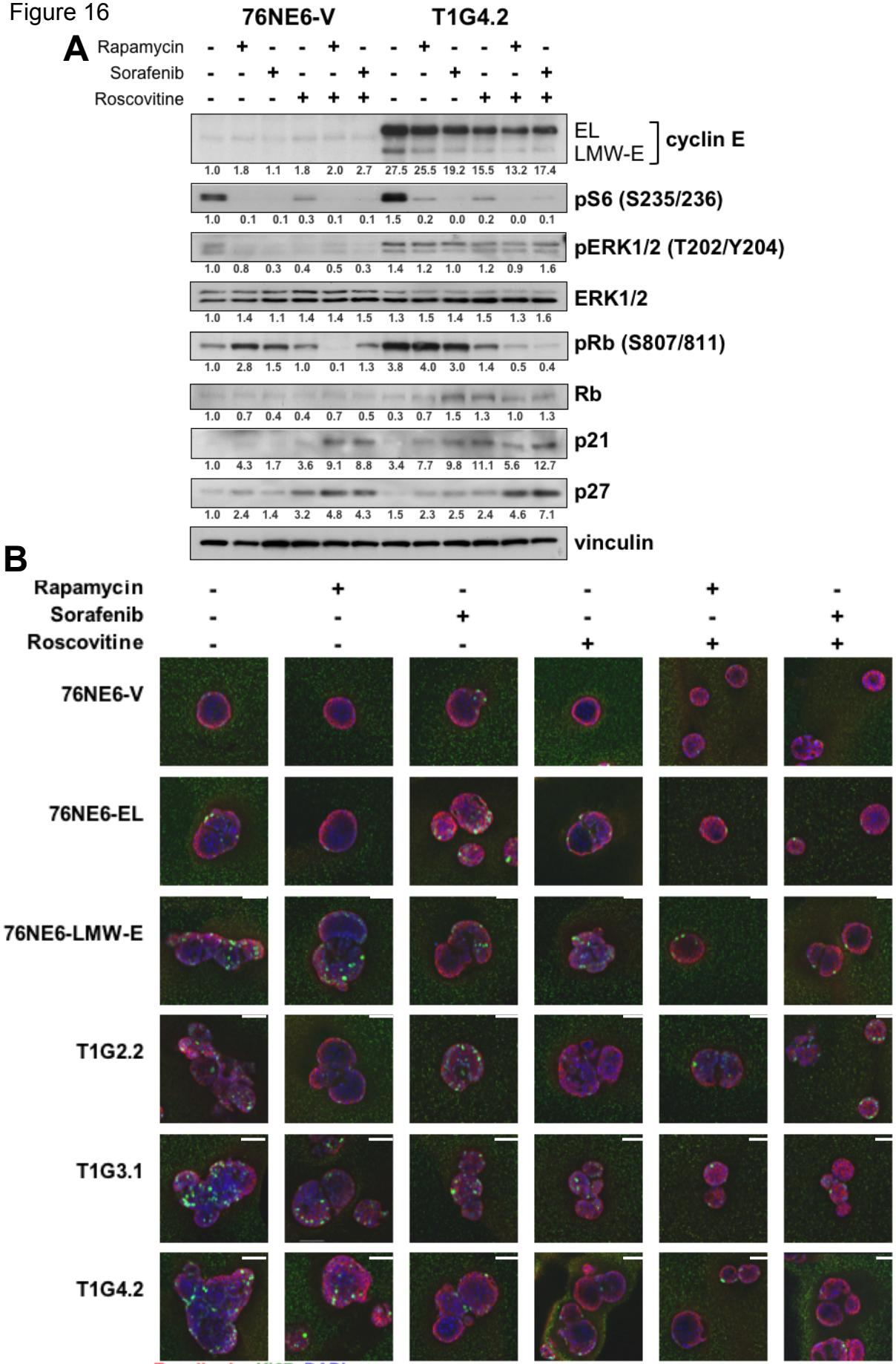
A
76NE6-V
T1G4.2
Rapamycin - + - - + - - + - - + -
Sorafenib - - + - - + - - + - - +
Roscovitine - - - + + + - - - + + +
EL
LMW-E
cyclin E
1.0 1.8 1.1 1.8 2.0 2.7 27.5 25.5 19.2 15.5 13.2 17.4
pS6 (S235/236)
1.0 0.1 0.1 0.3 0.1 0.1 1.5 0.2 0.0 0.2 0.0 0.1
pERK1/2 (T202/Y204)
1.0 0.8 0.3 0.4 0.5 0.3 1.4 1.2 1.0 1.2 0.9 1.6
ERK1/2
1.0 1.4 1.1 1.4 1.4 1.5 1.3 1.5 1.4 1.5 1.3 1.6
pRb (S807/811)
1.0 2.8 1.5 1.0 0.1 1.3 3.8 4.0 3.0 1.4 0.5 0.4
Rb
1.0 0.7 0.4 0.4 0.7 0.5 0.3 0.7 1.5 1.3 1.0 1.3
p21
1.0 4.3 1.7 3.6 9.1 8.8 3.4 7.7 9.8 11.1 5.6 12.7
p27
1.0 2.4 1.4 3.2 4.8 4.3 1.5 2.3 2.5 2.4 4.6 7.1
vinculin
B
Rapamycin - + - - + -
Sorafenib - - + - - +
Roscovitine - - - + + +
76NE6-V
76NE6-EL
76NE6-LMW-E
T1G2.2
T1G3.1
T1G4.2
E-cadherin; Ki67; DAPI

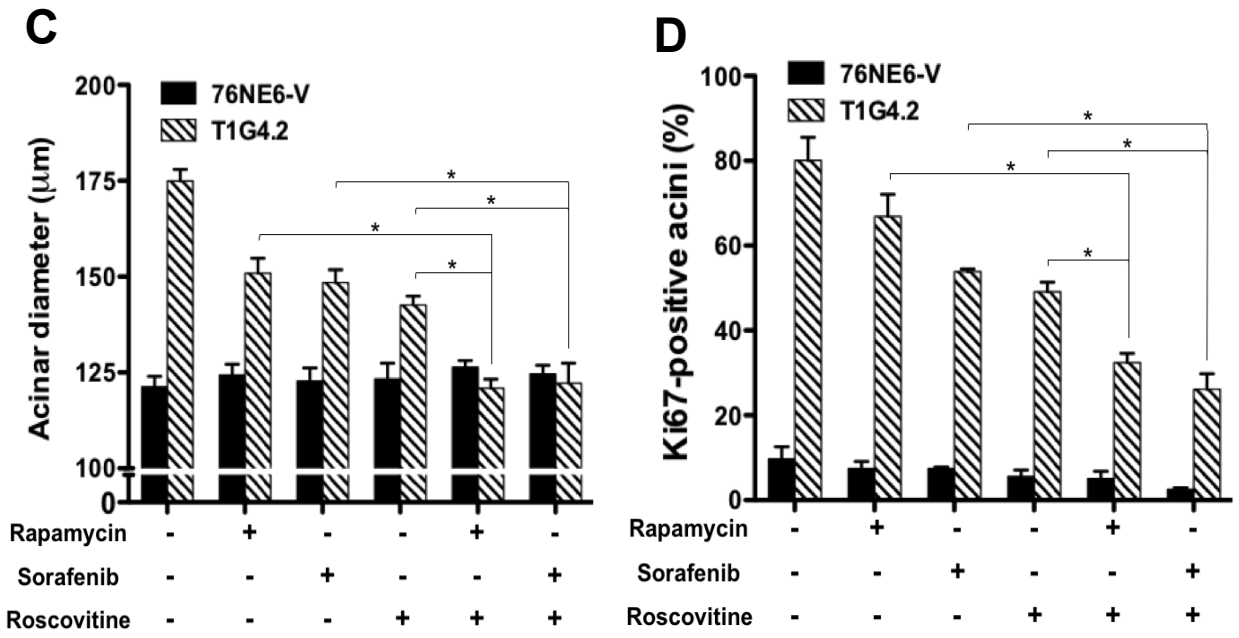

Figure 16: Combination drug treatment prevents induction of aberrant acinar development by LMW-E. (A) Cells were seeded on Matrigel for 24 hours and then treated with rapamycin, sorafenib, and roscovitine as indicated. Medium containing drugs was replaced every 4 days, and lysates were collected on day 15 for Western blot analysis with the indicated antibodies. (B) On day 15 of Matrigel culture, cells grown as in (A) were fixed and stained with E-cadherin (red) and Ki67 (green), and nuclei were counterstained with DAPI (blue). Scale bar = 50 μm. (C) The diameters of the acini were measured and averaged from three independent experiments. Error bars = SEM (Student *t* test, *p<0.05). (D) The number of Ki67-positive cells per acinus was counted and averaged from three independent experiments. Error bars = SEM (Student *t* test, *p<0.05).

Figure 17

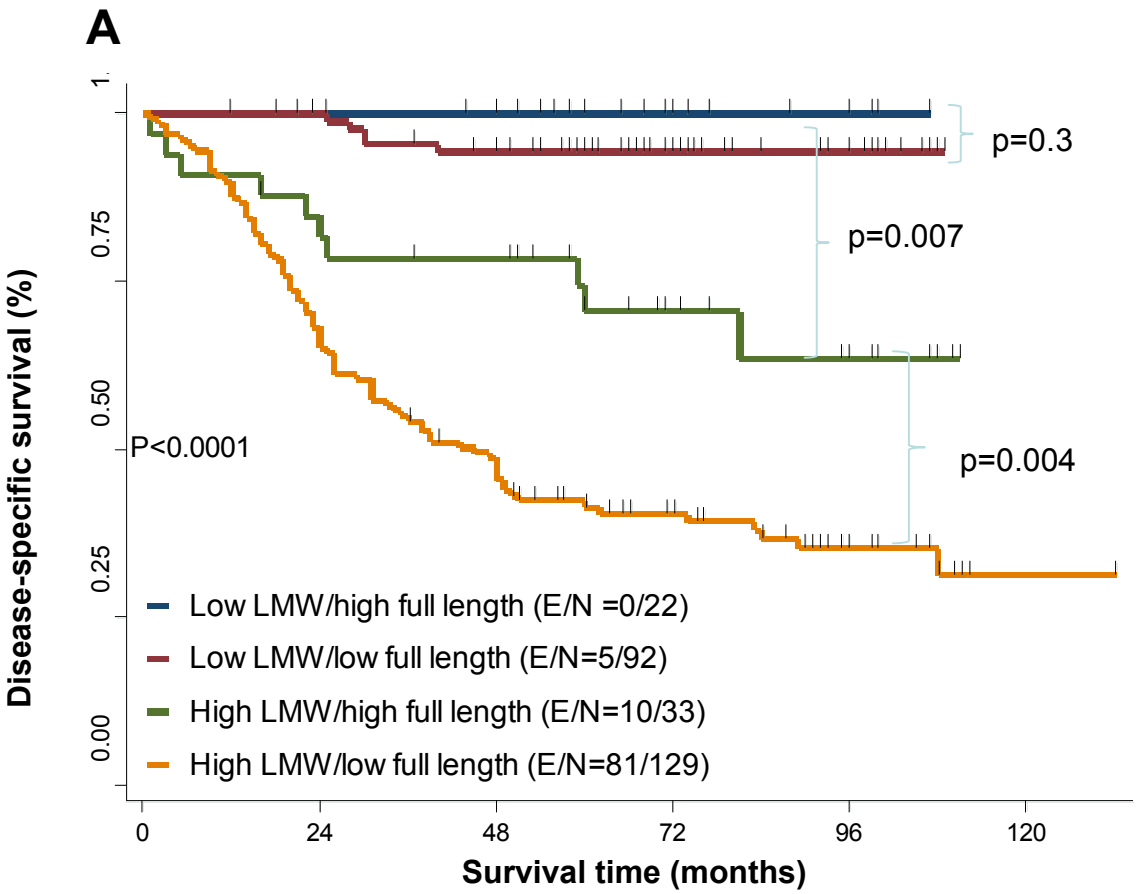
A
Disease-specific survival (%)
0.00
0.25
0.50
0.75
1.
P<0.0001
p=0.3
p=0.007
p=0.004
Low LMW/high full length (E/N =0/22)
Low LMW/low full length (E/N=5/92)
High LMW/high full length (E/N=10/33)
High LMW/low full length (E/N=81/129)
0
24
48
72
96
120
Survival time (months)

Figure 17

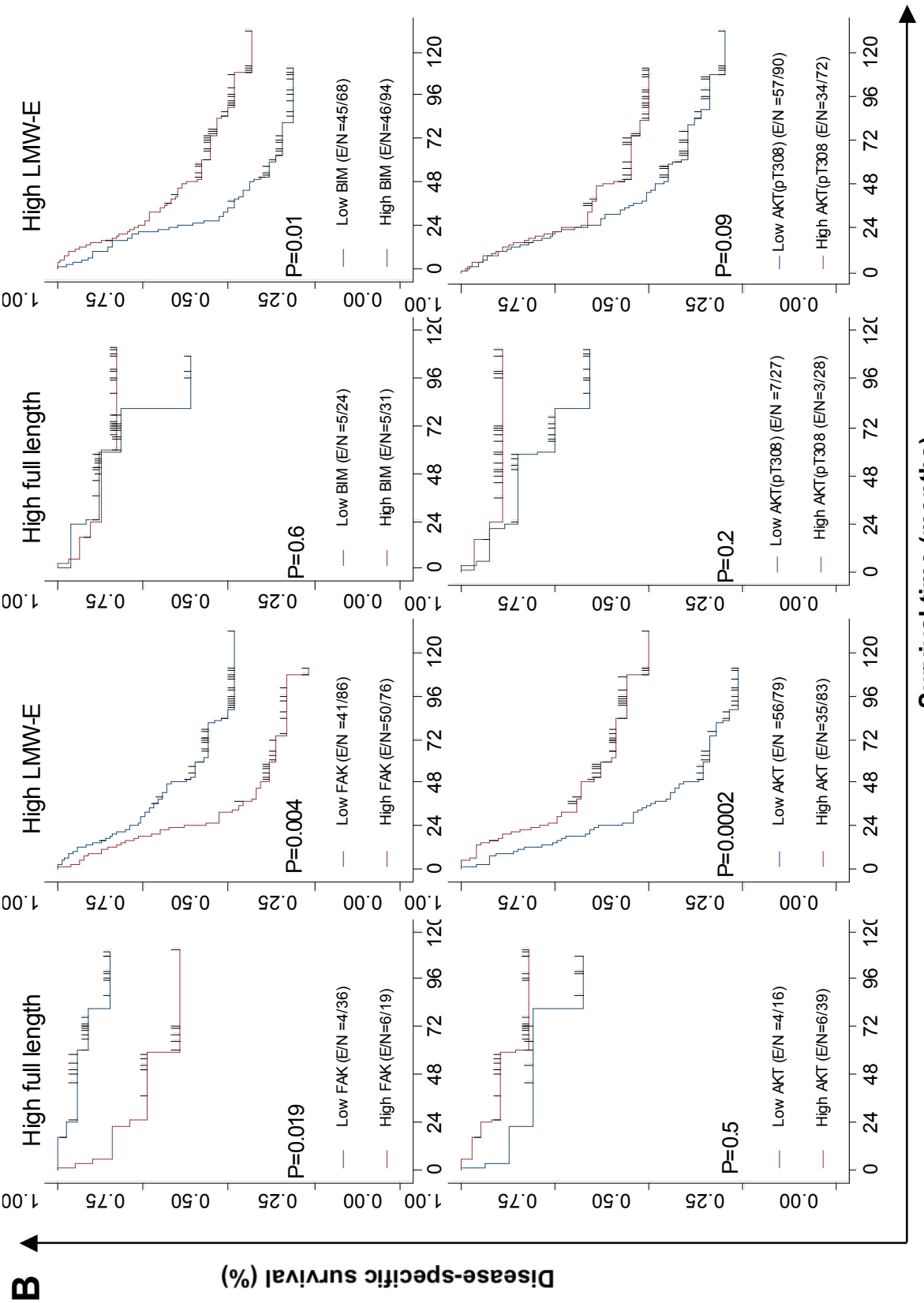
B
Disease-specific survival (%)
Survival time (months)
High full length
High LMW-E
High full length
High LMW-E
High LMW-E
P=0.019
Low FAK (E/N =4/36)
High FAK (E/N=6/19)
P=0.004
Low FAK (E/N =41/86)
High FAK (E/N=50/76)
P=0.6
Low BIM (E/N =5/24)
High BIM (E/N=5/31)
P=0.01
Low BIM (E/N =45/68)
High BIM (E/N=46/94)
P=0.5
Low AKT (E/N =4/16)
High AKT (E/N=6/39)
P=0.0002
Low AKT (E/N =56/79)
High AKT (E/N=35/83)
P=0.2
Low AKT(pT308) (E/N =7/27)
High AKT(pT308 (E/N=3/28)
P=0.09
Low AKT(pT308) (E/N =57/90)
High AKT(pT308 (E/N=34/72)
0.00
0.25
0.50
0.75
1.00
0
24
48
72
96
120

Figure 17

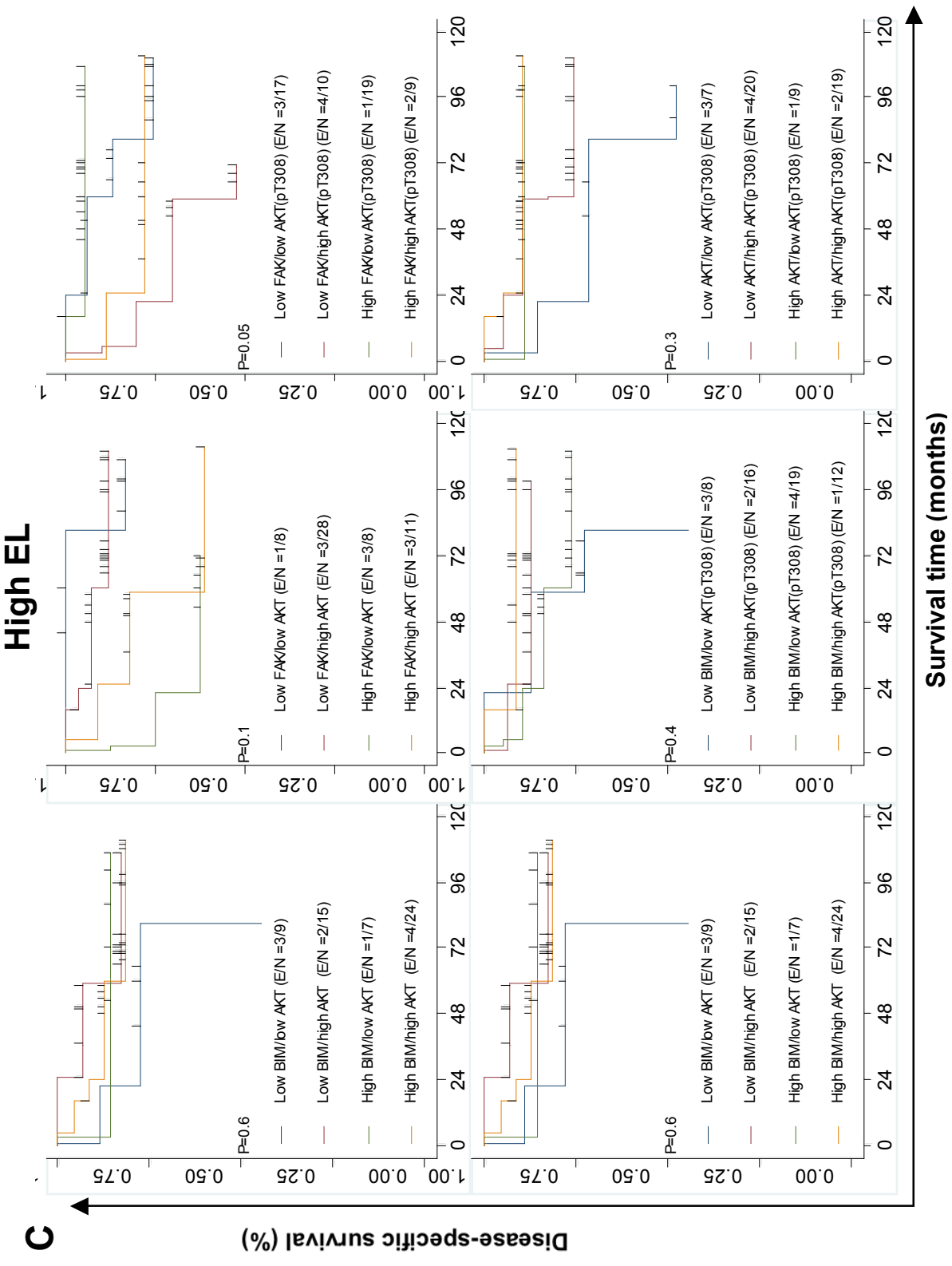
C
High EL
Disease-specific survival (%)
Survival time (months)
P=0.6
P=0.1
P=0.4
P=0.6
P=0.05
P=0.3
Low BIM/low AKT (E/N =3/9)
Low BIM/high AKT (E/N =2/15)
High BIM/low AKT (E/N =1/7)
High BIM/high AKT (E/N =4/24)
Low FAK/low AKT (E/N =1/8)
Low FAK/high AKT (E/N =3/28)
High FAK/low AKT (E/N =3/8)
High FAK/high AKT (E/N =3/11)
Low BIM/low AKT(pT308) (E/N =3/8)
Low BIM/high AKT(pT308) (E/N =2/16)
High BIM/low AKT(pT308) (E/N =4/19)
High BIM/high AKT(pT308) (E/N =1/12)
Low FAK/low AKT(pT308) (E/N =3/17)
Low FAK/high AKT(pT308) (E/N =4/10)
High FAK/low AKT(pT308) (E/N =1/19)
High FAK/high AKT(pT308) (E/N =2/9)
Low AKT/low AKT(pT308) (E/N =3/7)
Low AKT/high AKT(pT308) (E/N =4/20)
High AKT/low AKT(pT308) (E/N =1/9)
High AKT/high AKT(pT308) (E/N =2/19)
0.00
0.25
0.50
0.75
1.00
0
24
48
72
96
120

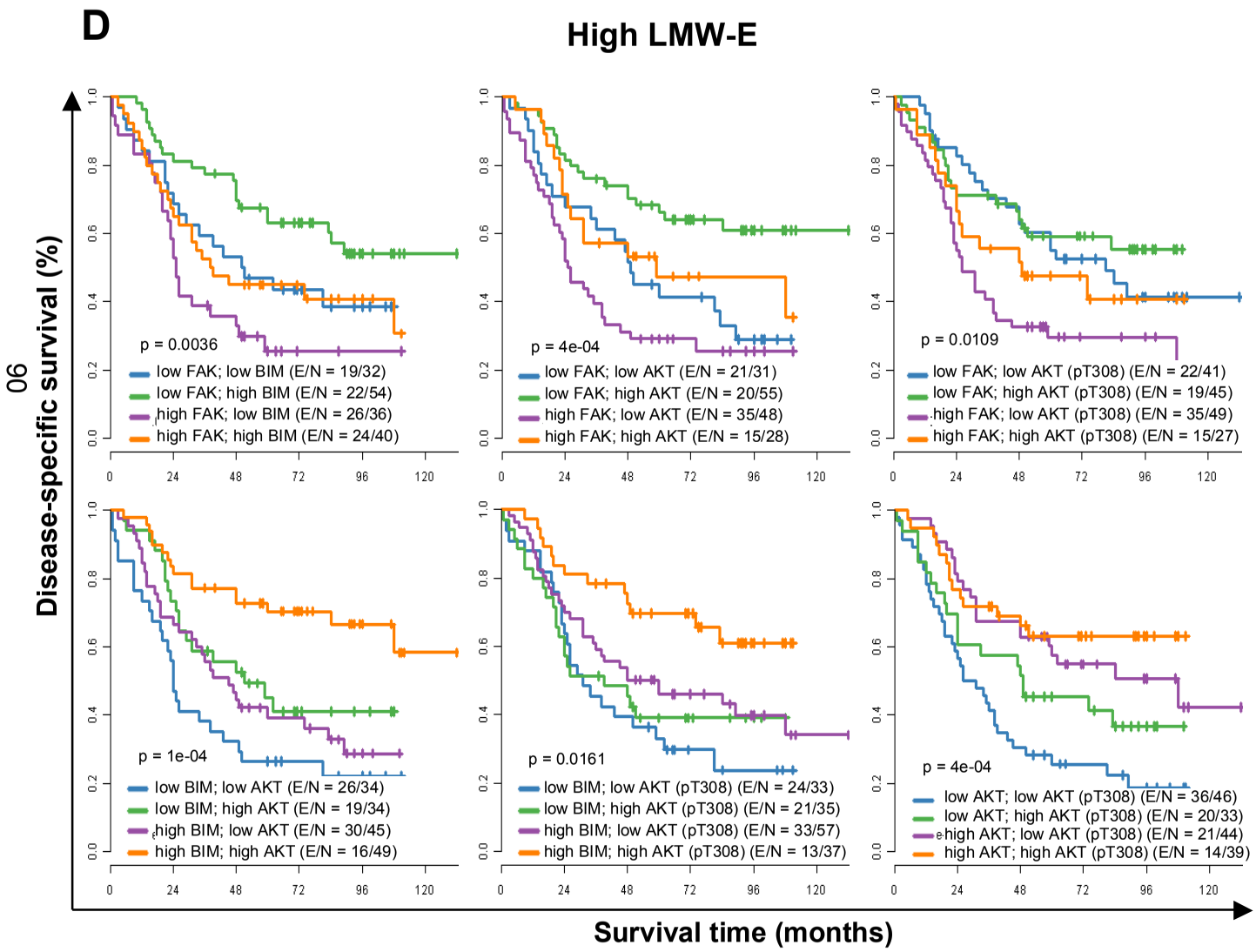

Figure 17: Activated b-Raf-ERK1/2-mTOR signaling pathway and high LMW-E expression predict poor survival in breast cancer patients. (A) Kaplan-Meier estimates of disease-specific survival based on the expression of low and high EL and LMW-E measured by Western blot analysis of 276 breast cancer patient samples. (B) Bivariate analysis of cyclin E protein levels in association with FAK, BIM, Akt and pAkt (T308) protein levels obtained from RPPA analysis. The expression levels of FAK, BIM, Akt and pAkt (T308) were dichotomized using their median values from all 276 patient samples. (C & D) Multivariate analysis was performed by including only those patients with high EL (C) and LMW-E (D) expression and examining LMW-E expression along with the expression of FAK, BIM, Akt, and pAkt (T308) levels. All p values are based on log-rank test.

mTOR pathway revealed that among breast cancer patients with high LMW-E expression, those with high FAK levels had significantly worse DSS than those with low FAK levels (p=0.0042) (Figure 17B). In contrast, among patients with high LMW-E expression, low BIM or low total Akt levels was associated with worse survival. Additionally, the overall DSS of patients with high LMW-E combined with these proteins in the b-Raf-ERK1/2-mTOR pathway was dramatically worse than in the patients with high full-length cyclin E expression (Figure 17B).

To determine whether these individual proteins collaborate to reduce patient survival, we performed multivariate analysis by analyzing patients with high LMW-E expression and combining 2 additional proteins. We found that patients with high LMW-E, high FAK, and low BIM, Akt, or pAkt (T308) experienced significantly worse DSS than the other groups ($p<0.05$) (Figure 17D). In addition, patients with high LMW-E, low BIM, and low Akt or pAkt (T308) experienced significantly worse DSS ($p<0.05$). Interestingly, we were not able to find statistical significance between full-length cyclin E expression in the same multivariate analysis with these proteins (Figure 17C). Essentially, our statistical analysis suggests that it is likely that LMW-E, FAK, BIM, Akt, and pAkt (T308) function in the same pathway to adversely affect patient survival in breast cancer.

2.4. CONCLUSIONS

The extracellular matrix provides environmental cues that induce differentiation and senescence of normal epithelial cells, and this response is lost when a cell transforms into a cancer cell. The acinar morphogenesis assay is an *in vitro* model system that can clearly distinguish the difference in growth behavior between normal epithelial cells and tumor cells (224, 232). The results from this study demonstrate that immortalized hMECs growth arrest and form differentiated and polarized acinar structures in laminin rich basement membrane while breast cancer cell lines fail to exhibit these behaviors. The morphological difference between normal and cancer cells displayed on Matrigel culture is because signaling from the extracellular matrix greatly influences the progression of the cell cycle intracellularly. Previous studies have demonstrated that malignant breast cancer cells express

high levels of β1-integrin receptor and exhibit disorganized distribution of the receptor in the acinar structures (245). Treatment of these structures with a blocking b1-integrin antibody reverts the aberrant morphologies, downregulates cyclin D expression while upregulating $p21^{Cip1}$ levels (245). Therefore, cell cycle regulation is critical for the maintenance of the integrity of the differentiation state of the cells and tissue. Without this regulation, the cells ignore the signals provided from the surrounding and become highly proliferative and cancerous. The difference in cellular proliferation is observed in cells cultured on monolayer and 3D matrix. Immortalized hMECs (76NE6, 76NF2V, and MCF-10A) exhibited growth arrest when cultured on 3D Matrigel compared with those cultured on monolayer.

High rate of proliferation resulting from deregulated G1-S phase transition mediated by overactive LMW-E/CDK2 complex is morphologically distinguishable during acinar morphogenesis. This uncontrolled proliferation is apparent by high Ki67 staining in the matrix-attached cells of the LMW-E-expressing acini but not in EL and vector control acini. The highly proliferative luminal cells may also explain the large and non-spherical acinar structures since coordination of cellular arrest and differentiation is lost. In addition to hyperactive proliferation, the LMW-E-expressing acini also downregulate bim indicating failure of the central cells to undergo apoptosis thus leaving a filled lumen (243). Elevated proliferation and reduced apoptosis observed in the acinar structures may explain the ability of LMW-E to induce tumor growth in the mouse mammary fat pad.

While the cyclin E/CDK2 complex is the accelerator of the G1-S checkpoint, p53 is the brake. Acting as a tumor suppressor, one of the major functions of p53 is to activate $p21^{Cip1}$ transcription in response to DNA damage, which in turn inhibits the cyclin E/CDK2 complex (246). The molecular link between cyclin E overexpression and loss of p53 control in breast cancer has been suggested in a number of reports. In one study, 56% of breast cancer patients with high cyclin E content were found to also possess p53 gene mutations (242). Furthermore, in our transgenic mouse model, overexpression of LMW-E is sufficient to induce mammary adenocarcinomas with 25% of the tumors advancing to metastasis (180). Moreover, these mice were found to select for loss of heterozygosity (LOH) of *p53*

and spontaneous inactivation of the ARF-p53 pathway. The aberrant acinar phenotypes induced by LMW-E worsen with loss of p53 expression. Therefore, the counterbalance between LMW-E and p53 has biochemical and functional implications in normal mammary acinar development, and deregulation of this process could act as the first step of derailment into malignancy.

Elafin is an elastase inhibitor and thus can prevent the generation of LMW-E. We recently reported that elafin is transcriptionally down regulated in most tumor cell lines, rendering the generation of LMW-E in tumor but not in normal cells (210). Ectopic elafin expression is able to some extent induce MDA-MB-231 cells to form spherical structure from single cell morphology. Furthermore, results from the xenograft study suggest that perhaps LMW-E-mediated tumorigenesis is due to elafin downregulation since the *in vivo* passaged tumors exhibit high LMW-E expression and suppressed elafin protein level. Research from our lab indicate that elafin is upregulated upon growth factor starvation or basement membrane detachment to elicit cell cycle arrest and or apoptosis, depending on the cell's pRb status. While the mechanism of elafin transcriptional downregulation remains to be elucidated, it is possible that loss of elastase inhibition mediated by elafin is responsible for the high levels of LMW-E in the xenograft tumors.

LMW-E is necessary and sufficient for growth of cancer cells *in vivo.* Xenograft transplantation experiment indicates that 74% of injection of hMECs expressing LMW-E led to tumor development whereas the percentage of tumor formation with injection of EL-expressing hMECs was 10 folds lower. This observation is consistent with previous study using transgenic mouse model to illustrate that LMW-E is a stronger oncogene than EL (180). Moreover, LMW-E expression is selected with increasing passaging of the tumor cells through the mice suggesting that LMW-E provides advantageous growth and survival for the tumor. With each generation of passaging, the LMW-E-expressing tumors developed at higher efficiency compared to the first generation. The microenvironment can exert selective pressure to induce genetic and epigenetic changes to favor progression of the tumor (247).

Our previous studies showed that LMW-E isoforms form tighter complexes with CDK2 compared to EL isoform and thereby exhibit higher kinase activity (175,

221). Furthermore, the LMW-E/CDK2 complexes are significantly more resistant to inhibition by p21 and p27 over EL/CDK2 complexes (175). Alteration in the interaction with CDK2 and inhibitory response to CKIs explains the difference in the oncogenicity between EL and LMW-E isoforms described in this report. Interestingly, the oncogenicity of LMW-E and formation of multiacinar complexes are strictly dependent on CDK2 kinase activity suggesting that perhaps unbound LMW-E exhibits no oncogenic activity. Therefore, CDK2 kinase activity presents as an ideal target to treat patients with high LMW-E expression. Roscovitine treatment can rescue the formation of large and multi-acinar complexes induced by LMW-E while showing no toxic effects on parental control acini. In the literature, roscovitine has proven to be an effective therapeutic agent in targeting numerous types of tumor cells including breast cancer, non-small cell lung cancer, sarcoma, multiple myeloma and lymphoma (173, 178, 198, 248, 249). Since the tumorigenic activity of LMW-E strongly depends on CDK-associated kinase activity, roscovitine becomes an apparent choice for designing therapeutic strategies for cancer patients with high LMW-E expression. The fact that LMW-E requires CDK2 kinase activity to drive multiacinar complexes and promote tumor-initiating activity of hMECs in mice suggests that LMW-E itself has no intrinsic oncogenic activity. Therefore, treatment of tumors with high LMW-E protein levels can be achieved by inhibiting CDK2 kinase activity. Our data demonstrate that combination treatment using roscovitine together with rapamycin or sorafenib of LMW-E-expressing acini efficiently prevents the aberrant morphogenetic phenotypes without toxic effects on hMECs lacking LMW-E expression.

The results from proteomic analysis demonstrated a marked contrast in the protein expression profiles of cells grown on monolayer and cells grown in 3D culture and illustrated a high similarity between cells in 3D culture and human tumor tissues, thus establishing a bridge between the 3D culture system and human tissues and further supporting the use of this culture system for biological study (250). In fact, gene expression signatures of mammary cells extracted from this 3D culture system can be reliably used to predict patient outcome in which the signature of growth-arrested and well-organized hMECs predicts favorable clinical

outcome (229, 251). Data from this analysis also allowed for the delineation of a signaling pathway that is deregulated in breast cancer patients who express high LMW-E levels. We demonstrated that tumors and cell lines with high LMW-E expression have upregulated b-Raf-ERK1/2-mTOR signaling, which has been reported to result in enhanced cell survival and reduced apoptosis (252-254).

In this chapter, multiple experimental systems were employed to explore the role of LMW-E with CDK2 in tumorigenesis. The results obtained indicate that LMW-E induces aberrant acinar morphologies and is clearly a much stronger oncogene compared to EL. More importantly, these oncogenic phenotypes mediated by LMW-E are dependent on its ability to interact with CDK2 to exert its kinase activity. Furthermore, proteomic analysis also identifies a signaling pathway involving raf-ERK1/2-mTOR that is activated in tumor cells with high LMW-E expression and associate with poor patient outcome. Clinically, there is a high percentage of breast cancer patients whose expression of LMW-E significantly predicts poor prognosis and adverse clinical outcomes (160). Our data suggest that the combination of roscovitine with either rapamycin or sorafenib should be evaluated as a therapeutic strategy to treat breast cancer patients with high LMW-E expression.

CHAPTER 3: **LMW-E INDUCES THE EMT AND ENRICHES FOR CELLS WITH CSC PROPERTIES**

3.1. INTRODUCTION

3.1a. The cancer stem cell (CSC) theory

Cancer is a multi-step heterogeneous disease caused by accumulation of genetic and epigenetic alterations that lead to uncontrolled growth of normal cells. This theory is supported by epidemiological data demonstrating that breast cancer development occurs many years after the actual oncogenic event (255, 256). Indeed, stem cells or progenitor cells are believed to be more susceptible to these alterations since they endure longer lifespan and thus are able to gain sufficient mutations to initiate and sustain tumor development (257). However, recent research in this field suggests that CSCs can in fact arise from a differentiated cell of origin.

The CSC theory states that there is a small population of cells within the tumor mass that possess unique properties shared by stem cells such as self-renewal capacity, multi-potency, and unlimited proliferation (257, 258). More specifically, CSCs have the ability to proliferate extensively and give rise to diverse cell types with reduced development or proliferation potential. Recent research presents vast evidence supporting the existence of CSCs in both hematological cancers as well as solid tumors (259-269). The Hierarchy stem cell model states that there are different subpopulations of cells within the tumor mass that possess different capabilities of self-renewal and differentiation (Figure 18A) (257, 260). This model emphasizes that only a small definable subset of tumor cells has the potential to initiate tumor growth and reproduce the hierarchy of cells that comprise the tumor. Indeed, numerous studies reported that many tumors are heterogeneous and contain many cell types thus suggesting that the few CSCs are multi-potent (270-274). In contrast, the Stochastic model predicts that the process of each individual cell within a tumor to self-renew and differentiate occurs randomly and can be predicted by statistics (Figure 18B) (257, 258, 275). This model maintains that the tumor is composed of a homogeneous population of cells and every cell

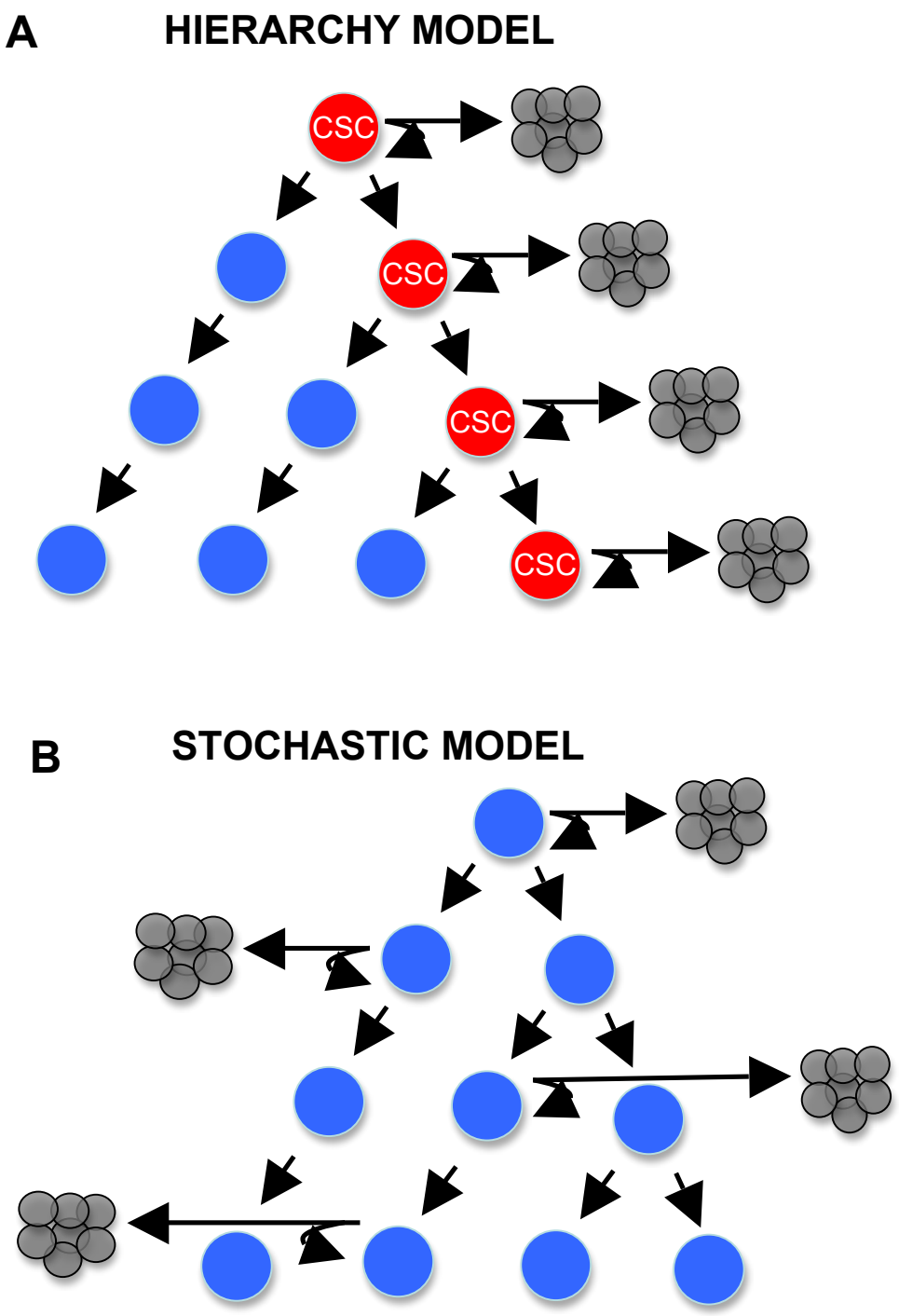

Adapted from *Nature* 2001;414(6859):105-11.

Figure 18: CSC models. (A) In the Hierarchy model, only a small subset of cells termed CSCs (red cells) are capable of self-renewal and form new tumors. The more differentiated cells do not possess self-renewal capability (blue cells), cannot form new tumors, and eventually reach terminal differentiation. (B) The Stochastic model argues that the tumor is composed of a homogenous population and every cell in the tumor has an equal but small chance to self-renew and form new tumors.

has a low but equal chance of acquiring tumorigenic potential. Clonal outgrowth of an individual cell due to genetic/epigenetic insult leads to selection and accumulation of this dominant population that then forms the bulk of the tumor (276). Currently there is no clear evidence that is sufficient to distinguish between these two models suggesting that they are not mutually exclusive. While the discussion on the origin of tumor cells and how to appropriately define these cells is ongoing, research in the last few years have further strengthen the fact that these CSCs are important in tumor initiation, maintenance, metastasis, and resistance to therapy.

3.1b. Molecular markers of mammary CSCs

CSCs are not only present in hematological cancers but are also identified in numerous solid tumors, most notably in breast cancer (263). Accumulating evidence from a number of publications indicate that mammary CSCs can be identified and isolated based on their expression for the $CD44^{hi}/CD24^{lo}$ surface markers, aldehyde dehydrogenase (ALDH) enzymatic activity, and the ability to form tumors at low cell numbers and mammospheres in low attachment and non-differentiating culture conditions (263, 277, 278). Early work by Al-Hajj and colleagues demonstrated that as few as 100 primary breast cancer cells that are defined by the $CD44^{hi}/CD24^{lo}$ cell surface expression pattern can form tumors when injected into the mammary fat pad of nude mice and also can be serially passaged while tens of thousands of cells with the $CD44^{hi}/CD24^{hi}$ phenotype cannot (263). Particularly, the *in vivo* passaged tumors from the second and third generations display similar population distribution as the original tumor suggesting that the $CD44^{hi}/CD24^{lo}$ population possess self-renewal capability as well as the ability to differentiate into non-CSCs.

Although, as of yet, there are no functions associated with this cell surface marker, $CD44^{hi}/CD24^{lo}$ cells are able to form mammosphere structures under non-adherent and non-differentiating culture condition, which is a functional test that has been reliably employed to investigate the self-renewal and differentiation capability of neuronal stem cells (279). While epithelial cells require basement attachment for survival and proliferation, Dontu and colleagues demonstrated that a single

mammary progenitor cell is able to proliferate and differentiate to form a floating mammosphere when cultured on non-adhesive substratum (277). Furthermore, mammospheres contain undifferentiated cells that are able to give rise to the 3 types of cells in the mammary gland, which are myoepithelial, ductal, and alveolar (luminal) epithelial cells (Figure1). Breast cancer cells grown in mammosphere culture condition exhibit increased tumorigenicity and downregulate CD24 expression, and these phenotypes can be reversed with passage in monolayer culture (280, 281).

Another functional marker identified to be associated with CSC is ALDH, which is a detoxifying enzyme that has been shown to be involved in early differentiation of stem cells by oxidizing retinol to retinoic acid (282) and is believed to mediate self-protection against some alkylating chemotherapeutic agents (283). Similar to the $CD44^{hi}/CD24^{lo}$ cells, sorted $ALDH^{hi}$ cells injected into xenograft mouse model are capable of recapitulating the phenotypic distribution of the original tumor (278). Although there is a small percentage of $CD44^{hi}/CD24^{lo}$ cells that are also $ALDH^{hi}$ (approximately 1% of the tumor population), as few as 20 cells with the $CD44^{hi}/CD24^{lo}/ALDH^{hi}$ phenotype are able to generate tumors in mice, which are 5 folds more tumorigenic compared to the $CD44^{hi}/CD24^{lo}$ population alone (278). Clinically, breast cancer patients whose tumors contain high ALDH expression are predicted to have poor clinical outcome (278, 284). Overall, the identification of these CSC markers have greatly facilitated our understanding of mammary tumor biology and allowed for examination into the mechanism of drug resistance and tumor relapse.

3.1c. The EMT connection to CSCs

The cells defined by the $CD44^{hi}/CD24^{lo}$ antigenic phenotype are enriched in tumor-initiating cells, exhibit enhanced tumor invasiveness, and can be generated through induction of the EMT (263, 285, 286). Mani and colleagues first reported that induction of the EMT by ectopic expression of twist, TGFβ1 or snail results in an enrichment of the $CD44^{hi}/CD24^{lo}$ population, mammosphere formation, and tumorigenicity in hMECs (285). EMT is a developmental process in which epithelial

cells gain mesenchymal phenotypes and behaviors such as increased motility and invasion to allow formation of new tissues and organs (287). However, aberrant induction of the EMT in tumor cells is known to enhance proliferation and invasion (288). Indeed, acquisition of the EMT traits is thought to aid tumor cells to invade and migrate to form metastasis at distant organ and the reverse process termed mesenchymal-epithelial transition (MET) is necessary for successful colonization at the new tumor location.

3.1d. LMW-E associates with basal-like breast cancer

Analysis of the breast cancer subtypes indicated that the $CD44^{hi}/CD24^{lo}$ cell population is enriched in the basal-like breast tumors, which are clinically associated with poor prognosis (289, 290). The basal-like subtype of breast cancer was first defined by gene expression microarrays to be negative for ER, PR, and HER2, and positive for cytokeratin 5/6 and EGFR (10). Interestingly, the mammary tumors formed from overexpression of LMW-E also assume the basal-like phenotypes and resemble the morphological characteristics of the tumors caused by deregulation of the Wnt pathway, which are acinar, glandular, papillary, solid, and adenosquamous (180, 291). Rosner and colleagues demonstrated that the phenotypes of the tumors often predict the genotypes signifying that tumors that share the same morphological characteristics are predicted to exhibit deregulation to the same pathway (292). Recent analysis of our breast cancer patient samples further indicated that of the LMW-E-expressing tumors, triple negative (TN) tumors (negative receptor status for ER, PR, and HER2) expressed dramatically higher levels of LMW-E than other tumors with at least one positive receptor, and these TN patients are significantly more likely to experience tumor recurrence ($p = 0.045$). Given that the mammary tumors formed from ectopic expression of LMW-E assume the basal-like phenotypes and LMW-E expression is high in TN breast cancer patients, we speculate that the mechanism that specifically allows LMW-E to initiate and maintain breast cancer is through activation of the EMT as well as acquisition of mammary CSC characteristics.

3.1e. Anti-CSC therapy

Most chemotherapeutic agents are designed to target highly proliferative cells, which typically form the bulk of the tumor. CSCs however exhibit low proliferation index, and consequently they are resistant to many current cancer treatments including chemo- and radiation therapy (293, 294). More specifically, the $CD44^{hi}/CD24^{lo}$ population was reported to be enriched in the tumor mass after chemotherapy and these cells demonstrate enhanced mammosphere formation efficiency (295). The CSCs that remain after therapy are capable of regenerating a new tumor thereby leading to tumor relapse. In addition, CSCs express high levels of the multi-drug resistance proteins and the ATP-binding cassette (ABC) transporter family, which function by pumping chemotherapeutic agents out of the cell (296).

The overwhelming evidence supporting the existence of CSCs suggests that our conventional therapeutic approaches would only target the non-CSCs that make up the bulk of the tumor but spare the CSCs that are capable of regenerating the tumor post-treatment. As a result, we need to improve our therapeutic strategy by specifically targeting these CSCs in addition to eradicating the non-CSCs. A rational strategy to overcome this challenge is to combine agents that can target both the CSC and non-CSC populations. Recently, a large screen for small compounds that can specifically target the CSC population revealed that salinomycin, an antibacterial drug, exerts highly specific toxicity against $CD44^{hi}/CD24^{lo}$ cells compared to paclitaxel (297). Therefore, combination of this agent with a general chemotherapeutic agent such as doxorubicin, which can kill proliferating non-CSCs, will likely to result in complete remission.

3.1f. Hypothesis and Specific Aims

Initiation and maintenance of cancer depends on a strong oncogene that can elicit multiple downstream effects to convert a normal cell to a tumor cell. We believe that the tumorigenicity of LMW-E is mediated through induction of the EMT that leads to enrichment of the CSC population, and these tumor cells can be effectively targeted with combination treatment using doxorubicin and salinomycin.

Additionally, the ProtoArray microarray analysis, which will be discussed in greater details in the Results section, will be used to identify novel substrate(s) of the LMW-E/CDK2 complex that will allow for elucidation into the mechanism of LMW-E-mediated mammary tumorigenesis. The following specific aims are designed to address this hypothesis:

1. Understand the role of LMW-E in the induction of the EMT
2. Analyze the CSC properties of cells induced with LMW-E expression
3. Identify a therapeutic regimen to target the LMW-E-induced CSCs
4. Identify novel LMW-E/CDK2-associated substrates and/or interacting proteins

Briefly, the tumor-derived cells (TDCs) isolated from *in vivo* passaging exhibited phenotypes characteristic of the EMT, which are reduced cell-cell contact by downregulation of E-cadherin, upregulated gene expression profile associated with the EMT, and enhanced basement membrane invasion. Moreover, the LMW-E-expressing tumor cells demonstrated an increase in the $CD44^{hi}/CD24^{lo}$ population, and examination of patient tumor samples indicated that cytoplasmic cyclin E IHC staining significantly associate with high $CD44^{hi}/CD24^{lo}$ score compared to nuclear cyclin E staining ($p = 0.0435$). Further analysis for the CSC characteristics revealed that the TDCs possess self-renewal capability by forming mammosphere structures and also upregulated ALDH expression and enzymatic activity. Combination drug treatment with doxorubicin and salinomycin reduced the CSC population and synergistically killed the CSCs while sparing normal cells that do not express LMW-E. Finally, ProtoArray analysis revealed that LMW-E/CDK2 phosphorylates Hbo1 in the N-terminal domain, which demonstrated no effects on the *in vitro* histone acetyltransferase activity of Hbo1. Co-expression of LMW-E/CDK2 with Hbo1 in HEK293T resulted in an enrichment of cells with CSC properties and knockdown of Hbo1 in the TDCs reduced these properties. Taken together, these data suggest that Hbo1 is downstream of LMW-E/CDK2 overactive kinase activity, and increased Hbo1's HAT activity may be critical for the CSC phenotypes observed.

3.2. MATERIALS and METHODS

3.2a. General reagents

Antibodies used for western blot analysis are: E-cadherin and ALDH (BD Bioscienes, Sparks, MD), CDK2 and CD24 (Santa Cruz Biotechnology Santa Cruz, CA), CD44 (Cambridge, MA), Hbo1 (Proteintech Group, Chicago, IL), FLAG-tag (Sigma, St. Louis, MO), Myc-tag (Cell Signaling Technology, Boston, MA).

3.2b. Brightfield and indirect immunofluorescence analysis

Cells grown on tissue culture dish were photographed using the Leica DM 4000M microscope (Buffalo Grove, IL) at 5X objective with an attached digital camera, and images were processed with the Photoshop software (Version 11.0.2). Indirect immunofluorescence analysis was performed as described in chapter II with minor modifications. Cells were grown directly on the 8-chamber slides for monolayer culture and the E-cadherin primary antibody (BD) was incubated in IF buffer at 1:200 dilution overnight at 4°C. The cells were incubated with Alexa fluor-conjugated mouse secondary antibodies (Molecular Probes, Carlsbad, California), counterstained with 4',6-diamidino-2-phenylindole (DAPI) (Sigma, St. Louis, MO) for 15 min at RT, and mounted with antifade solution (Molecular Probes). Confocal analyses were performed using the Olympus FV300 laser scanning confocal microscope (Olympus America, Inc., Center Valley, PA) using the exact same setting for all samples.

3.2c. Transwell invasion assay

For each sample, 100 μl of 1 mg/ml Matrigel in serum free-cold MEM media was aliquoted into the upper chamber of 24-well transwell plate (Corning, Corning, NY) and incubated at 37^{o}C for at least 4-5 hours for adequate gelling. The cells were washed and suspended in serum free medium at a 1x10^{6} cells/ml concentration. One hundred μl of cell suspension was transferred onto the upper chamber containing the Matrigel layer. The lower chamber of the transwell was filled with 600 μl of complete media containing 10 μg/ml fibronectin as an adhesive substrate. After 24 hours, the cells were fixed with 4% formaldehyde for 15 minutes, rinsed with PBS, and stained with 0.2% crystal violet for 10 minutes. The crystal

violet was rinsed with excess ddH_2O and the top chamber containing the Matrigel was thoroughly cleansed with Q-tips and the invaded cells were photographed with a light microscope. For quantification, the cells on the top and bottom of the chamber are collected using trypsin and counted using the culture counter. Each sample was counted 3 times and each experiment was repeated independently 3 times.

3.2d. Quantitative RT-PCR analysis

Total RNA was isolated from cell culture with TRIzol reagent according to the manufacture's protocol (Invitrogen). After treatment with DNase I (NEB, Ipswich, MA), 1 μg of the RNA samples was reverse-transcribed using Transcriptor First Strand cDNA Synthesis Kit (Roche, Branford, CT) with the control reactions excluding reverse transcriptase. Realtime PCR was done with aliquots of the cDNA samples mixed with SYBR Green Master Mix (Sigma). The primer sequences were: cyclin E forward 5'-TGTGTCCTGGATGTTGACTG-3', reverse 5'-CAAGCTGTCTCTGTGGGTCT-3'; E-cadherin forward 5'-TGCCCAGAAAATGAAAAAGG, reverse 3'-GTGTATGTGGCAATGCGTTC; N-cadherin forward 5'-ACAGTGGCCACCTACAAAGG, reverse 3'-CCGAGATGGGGTTGATAATG; Twist forward 5'-GGAGTCCGCAGTCTTACGAG, reverse 3'-TCTGGAGGACCTGGTAGAGG; Slug forward 5'-GGGGAGAAGCCTTTTTCTTG, reverse 3'-TCCTCATGTTTGTGCAGGAG; Vimentin forward 5'-GAGAACTTTGCCGTTGAAGC, reverse 3'-GCTTCCTGTAGGTGGCAATC; and GAPDH forward 5'-ACCCAGAAGACTGTGGATGG-3', reverse 5'-CTGGACTGGACGGCAGATCT-3';

3.2e. CD24/CD44 FACS analysis

To perform doublestaining of the cell surface markers, 500,000 cells were washed 3 times with PBS containing 1% horse serum and resuspended with 10 μl PE anti-mouse CD24, 10 μl APC anti-mouse CD44 (BD Pharmingen, San Jose, CA, USA) and 30 μl of the 1% serum PBS buffer. The samples were incubated for 20 minutes on ice, washed with 1% serum PBS buffer, analyzed with the FACS

Calibur, and the data was analyzed by the Flowjo software (version 8.8.6) (Tree Star, Inc., Ashland, OR). Cells only and single antibody label were used to set up the gates for analysis. For cell sorting experiments, antibody staining was performed similarly but under sterile condition and sorted using the FACSAria cell sorter (BD, Franklin Lakes, NJ).

3.2f. Study patients, Western blot analysis, and immunohistochemical staining

The target population for the study is women with a diagnosis of invasive breast cancer stages I, II and III who are scheduled for surgery to remove the breast cancer with axillary lymph node dissection or sentinel lymph node dissection. IHC analyses of Cyclin E and CDK2 will be performed using available paraffin-embedded tumor specimens from residual tissue prepared and archived by the MDACC Institutional Tissue Bank per the standard procedure for surgical cases. Results of the IHC analyses compared with results previously obtained by Western Blot analysis of freshly resected surgical tissue.

Lysates were prepared from freshly resected surgical tissues as described previously (165,228) and subjected to Western blot analysis using cyclin E monoclonal antibody HE12 from Santa Cruz Biotechnology (Santa Cruz, CA). Densitometry of the Western blots were measured using the IP-Lab Gel software (Scanalytics) and normalized to β-actin protein levels. Full-length, LMW-E, and total cyclin E densitometric values were separated into low (less than or equal to normal tissues) and high groups (higher than the levels found in normal tissues).

Tumor tissues from 118 breast cancer patients were subjected to double IHC staining with antibodies to CD24 (Clone SN3b, 1:400) and CD44 (Clone 156-3C11, 1:800) from Neomarkers (Thermo Fisher, Fremont, CA). Briefly, sections were deparaffinized in xylene, rehydrated in ethanol, antigen retrieval in Tris-ethylenediamine tetraacetic acid buffer (pH 9.0) at 125^{o}C for 5 minutes. The DAKO EnVision G2 Doublestain System Rabbit/Mouse (diaminobenzidene (DAB+)/Permanent Red) kit was used for detection of CD44 and CD24. CD44 was detected with Permanent Red and CD24 was detected using DAB. In general,

CD24 staining was detected mainly in the cytoplasm and CD44 staining was mainly in the membrane as noted previously (289). Scoring was done blindly by 2 investigators blinded to patient annotation and the percentage of $CD44^{hi}/CD24^{lo}$ tumor cells were scored as follows: 0 (0%), 1 (1-10%), 2 (11-25%), 3 (26-50%), 4 (51-75%), 5 (76-100%).

Cyclin E IHC was accomplished using C-terminal cyclin E (C-19) antibody detecting both EL and LMW-E forms (Santa Cruz Biotechnology, Inc., Santa Cruz, CA), diluted at 1:2000 in normal goat serum. Cyclin E staining intensity and percent positivity were evaluated both in the nucleus and cytoplasm of cancer cells. We identify four different phenotypes of cyclin E distinguished with respect to predominant nuclear or cytoplasmic localization of staining. Breast tumors were considered negative when no staining was detected either in the nucleus or in the cytoplasm (score = 1). Among the cases evaluated as cyclin E positive, if the score assigned to the nucleus exceeded the score assigned to the cytoplasm, cyclin E expression was considered predominantly nuclear (score = 2). When the nucleus and the cytoplasm received equal scores, cyclin E expression was considered both nuclear and cytoplasmic (score = 3). If cytoplasmic staining was graded higher than nuclear staining, cyclin E expression was considered predominantly cytoplasmic (score = 4).

3.2g. Soft agar transformation and mammosphere formation assays

For soft agar transformation assay, the base agar was made by mixing 90 ml 10% FBS MEM with 22.5 ml 2.4% Noble agar (DIFCO, Lawrence, KS). The solution was heated to melt the agar and then aliquot to 6-well plates with 1 ml per well and allowed to solidify at RT. For the top agar, 2000 cells were mixed with 850 μl 10% FBS MEM and 125 μl 2.4% agar and transferred to the base agar for each well of 6-well plate. The cells were cultured for 15 days, stained with 0.005% crystal violet in 25% methanol for 1.5 hours, washed with ddH_20 and counted using the GelCount (Oxford Optronix Ltd., Oxford, UK). For mammosphere culture, cells were plated at 40,000 cells/ml in ultra-low attachment plates (Corning, Corning, NY) in MEM media (Media Tech, Manassas, VA) containing 1% methylcellulose (Sigma, St. Louis, MO)

and supplemented with 20 ng/mL EGF and B27 (Invitrogen, Carlsbad, CA). For quantification, 10% v/v 5 mg/ml MTT solution was added to each well after 7 days in culture, incubated for 1 hour at 37^{o}C and counted using the GelCount software.

3.2i. ALDEFLUOR assay

All contents of the ALDEFLUOR assay are included in the kit from Stem Cell Technologies (Durham, NC). To measure the ALDH enzymatic activity, 1 million cells were washed in assay buffer. For each sample, ALDH substrate (1 μmol/l BAAA) and ALDH inhibitor (50 mmol/l DEAB) were added to 500,000 cells in separate tubes and incubated at 37^{o}C for 1 hour. The cells were washed in assay buffer and analyzed with FACS Calibur. The DEAB sample was used to gate each individual sample to achieve less than 2% positive.

3.2h. Drug treatment & high-throughput survival assay (HTSA)

For CD24/CD44 FACS analysis, cells were seed at 20,000 cells/cm^2 density on 6-well plates 24 hours before drug treatment (day 0) (Figure 19A). On day 1, medium containing varying doxorubicin or salinomycin concentrations was added to the cells and replaced every 2 days for a total of 4 days. On day 5, the cells were allowed to recover for 3 days in drug-free medium before FACS analysis. For HTSA, cells were seeded at 3,000 cells/cm^2 density for 24 hours in 96-well plates and medium containing doxorubicin or salinomycin were added on days 1 and 3 (Figure 19B). The cells were allowed to recover for 5 days in drug-free media before analysis. On day 10, 50 μl of 2.5 mg/ml MTT solution (Sigma) was added to each well and incubated at 37°C for 4 hours in the dark. The media were removed and 100 μl of solubilization solution (0.04 N HCl, 1% SDS, in isopropyl alcohol) was added per well and gently rocked for 1 hour. After solubilization, cell viability was measured at 590 nm absorbance using the Wallac-Victor3 multilabel plate reader (PerkinElmer, Waltham, MA). At least 3 independent experiments were performed for each analysis.

3.2i. ProtoArray Human Protein Microarray analysis

A

CD44/CD24 FACS ANALYSIS

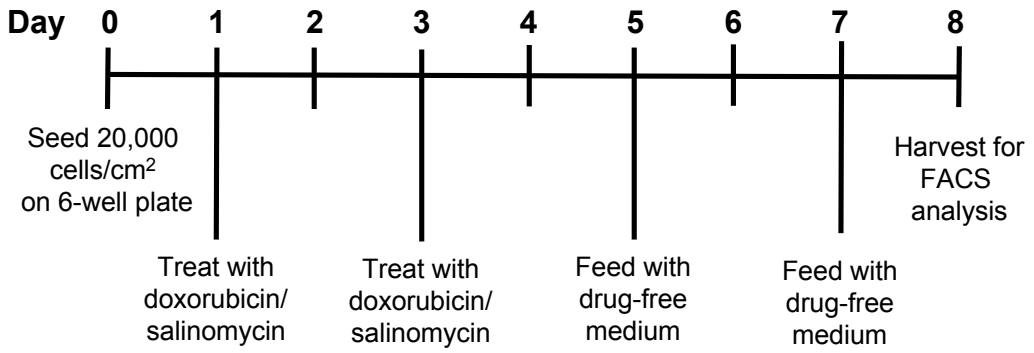

B

HTSA

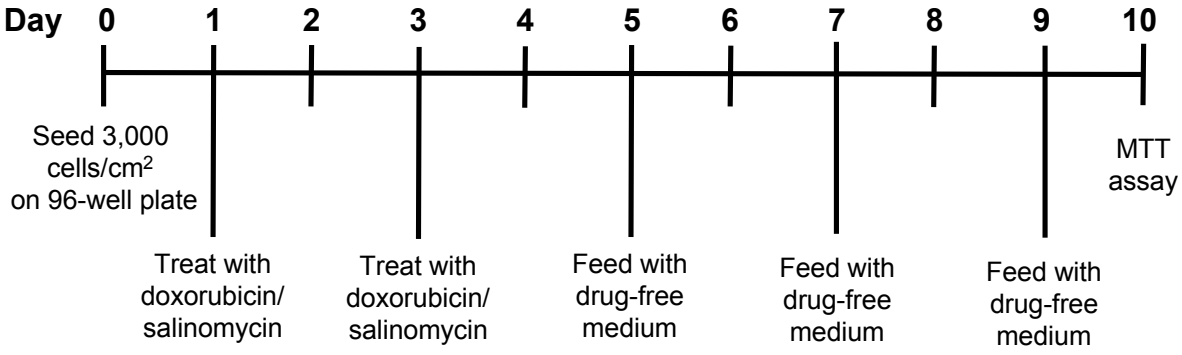

Figure 19: Schematic of the doxorubicin and salinomycin combination treatment. (A) For CD24/CD44 FACS analysis, the cells were seeded at 20,000 cells/cm^2 density on 6-well plates on day 0. On days 1 and 3, medium containing doxorubicin or salinomycin was added to the cells. On days 5 and 7, the cells were fed with drug-free medium and harvested for FACS analysis on day 8. (B) For the HTSA, the cells were seeded at 3,000 cells/cm^2 density on 96-well plates on day 0. On days 5, 7, and 9, the cells were fed with drug-free medium and subjected to the MTT assay on day 10.

The ProtoArray human protein microarrays (Invitrogen, Carlsbad, CA) contain more than 6,100 kinase substrates expressed as N-terminus GST fusion (www.invitrogen.com/protoarray). Purified FLAG-EL/CDK2 and FLAG-LMW-E/CDK2 complexes were produced in sf9 insect cells, purified by IP with FLAG-tagged antibody and eluted with 3X FLAG peptide (Sigma, St. Louis, MO). Arrays were incubated either with recombinant active EL/CDK2 or LMW-E/CDK2 at a concentration of 50 nM in the presence of ^{33}P-γ-ATP for 1 hour at 30°C. After washing and drying, arrays were exposed to X-ray film overnight. Imaging and data analysis were performed as recommended by the manufacturer. Briefly, the films were scanned to obtain 50 μm resolution and the arrays were aligned using the ProtoArray(R) Prospector Imager. The radioactive spots were quantified and analyzed using the ProtoArray(R) Prospector Analyzer, and the EL/CDK2 and LMW-E/CDK2 arrays were compared directly.

3.2i. Cyclin E/CDK2 substrate screening using ATP analog

pVL1392-hCDK2 F80G mutant was generated using the QuikChange XL site-directed mutagenesis (Qiagen) per instruction provided by the manufacturer. CDK2 (wild type and F80G), EL and LMW-E were expressed, purified from sf9 insect cells, and incubated with GST-Rb, ATP or PE- ATP-γ-S (BioSite, Täby, Sweden) at 30°C for 30 minutes. The samples were boiled with 2x sample buffer and separated by SDS-PAGE. The gel was fixed in 50% (v/v) ethanol in water with 10% (v/v) acetic acid and stained with 0.1% (w/v) Coomassie blue R350.

The ATP analog (PE-ATP-γS) can fit into the ATP pocket of the F80G CDK2 but not the wild-type CDK2 kinase. The replacement of the γ-phosphoryl oxygen with sulfur allows for specific tagging of the substrates with the thiophosphate group. Thio-containing groups can react with iodoacetyl-agarose to form covalent bond while unbound peptides are washed away. Thiophosphopeptides are specifically liberated by oxidation-promoted hydrolysis of the sulfur-phosphorus bond and recovered peptides can be analyzed by nanoscale liquid chromatography coupled to a Q TRAP tandem mass spectrometer.

3.2j. HAT activity colorimetric assay

To obtain purified proteins, pEXP-N-Myc-Hbo1 (wt, T88A, T88D), pEXP-N-SFB-(EL, LMW-E, CDK2) were transfected into HEK293T cells using LipoD293 transfection reagents (SignaGen, Rockville, MD) and lysates were harvested 24 hours later. The proteins were purified by IP using Myc-tag or FLAG-tag antibodies and purified Myc-tagged proteins were left on beads in 1x wash buffer, while purified FLAG-tagged proteins were eluted using 3X FLAG peptides (Sigma, St. Louis, MO). The HAT activity colorimetric assay kit was purchased from MBL International (Woburn, MA) and performed according to manufacturer's instructions. Briefly, purified proteins or 25 μg of HeLa nuclear extract (positive control supplied with the kit) were diluted in 40 μl water per well of 96-well plates. The samples were mixed with the assay mix, which contains 50 μl of 2X HAT assay buffer, 5 μl HAT substrate I, 5 μl HAT substrate II, and 5 μl NADH generating enzyme. The plates were incubated at 37°C for 2 hours and the samples were read at 440 nm using the Wallac-Victor3 multilabel plate reader (PerkinElmer, Waltham, MA).

3.2k. Lentiviral packaging and infection of shRNAs

All shRNA constructs were purchased from Thermo Scientific (Open Biosystem, Huntsville, AL). To generate lentivirus expressing shRNAs, HEK293T cells were co-transfected with pCMVdeltaR8.2, pMD2.G, and pGIPZ-(empty, shGAPDH, or shHbo1) using LipoD293 transfection reagents (SignaGen, Gaithersburg, MD). The supernatants containing the virus were filtered through 0.45 μm filter and directly added to cells for infection. GFP expression was confirmed prior to selection with 0.5 μg/ml puromycin.

3.3. RESULTS

3.3a. LMW-E-expressing tumor cells exhibit reduced cell-cell contact and enhanced invasion

One unique feature of mammary epithelial cells is that they tend to form isolated islands when cultured as a monolayer by forming tight junctions with nearby cells. In the previous chapter, we have extensively described the tumorigenic

phenotypes of hMECs with exogenous LMW-E expression through 3 serial *in vivo* passaging generations. In addition to deregulating mammary acinar morphogenesis, we observed that the TDCs display reduced cell-cell contact by growing further away from neighbor cells. To examine cell-cell adhesion, the TDCs were immunostained with E-cadherin, a transmembrane protein that maintains cell adhesion by ensuring that the cells within a tissue are bound together. Figure 20A clearly shows that the LMW-E-expressing cells demonstrate dramatically reduced E-cadherin expression, particularly at the membrane junction, while the parental 76NE6 cells display strong membranous E-cadherin staining (white arrows). Downregulation of E-cadherin protein levels are confirmed by Western blot analysis demonstrating that cells with LMW-E expression have reduced E-cadherin protein levels (Figure 20B & C).

Cellular invasion is one of the critical events leading to successful metastasis and requires migration of the tumor cells through the basement membrane to invade the surrounding tissues (298). Given that E-cadherin regulates cellular adhesion, downregulation of E-cadherin is known to be associated with tumor progression and metastasis. Cells with E-cadherin knockdown are more motile resulting in their enhanced ability to penetrate the basement membrane and thus invade into surrounding tissues to form metastasis (299, 300). The Boyden chamber invasion assay was performed to investigate whether LMW-E expression enhances cellular invasiveness. The cells were seeded on a microporous transwell insert on top of a thin layer of Matrigel with fibronectin on the other side of the membrane to act as a chemo-attractant. After 24 hours, the cells that have invaded to the bottom side of the membrane were stained with crystal violet for visualization. Figure 20D shows that while the vector control cells were unable to invade through the Matrigel basement membrane, cells with cyclin E expression were highly invasive. More specifically, quantification of the invaded cells demonstrate that while all cells with cyclin E expression invade significantly more than vector control cells, the 76NE6-LMW-E and TDCs combined invade significantly more than the 76NE6-EL cells ($p < 0.05$) (Figure 20E). Collectively, we provide evidence suggesting that overexpression of LMW-E downregulates E-cadherin expression and thereby

Figure 20

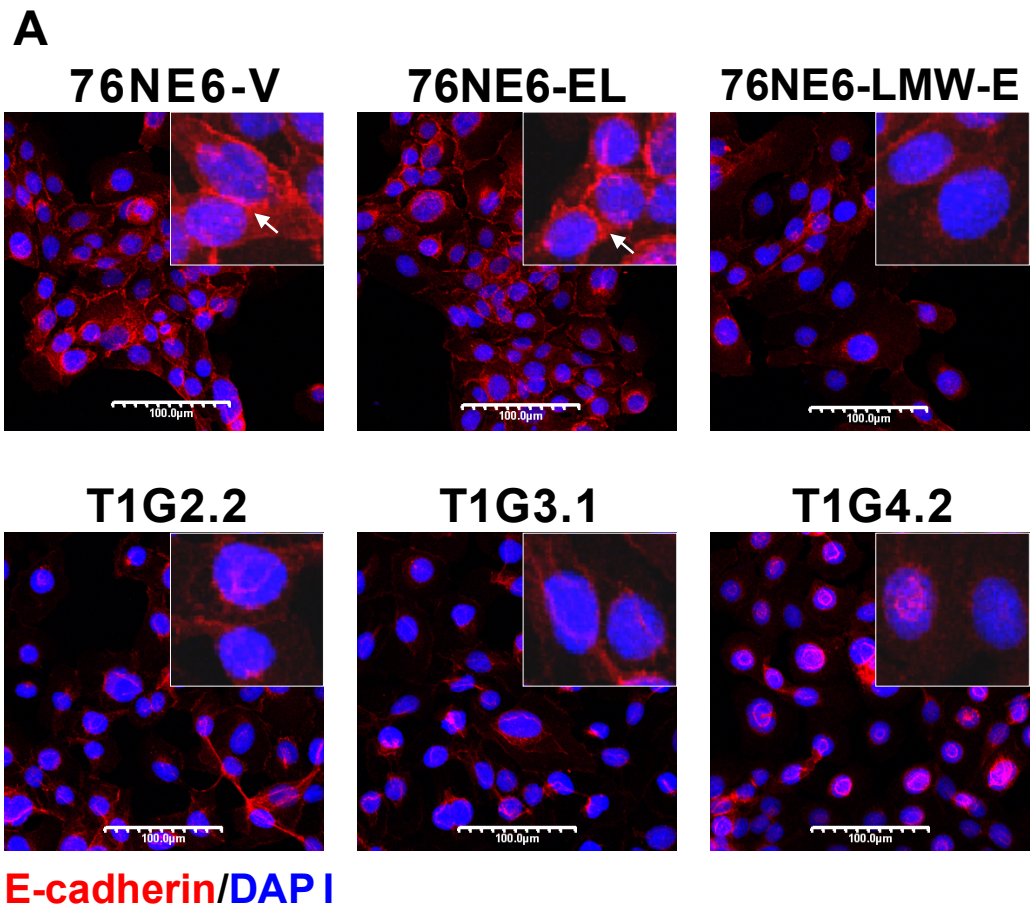
A
76NE6-V
76NE6-EL
76NE6-LMW-E
T1G2.2
T1G3.1
T1G4.2
E-cadherin/DAPI

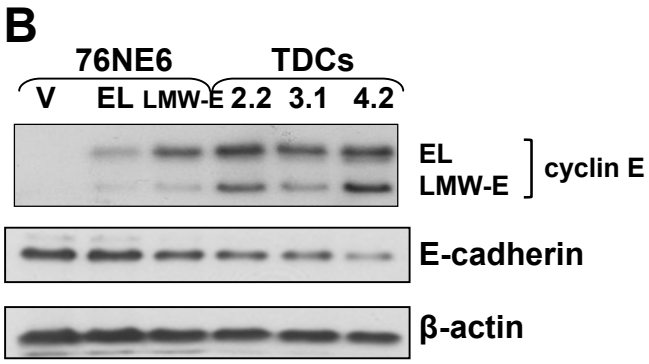
B
76NE6
TDCs
V
EL
LMW-E
2.2
3.1
4.2
EL
LMW-E
cyclin E
E-cadherin
β-actin

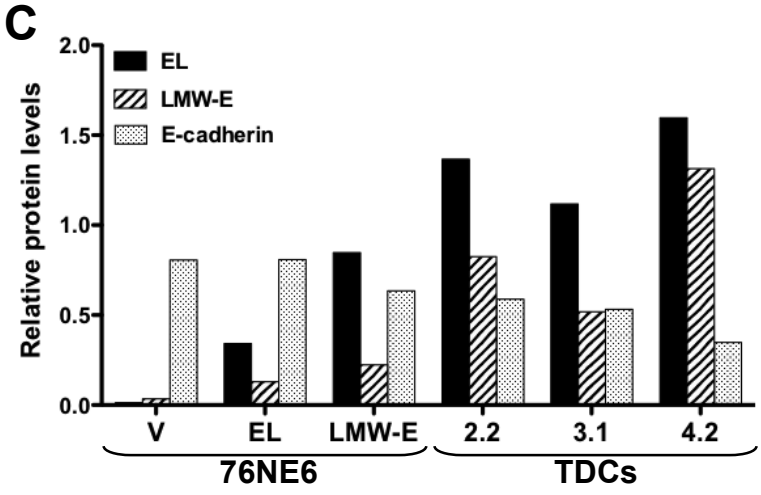
C
Relative protein levels
2.0
1.5
1.0
0.5
0.0
EL
LMW-E
E-cadherin
V
EL
LMW-E
2.2
3.1
4.2
76NE6
TDCs

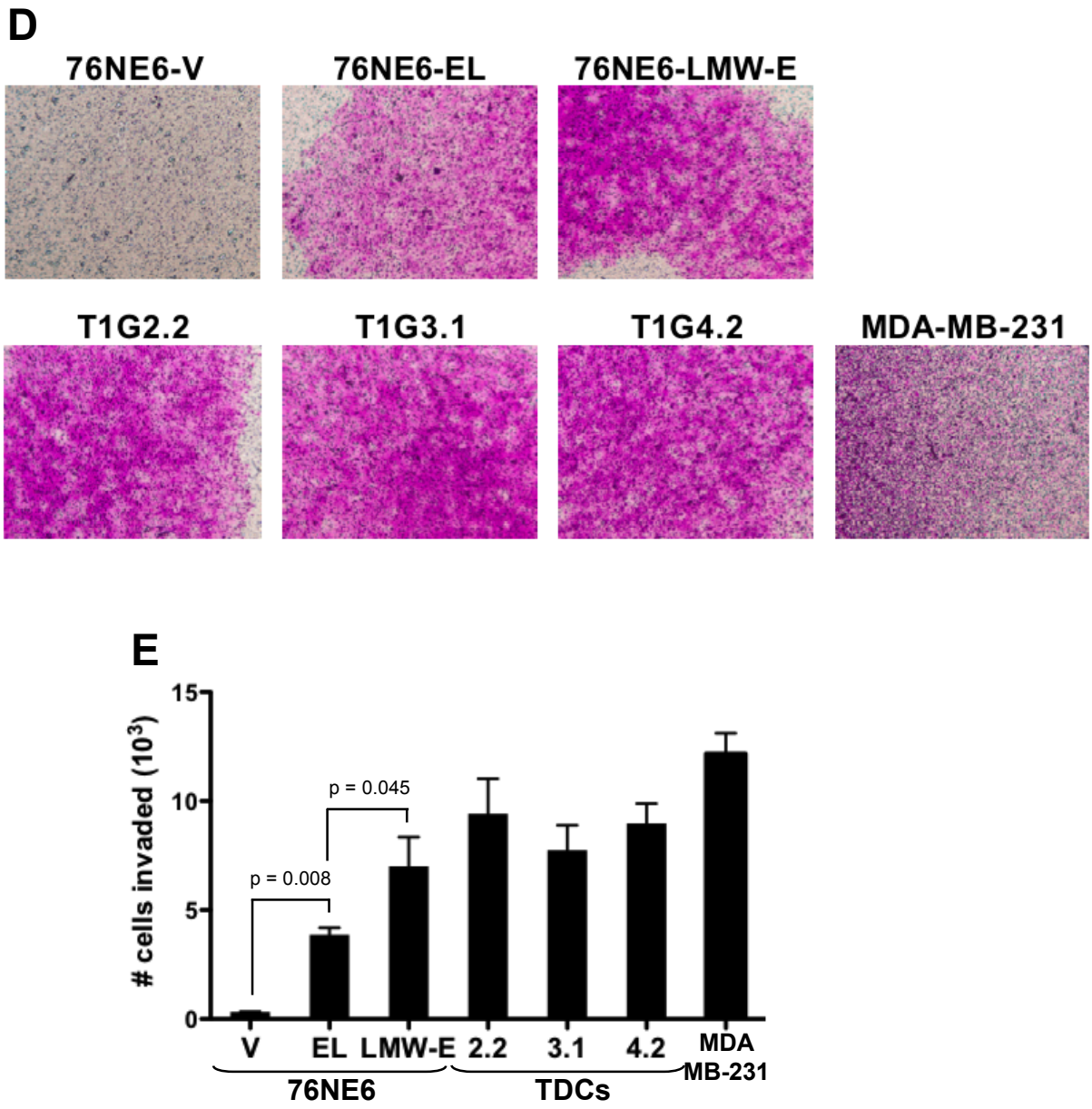

Figure 20: LMW-E-expressing tumor cells exhibit reduced cell-cell contact and enhanced invasion. (A) Cells were fixed and immunostained with E-cadherin antibody and nuclei were counterstained with DAPI (scale bar = 100 μm). (B) Lysates were extracted and subjected to Western blot analysis with antibodies against cyclin E, E-cadherin, and β-actin. (C) Densitometric values of the Western blot analysis. (D) Cells were seeded on Matrigel-coated transwell chamber and incubated on top of fibronectin-containing media for 24 hours. The cells on top of the membrane were removed and the cells remaining on the bottom were stained with crystal violet and images were taken with a light microscope. (E) After 24 hours incubation, the cells on the bottom of the transwell were collected and counted. Statistical analysis used was unpaired student's *t*-test.

enhance the invasiveness of hMECs.

3.3b. LMW-E activates gene expression associated with the EMT

Loss of cell-cell contact and reduced E-cadherin expression typically signify that the cells have undergone the morphogenetic reprogramming from epithelial to mesenchymal phenotype, which is commonly known as the epithelial-mesenchymal transition or EMT. The EMT is an epigenetic process that involves modulation of numerous transcription factors to transform the cells from epithelial to mesenchymal characteristic to allow them to migrate and invade through the basement membrane. The transcriptional levels of genes known to be involved in the EMT were analyzed by realtime qRT-PCR. Firstly, analysis of cyclin E mRNA level confirmed high expression in the 76NE6-LMW-E and the TDCs and these cells exhibited downregulation of E-cadherin (Figure 21A & B). Furthermore, in the cells that show high cyclin E expression, they also upregulate N-cadherin, twist, slug, and vimentin mRNA levels, which are the genes associated with the EMT (Figure 21C-F). Interestingly, we observed that the levels of cyclin E protein as well as mRNA transcript were much higher in the 76NE6-LMW-E cells compared to the 76NE6-EL cells (Figure 20B, 20C & 21A), which is a phenomenon that was also observed in the transgenic mouse model with overexpression of LMW-E. We speculate that high LMW-E protein levels may lead to hyperactive G1-S transition causing a positive feedback loop through activation of E2F, and increased E2F activity has been shown to stabilize cyclin E by reducing conjugation with ubiquitin (301). Additionally, cyclin E transcription has been reported to be positively regulated by the E2F transcription factor, and in fact, the cyclin E promoter does contains several E2F binding sites (302). Taken together, exogenous LMW-E expression in the 76NE6 cells resulted in reduced cell-cell adhesion and induced transcriptional changes that are featured as the EMT.

3.3c. LMW-E expression enriches for the $CD44^{hi}/CD24^{lo}$ population

As the connection between induction of the EMT and generation of cells with CSC properties was recently demonstrated, we suspect that the tumorigenicity of

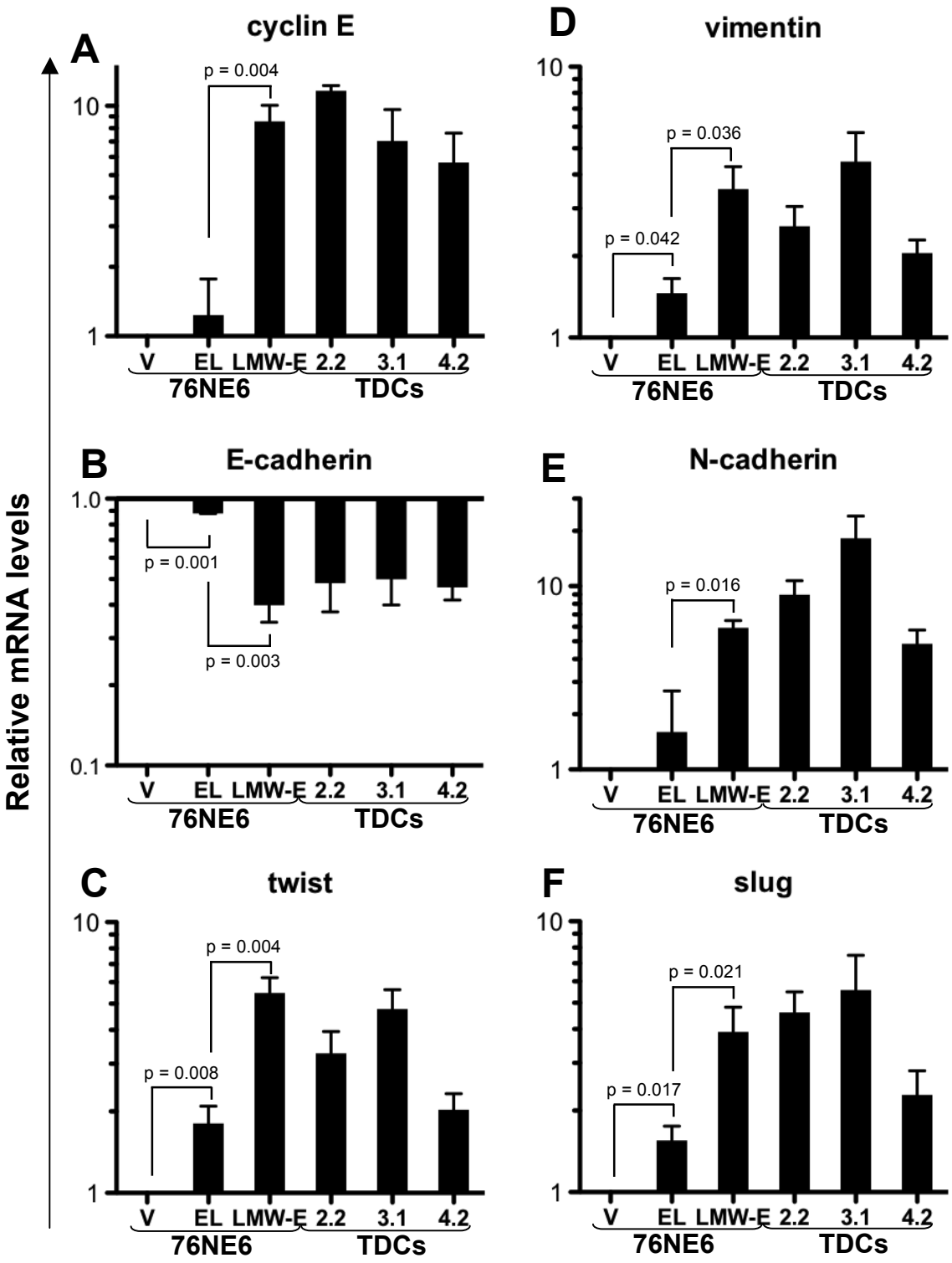

Figure 21: LMW-E activates gene expression associated with the EMT. (A – F) Cells were grown in monolayer culture to 70% confluency and RNA were extracted and subjected to qRT-PCR analysis for the mRNA levels of cyclin E (A), E-cadherin (B), twist (C), vimentin (D), N-cadherin (E), and slug (F). These values were normalized against GAPDH mRNA levels and statistical analysis used was unpaired student's *t*-test.

LMW-E could be due to its ability to induce the EMT and enrich for CSCs. To date, many surface markers have been demonstrated to be unique CSC markers, and $CD44^{hi}/CD24^{lo}$ is the best well-established markers for mammary CSCs. We aim to investigate whether ectopic expression of EL or LMW-E in the 76NE6 cells and whether *in vivo* passaging of these cells would enrich for this population. The cells were stained using antibodies to the surface markers CD24 and CD44 that are conjugated to different fluorophores, and their relative expression levels were measured by FACS analysis (Figure 22).

The majority of the 76NE6-vector cells were $CD44^{hi}/CD24^{hi}$ with only 1.5% of the population was $CD44^{hi}/CD24^{lo}$ (Figure 22A & B). While stable expression of EL increased the $CD44^{hi}/CD24^{lo}$ population to approximately 10%, the 76NE6-LMW-E cells have significantly more $CD44^{hi}/CD24^{lo}$ population compared to the 76NE6-EL cells ($p = 0.001$) (Figure 22A & B). The difference was more remarkable in the TDCs, in which most of the clones contained approximately 10 folds higher of this CSC population. Furthermore, Western blot analysis using CD24 and CD44 antibodies confirmed that indeed LMW-E-expressing cells downregulated CD24 and upregulated CD44 protein levels (Figure 22C). Since *in vivo* passaging led to enhancement of LMW-E expression as well as enrichment for the $CD44^{hi}/CD24^{lo}$ population, we believe that cyclin E may be involved in selecting for this CSC population. In fact, correlation analysis revealed that cyclin E expression level positively correlate with the $CD44^{hi}/CD24^{lo}$ population with $R^2 = 0.853$ ($p < 0.0001$) indicating that cells with high cyclin E expression are also statistically likely to be $CD44^{hi}/CD24^{lo}$ (Figure 22D).

3.3d. Cytoplasmic cyclin E expression correlates with high $CD44^{hi}/CD24^{lo}$ population in breast cancer patient tissue

Given that cyclin E expression positively associates with the $CD44^{hi}/CD24^{lo}$ population in hMECs, we now aim to determine whether this correlation also exists in breast cancer patient samples. A total of 118 breast cancer patient tissues were analyzed for the CD24 and CD44 expression by double IHC staining on the tissue sections and visualized with 3,3'-Diaminobenzidine (DAB) and permanent red,

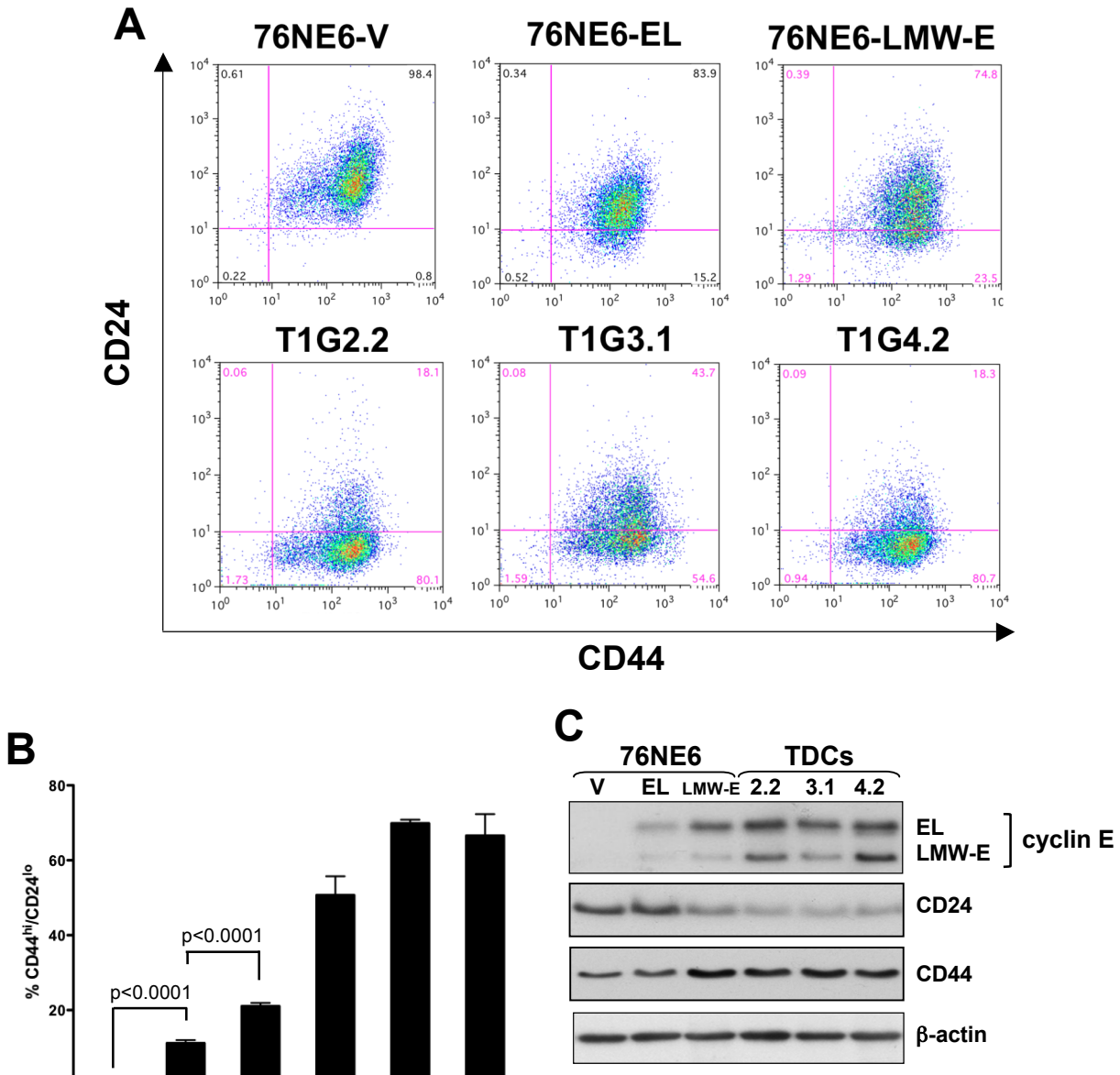

Figure 22: LMW-E expression enriches for the CD44^{hi}/CD24^{lo} population. (A & B) Cells were incubated with PE-CD24 and APC-CD44 antibodies and analyzed with a FACS Calibur. Statistical analysis used was unpaired student's *t*-test. (C) Lysates were extracted and subjected to Western blot analysis with antibodies against cyclin E, CD24, CD44, β-actin. (D) Percent of CD44^{hi}/CD24^{lo} population were subjected to correlation analysis versus cyclin E mRNA levels.

respectively (Figure 23A). The slides were given a score of 0 to 5 that correspond to a range of the percentage of the $CD44^{hi}/CD24^{lo}$ population as follows: 0 (0%), 1 (1-10%), 2 (11-25%), 3 (26-50%), 4 (51-75%), 5 (76-100%). In addition, these same tissue slides were also subjected to IHC staining using antibody to cyclin E (Figure 23B). We scored the cyclin E staining based on its intensity as well as localization. Breast tumors were considered negative when no staining was detected either in the nucleus or in the cytoplasm (score = 1). Among the cases evaluated as cyclin E positive, if the score assigned to the nucleus exceeded the score assigned to the cytoplasm, cyclin E expression was considered predominantly nuclear (score = 2). When the nucleus and the cytoplasm received equal scores, cyclin E expression was considered both nuclear and cytoplasmic (score = 3). If cytoplasmic staining was graded higher than nuclear staining, cyclin E expression was considered predominantly cytoplasmic (score = 4). Lastly, lysates prepared from these patient samples were also analyzed for the protein levels of EL and LMW-E by Western blot followed by densitometric analysis (Figure 23C). Statistical analysis was applied to data obtained from 1) CD24/CD44 double IHC staining, 2) cyclin E IHC staining, and 3) EL versus LMW-E protein levels from Western blot analysis.

Statistical analysis revealed that more than 60% of the patient tissues contain less than 10% of the $CD44^{hi}/CD24^{lo}$ population, and this patient distribution was similar to that previously reported (Table 9) (289). More specifically, we found that cytoplasmic staining of cyclin E significantly correlated with high percentage of the $CD44^{hi}/CD24^{lo}$ population ($p = 0.0435$), and the fact that the patient sample was relatively small further demonstrates the strength of the relationship between these two factors (Figure 24A). In fact, when cytoplasmic versus nuclear cyclin E IHC scores were compared with the densitometry values from Western blot analysis of the patient tissues, we found that high LMW-E expression levels significantly associated with cytoplasmic cyclin E staining ($p = 0.0194$) while full-length and total cyclin E expression levels did not (Figure 24B-D). Since LMW-E lacks an N-terminal nuclear signal sequence, previous report has shown that LMW-E preferentially accumulates in the cytoplasm, and these results further support this observation (169). In conclusion, similar to our cell line data, breast cancer patients who have

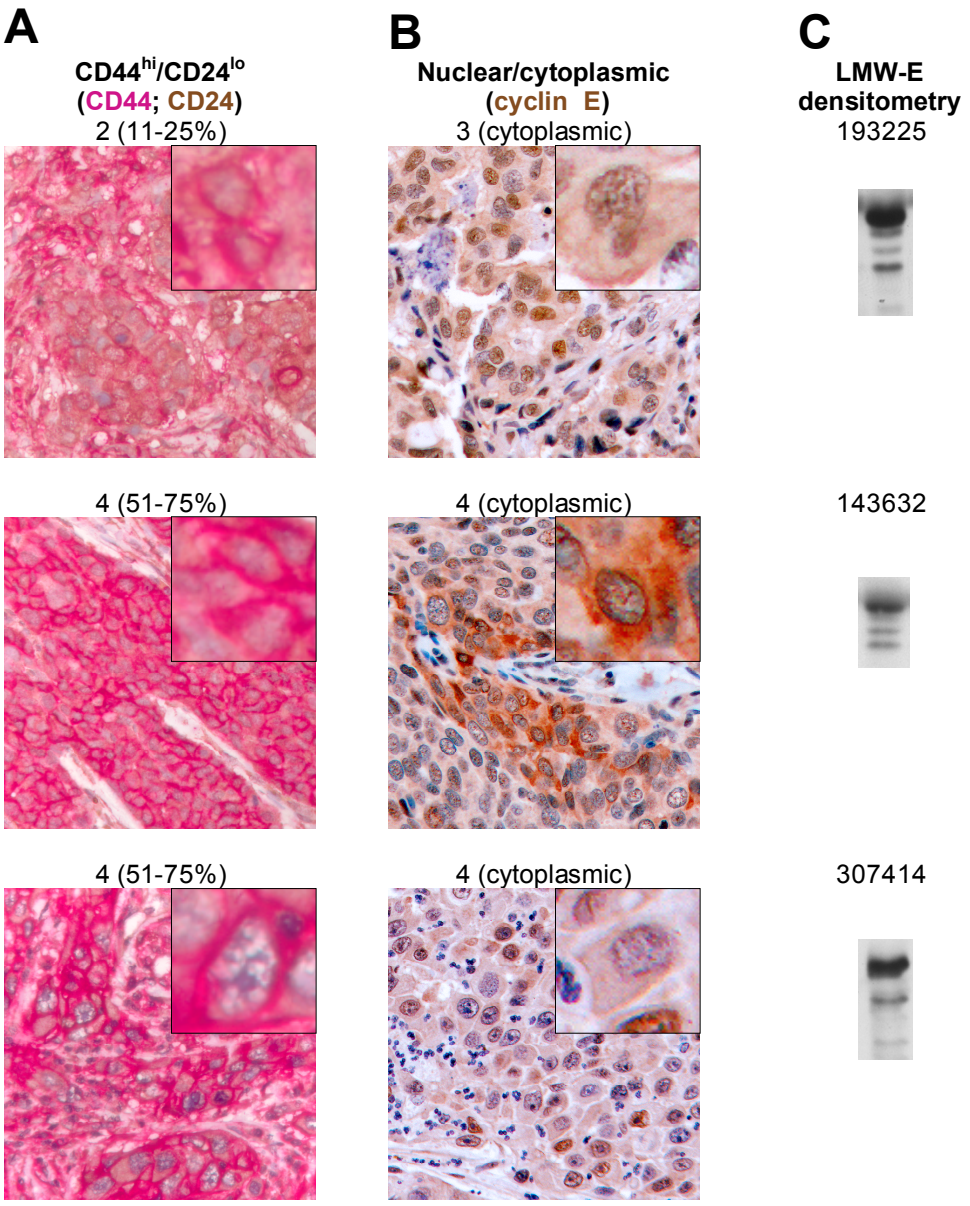

Figure 23: IHC analysis for CD24, CD44 and cyclin E expression in breast cancer patient samples. (A) A total of 118 breast cancer patient tissue slides were subjected to IHC double staining with CD24 and CD44 antibodies and scored for %CD44^{hi}/CD24^{lo}. (B) IHC single staining using cyclin E antibody and scored with respect to intensity as well as cytoplasmic versus nuclear localization (1: no staining, 2: nuclear > cytoplasmic, 3: nuclear = cytoplasmic, 4: nuclear < cytoplasmic). The slides were scored blindly by 2 independent investigators. (C) Cyclin E EL and LMW-E protein levels were measured by Western blot analysis from breast cancer patient tissues and quantified by densitometry. Shown here are representative samples to illustrate the IHC staining that reflect the scoring assigned and the LMW-E protein levels by densitometry.

Table 9. $CD44^{hi}/CD24^{lo}$ patient distribution		
Score (%$CD44^{hi}/CD24^{lo}$)	**N**	**%**
0 (0%)	37	31
1 (1 – 10%)	35	30
2 (11 – 25%)	20	17
3 (25 – 50%)	14	12
4 (51 - 75%)	10	8
5 (76 – 100%)	2	2
total	118	100
The CD24 and CD44 double staining was given a score from 0 to 5 for the respective percentage of $CD44^{hi}/CD24^{lo}$ population in the tissue slide. At least 3 images from different regions of each patient slide were scored and averaged. N represents number of patients and % is the percentage of total patient population with that particular score.		

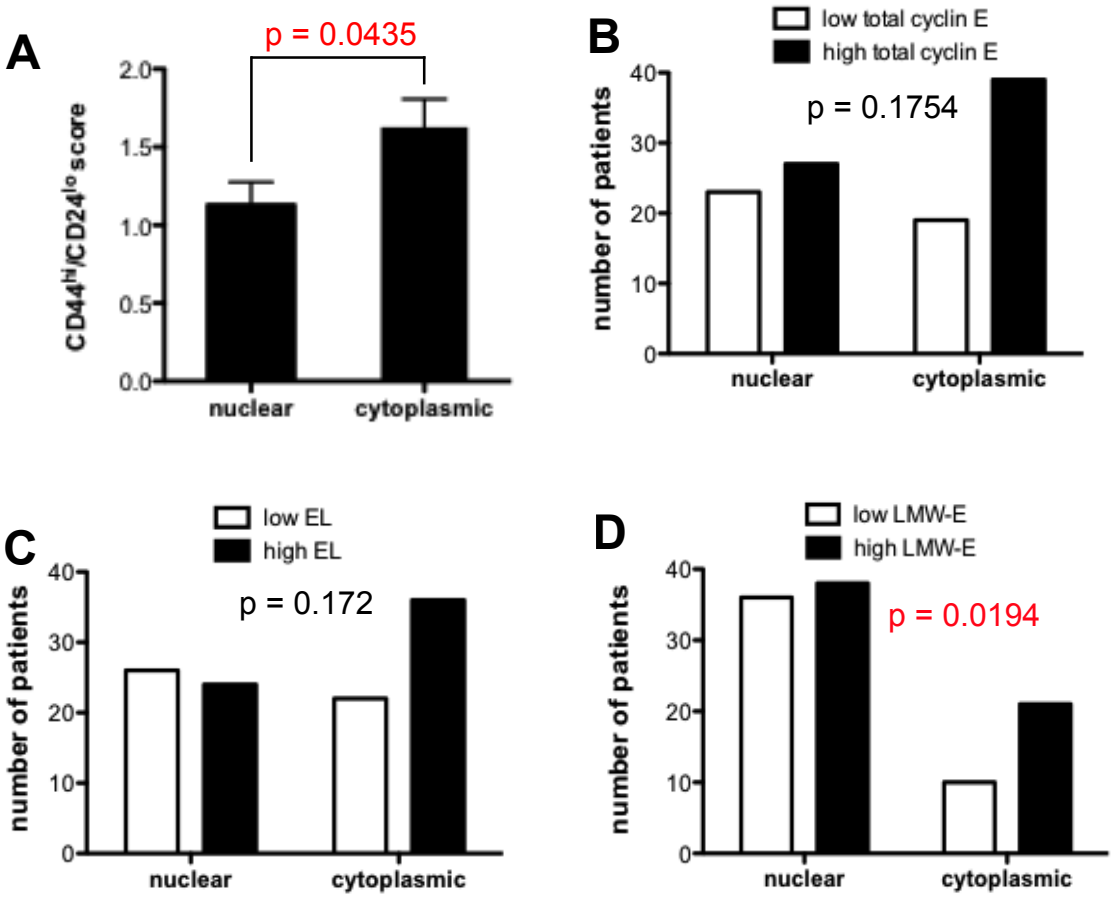

<u>Figure 24:</u> Cytoplasmic cyclin E expression correlates with high CD44^{hi}/CD24^{lo} score in breast cancer patient tissue. (A Patient tissues were subjected to IHC analysis using CD24, CD44, and cyclin E antibodies. The CD44^{hi}/CD24^{lo} scores were correlated to the nuclear versus cytoplasmic cyclin E staining scores. Statistical analysis used was unpaired student's *t*-test. The cyclin E nuclear and cytoplasmic staining scores were correlated with total cyclin E (B), EL (C), and LMW-E (D) protein levels from densitometry of Western blot analysis. Statistical analysis used was Pearson's chi-square test.

high $CD44^{hi}/CD24^{lo}$ population significantly correlate with cytoplasmic cyclin E, and we have demonstrated that cytoplasmic cyclin E protein represents the LMW isoforms.

3.3e. LMW-E-expressing cells exhibit enhanced anchorage-independent growth, self-renewal capability, and ALDH activity

LMW-E expression increased with *in vivo* passaging suggesting that perhaps LMW-E provided oncogenic advantage to tumor-initiating cells that will continue to select for those cells possessing tumorigenic phenotypes such as transformation. Anchorage independent growth is one of the characteristics of neoplastic cellular transformation and is traditionally tested by culturing cells on soft agar medium. The cells were embedded in between 2 layers of soft agar at 200 cells/cm^2 density. After 15 days in culture, the plates were stained with crystal violet and automatically counted using the GelCount software. As expected, the LMW-E-expressing cells formed more transformed colonies compared to cells with vector and EL expression (Figure 25A). To confirm that the $CD44^{hi}/CD24^{lo}$ cells have higher tumorigenic potential than the $CD44^{hi}/CD24^{hi}$ cells, these cells were sorted into these 2 respective populations and subjected to soft agar transformation assay. The results obtained clearly demonstrated that the sorted $CD44^{hi}/CD24^{lo}$ population was able to form much more colonies than unsorted cells, and the $CD44^{hi}/CD24^{hi}$ population was unable to sustain growth on soft agar (Figure 25A). These observations may explain the ability of LMW-E-expressing cells to form tumor *in vivo* due to the high $CD44^{hi}/CD24^{lo}$ population that allow them to grow in the absence of a basement membrane compared to EL-expressing cells.

In addition to the $CD44^{hi}/CD24^{lo}$ population, mammary CSCs also possess self-renewal capability and thus a single cell can give rise to multiple lineages of more differentiated cell types to form a mammosphere (277). Although similar to the soft agar transformation assay in some aspects, the mammosphere formation assay specifically tests the ability of cells to grow in an ultra-low attachment dish in the presence of high EGF and no serum, which is a non-differentiating culture condition. CSCs are able to undergo proliferation and self-renewal to form a floating colony

Figure 25

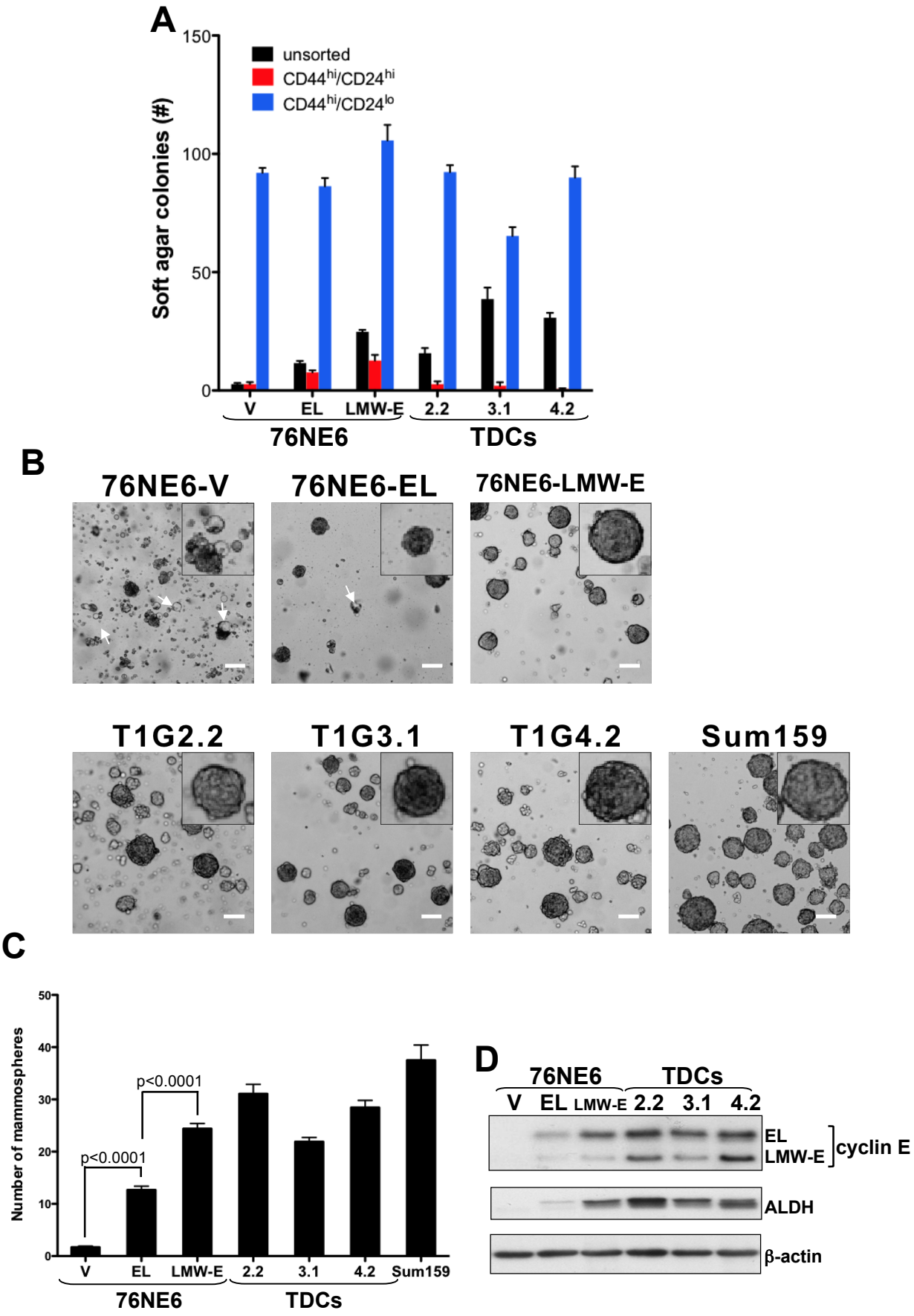
A
Soft agar colonies (#)
150
100
50
0
unsorted
CD44hi/CD24hi
CD44hi/CD24lo
V
EL
LMW-E
2.2
3.1
4.2
76NE6
TDCs
B
76NE6-V
76NE6-EL
76NE6-LMW-E
T1G2.2
T1G3.1
T1G4.2
Sum159
C
Number of mammospheres
50
40
30
20
10
0
p<0.0001
p<0.0001
V
EL
LMW-E
2.2
3.1
4.2
Sum159
76NE6
TDCs
D
76NE6
TDCs
V
EL
LMW-E
2.2
3.1
4.2
EL
LMW-E
cyclin E
ALDH
β-actin

Figure 25

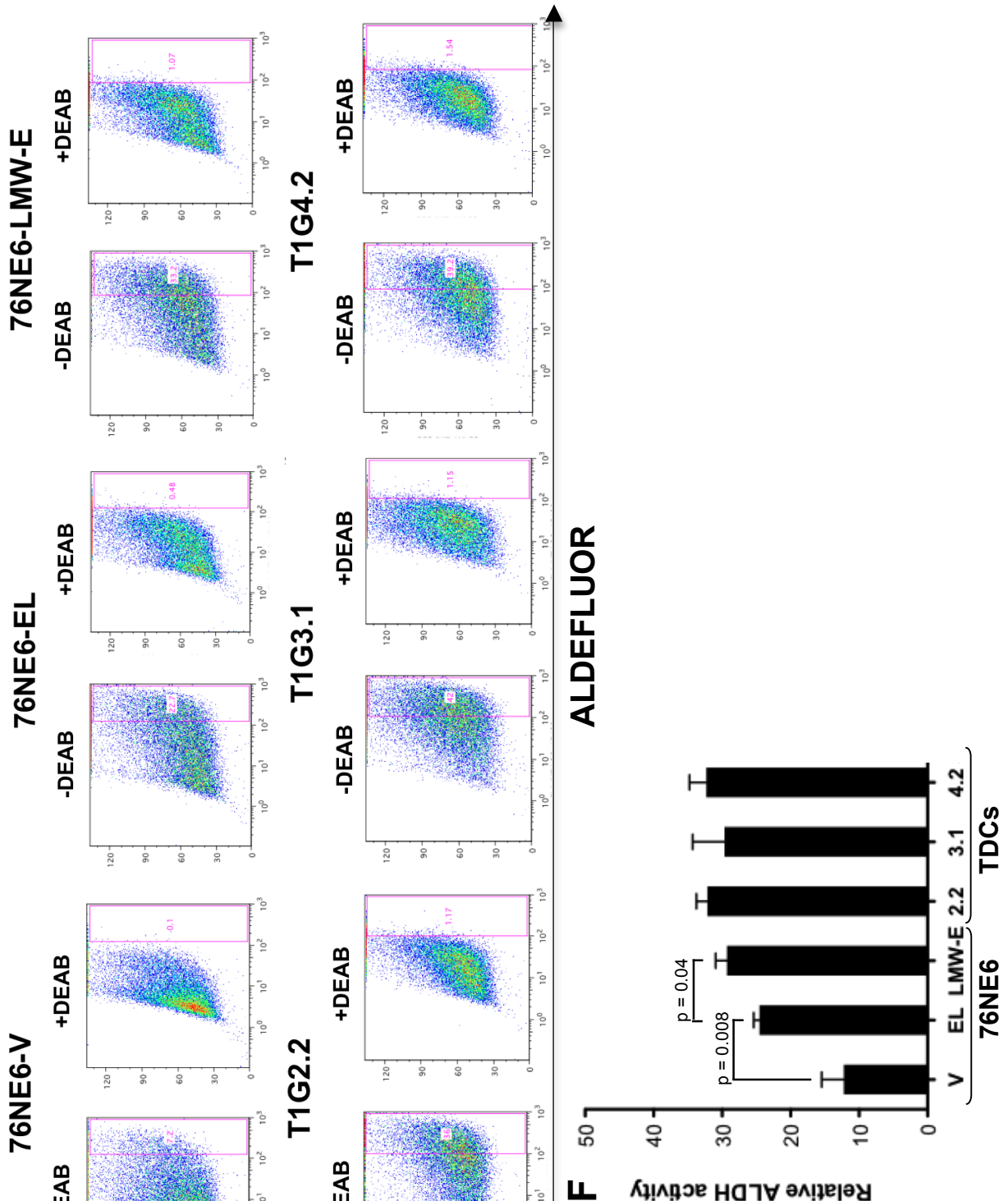
E
SSC
76NE6-V
76NE6-EL
76NE6-LMW-E
-DEAB
+DEAB
T1G2.2
T1G3.1
T1G4.2
ALDEFLUOR
F
Relative ALDH activity
p = 0.008
p = 0.04
V
EL
LMW-E
2.2
3.1
4.2
76NE6
TDCs

<u>Figure 25:</u> LMW-E-expressing cells exhibit enhanced anchorage-independent growth, self-renewal capability, and ALDH activity. (A) Anchorage-independent growth was tested by culturing cells in soft agar medium. Unsorted cells and cells stained with CD24 and CD44 conjugated antibodies and sorted for the $CD44^{hi}/CD24^{hi}$ and $CD44^{hi}/CD24^{lo}$ populations were seeded in soft agar culture. After 15 days in culture, the colonies were stained with crystal violet and counted using the GelCount program. (B) Representative brightfield images of cells cultured on ultra-low attachment plates for 7 days (scale bar =100 μm). The vector control cells undergo apoptosis as apparent by extensive membrane blebbing (white arrows). (C) MTT solution was added to the mammosphere cultures at 500 μg/ml concentration and incubated at 37^{o}C for 1 hour. Number of mammospheres were quantified using the automated GelCount program and statistical analysis used was unpaired student's *t*-test. (D) Lysates from mammosphere cultures were extracted and subjected to Western blot analysis with antibodies to cyclin E, ALDH, and β-actin. (E & F) ALDELUOR assay was performed on cells grown on monolayer. For each sample, 500,000 cells were incubated with the ALDH substrate alone or with the ALDH inhibitor (DEAB) and subjected to FACS analysis. The ALDH activity is obtained by subtracting the DEAB inhibitor value and the statistical analysis used was unpaired student's *t*-test.

while differentiated epithelial cells undergo anoikis, which is apoptosis due to lack of basement membrane attachment (277). As expected, the 76NE6-vector control cells underwent apoptosis as apparent by extensive membrane blebbing (Figure 25B). In contrast, the 76NE6-LMW-E and the TDCs were able to form larger and more mammospheres compared to those formed by the 76NE6-EL cells (Figure 25B). Sum159 is a breast cancer cell line that has been shown to contain very high percentage of the $CD44^{hi}/CD24^{lo}$ population and form very robust and reliable mammospheres and therefore are used in this experiment as a positive control (303). To quantify the number of mammospheres formed and confirm the viability of the cells in these structures, MTT (3-(4,5-Dimethylthiazol-2-yl)-2,5-diphenyltetrazolium bromide) was added to the cells after 7 days in culture and the viable colonies were automatically counted using the GelCount software. Statistical analysis revealed that cells with LMW-E expression formed significantly more mammospheres than cells with full-length cyclin E expression ($p < 0.05$) (Figure 25C).

High ALDH protein and enzymatic levels are found to be associated with CSC phenotypes such as high $CD44^{hi}/CD24^{lo}$ population and mammosphere formation (278). Western blot analysis of the mammosphere cultures showed that the 76NE6-LMW-E cells and the TDCs indeed express high LMW-E and ALDH protein levels compared to the 76NE6-EL and vector control cells (Figure 25D). Therefore, we subjected the cells to the ALDEFLUOR assay to measure the ALDH enzymatic activity by FACS analysis. Briefly, the cells were incubated with Bodipy-aminoacetaldehyde (BAAA), an ALDH substrate that can freely diffuse across the plasma membrane (304). The presence of ALDH inside the cell catalyzes the substrate into Bodipy-aminoacetate (BAA), which is fluorescent and can be detected with flow cytometry. Diethylamino-benzaldehyde (DEAB) is an inhibitor of ALDH and is used to normalize the ALDH activity. The results obtained showed that the 76NE6-LMW-E cells and the TDCs exhibit high ALDH activity compared to the 76NE6-EL and vector control cells (Figure 25E). Statistical analysis demonstrated that the LMW-E-expressing cells have higher ALDH enzymatic activity compared to cells expressing EL ($p < 0.05$) (Figure 25F). Collectively, the evidences presented

here suggest that LMW-E enriches for cells with CSC properties by upregulating the ALDH activity level and enabling hMECs to survive and undergo self-renewal in the absence of basement membrane attachment thus explaining the enhanced tumorigenicity of LMW-E over full-length cyclin E.

3.3f. Doxorubicin synergizes with salinomycin to kill LMW-E-expressing tumor cells

Salinomycin is a pharmacological agent recently identified from a large screen of small molecule inhibitors to specifically kill CSCs (297). Particularly, breast cancer cells treated with salinomycin demonstrated a decrease in the $CD44^{hi}/CD24^{lo}$ population, reduction in their ability to form mammospheres, and the 4T1 xenograft tumors formed less metastasis compared to parallel paclitaxel treatment (297). Therefore, we aim to determine whether salinomycin can specifically target the $CD44^{hi}/CD24^{lo}$ population in the tumor cells with LMW-E expression. The cells were treated with salinomycin for 4 days and then allowed to recover in drug-free medium for 3 days (Figure 19A). The cells were then harvested and stained with PE-CD24 and APC-CD44 conjugated antibodies, and the $CD44^{hi}/CD24^{lo}$ population was measured by FACS analysis. The results showed that salinomycin treatment reduced the $CD44^{hi}/CD24^{lo}$ population in a dose dependent manner (Figure 26A). More specifically, the TDCs contain approximately 80% of the $CD44^{hi}/CD24^{lo}$ population in which only 10% of these cells remained after treatment with 8 μM salinomycin. Additionally, salinomycin treatment also effectively disrupted their ability to form mammospheres (Figure 26B). Similar to the results previously published, we also showed that salinomycin demonstrated high effectiveness in targeting the phenotypes associated with CSCs that are induced with LMW-E expression (297).

Most highly proliferative cancer cells are sensitive to conventional chemotherapies drugs while CSCs are believed to be more resistant to them thus resulting in high frequency of tumor relapse (293). Doxorubicin, a common chemotherapeutic agent, is an anthracycline antibiotic, which functions by intercalating DNA and thereby inhibits DNA replication. As anticipated, doxorubicin

Figure 26

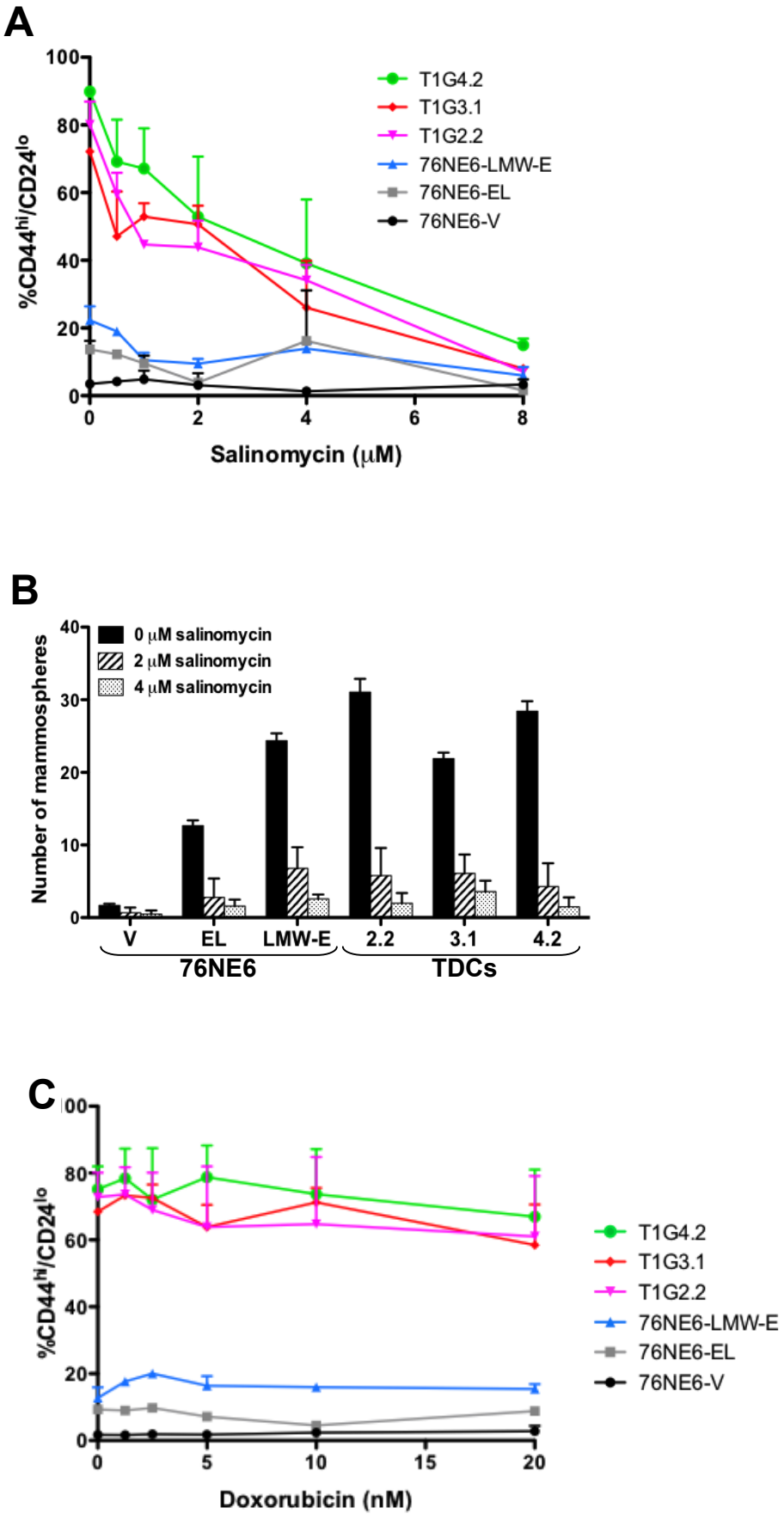
A
100
80
60
40
20
0
%CD44hi/CD24lo
0
2
4
6
8
Salinomycin (μM)
T1G4.2
T1G3.1
T1G2.2
76NE6-LMW-E
76NE6-EL
76NE6-V
B
40
30
20
10
0
Number of mammospheres
0 μM salinomycin
2 μM salinomycin
4 μM salinomycin
V
EL
LMW-E
2.2
3.1
4.2
76NE6
TDCs
C
100
80
60
40
20
0
%CD44hi/CD24lo
0
5
10
15
20
Doxorubicin (nM)
T1G4.2
T1G3.1
T1G2.2
76NE6-LMW-E
76NE6-EL
76NE6-V

Figure 26

D

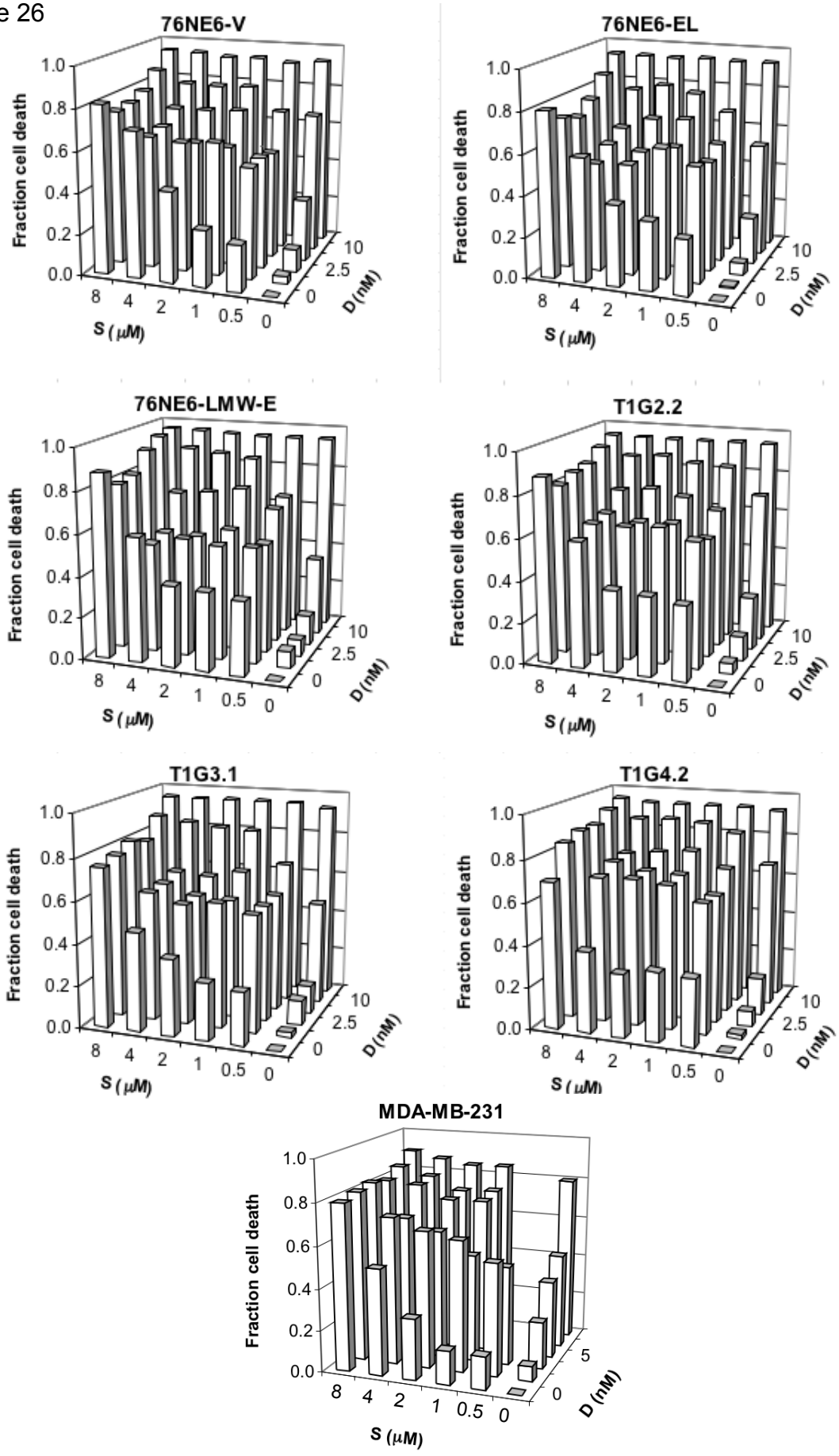
76NE6-V
76NE6-EL
76NE6-LMW-E
T1G2.2
T1G3.1
T1G4.2
MDA-MB-231
Fraction cell death
1.0
0.8
0.6
0.4
0.2
0.0
S (μM)
8
4
2
1
0.5
0
D (nM)
10
2.5
0
5

Figure 26

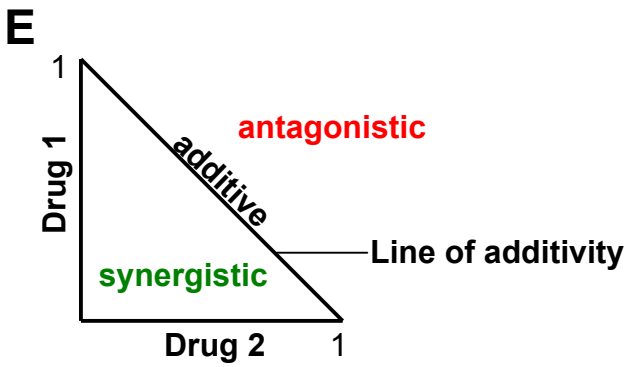
E
1
Drug 1
antagonistic
additive
synergistic
Line of additivity
Drug 2
1

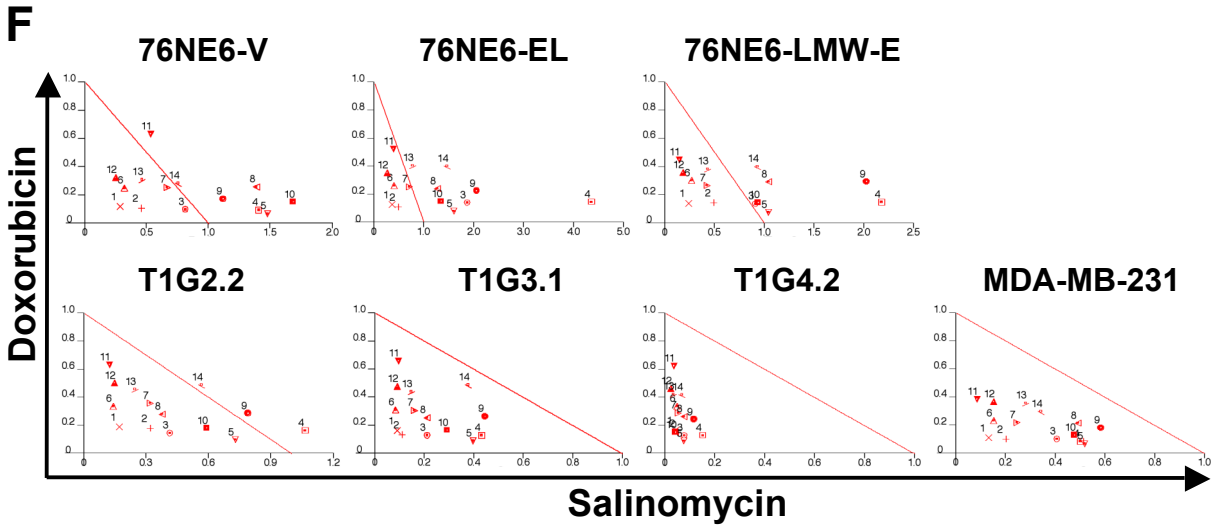
F
76NE6-V
76NE6-EL
76NE6-LMW-E
T1G2.2
T1G3.1
T1G4.2
MDA-MB-231
Doxorubicin
Salinomycin

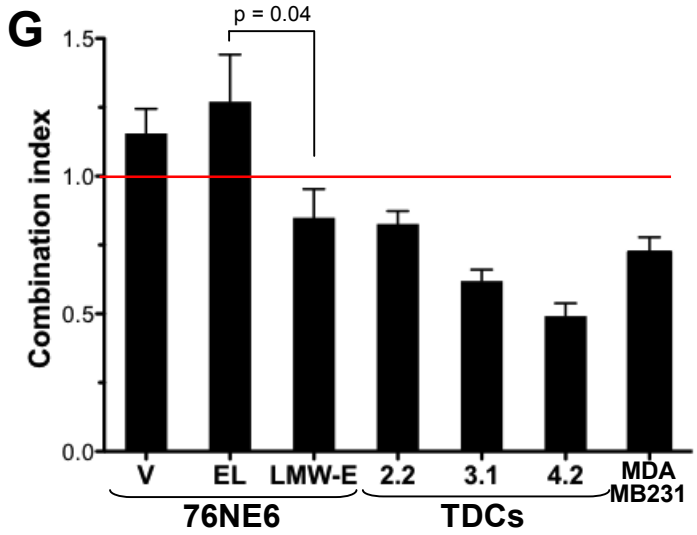
G
p = 0.04
Combination index
1.5
1.0
0.5
0.0
V
EL
LMW-E
2.2
3.1
4.2
MDA MB231
76NE6
TDCs

Figure 26: Doxorubicin synergizes with salinomycin to kill LMW-E-expressing tumor cells. (A) Cells were seeded on monolayer for 24 hours and treated with salinomycin for 4 days with the drug-containing media replaced every 48 hours. After 3 days of recovery in drug-free medium, the cells were trypsinized and stained for PE-CD24 and APC-CD44 antibodies and analyzed by FACS analysis. (B) Cells were seeded on ultra-low attachment plates on day 0 and then treated with salinomycin on days 1 and 3. On day 7, MTT solution was added to the mammosphere cultures and incubated at 37^{o}C for 1 hour. Number of mammospheres were quantified using the automated GelCount program. (C) Cells were seeded on monolayer for 24 hours and treated with doxorubicin and analyzed by FACS as in (A). (D) HTSA was performed to examine the toxicity of combining doxorubicin and salinomycin. Cells were seeded at 3000 cells/cm^2 density in 96-well plates on day 0, treated with doxorubicin on day 1 and then with salinomycin on day 3, and allowed to recover for 5 days in drug-free medium. On day 11, MTT solution was added to the cells and cell viability was measured at 590nm absorbance using a spectrophotometer. (E) An isobologram illustrates the effects of the combined drugs calculated from the Calcusyn software. The combination indices calculated that lay above the line of additivity represent antagonistic, on the line are additive and underneath the line are synergistic effect. (F) The results obtained from A were subjected to calculation using the Calcusyn software. The isobolograms shown are representative from 3 independent experiments. (G) The combination indices were averaged from 3 independent experiments and the statistical analysis used was unpaired student's *t*-test.

treatment with increasing drug concentration did not affect the distribution of the $CD44^{hi}/CD24^{lo}$ population of any of the cell line tested (Figure 26C). These observations led us to develop a combination treatment regimen in which the LMW-E tumor cells will be first treated with doxorubicin to eliminate the non-CSC population and then followed by salinomycin to target the CSC population. One advantage of combining drug treatment is that it allows for administration of the drugs at low concentration and therefore lessens the toxic side effects. To achieve this goal, the combined drugs must exert a synergistic effect in which the outcome is greater than the sum of the single agent alone. To examine the toxicity of combining doxorubicin and salinomycin, we utilized the high-throughput survival assay (HTSA). After seeding at 3000 cells/cm^2 density for 24 hours in 96-well plates, the cells were first treated with doxorubicin for 48 hours, followed by salinomycin for 48 hours, and then allowed to recover for 5 days in drug-free medium (Figure 19B). On the 10^{th} day, MTT solution was added to the cells and cell viability was measured at 590 nm absorbance using a spectrophotometer. While the IC_{50} of doxorubicin and salinomycin alone were approximately 7.5 nM and 3 μM, respectively, the combination of these drugs resulted in higher fraction of cell death (Figure 26D).

The Calcusyn software was used to calculate the combined drug effects on the viability of the cells. This program analyzes the effects from the 2 drugs and generates an isobologram, a graph that displays the effects of the combined drugs: synergistic, additive, or antagonistic (Figure 26E). The Calcusyn program calculates a combination index based on the fractions of cell death due to doxorubicin and salinomycin treatments, and a line of additivity is placed at a value of 1 on each axis. A combination index of 1 represents additive effect, greater than 1 represents antagonistic effect, and less than 1 represents synergistic effect. The isobolograms of the 76NE6-V and 76NE6-EL cells indicated that the combined drug treatment resulted in additive to antagonistic effects (Figure 26F). In contrast, the drug treatment demonstrated a clear synergistic effect in the LMW-E-expressing cells (76NE6-LMW-E, T1G2.2, T1G3.1, and T1G4.2). An average of the combination indices revealed that the doxorubicin and salinomycin combination resulted in

additive/antagonistic effects in the 76NE6-V and 76NE6-EL cells but synergistic effects in the 76NE6-LMW-E and the TDCs (Figure 26G). These results suggest a promising and effective therapeutic strategy of combining doxorubicin and salinomycin to treat breast cancer patients who have high levels of LMW-E expression and high CSC population.

3.3g. Identification of human EL/CDK2 and LMW-E/CDK2 substrates

To elucidate the signaling pathway downstream of LMW-E, we utilized two distinct methods to discover potential substrates/interacting partners for EL/CDK2 and LMW-E/CDK2 on a proteome-wide scale: (1) the ProtoArray® Human Protein Microarray from Invitrogen and (2) the chemical/genetic manipulation of CDK2 approach.

In the first approach, we purified recombinant EL/CDK2 and LMW-E/CDK2 complexes from insect cell lysates and confirmed that the complexes were active using GST-Rb as substrates in a kinase assay (Figure 27A & B). The microarrays, which contain more than 9,000 unique human proteins, were incubated either with recombinant active EL/CDK2 or LMW-E/CDK2 at a concentration of 50 nM in the presence of ^{33}P-γ-ATP for 1 hour at 30°C. The radioactive signals were directly compared to generate a list of proteins that were most differentially phosphorylated by EL/CDK2 and LMW-E/CDK2 complexes (Figure 27C). Our screen identified a total of 146 potential substrates to both EL/CDK2 and LMW-E/CDK2 complexes (Table 10). Interestingly, we only identified 4 proteins (myotilin, tomosyn, PRP38 pre-mRNA processing factor 38 (PRPF38A), and p27^{Kip1}) that were phosphorylated by EL/CDK2 significantly more than by LMW-E/CDK2 as compared to the 14 (histone acetyltransferase binding to ORC (Hbo1), RAD51 associated protein 1 (RAD51AP1), non-metastatic cells 1/2 (NME1/E2), protein regulator of cytokinesis 1 (PRC1), cyclin-dependent kinase 2-interacting protein (CINP), ligase III (LIG3), mitochondrial GTPase 1 (MTG1), polypeptide N-acetylgalactosaminyltransferase 10, mitochondrial ribosomal protein L40 (MRPL40), tektin 2 (testicular) (TEKT2), Ribosomal protein S6 kinase alpha-5, interleukin-1 receptor-associated kinase 3 (IRAK3), FAD-dependent oxidoreductase domain containing 1 (FOXRED1), and cell

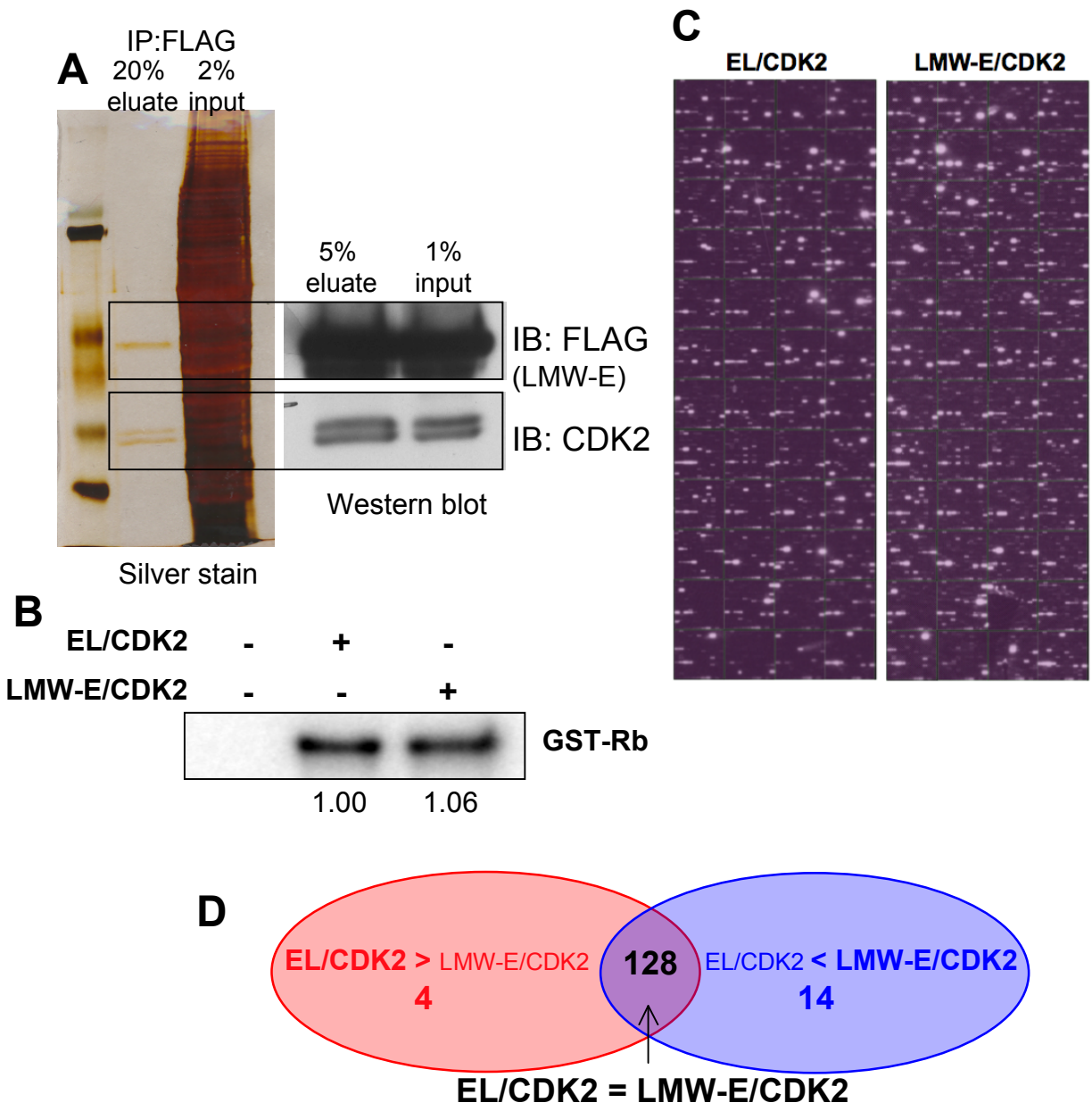

Figure 27: Identification of human EL/CDK2 and LMW-E/CDK2 substrates using the ProtoArray microarray. (A) FLAG-EL/CDK2 and FLAG-LMW-E/CDK2 complexes were expressed in sf9 insect cells, purified by IP with FLAG-tagged antibody, eluted with 3X FLAG peptide and visualized by silver stain and Western blot analysis. (Only LMW-E/CDK2 results are shown here). (B) *In vitro* kinase assay using purified EL/CDK2 and LMW-E/CDK2 kinase complexes with GST-Rb as substrate to confirm the relative amount of the kinase complexes for use in the microarray analysis. The kinase assay was performed with ^{32}P-γ-ATP, separated by SDS-PAGE and exposed to x-ray films. (C) The microarrays were incubated either with recombinant EL/CDK2 or LMW-E/CDK2 in the presence of ^{33}P-γ-ATP and the radioactive signals were exposed to x-ray films. (D) Venn diagram showing the number of proteins whose phosphorylation signal by EL/CDK2 is greater than LMW-E/CDK2 by more than 1.5 (red), LMW-E/CDK2 signal is greater than EL/CDK2 signal by 1.5 (blue) and EL/CDK2 and LMW-E/CDK2 signals are between 0.5 and 1.5 (black).

Table 10. Potential substrates to both EL/CDK2 and LMW-E/CDK2 complexes from the ProtoArray Microarray analysis. Proteins that are phosphorylated by EL/CDK2 more than LMW-E/CDK2 are highlighted in yellow. Proteins that are phosphorylated by LMW-E/CDK2 more than EL/CDK2 are highlighted in pink.

	Protein
1	cyclin-dependent kinase inhibitor 1B (p27, Kip1) (CDKN1B)
2	myotilin (MYOT)
3	syntaxin binding protein 5 (tomosyn) (STXBP5)
4	PRP38 pre-mRNA processing factor 38 (PRPF38A)
5	E2F transcription factor (E2F)
6	Proto-oncogene tyrosine-protein kinase MER
7	hydrolethalus syndrome 1 (HYLS1)
8	Phosphatidylinositol 4-kinase beta
9	Ribosomal protein S6 kinase
10	sciellin (SCEL)
11	Rho GTPase-activating protein 15
12	Bruton agammaglobulinemia tyrosine kinase (BTK)
13	Fibroblast growth factor receptor 2
14	Peripheral plasma membrane protein CASK
15	BRCA1 associated protein-1 (BAP1)
16	ankyrin repeat and sterile alpha motif domain containing 3 (ANKS3)
17	schlafen-like 1 (SLFNL1)
18	BMP-2-inducible protein kinase
19	Receptor tyrosine-protein kinase erbB-2
20	Dual specificity protein kinase CLK1
21	platelet-derived growth factor receptor (PDGFR)
22	BTB (POZ) domain containing 12 (BTBD12)
23	anaplastic lymphoma kinase (Ki-1) (ALK)
24	met proto-oncogene (MET)
25	serum/glucocorticoid regulated kinase (SGK)
26	pim oncogene (PIM)
27	fms-related tyrosine kinase 1 (FLT1)
28	WEE1 homolog (WEE1)
29	Interleukin-1 receptor-associated kinase (IRAK)
30	PRKR interacting protein 1 (IL11 inducible) (PRKRIP1)
31	Ephrin type-B receptor 1
32	cyclin E2 (CCNE2)
33	Rho-associated protein kinase 2
34	PTK2B protein tyrosine kinase 2 beta (PTK2B)
35	REX2, RNA exonuclease 2 homolog (REXO2)
36	ret proto-oncogene (RET)
37	epidermal growth factor receptor (EGFR)
38	tau tubulin kinase 2 (TTBK2)
39	Dual specificity tyrosine-phosphorylation-regulated kinase 1B
40	Eukaryotic translation initiation factor 2-alpha kinase 3
41	F-box/WD repeat-containing protein 11
42	p21 (CDKN1A)-activated kinase (PAK)
43	Proto-oncogene tyrosine-protein kinase FER
44	inhibitor of kappa light polypeptide gene enhancer in B-cells (IKBKB)
45	death-associated protein kinase (DAPK)
46	tropomyosin 4 (TPM4)
47	Receptor tyrosine-protein kinase erbB-4
48	CHK1 checkpoint homolog (CHEK1)
49	mitogen-activated protein kinase kinase kinase kinase (MAP4K)

Table 10. Potential substrates to both EL/CDK2 and LMW-E/CDK2 complexes from the ProtoArray Microarray analysis. Proteins that are phosphorylated by EL/CDK2 more than LMW-E/CDK2 are highlighted in yellow. Proteins that are phosphorylated by LMW-E/CDK2 more than EL/CDK2 are highlighted in pink.

	Protein
50	TTK protein kinase (TTK)
51	TANK-binding kinase 1 (TBK1)
52	MAP kinase-interacting serine/threonine-protein kinase
53	doublecortin and CaM kinase-like 2 (DCAMKL2)
54	bone morphogenetic protein receptor, type IB (BMPR1B)
55	transforming growth factor, beta receptor II (TGFBR2)
56	B lymphoid tyrosine kinase (BLK)
57	cyclin-dependent kinase 5 (CDK5)
58	Basic fibroblast growth factor receptor 1
59	BMX non-receptor tyrosine kinase (BMX)
60	dystrophin
61	Activin receptor type-2A
62	Cartilage intermediate layer protein 2
63	Inhibitor of nuclear factor kappa-B kinase
64	Tyrosine-protein kinase ABL2
65	TYRO3 protein tyrosine kinase (TYRO3)
66	protein kinase D (PRKD)
67	SFRS protein kinase 3 (SRPK3)
68	alanine-glyoxylate aminotransferase 2-like 2 (AGXT2L2)
69	calcium/calmodulin-dependent protein kinase kinase 2 (CAMKK2)
70	3-phosphoinositide dependent protein kinase-1 (PDPK1)
71	RIO kinase (RIOK)
72	Cas scaffolding protein family member 4
73	protein kinase C (PRKC)
74	Insulin receptor
75	Wolf-Hirschhorn syndrome candidate 1 (WHSC1)
76	spleen tyrosine kinase (SYK)
77	leukocyte tyrosine kinase (LTK)
78	phosphorylase kinase
79	microcephaly (MCPH1)
80	NCK adaptor protein 2 (NCK2)
81	SNF1-like kinase 2 (SNF1LK2)
82	suppressor of cytokine signaling 2 (SOCS2)
83	MAP/microtubule affinity-regulating kinase (MARK)
84	Macrophage-stimulating protein receptor
85	polo-like kinase 1 (PLK1)
86	Protein tyrosine kinase 2
87	MAP kinase-activated protein kinase 2
88	Glycogen synthase kinase-3 beta
89	IL2-inducible T-cell kinase (ITK)
90	Tyrosine-protein kinase FRK
91	CDC-like kinase (CLK)
92	myomegalin (PDE4DIP)
93	casein kinase 1
94	hypothetical protein MGC42105 (MGC42105)
95	male-specific lethal 3-like 1 (MSL3L1)
96	PTK2 protein tyrosine kinase 2 (PTK2)
97	cGMP-dependent protein kinase 1

Table 10. Potential substrates to both EL/CDK2 and LMW-E/CDK2 complexes from the ProtoArray Microarray analysis. Proteins that are phosphorylated by EL/CDK2 more than LMW-E/CDK2 are highlighted in yellow. Proteins that are phosphorylated by LMW-E/CDK2 more than EL/CDK2 are highlighted in pink.

	Protein
98	Band 4.1-like protein 4A
99	ephrin receptor B4 (EPHB4)
100	homeodomain interacting protein kinase (HIPK)
101	TBC1 domain family, member 22A (TBC1D22A)
102	splicing factor, arginine/serine-rich 2B (SFRS2B)
103	fyn-related kinase (FRK)
104	Small conductance calcium-activated potassium channel protein 2
105	Cyclin-dependent kinase-like 2
106	family with sequence similarity 122A (FAM122A)
107	inositol(myo)-1(or 4)-monophosphatase 1 (IMPA1)
108	G patch domain containing 2 (GPATCH2)
109	testis-specific serine kinase 2 (TSSK2)
110	chromodomain helicase DNA binding protein 2 (CHD2)
111	mitogen-activated protein kinase kinase kinase (MAP3K)
112	casein kinase 2
113	ets variant gene 3 (ETV3)
114	TAO kinase 3 (TAOK3)
115	HIRA interacting protein 3 (HIRIP3)
116	PRP40 pre-mRNA processing factor 40 (PRPF40A)
117	feline sarcoma oncogene (FES)
118	Focal adhesion kinase 1
119	SH3 and cysteine rich domain (STAC)
120	cyclin G associated kinase (GAK)
121	phytanoyl-CoA 2-hydroxylase interacting protein-like (PHYHIPL)
122	mitogen-activated protein kinase (MAPK)
123	SMAD family member 3 (SMAD3)
124	G protein-coupled receptor kinase (GRK)
125	ribosomal protein S10 (RPS10)
126	ribosomal protein L41 (RPL41)
127	NUAK family (NUAK2)
128	SLAIN motif family, member 2 (SLAIN2)
129	Cytoplasmic tyrosine-protein kinase BMX
130	cell division cycle associated 7 (CDCA7)
131	Ephrin receptor A1 (EPHA1)
132	tripartite motif-containing 63 (TRIM63)
133	mitochondrial GTPase 1 (MTG1)
134	non-metastatic cells 1 (NME1)
135	Polypeptide N-acetylgalactosaminyltransferase 10
136	MYST histone acetyltransferase 2 (MYST2)
137	mitochondrial ribosomal protein L40 (MRPL40)
138	tektin 2 (testicular) (TEKT2)
139	Ribosomal protein S6 kinase alpha-5
140	interleukin-1 receptor-associated kinase 3 (IRAK3)
141	FAD-dependent oxidoreductase domain containing 1 (FOXRED1)
142	cell division cycle 2 (CDC2)
143	RAD51 associated protein 1 (RAD51AP1)
144	protein regulator of cytokinesis 1 (PRC1)
145	cyclin-dependent kinase 2-interacting protein (CINP)
146	ligase III (LIG3)

division cycle 2 (CDC2)) potential substrates that were preferentially phosphorylated by LMW-E/CDK2 suggesting that by losing the N-terminal portion, the LMW-E/CDK2 kinase complex is able to specifically interact and phosphorylate additional proteins (Figure 27D). We chose 6 top candidates from the list of 14 potential substrates that were phosphorylated by LMW-E/CDK2 at higher intensity than by EL/CDK2 (Hbo1, CINP, LIG3, PRC1, RAD51AP1, and NME1/E2) to further validate using *in vitro* kinase assay (Table 11). These 6 genes were tagged with a Myc-tag, expressed in HEK293T cells, and purified by IP using Myc-tagged antibody. The purified proteins were then subjected to the *in vitro* kinase assay as substrates to the EL/CDK2 and LMW-E/CDK2 kinase complexes (Figure 28). The results from the kinase assay revealed that Hbo1, CINP, LIG3, and PRC1 were indeed phosphorylated by both the EL/CDK2 and LMW-E/CDK2 kinase complexes, and the phosphorylation was efficiently inhibited with addition of roscovitine (Figure 28A-D). However, we could not detect any phosphorylation signal with RAD51AP1 and NME1/E2 as substrates (Figure 28E & F).

The second screening approach involves generating a modified CDK2 kinase that can accept an ATP analog to facilitate covalent modification and subsequent purification of substrate peptides (Figure 29A & B) (305). CDK2 F80G mutant was generated by amino acid exchange at a conserved bulky phenylalanine residue in the ATP binding pocket to a smaller glycine amino acid to allow this mutant CDK2 to use PE-ATP-γS as a substrate. The γ sulfur group in the PE-ATP-γS analog allows for specific tagging of the substrates with the thiophosphate group, which can be used to identify any peptide that has been phosphorylated by CDK2 F80G. Then incubated with GST-Rb, both EL/CDK2 F80G and LMW-E/CDK2 F80G kinase complexes can use both ATP and PE-ATP-γS to phosphorylate GST-Rb as indicated by its electromobility shift while the wild type CDK2 kinase complexes can only use ATP, but not PE-ATP-γS (Figure 29C). The next steps will be to phosphorylate cell lysates *in vitro* using EL/CDK2 F80G and LMW-E/CDK2 F80G with PE-ATP-γ-S as substrate, digest the protein mixture, capture the thiophosphopeptides with thiopropyl sepharose, and the thiophosphopeptides will be specifically released by treatment of the resin with a strong base. The recovered

Table 11. Candidate substrates of the LMW-E/CDK2 complexes identified from the ProtoArray Microarray	
CANDIDATE SUBSTRATES	**FUNCTION(S)**
Hbo1 (histone acetyltransferase binding to ORC)	• Plays critical roles in gene-specific transcription regulation, DNA damage response, repair, and DNA replication • CDK11(p58) interacts with Hbo1 and enhances its HAT activity (311) • Hbo1 enhances anchorage-independent growth of breast cancer cells (312) • Hbo1 is highly expressed in breast cancer tissues and correlates positively with histology grade in ERa positive tumors (313)
CINP (cyclin-dependent kinase 2 interacting protein)	• Involved in replication and ATR-mediated checkpoint signaling
LIG3 (ligase 3)	• Catalyzes the joining of DNA ends (excision repair)
PRC1 (protein regulator of cytokinesis 1)	• High level during S and G2/M and drop dramatically after cell exit mitosis and enter G1
RAD51AP1 (RAD51 associated protein 1)	• Participates in a common DNA damage response by mediating homologous recombination
NME1/E2 (non-metastatic cells 1/2)	• Reduced mRNA transcript levels in highly metastatic cells

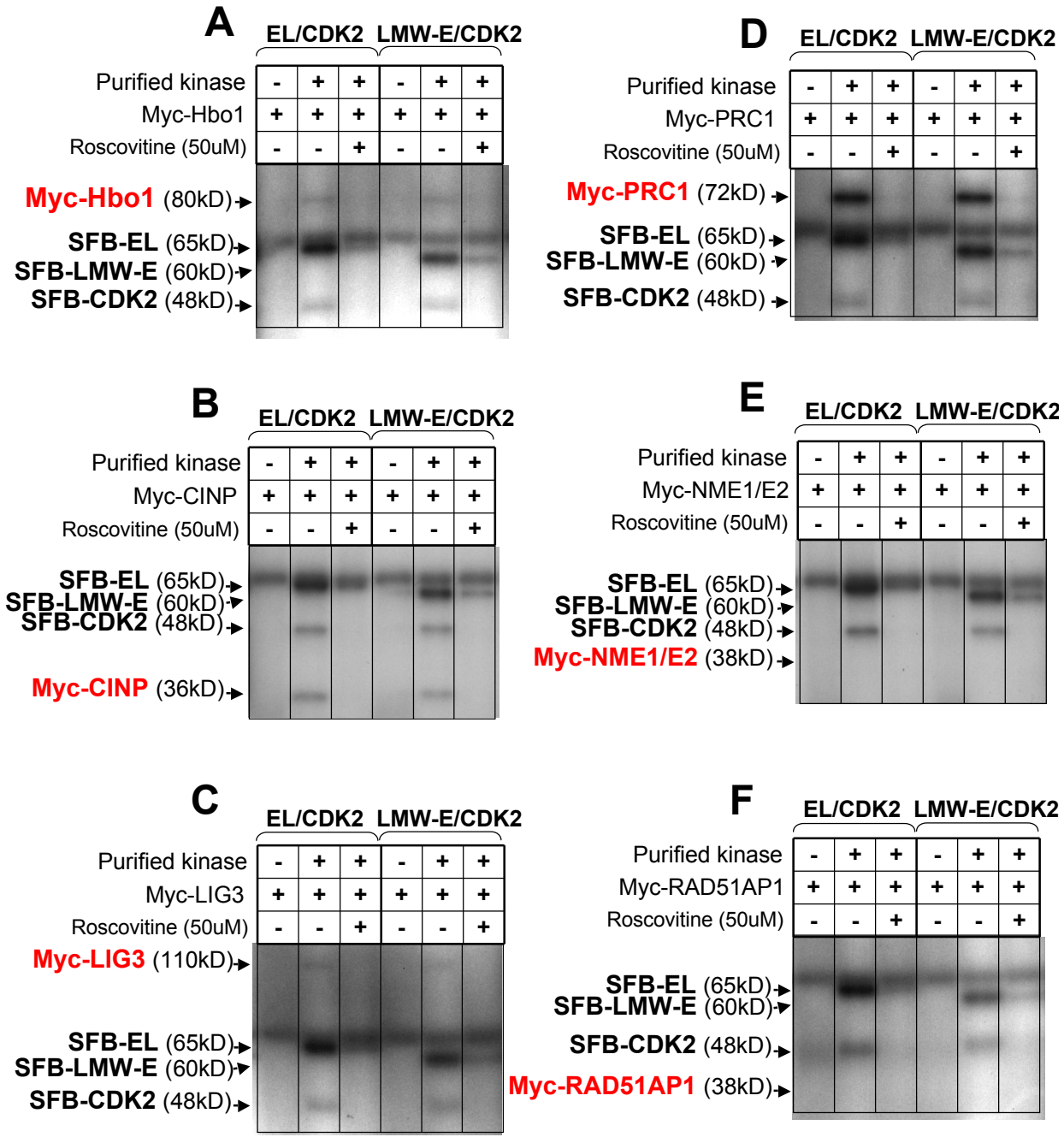

<u>Figure 28:</u> Hbo1, CINP, LIG3 and PRC1 are phosphorylated by both EL/CDK2 and LMW-E/CDK2 kinase complexes. (A) Purified EL/CDK2 and LMW-E/CDK2 kinase complexes were subjected to *in vitro* kinase assay using purified Myc-tagged Hbo1 (A), CINP (B), LIG3 (C), PRC1 (D), NME1/E2 (E) and RAD51AP1 (F) as substrates. The kinase assays were performed with ^{32}P-γ-ATP, separated by SDS-PAGE and exposed to x-ray films.

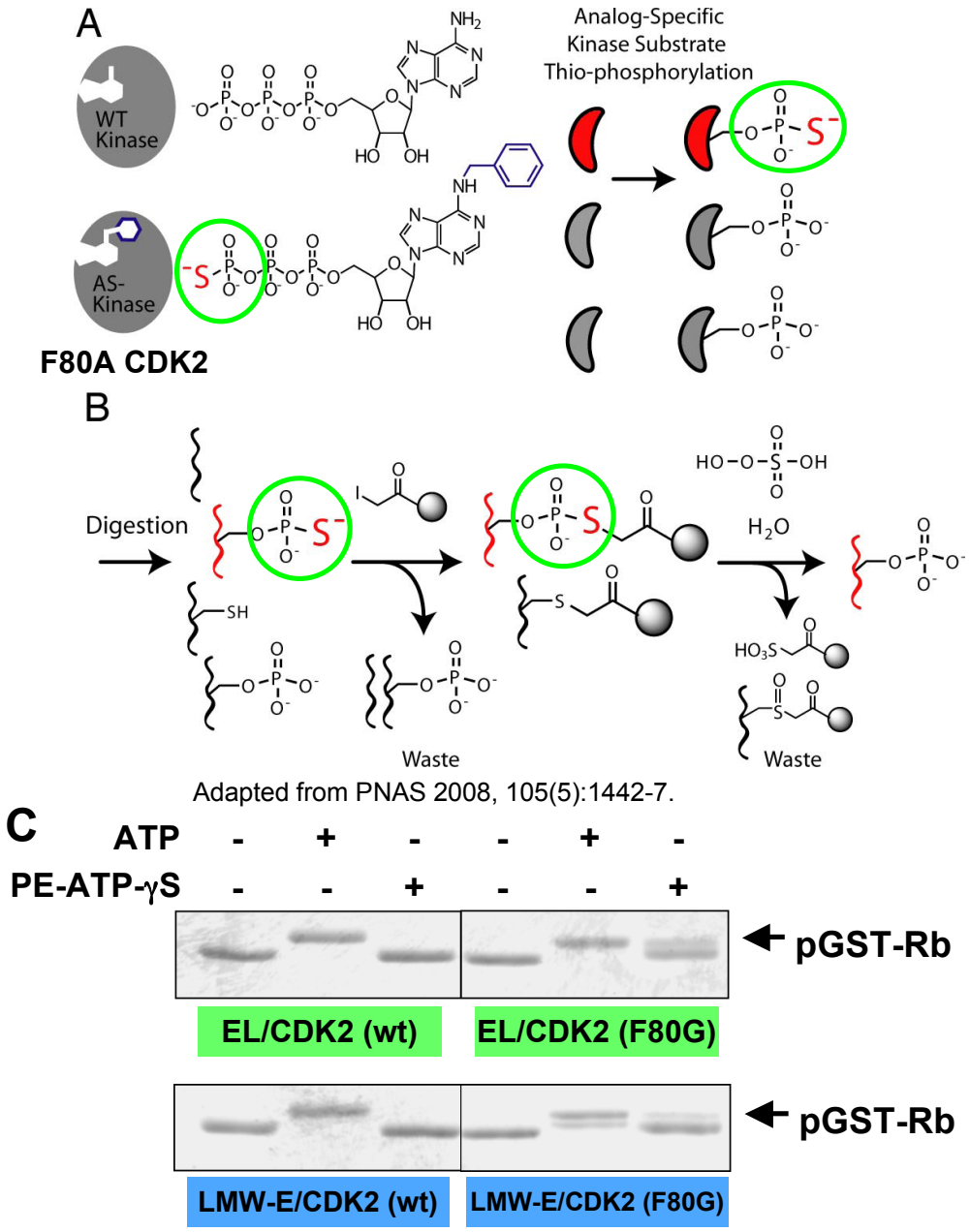

Figure 29: EL/CDK2 and LMW-E/CDK2 substrate screening using ATP analog and F80G CDK2. (Adapated from PNAS 2008, 105(5):1442-7.) (A) Schematic of the screening approach demonstrating that the ATP analog (PE-ATP-γS) can fit into the ATP pocket of the F80G CDK2 but not the wild-type CDK2 kinase. The replacement of the γ-phosphoryl oxygen with sulfur allows for specific tagging of the substrates with the thiophosphate group. (B) Thio-containing groups can react with iodoacetyl-agarose to form covalent bond while unbound peptides are washed away. Thiophosphopeptides are specifically liberated by oxidation-promoted hydrolysis of the sulfur-phosphorus bond and recovered peptides can be analyzed by nanoscale liquid chromatography coupled to a Q TRAP tandem mass spectrometer. (C) *In vitro* kinase assay with wild-type and F80G CDK2 mutant in complex with EL or LMW-E in the presence of either ATP or PE-ATP-γS and GST-Rb. The samples were separated by SDS-PAGE and stained with Coomassie blue. The top band represents pGST-Rb and the bottom band represents the unphosphorylated form.

peptides will be subjected to liquid chromatography-MS/MS analysis to identify and to compare the substrate peptides phosphorylated by EL/CDK2 and LMW-E/CDK2 kinase complexes. Since the first screening method produced a number of interesting hits and given the time constraint, we decided to postpone this experiment and focus our studies on the discovered potential hits.

3.3h. Hbo1 is a novel substrate of the cyclin E/CDK2 complex

From the 2 independent ProtoArray microarray experiments, Hbo1 (histone acetyltransferase (HAT) binding to ORC1 (origin recognition complex 1)) was among the top potential hits with phosphorylation signal by LMW-E/CDK2 being 3 folds higher than that by EL/CDK2 (Figure 30A). Hbo1 is a member of the MYST family (named after its original 4 founding members: **M**OZ, **Y**bf2/Sas3, **S**as2, **T**IP60), which is highly conserved from yeast to humans, and has been implicated in regulating gene expression, DNA replication, and DNA repair (306-311). The Hbo1 protein structure contains a defining MYST domain consisting of an acetyl-CoA binding motif, a zinc finger, and a serine-rich region. During S phase, ORC is a key protein for initiating DNA replication by recruiting components for the formation of the pre-replication complex (pre-RC). Hbo1 was first identified to bind to ORC1 and subsequently shown to interact with MCM-2 to positively regulate the assembly of the pre-RC and DNA replication initiation (306, 311-313).

The coding region of Hbo1 has been shown to be a common site for retroviral integration and has been linked to B/T-cell lymphoma and myeloid leukemia in mice (314). Additionally, in a screen for genetic alterations and oncogenic pathways in breast cancer, Hu and colleagues identified the coding region of Hbo1 with recurrent chromosomal gain in ER+/PR+/HER2+ tumors (315). Furthermore, ectopic overexpression of Hbo1 in MCF7 and SKBR3 cells enhanced soft agar colony formation while knockdown of Hbo1 with siRNA blocked S phase progression and reduced cell proliferation (315, 316). These data suggest that Hbo1 plays a role in supporting the oncogenic transformed state, and genetic amplification at this chromosomal region implicates Hbo1 as an important oncogene in breast cancer. Aside from interacting with the pre-RC, Hbo1 has been

Figure 30

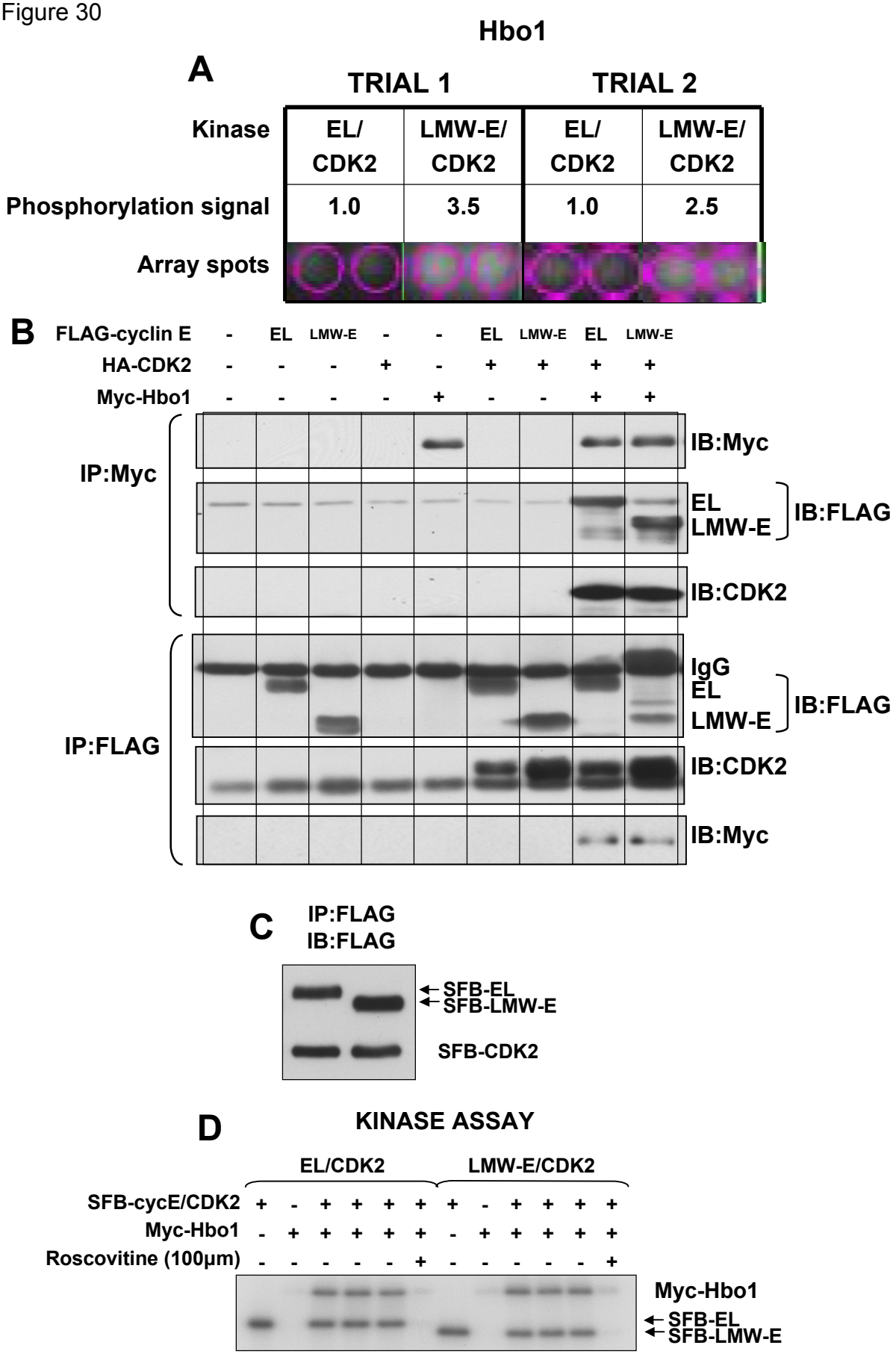
Hbo1
A
TRIAL 1
TRIAL 2
Kinase
EL/ CDK2
LMW-E/ CDK2
EL/ CDK2
LMW-E/ CDK2
Phosphorylation signal
1.0
3.5
1.0
2.5
Array spots
B
FLAG-cyclin E
HA-CDK2
Myc-Hbo1
IP:Myc
IB:Myc
EL
LMW-E
IB:FLAG
IB:CDK2
IP:FLAG
IgG
EL
LMW-E
IB:FLAG
IB:CDK2
IB:Myc
C
IP:FLAG
IB:FLAG
SFB-EL
SFB-LMW-E
SFB-CDK2
D
KINASE ASSAY
EL/CDK2
LMW-E/CDK2
SFB-cycE/CDK2
Myc-Hbo1
Roscovitine (100μm)
Myc-Hbo1
SFB-EL
SFB-LMW-E

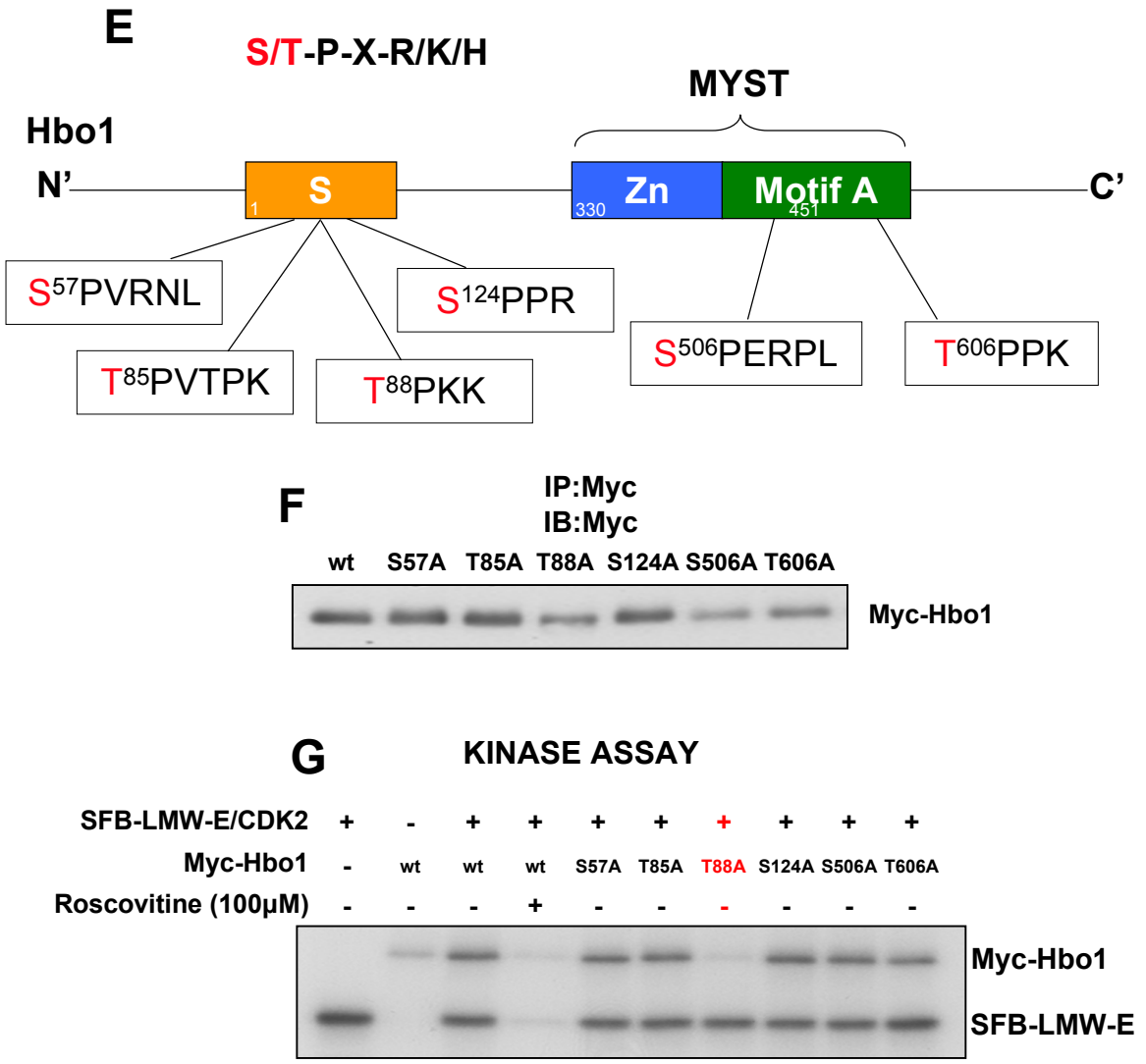

Figure 30: Hbo1 is a novel substrate of the cyclin E/CDK2 complex. (A) The ProtoArray microarray experiment was performed in two independent experiments. The phosphorylation signals indicate relative radioactive signal detected in the microarray spots. (B) FLAG-EL or LMW-E, HA-CDK2, and Myc-Hbo1 constructs were transfected into HEK293T cells and IP with either Myc-tagged or FLAG-tagged antibodies and probed with the indicated antibodies. (C) SFB-EL or SFB-LMW-E was co-transfected with SFB-CDK2 into HEK293T cells, purified using FLAG-tagged antibody, eluted with 3X FLAG peptide and visualized by Western blot analysis. Myc-Hbo1 was transfected into HEK293T cells, purified using Myc-tagged antibody and the bead-Myc protein complex was resuspended in 1X wash buffer. (D) The EL/CDK2 or LMW-E/CDK2 kinase complex was incubated with purified Hbo1 in the presence of ^{32}P-γ-ATP and with or without roscovitine. The samples were separated by SDS-PAGE and exposed to x-ray films. (E) Schematic of the Hbo1 gene construct with the potential phosphorylation sites predicted based on the CDK2 consensus phosphorylation motif (S/T-P-X-R/K/H). (F & G) The six potential phosphorylation sites were mutated to alanine, expressed, purified and subjected to similar kinase assay as in (D).

demonstrated to bind to AR (androgen receptor) and NF-κB to mediate transcriptional repression (308, 309). Furthermore, Hbo1 is highly expressed in breast cancer tissues and correlates positively with histology grade in ERα positive tumors (317). Given the important role of Hbo1 in breast cancer, we decided to further investigate its relationship with cyclin E/CDK2 in mediating mammary tumorigenesis.

Since the ProtoArray results showed that Hbo1 was phosphorylated by the cyclin E/CDK2 complex, the first question to address is does Hbo1 interact directly with this kinase complex? DNA plasmids containing FLAG-EL or LMW-E, HA-CDK2, and Myc-Hbo1 were transiently transfected into HEK293T cells followed by IP/Western analysis. Immunoprecipitation using Myc-tagged antibody showed that EL and LMW-E as well as CDK2 were pulled-down along with Hbo1 (Figure 30B). Moreover, IP using FLAG-tagged antibody also pulled-down Hbo1 along with EL or LMW-E, and CDK2. These results indicated that Hbo1 exists in the same protein complex with EL/CDK2 and LMW-E/CDK2, at least in this *in vitro* experimental condition.

To confirm whether Hbo1 is a substrate of the cyclin E/CDK2 kinase complex, the EL/CDK2 and LMW-E/CDK2 kinase complexes and Myc-Hbo1 proteins were purified by IP with FLAG-tagged and Myc-tagged antibodies (Figure 30C). Results from the *in vitro* kinase assay showed that both EL/CDK2 and LMW-E/CDK2 kinase complexes phosphorylate Hbo1 at relatively similar levels, and addition of roscovitine efficiently inhibited the phosphorylation signal (Figure 30D). Perhaps the reason that we cannot detect a difference in the extent of Hbo1 phosphorylation between the EL/CDK2 and LMW-E/CDK2 complexes is due to the saturated concentrations of the kinase as well as the substrate in this *in vitro* kinase assay condition compared to the condition performed for the ProtoArray. (The kinase concentration was 50 nM in the microarray experiment and was approximately 500 nM in this *in vitro* kinase assay.) Additionally, since the LMW-E isoforms are overexpressed in breast cancer, we speculate that it is these truncated forms of cyclin E in complex with CDK2 that phosphorylate Hbo1 and not the full-length cyclin E form.

Based on the consensus CDK2 phosphorylation motifs (S/T-P-X-R/K/H and R-X-L), there are six potential phosphorylation sites on the Hbo1 gene sequence (Figure 30E), and these sites were mutated to alanine to identify which site is being phosphorylated by the LMW-E/CDK2 complex. The mutant proteins were transfected into HEK293T cells, purified by IP, and then followed by kinase assay (Figure 30F). Of the six potential sites, LMW-E/CDK2 phosphorylate Hbo1 at T88 since the T88A mutant showed abolished radioactive signal (Figure 30G). Collectively, the Protoarray analysis led us to discover Hbo1 as a novel substrate of the LMW-E/CDK2 complex that may mediate critical downstream signaling to contribute to the oncogenic potential of LMW-E in breast cancer.

3.3i. Cyclin E/CDK2 phosphorylation of Hbo1 does not affect the HAT activity of Hbo1

A recent study reported that $CDK11^{p58}$ interacts with Hbo1 in the nucleus and enhances Hbo1's HAT activity leading us to speculate that the interaction and phosphorylation of Hbo1 by the cyclin E/CDK2 complex may also affect the HAT activity of Hbo1 (318). The Myc-Hbo1 (wt, T88A, and T88D), SFB-EL, SFB-LMW-E, and SFB-CDK2 constructs were purified by IP with Myc or FLAG-tagged antibody and then subjected to an *in vitro* HAT activity colorimetric assay (Figure 31A & B). As shown in Figure 31C, phosphorylation of Hbo1 at T88 did not alter Hbo1's HAT activity since the T88A and T88D mutants exhibited similar HAT activity levels to wild type Hbo1. Furthermore, inhibition of the kinase activity of EL/CDK2 and LMW-E/CDK2 by addition of roscovitine did not affect the HAT activity level. Perhaps the phosphorylation of Hbo1 at T88 may affect its binding to other proteins or to DNA but not necessarily alter its function as a HAT. In fact, it has been demonstrated that CDK1 phosphorylates Hbo1 at T85/T88 to create a docking site for polo-like kinase 1 (Plk1) (319). The recruited Plk1 subsequently phosphorylates Hbo1 at S57 and activates the HAT enzymatic activity of Hbo1. We speculate that in the cellular context, phosphorylation of Hbo1 by the LMW-E/CDK2 complex at T88 may also create docking site for Plk1 or perhaps other kinases/proteins to be recruited to regulate Hbo1's HAT activity. Alternatively, the HAT activity of Hbo1 is not required

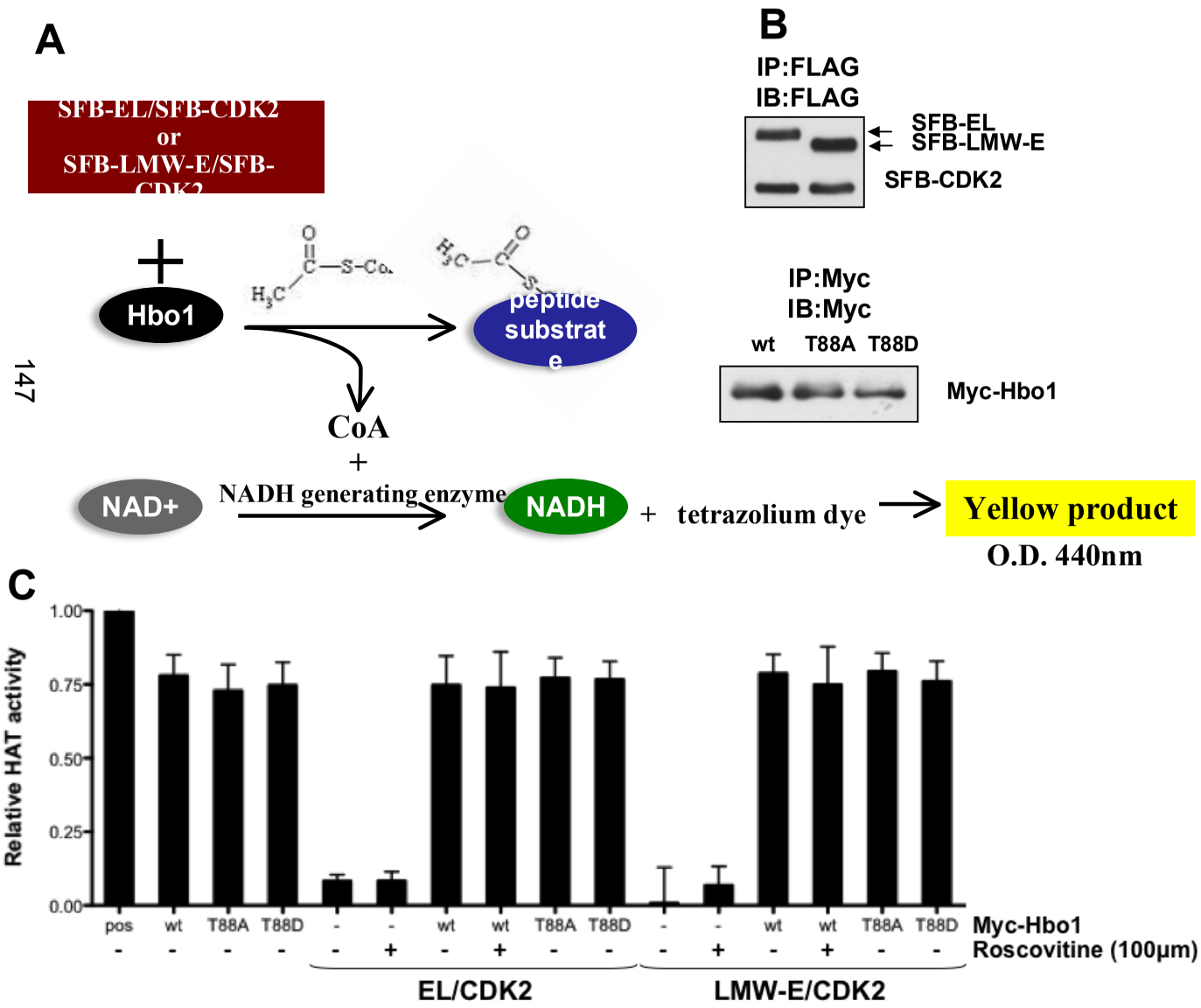

Figure 31: Cyclin E/CDK2 phosphorylation of Hbo1 does not affect the HAT activity of Hbo1. (A) Schematic of the colorimetric HAT activity assay. As a HAT, Hbo1 transfers the acetyl group to the peptide substrate leaving coenzyme A to react with NAD+ to generate NADH in the presence of NADH generating enzyme. NADH then reacts with a tetrazolium dye giving rise to a yellow color product that can be detected at 440nm optical density. (B) SFB-EL or SFB-LMW-E was co-transfected with SFB-CDK2 into HEK293T cells, purified using FLAG-tagged antibody, and eluted with 3X FLAG peptide. Myc-Hbo1 was transfected into HEK293T cells, purified using Myc-tagged antibody and the bead-Myc protein complex was resuspended in 1X wash buffer. The purified proteins were visualized by immunoblotting. (C) Results from the HAT activity assay with the values first subtracted from a water control and then normalized to the positive control, which used HeLa nuclear extract as a source of HAT.

for its transcriptional repression function. In fact, two independent reports indicated that the N-terminal region of Hbo1 (in which the T88 site is located) is necessary to repress AR and NF-κB transcriptional activation while the C-terminal domain (which contains the HAT domain) displays no effect (317,318).

3.3j. Hbo1 is overexpressed in breast cancer cell lines and co-expression with LMW-E/CDK2 enhances self-renewal capability of hMECs.

If Hbo1 is a novel downstream substrate of the cyclin E/CDK2 complex, we next hypothesize that Hbo1 may play a role in inducing the CSC properties of the LMW-E-expressing cells. We first determined that Hbo1 is highly expressed in 13 of the 18 breast cancer cell lines tested compared to the relatively low levels in the 3 hMEC cell lines (Figure 32A). Interestingly, we observed no significant correlation between Hbo1 expression and the different breast cancer subtypes (Figure 32A). Furthermore, in our cell line model system, the 76NE6-LMW-E, T1G2.2, T1G3.1, and T1G4.2 cells also express high level of Hbo1 protein compared to the 76NE6-vector and 76NE6-EL cells (Figure 32B). To determine if transient co-expression of Hbo1 with EL/CDK2 or LMW-E/CDK2 enriches for the CSC population, these constructs were transfected into HEK293T cells and examined the change in the $CD44^{hi}/CD24^{lo}$ population four days later. Results from FACS analysis clearly showed that while expression of EL/CDK2 and LMW-E/CDK2 led to an increase in the $CD44^{hi}/CD24^{lo}$ population compared to control cells, co-expression with Hbo1 further doubled this population (Figure 32C). More importantly, the increase in the $CD44^{hi}/CD24^{lo}$ population by LMW-E expression was significantly more than with EL expression ($p = 0.042$). Additionally, Western blot analysis confirmed that co-expression of Hbo1 with EL/CDK2 and LMW-E/CDK2 resulted in reduced CD24 and elevated ALDH protein levels (Figure 32D). While the HEK293T cells facilitate efficient overexpression of proteins, they are however not an ideal model system to examine physiologically relevant biological processes. Therefore, we co-expressed cyclin E (EL or LMW-E), CDK2, and Hbo1 in the 76NE6 cells via lentiviral infection and generated stable cell lines through antibiotic selection (Figure 32E). Examination of the $CD44^{hi}/CD24^{lo}$ population by FACS analysis revealed no

Figure 32

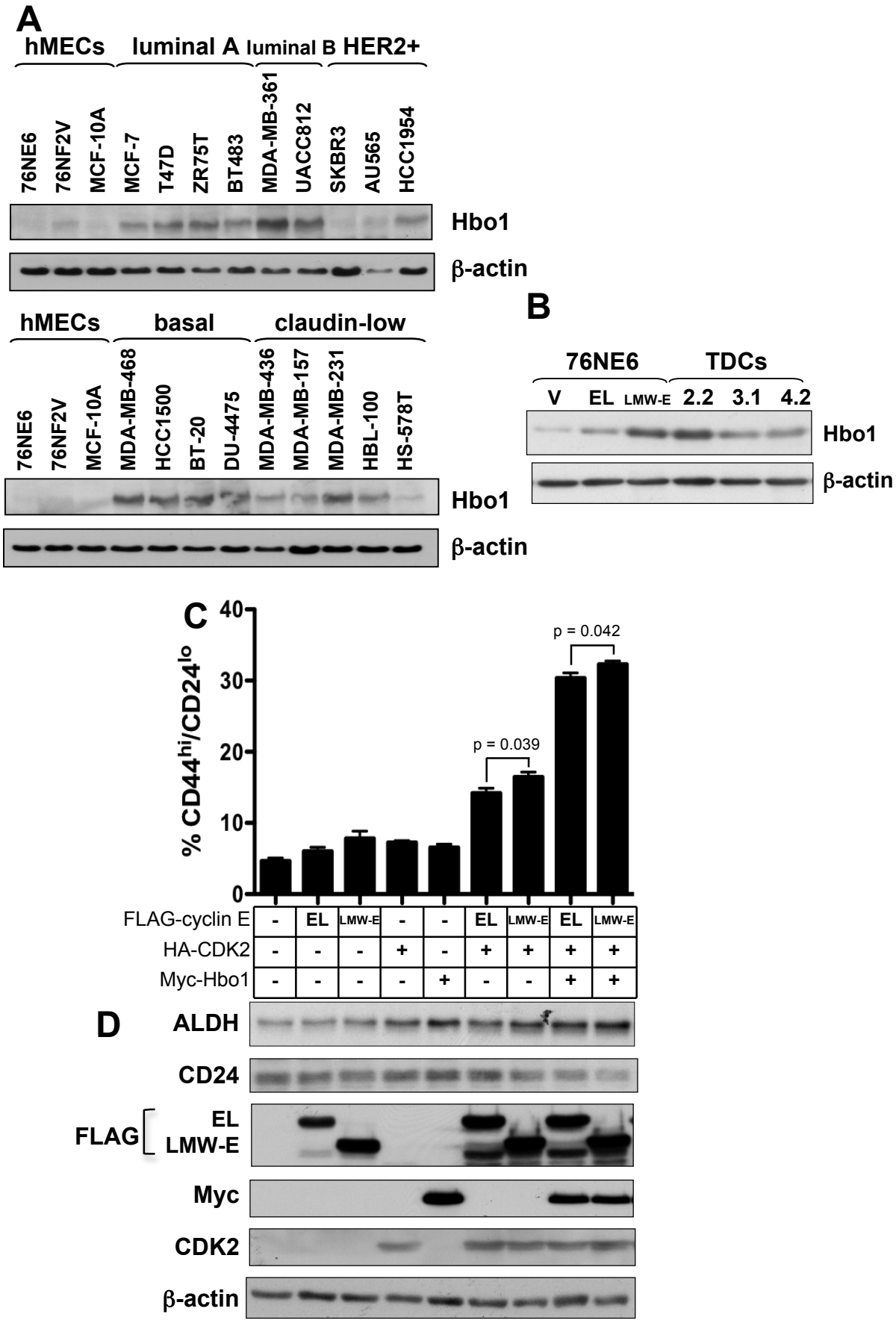
A
hMECs
luminal A
luminal B
HER2+
76NE6
76NF2V
MCF-10A
MCF-7
T47D
ZR75T
BT483
MDA-MB-361
UACC812
SKBR3
AU565
HCC1954
Hbo1
β-actin
hMECs
basal
claudin-low
76NE6
76NF2V
MCF-10A
MDA-MB-468
HCC1500
BT-20
DU-4475
MDA-MB-436
MDA-MB-157
MDA-MB-231
HBL-100
HS-578T
Hbo1
β-actin
B
76NE6
TDCs
V
EL
LMW-E
2.2
3.1
4.2
Hbo1
β-actin
C
% CD44hi/CD24lo
40
30
20
10
0
p = 0.042
p = 0.039
FLAG-cyclin E
HA-CDK2
Myc-Hbo1
D
ALDH
CD24
FLAG
EL
LMW-E
Myc
CDK2
β-actin

Figure 32

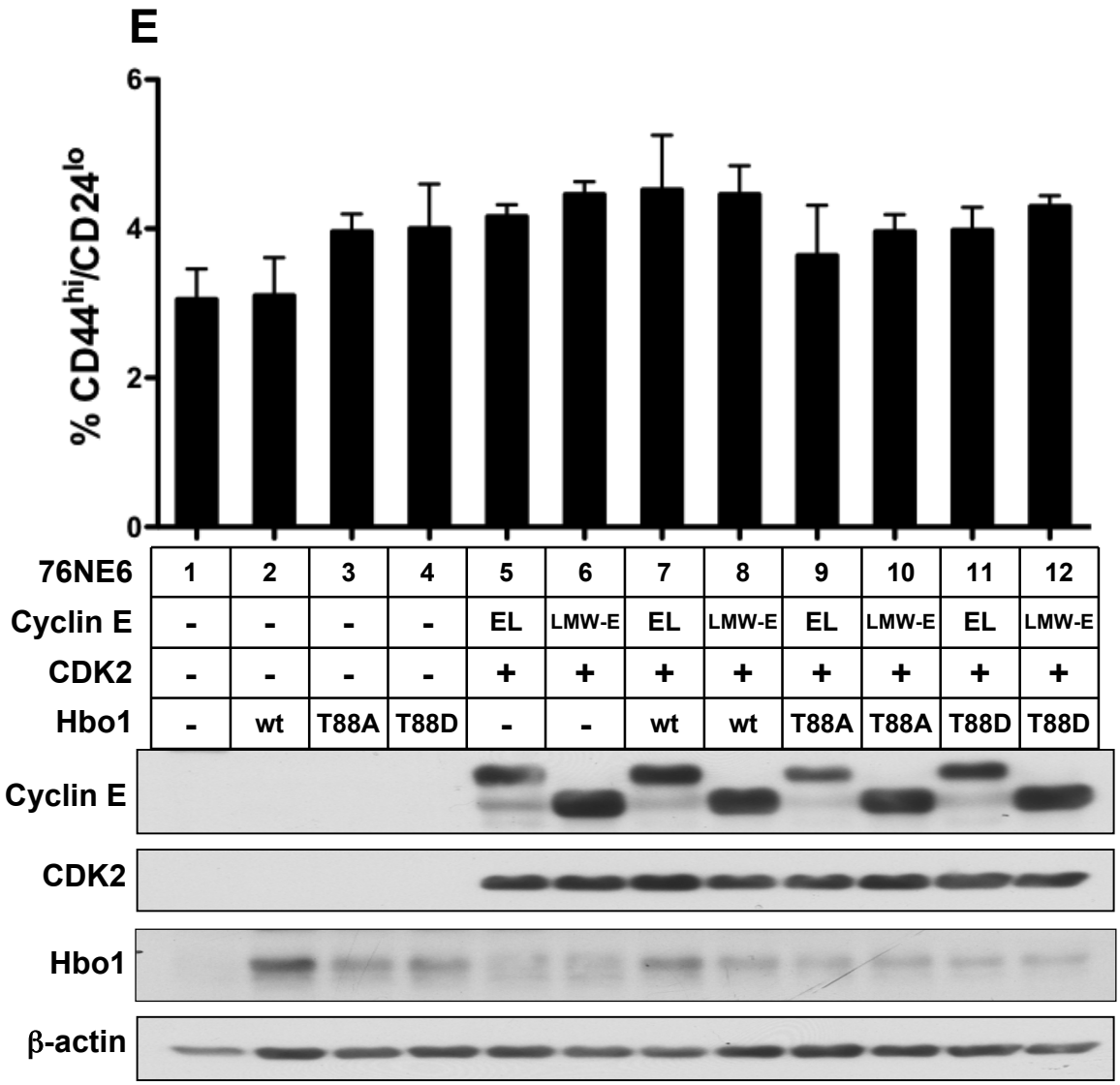
E
% CD44hi/CD24lo
6
4
2
0
76NE6
1 2 3 4 5 6 7 8 9 10 11 12
Cyclin E
- - - - EL LMW-E EL LMW-E EL LMW-E EL LMW-E
CDK2
- - - - + + + + + + + +
Hbo1
- wt T88A T88D - - wt wt T88A T88A T88D T88D
Cyclin E
CDK2
Hbo1
β-actin

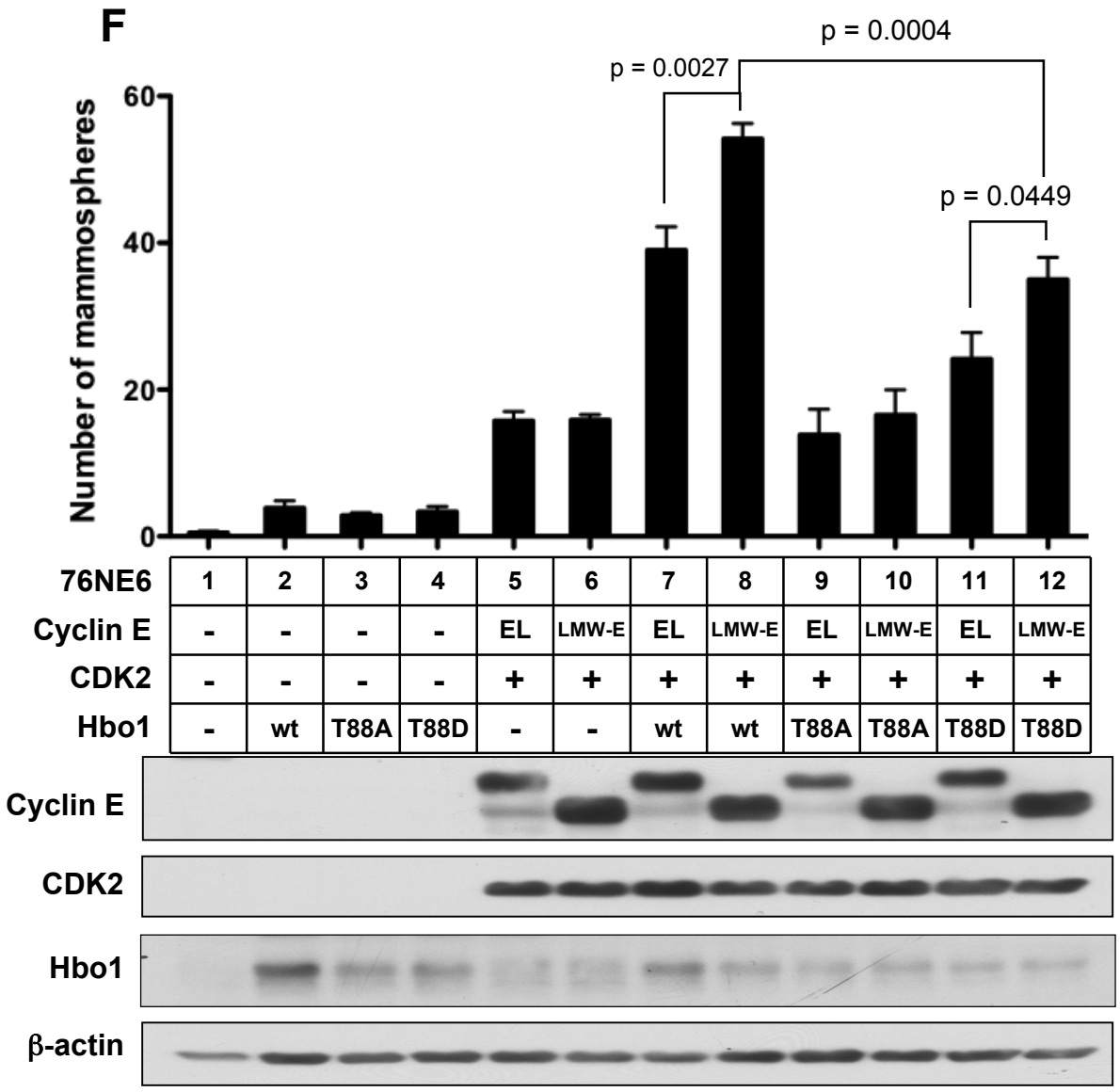

Figure 32: Hbo1 is overexpressed in breast cancer cell lines and co-expression with LMW-E/CDK2 enhances self-renewal capability of hMECs. (A) Cell lysates from 3 hMECs lines and 18 breast cancer cell lines were subjected to Western blot analysis with antibodies to Hbo1 and β-actin. (B) The 76NE6 stable cell panel and the TDCs were subjected to similar analysis as in (A). (C) SFB-EL or SFB-LMW-E, HA-CDK2, and Myc-Hbo1 constructs were co-transfected into HEK293T cells. Four days later, the cells were subjected to CD24/CD44 FACS and (D) Western blot analysis. The FACS results were averaged from 3 independent experiments and the statistical analysis used was unpaired student's *t*-test. (E & F) Lentivirus were generated in HEK293T cells carrying the EL, LMW-E, CDK2, or Hbo1 (wt, T88A, or T88D) constructs were used to infect the 76NE6 cells and stable expression was achieved by selection with 20 μg/ml blasticidin for 2 weeks. The cells were then subjected to CD44/CD24 FACS analysis (E) and mammosphere culture (F). The FACS and mammosphere formation results were averaged from at least 2 independent experiments and the statistical analysis used was unpaired student's *t*-test.

statistical difference between the different stable cell lines (Figure 32E). In contrast, when we tested the ability of these cells to form mammospheres, we found that the 76NE6 cells co-expressing wild-type Hbo1 with the LMW-E/CDK2 complex (76NE6-8) formed significantly more mammospheres than those co-expressing the EL/CDK2 complex (76NE6-7) ($p = 0.0027$) (Figure 32F). Additionally, co-expression of the T88A Hbo1 mutant in the 76NE6 cells (76NE6-9,10) reduced the number of mammospheres to similar levels as in the cells without Hbo1 overexpression (76NE6-5,6) suggesting that the phosphorylation of Hbo1 by the cyclin E/CDK2 complex is critical for the enhanced self-renewal capability of these cells. Interestingly, the cells with the T88D Hbo1 phosphorylation mimetic expression (76NE6-11,12) also demonstrated reduced mammosphere formation compared to wild-type Hbo1 (76NE6-7,8). We speculate that the aspartic acid substitution is not an ideal phosphorylation mimetic for phospho-threonine as it has one less chemical bond. Perhaps glutamate will be a better substitution for phospho-threonine mimetic and may explain the importance of the phosphorylation of Hbo1 at T88 by the cyclin E/CDK2 complex to generate a docking site for protein recruitment. Collectively, these results indicate that Hbo1 along with LMW-E/CDK2 function to alter the physiology of the cell as manifested in the properties associated with CSCs.

3.3k. Knockdown of Hbo1 reduced the properties associated with CSCs.

To investigate whether Hbo1 plays a role in enriching for the CSC population, shRNAs targeting the Hbo1 mRNA transcript with an internal ribosome entry site for GFP were packaged into lentivirus with HEK293T cells and used to infect the 76NE6-V, EL, LMW-E, T1G2.2, T1G4.2 and Sum159 cells. After two week of 0.5 μg/ml puromycin selection, approximately 98% of the cells express high levels of GFP suggesting that the shRNAs were integrated successfully (Figure 33A). Western blot analysis indicated that the two shHbo1 constructs were efficient at knocking down Hbo1 protein levels (Figure 33B). Additionally, FACS analysis for CD44/CD24 expression revealed that knockdown of Hbo1 significantly reduced the $CD44^{hi}/CD24^{lo}$ population as well as the ability of the cells to form mammosphere structures compared to the shControl cells (Figure 33C & D). Furthermore, we

Figure 33

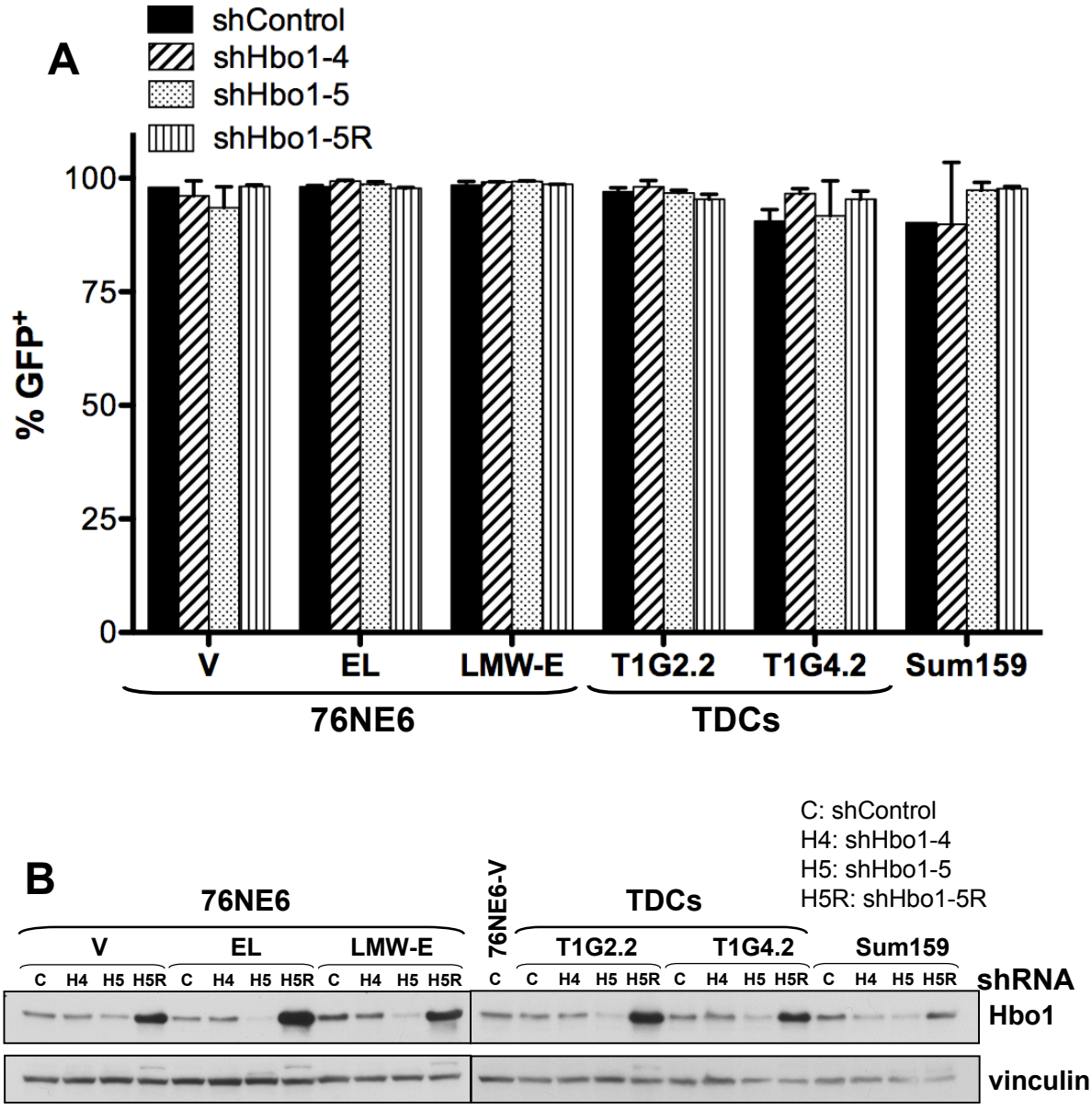
A
shControl
shHbo1-4
shHbo1-5
shHbo1-5R
% GFP+
100
75
50
25
0
V
EL
LMW-E
T1G2.2
T1G4.2
Sum159
76NE6
TDCs
B
C: shControl
H4: shHbo1-4
H5: shHbo1-5
H5R: shHbo1-5R
76NE6
76NE6-V
TDCs
V
EL
LMW-E
T1G2.2
T1G4.2
Sum159
C H4 H5 H5R
shRNA
Hbo1
vinculin

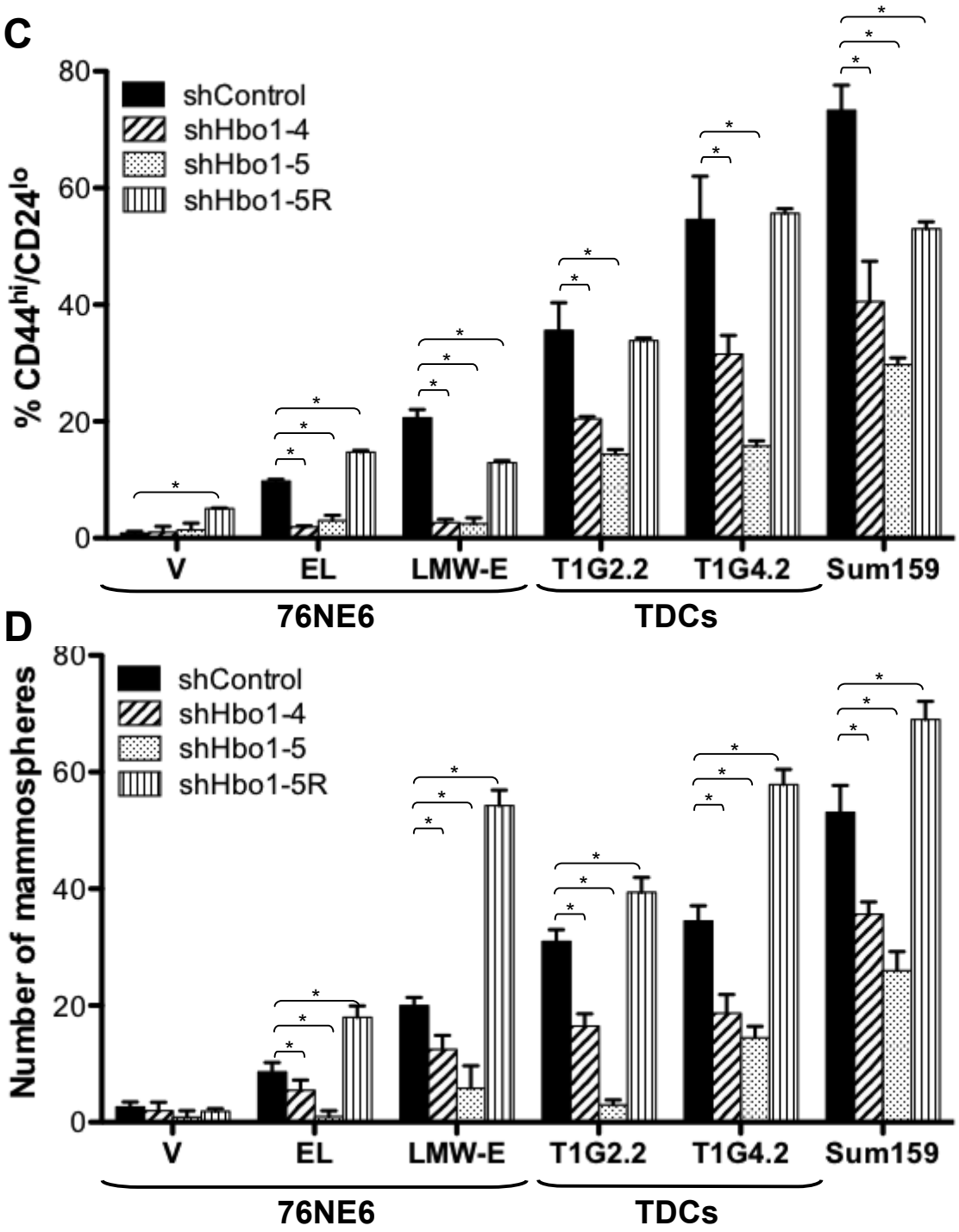

Figure 33: Knockdown of Hbo1 reduced the properties associated with CSCs. shControl, shHbo1-4, and shHbo1-5 lentivirus were produced in HEK293T cells and used to infect the 76NE6 stable cell panel, two of the TDCs and Sum159 cells. After selection with 0.5 μg/ml puromycin for 2 weeks, the cells were subjected to (A) GFP FACS analysis, (B) Western blot analysis, (C) CD44/CD24 FACS analysis, and (D) mammosphere formation assay. These cells were then infected with lentivirus carrying the shHbo1-5R construct and selected with 20 μg/ml blasticidin for 2 weeks followed by similar in vitro analysis. The FACS and mammosphere formation results were averaged from at least 2 independent experiments and the statistical analysis used was unpaired student's *t*-test (*p<0.05).

rescued Hbo1 expression by infecting the cells with an shHbo1-5 resistant construct (shHbo1-5R) by taking advantage of the wobble effect of the amino acid code and select for stable expression with 20 μg/ml blasticidin for two weeks (Figure 33B). Analysis of the CSC properties of these cells showed that re-expression of the shHbo1-5R construct rescued the reduced $CD44^{hi}/CD24^{lo}$ population as well as the number of mammosphere formation (Figure 33C & D). Collectively, our findings implicate that the presence of Hbo1 in LMW-E-expressing cells enhanced the properties associated with CSCs, which can be reduced by knockdown of Hbo1 expression.

3.4. CONCLUSIONS

The role of LMW-E in breast cancer was first strongly established by its association with patient samples and poor clinical outcome and was subsequently reinforced by the demonstration that transgenic mice with ectopic LMW-E expression develop mammary carcinoma and metastasis at significantly higher frequency compared to transgenic mice with EL expression (160, 180). In chapter 2, we described similar findings in xenograft mouse model in which hMECs expressing LMW-E/CDK2 yielded higher tumor incidence compared to cells with EL/CDK2 expression.

By expressing LMW-E, the 76NE6 mammary epithelial cells underwent a morphological switch by adopting mesenchymal characteristics as well as CSC properties. That is, these cells altered gene expression that is consistent with the EMT and demonstrated increased invasiveness through the basement membrane. In addition, LMW-E-expressing cells contain a high percentage of the $CD44^{hi}/CD24^{lo}$ population, were able to form mammospheres in non-adherent culture, and upregulated the expression and enzymatic activity of ALDH. More importantly, the fact that the phenotypes observed were more robust with exogenous LMW-E overexpression than with EL overexpression provides evidence for the difference in their tumorigenic potential.

Furthermore, we observed a strong positive association between LMW-E expression and the $CD44^{hi}/CD24^{lo}$ population in the tumor cell line model,

particularly in the cells obtained from *in vivo* passaging in which both the levels of LMW-E expression and the $CD44^{hi}/CD24^{lo}$ population showed dramatic elevation compared to the stable cell lines. This connection was further strengthened by the clinical examination of breast cancer patient tissues in which LMW-E expression associated with tumors that contain high $CD44^{hi}/CD24^{lo}$ population suggesting that perhaps breast cancer cells with LMW-E expression are CSCs. More importantly, statistical analysis also revealed a significant association between LMW-E expression and their cytoplasmic localization from IHC staining of the tumor tissues thus implicating a more efficient way to identify LMW-E expression in tumor tissues by IHC rather than by Western blot analysis.

Given that the understanding of breast CSCs has only recently evolved, clinical therapy aimed at targeting these cells is currently under active investigation. In a large screen for small molecule inhibitors that can specifically kill CSCs, Gupta and colleagues identified salinomycin as a potent agent that can abrogate the phenotypes associated with CSCs and thereby reduce tumor aggressiveness and regrowth (297). Although the mechanism of salinomycin-induced CSC death is currently unclear, it is speculated that it may be due to its function as a potassium ionophore since nigericin, another potassium ionophore, was also identified as a CSC inhibitor in the same screening study (297). Recently, salinomycin was reported to sensitize cancer cells to doxorubicin and etoposide leading to increased DNA damage and apoptosis (320). In our study, we also demonstrated that the combination of doxorubicin and salinomycin effectively targeted both the tumor bulk (non-CSCs) as well as the CSCs. Doxorubicin is a strong anti-tumor agent; however, due to its life-threatening cardiac toxicity, doxorubicin's use in the clinic is limited (321, 322). Similarly, salinomycin also has a narrow therapeutic window due to its high toxicity. However, the synergistic effects mediated by salinomycin and doxorubicin in LMW-E tumor cells but not in control and EL-expressing cells may allow for administration of these drugs at a lower and thus less toxic dose in patients with high LMW-E protein levels.

Our screen for novel substrates of the cyclin E/CDK2 complex identified Hbo1, which is a HAT that can alter the expression pattern of multiple genes. The

consensus phosphorylation motif for CDK2 is S/T-P-X-R/K/H, and we found that cyclin E/CDK2 phosphorylated Hbo1 at T^{88}PKK confirming that the phosphorylation is specific. T88 is located within the N-terminal serine-rich region of the Hbo1 gene, which is the regulatory domain, while the C-terminal region contains the Zn-finger and a HAT domain that carries out the enzymatic function (306, 311). Plk1 was previously shown to phosphorylate Hbo1 at S57A, which is in the regulatory N-terminal region, and this phosphorylation exerts positive control over the HAT activity indicating that this domain is critical in regulating the enzymatic activity of Hbo1 (319). The fact that co-expression of Hbo1 with LMW-E/CDK2 further increased the CSC properties of both HEK293T and 76NE6 cells while knockdown of Hbo1 expression reduced the $CD44^{hi}/CD24^{lo}$ population and mammosphere formation ability suggests that Hbo1 plays a role downstream of LMW-E in enriching for the CSC population. Even though results from the *in vitro* HAT activity assay indicated that LMW-E/CDK2 phosphorylation of Hbo1 did not directly affect its HAT activity, in the cellular physiological context, this phosphorylation may create a docking site to recruit other kinases to further phosphorylate Hbo1 and thereby alter its HAT activity. Indeed this phenomenon has been previously observed in which CDK1 phosphorylates Hbo1 to recruit further phosphorylation by Plk1 to increase the HAT activity of Hbo1 (319).

Although the role of cyclin E has been strictly confined to the control of the cell cycle, our data suggest that when deregulated, such as cleavage into LMW isoforms, this oncogene is capable of inducing phenotypes associated with the EMT and CSCs, which are further enhanced with the co-expression of Hbo1. Moreover, phosphorylation of Hbo1 in the regulatory N-terminal region by the LMW-E/CDK2 complex implicates potential alteration in the regulation of gene transcription associated with the EMT and CSCs. More importantly, combination treatment using doxorubicin and salinomycin produced synergistic effect on cancer cellular toxicity and thus further encourages investigation onto other drug combinations that target both the CSC and non-CSC populations to bring to the clinic.

CHAPTER 4: **CONCLUDING REMARKS AND FUTURE DIRECTIONS**

4.1. HIGHLIGHT OF MAJOR FINDINGS

The role of LMW-E in breast cancer has been well documented for more than a decade, and research from this dissertation has shed light into our understanding of how LMW-E deregulate the cells in the mammary gland as well as provide possible therapeutic implications to intervene this process. The central hypothesis of this dissertation is that **LMW-E initiates and maintains mammary tumor via deregulation of mammary acinar morphogenesis, induction of the EMT, and generation of cells with CSC properties**. The data obtained from this dissertation provided answers to the following five questions that were raised at the end of chapter 1.

1. **Is LMW-E capable of initiating and maintaining tumor development?**

- Both stable and inducible LMW-E expression systems are capable of rendering a nontumorigenic hMEC tumorigenic. Moreover, the tumorigenic potential mediated by LMW-E is approximately 10 folds stronger compared to that of EL.

2. **What effect does LMW-E have on the proliferation and architecture of the mammary acini, and if so, can inhibition of LMW-E by pharmacological agents rectify these defects?**

- LMW-E induced hyper-proliferation during mammary acinar morphogenesis causing formation of large and misshapen acinar structures. Treatment of these acini using combination of rapamycin and roscovitine or sorafenib and roscovitine prevents development of these phenotypes.

3. **What signaling pathway is deregulated in breast tumors with high LMW-E expression?**

- Proteomic analysis identified the b-raf/ERK2/mTOR pathway is activated in both breast cancer patient tissues and cells with high LMW-E levels. More importantly, expression levels of the proteins from this pathway along with LMW-E predicted poor clinical outcome.

4. **Does LMW-E induce tumor initiation, progression, and metastasis by**

altering gene expression to enhance invasiveness and self-renewal capability?

- LMW-E altered the gene signature associated with the EMT thereby reducing cell-cell contact and enhancing cellular invasion. Furthermore, LMW-E enriched for cells with CSC properties and, in breast cancer patient samples, cytoplasmic cyclin E significantly correlated with the $CD44^{hi}/CD24^{lo}$ mammary CSC population. Combination treatment using salinomycin and doxorubicin demonstrated synergistic toxicity in LMW-E-expressing cells but not in control and EL-expressing cells.

5. **Are these phenotypes driven by previously unidentified substrate(s) of the LMW-E/CDK2 complex?**

- ProtoArray microarray analysis identified Hbo1 as a novel substrate of cyclin E/CDK2. Co-expression of Hbo1 with LMW-E/CDK2 resulted in an enrichment of the CSC population while knockdown of Hbo1 expression significantly reduced the CSC population.

4.2. FUTURE DIRECTIONS

While research from this dissertation has addressed some of the critical aspects of LMW-E deregulation in mammary tumorigenesis, the data generated inevitably raised new questions that are essential to further understand this process in order to apply therapeutic intervention in the clinical setting.

Firstly, we identified several different therapeutic strategies involving combining pharmacological agents to specifically target mammary tumor cells with high LMW-E expression. The first strategy was to target the activated b-Raf-ERK1/2-mTOR pathway by combining roscovitine with rapamycin or sorafenib, which was effective at preventing the formation of hyperproliferative mammary acinar structures in LMW-E-expressing cells. In the inducible transgenic mouse model with LMW-E expression, we also observed similar hyperproliferation of the terminal end buds and activated MAPK pathway. Therefore, this mouse model is valuable to test the preclinical effectiveness of combining roscovitine with rapamycin or sorafenib at both preventing LMW-E-induced mammary tumor development as

well as inducing tumor toxicity post tumor formation. This therapeutic strategy is anticipated to demonstrate strong anti-tumor effect in the mouse model since we observed activation of the MAPK pathway in this mouse model and strong correlation between high LMW-E expression and activation of the b-raf/ERK/mTOR pathway with patient survival outcome.

The second therapeutic approach that we identified was by combining salinomycin with doxorubicin to target the LMW-E-induced CSCs. Again, the inducible transgenic mouse model with LMW-E expression is valuable to test the effectiveness of this drug combination. However, it is necessary to first determine whether the LMW-E-induced mammary tumors in the transgenic mice also demonstrate features of the EMT and enrichment for mammary CSCs. We speculate that the LMW-E-mediated mammary tumors likely undergo the EMT to facilitate metastasis development since it was reported that approximately 25% of LMW-E-tumor-bearing mice formed distant metastasis (180). If the salinomycin and doxorubicin combination proves to be effective at targeting the LMW-E-induced mammary tumors in the mouse model, this therapeutic strategy will undoubtedly implicate possible clinical application for breast cancer patients with high LMW-E expression given the fact that we have also provided evidence demonstrating a positive correlation between cytoplasmic cyclin E and the $CD44^{hi}/CD24^{lo}$ CSC population.

We ended this project with the finding that Hbo1 is a novel substrate of the cyclin E/CDK2 kinase complex. Given that the cyclin E/CDK2 complex has been shown to be involved during the assembly of the prereplication complex (pre-RC), it is not surprising that Hbo1 (a HAT binding to ORC1) was found to be a substrate of this kinase complex. DNA replication requires the assembly of the pre-RC, which is formed by the sequential loading of Cdc6/Cdcl8, Cdtl, and MCM2-7. More specifically, the interaction between cyclin E/CDK2 and Cdc6 was found to be critical for the initiation and maintenance of DNA replication at the G1-S phase boundary (115, 116). Recently, Hbo1 was reported to be important for the chromatin loading of the MCM2-7 since depletion of Hbo1 blocked MCM2-7 assembly into the pre-RC and subsequently inhibited DNA replication (313). Therefore, it is intriguing

to investigate the mechanistic function of cyclin E/CDK2 phosphorylation of Hbo1 on DNA replication licensing in the normal cellular context as well as the consequence of deregulated phosphorylation of Hbo1 due to hyperactive LMW-E/CDK2 activity in tumor cells. Perhaps phosphorylation of Hbo1 by the cyclin E/CDK2 complex provides a docking site on Hbo1 to recruit other proteins required for the assembly of the pre-RC. However, aberrant cyclin E/CDK2 kinase activity manifested by LMW-E/CDK2, whose activity has been shown to be deregulated throughout the cell cycle, can cause untimely DNA replication leading to genomic instability (173,184). Indeed, one mechanism of cyclin E-mediated oncogenesis is through inducing genomic instability (162-164) and tumor cells with *p53* loss and cyclin E overexpression were observed to have elevated frequency of centrosomal hyperamplification (120). In fact, in response to DNA replication fork arrest and hyperosmotic shock, stablized p53 has been shown to interact with Hbo1 and negatively regulates its HAT activity (307). Therefore, aberrant Hbo1 HAT activity due to lack of repression by p53 and overexpression of cyclin E may lead to deregulated DNA replication and predispose the cell to genomic instability.

Studies have shown that Hbo1 is the major HAT for histone H4 acetylation *in vivo,* however recent work by Kueh and colleagues demonstrated that Hbo1 is also necessary for H3K14 acetylation to transcriptionally activate genes associated with embryonic development (313, 316, 323, 324). While H4 acetylation is linked with DNA replication, H3 acetylation is thought to control transcriptional activity suggesting that aside from playing an important role during replication licensing in S-phase, Hbo1 also exerts control over gene expression (323). In fact, Hbo1 has been shown to affect the transcriptional activity of a few transcription factors such as ER, PR, AR and NF-κB (308-310). Interestingly, the N-terminal region of Hbo1 exerts repression of AR and NF-κB transcriptional activation while the C-terminal domain displays no effect suggesting that the HAT activity of Hbo1, which is located in the C-terminal region, is not necessarily required for Hbo1 to mediate transcriptional regulation (308, 309). Particularly, Contzler and colleagues further demonstrated that the mechanism of Hbo1-mediated suppression of NF-κB transcriptional activity is not through binding directly to NF-κB nor to the κB

consensus sequence but perhaps via interaction with NF-κB's coactivator(s) and thereby squelching them from NF-κB (309). One likely possible coactivator is SRC-1 since it has been shown to co-IP with the N-terminal domain but not the C-terminal region of Hbo1, and the interaction between these two proteins cooperates to enhance the transcriptional activities mediated by ER and PR (310). Finally, studies have shown that the N-terminal domain of Hbo1 is able to mediate transcriptional control both *in trans* and *in cis* thus implicating that this domain of Hbo1 is critical for the recruitment and binding of other factors to Hbo1 to regulate gene expression (325, 326). Therefore, phosphorylation of Hbo1 at T88 by the cyclin E/CDK2 complex may affect the ability of Hbo1 to regulate the transcriptional activities of PR, AR, NF-κB, and perhaps other transcription factors yet to be identified. This speculation can be addressed by using the T88A and T88D (or T88E) Hbo1 mutants to examine the extent of Hbo1's regulation on the transcriptional activities of ER, PR, AR and NF-κB through the use of a luciferase gene reporter assay.

In addition, *in vitro* HAT activity assay also showed that phosphorylation of Hbo1 at T88 by the cyclin E/CDK2 complex did not affect the HAT activity of Hbo1. Similar to the context of CDK1 phosphorylation and subsequent recruitment of Plk1 to Hbo1, we speculate that phosphorylation of Hbo1 by cyclin E/CDK2 also provides docking site for other proteins to bind to Hbo1. Again, T88A and T88D (or T88E) Hbo1 mutants can be used to co-IP possible interacting proteins and then identified via mass spectrometry. Alternatively, the retrovirus-based protein-fragment complementation assay can also be used to screen for interacting proteins to Hbo1 when phosphorylated at T88. This approach involves fusing the N-terminal half of the GFP gene to the Hbo1 mutants and the C-terminal half of the GFP gene is fused to an endogenously expressed protein through an in-frame exon trap. The difference in the hits obtained between the two mutants will uncover the proteins that interact specifically to Hbo1 when the T88 site is phosphorylated. Given that the N-terminal domain of Hbo1 is critical for its regulation of gene transcription, the identified interacting proteins to pT88 Hbo1 will further reveal other transcription

factors and co-activators that are critical in controlling the gene transcriptional activity of Hbo1.

Although the *in vitro* kinase assay was understandably not adequate in distinguishing the difference in the extent of phosphorylation between EL/CDK2 and LMW-E/CDK2 complexes, it is likely that high LMW-E levels in the tumor tissues of patients are responsible for phosphorylation of Hbo1. To address this hypothesis, an antibody specific to phospho-T88 Hbo1 can be produced and used for immunoblot analysis of our patient data set to correlate with LMW-E protein levels. Furthermore, the level of Hbo1 phosphorylation can also be analyzed for association with the percentage of the $CD44^{hi}/CD24^{lo}$ population as well as survival outcome in patients. These findings will better define the molecular deregulation mediated by LMW-E and thus bring us closer to identifying a therapeutic approach that is specific for patients with high LMW-E expression. For instance, a combination between a CDK inhibitor (i.e. roscovitine) and salinomycin might be effective at inhibiting the CSC population in patients with high LMW-E expression. Although CDK inhibitors such as flavopiridol and roscovitine have demonstrated unimpressive response in clinical trials as a single agent, it must be noted that the patients in these trials were not selected based on LMW-E levels (327, 328). By inhibiting the CSC population in the high LMW-E-expressing tumors, we may be able to achieve favorable outcome and avoid tumor relapse due to the specific targeting of the CSCs. In addition, another possible target is Hbo1 using HAT inhibitor if the HAT activity of Hbo1 were found to be important in enriching for the CSC populations. However, similar to HDACs, HATs also have both oncogenic and tumor suppressive roles in cancer biology thus complicating its use in the clinic. To date, there are a few HAT inhibitors available for mechanistic studies as possible antitumor agents such as garcinol, anacardic acid, and curcumin, which are among the natural inhibitors found in plants. Particularly, anacardic acid was shown to be a radiation sensitizer while garcinol and curcumin demonstrated strong cytotoxic effect in human leukemic cell lines (329, 330). As with all natural compounds, their mechanism of action is typically complex and non-specific and thus warrants more extensive investigation prior to use in the clinic. In contrast to the plant-derived

inhibitors, lys-CoA, which is a synthetic HAT inhibitor (lysine amino acid conjugated to coenzyme A), has been shown to exhibit highly specific and potent activity against HAT activity although its use *in vivo* has been limited due to high metabolic instability and cell impermeability (331). While HAT inhibitors are currently not ideal for clinical therapy, they can serve as valuable tools for mechanistic studies as proofs of principle.

4.3. SIGNIFICANCE

The incident rate of breast cancer worldwide is steadily increasing over the past few decades, and the problem of tumor recurrence remains difficult to address. Clinical studies demonstrated that a high percentage of breast cancer patients express LMW-E, and this occurrence is linked to adverse clinical outcomes (160). In this dissertation, we identified two therapeutic approaches of targeting breast tumor cells with high LMW-E expression: 1) combination of roscovitine with sorafenib or rapamycin and 2) combination of doxorubicin and salinomycin. We believe that the results from this study provided important preclinical basis for the use of these agents first in the animal model and hopefully into the clinic in the near future. Furthermore, the identification of Hbo1 as a downstream substrate of the LMW-E/CDK2 complex undoubtedly unveils additional mechanism of how LMW-E mediates mammary tumorigenesis.

REFERENCES

1. Bissell, M. J., A. Rizki, and I. S. Mian. 2003. Tissue architecture: the ultimate regulator of breast epithelial function. Curr Opin Cell Biol 15:753-762.
2. Romond, E. H., E. A. Perez, J. Bryant, V. J. Suman, C. E. Geyer, Jr., N. E. Davidson, E. Tan-Chiu, S. Martino, S. Paik, P. A. Kaufman, S. M. Swain, T. M. Pisansky, L. Fehrenbacher, L. A. Kutteh, V. G. Vogel, D. W. Visscher, G. Yothers, R. B. Jenkins, A. M. Brown, S. R. Dakhil, E. P. Mamounas, W. L. Lingle, P. M. Klein, J. N. Ingle, and N. Wolmark. 2005. Trastuzumab plus adjuvant chemotherapy for operable HER2-positive breast cancer. N Engl J Med 353:1673-1684.
3. Bang, Y. J., E. Van Cutsem, A. Feyereislova, H. C. Chung, L. Shen, A. Sawaki, F. Lordick, A. Ohtsu, Y. Omuro, T. Satoh, G. Aprile, E. Kulikov, J. Hill, M. Lehle, J. Ruschoff, and Y. K. Kang. 2010. Trastuzumab in combination with chemotherapy versus chemotherapy alone for treatment of HER2-positive advanced gastric or gastro-oesophageal junction cancer (ToGA): a phase 3, open-label, randomised controlled trial. Lancet 376:687-697.
4. Buzdar, A. U., M. Baum, and J. Cuzick. 2006. Letrozole or tamoxifen in early breast cancer. N Engl J Med 354:1528-1530; author reply 1528-1530.
5. Coombes, R. C., E. Hall, L. J. Gibson, R. Paridaens, J. Jassem, T. Delozier, S. E. Jones, I. Alvarez, G. Bertelli, O. Ortmann, A. S. Coates, E. Bajetta, D. Dodwell, R. E. Coleman, L. J. Fallowfield, E. Mickiewicz, J. Andersen, P. E. Lonning, G. Cocconi, A. Stewart, N. Stuart, C. F. Snowdon, M. Carpentieri, G. Massimini, J. M. Bliss, and C. van de Velde. 2004. A randomized trial of exemestane after two to three years of tamoxifen therapy in postmenopausal women with primary breast cancer. N Engl J Med 350:1081-1092.
6. Smith, I. E., and M. Dowsett. 2003. Aromatase inhibitors in breast cancer. N Engl J Med 348:2431-2442.
7. Geisler, J., N. King, G. Anker, G. Ornati, E. Di Salle, P. E. Lonning, and M. Dowsett. 1998. In vivo inhibition of aromatization by exemestane, a novel

irreversible aromatase inhibitor, in postmenopausal breast cancer patients. Clin Cancer Res 4:2089-2093.

8. Lonning, P. E. 2004. Aromatase inhibitors in breast cancer. Endocr Relat Cancer 11:179-189.
9. Hortobagyi, G. N. 1998. Treatment of breast cancer. N Engl J Med 339:974-984.
10. Perou, C. M., T. Sorlie, M. B. Eisen, M. van de Rijn, S. S. Jeffrey, C. A. Rees, J. R. Pollack, D. T. Ross, H. Johnsen, L. A. Akslen, O. Fluge, A. Pergamenschikov, C. Williams, S. X. Zhu, P. E. Lonning, A. L. Borresen-Dale, P. O. Brown, and D. Botstein. 2000. Molecular portraits of human breast tumours. Nature 406:747-752.
11. Calza, S., P. Hall, G. Auer, J. Bjohle, S. Klaar, U. Kronenwett, E. T. Liu, L. Miller, A. Ploner, J. Smeds, J. Bergh, and Y. Pawitan. 2006. Intrinsic molecular signature of breast cancer in a population-based cohort of 412 patients. Breast Cancer Res 8:R34.
12. Sorlie, T., R. Tibshirani, J. Parker, T. Hastie, J. S. Marron, A. Nobel, S. Deng, H. Johnsen, R. Pesich, S. Geisler, J. Demeter, C. M. Perou, P. E. Lonning, P. O. Brown, A. L. Borresen-Dale, and D. Botstein. 2003. Repeated observation of breast tumor subtypes in independent gene expression data sets. Proc Natl Acad Sci U S A 100:8418-8423.
13. Sotiriou, C., S. Y. Neo, L. M. McShane, E. L. Korn, P. M. Long, A. Jazaeri, P. Martiat, S. B. Fox, A. L. Harris, and E. T. Liu. 2003. Breast cancer classification and prognosis based on gene expression profiles from a population-based study. Proc Natl Acad Sci U S A 100:10393-10398.
14. Hoadley, K. A., V. J. Weigman, C. Fan, L. R. Sawyer, X. He, M. A. Troester, C. I. Sartor, T. Rieger-House, P. S. Bernard, L. A. Carey, and C. M. Perou. 2007. EGFR associated expression profiles vary with breast tumor subtype. BMC Genomics 8:258.
15. Prat, A., J. S. Parker, O. Karginova, C. Fan, C. Livasy, J. I. Herschkowitz, X. He, and C. M. Perou. 2010

. Phenotypic and molecular characterization of the claudin-low intrinsic subtype of breast cancer. Breast Cancer Res 12:R68.

16. Hennessy, B. T., A. M. Gonzalez-Angulo, K. Stemke-Hale, M. Z. Gilcrease, S. Krishnamurthy, J. S. Lee, J. Fridlyand, A. Sahin, R. Agarwal, C. Joy, W. Liu, D. Stivers, K. Baggerly, M. Carey, A. Lluch, C. Monteagudo, X. He, V. Weigman, C. Fan, J. Palazzo, G. N. Hortobagyi, L. K. Nolden, N. J. Wang, V. Valero, J. W. Gray, C. M. Perou, and G. B. Mills. 2009. Characterization of a naturally occurring breast cancer subset enriched in epithelial-to-mesenchymal transition and stem cell characteristics. Cancer Res 69:4116-4124.

17. Creighton, C. J., X. Li, M. Landis, J. M. Dixon, V. M. Neumeister, A. Sjolund, D. L. Rimm, H. Wong, A. Rodriguez, J. I. Herschkowitz, C. Fan, X. Zhang, X. He, A. Pavlick, M. C. Gutierrez, L. Renshaw, A. A. Larionov, D. Faratian, S. G. Hilsenbeck, C. M. Perou, M. T. Lewis, J. M. Rosen, and J. C. Chang. 2009. Residual breast cancers after conventional therapy display mesenchymal as well as tumor-initiating features. Proc Natl Acad Sci U S A 106:13820-13825.

18. Glinsky, G. V. 2007. Stem cell origin of death-from-cancer phenotypes of human prostate and breast cancers. Stem Cell Rev 3:79-93.

19. Kakarala, M., and M. S. Wicha. 2008. Implications of the cancer stem-cell hypothesis for breast cancer prevention and therapy. J Clin Oncol 26:2813-2820.

20. Coller, H. A., L. Sang, and J. M. Roberts. 2006. A new description of cellular quiescence. PLoS Biol 4:e83.

21. Peng, J., N. F. Marshall, and D. H. Price. 1998. Identification of a cyclin subunit required for the function of Drosophila P-TEFb. J Biol Chem 273:13855-13860.

22. Okamoto, K., and D. Beach. 1994. Cyclin G is a transcriptional target of the p53 tumor suppressor protein. Embo J 13:4816-4822.

23. Rickert, P., W. Seghezzi, F. Shanahan, H. Cho, and E. Lees. 1996. Cyclin C/CDK8 is a novel CTD kinase associated with RNA polymerase II. Oncogene 12:2631-2640.
24. Arellano, M., and S. Moreno. 1997. Regulation of CDK/cyclin complexes during the cell cycle. Int J Biochem Cell Biol 29:559-573.
25. Morgan, D. O. 1997. Cyclin-dependent kinases: engines, clocks, and microprocessors. Annu Rev Cell Dev Biol 13:261-291.
26. Fisher, R. P., and D. O. Morgan. 1994. A novel cyclin associates with MO15/CDK7 to form the CDK-activating kinase. Cell 78:713-724.
27. Sherr, C. J. 1994. G1 phase progression: cycling on cue. Cell 79:551-555.
28. Kowalczyk, A., R. K. Filipkowski, M. Rylski, G. M. Wilczynski, F. A. Konopacki, J. Jaworski, M. A. Ciemerych, P. Sicinski, and L. Kaczmarek. 2004. The critical role of cyclin D2 in adult neurogenesis. J Cell Biol 167:209-213.
29. Fantl, V., G. Stamp, A. Andrews, I. Rosewell, and C. Dickson. 1995. Mice lacking cyclin D1 are small and show defects in eye and mammary gland development. Genes Dev 9:2364-2372.
30. Sicinski, P., J. L. Donaher, S. B. Parker, T. Li, A. Fazeli, H. Gardner, S. Z. Haslam, R. T. Bronson, S. J. Elledge, and R. A. Weinberg. 1995. Cyclin D1 provides a link between development and oncogenesis in the retina and breast. Cell 82:621-630.
31. Huard, J. M., C. C. Forster, M. L. Carter, P. Sicinski, and M. E. Ross. 1999. Cerebellar histogenesis is disturbed in mice lacking cyclin D2. Development 126:1927-1935.
32. Sicinski, P., J. L. Donaher, Y. Geng, S. B. Parker, H. Gardner, M. Y. Park, R. L. Robker, J. S. Richards, L. K. McGinnis, J. D. Biggers, J. J. Eppig, R. T. Bronson, S. J. Elledge, and R. A. Weinberg. 1996. Cyclin D2 is an FSH-responsive gene involved in gonadal cell proliferation and oncogenesis. Nature 384:470-474.
33. Solvason, N., W. W. Wu, D. Parry, D. Mahony, E. W. Lam, J. Glassford, G. G. Klaus, P. Sicinski, R. Weinberg, Y. J. Liu, M. Howard, and E. Lees. 2000.

Cyclin D2 is essential for BCR-mediated proliferation and CD5 B cell development. Int Immunol 12:631-638.

34. Sicinska, E., I. Aifantis, L. Le Cam, W. Swat, C. Borowski, Q. Yu, A. A. Ferrando, S. D. Levin, Y. Geng, H. von Boehmer, and P. Sicinski. 2003. Requirement for cyclin D3 in lymphocyte development and T cell leukemias. Cancer Cell 4:451-461.
35. Ciemerych, M. A., A. M. Kenney, E. Sicinska, I. Kalaszczynska, R. T. Bronson, D. H. Rowitch, H. Gardner, and P. Sicinski. 2002. Development of mice expressing a single D-type cyclin. Genes Dev 16:3277-3289.
36. Kozar, K., M. A. Ciemerych, V. I. Rebel, H. Shigematsu, A. Zagozdzon, E. Sicinska, Y. Geng, Q. Yu, S. Bhattacharya, R. T. Bronson, K. Akashi, and P. Sicinski. 2004. Mouse development and cell proliferation in the absence of D-cyclins. Cell 118:477-491.
37. Assoian, R. K., and X. Zhu. 1997. Cell anchorage and the cytoskeleton as partners in growth factor dependent cell cycle progression. Curr Opin Cell Biol 9:93-98.
38. Buchkovich, K., L. A. Duffy, and E. Harlow. 1989. The retinoblastoma protein is phosphorylated during specific phases of the cell cycle. Cell 58:1097-1105.
39. Kato, J., H. Matsushime, S. W. Hiebert, M. E. Ewen, and C. J. Sherr. 1993. Direct binding of cyclin D to the retinoblastoma gene product (pRb) and pRb phosphorylation by the cyclin D-dependent kinase CDK4. Genes Dev 7:331-342.
40. Ohtani, K., J. DeGregori, and J. R. Nevins. 1995. Regulation of the cyclin E gene by transcription factor E2F1. Proc Natl Acad Sci U S A 92:12146-12150.
41. Lauper, N., A. R. Beck, S. Cariou, L. Richman, K. Hofmann, W. Reith, J. M. Slingerland, and B. Amati. 1998. Cyclin E2: a novel CDK2 partner in the late G1 and S phases of the mammalian cell cycle. Oncogene 17:2637-2643.
42. Zariwala, M., J. Liu, and Y. Xiong. 1998. Cyclin E2, a novel human G1 cyclin and activating partner of CDK2 and CDK3, is induced by viral oncoproteins. Oncogene 17:2787-2798.

43. Gudas, J. M., M. Payton, S. Thukral, E. Chen, M. Bass, M. O. Robinson, and S. Coats. 1999. Cyclin E2, a novel G1 cyclin that binds Cdk2 and is aberrantly expressed in human cancers. Mol Cell Biol 19:612-622.
44. Parisi, T., A. R. Beck, N. Rougier, T. McNeil, L. Lucian, Z. Werb, and B. Amati. 2003. Cyclins E1 and E2 are required for endoreplication in placental trophoblast giant cells. Embo J 22:4794-4803.
45. Geng, Y., Q. Yu, E. Sicinska, M. Das, J. E. Schneider, S. Bhattacharya, W. M. Rideout, R. T. Bronson, H. Gardner, and P. Sicinski. 2003. Cyclin E ablation in the mouse. Cell 114:431-443.
46. Ohtsubo, M., A. M. Theodoras, J. Schumacher, J. M. Roberts, and M. Pagano. 1995. Human cyclin E, a nuclear protein essential for the G1-to-S phase transition. Mol Cell Biol 15:2612-2624.
47. Girard, F., U. Strausfeld, A. Fernandez, and N. J. Lamb. 1991. Cyclin A is required for the onset of DNA replication in mammalian fibroblasts. Cell 67:1169-1179.
48. Walker, D. H., and J. L. Maller. 1991. Role for cyclin A in the dependence of mitosis on completion of DNA replication. Nature 354:314-317.
49. Liu, D., M. M. Matzuk, W. K. Sung, Q. Guo, P. Wang, and D. J. Wolgemuth. 1998. Cyclin A1 is required for meiosis in the male mouse. Nat Genet 20:377-380.
50. Murphy, M., M. G. Stinnakre, C. Senamaud-Beaufort, N. J. Winston, C. Sweeney, M. Kubelka, M. Carrington, C. Brechot, and J. Sobczak-Thepot. 1997. Delayed early embryonic lethality following disruption of the murine cyclin A2 gene. Nat Genet 15:83-86.
51. King, R. W., P. K. Jackson, and M. W. Kirschner. 1994. Mitosis in transition. Cell 79:563-571.
52. Brandeis, M., I. Rosewell, M. Carrington, T. Crompton, M. A. Jacobs, J. Kirk, J. Gannon, and T. Hunt. 1998. Cyclin B2-null mice develop normally and are fertile whereas cyclin B1-null mice die in utero. Proc Natl Acad Sci U S A 95:4344-4349.

53. Heald, R., M. McLoughlin, and F. McKeon. 1993. Human wee1 maintains mitotic timing by protecting the nucleus from cytoplasmically activated Cdc2 kinase. Cell 74:463-474.
54. McGowan, C. H., and P. Russell. 1993. Human Wee1 kinase inhibits cell division by phosphorylating p34cdc2 exclusively on Tyr15. Embo J 12:75-85.
55. Mueller, P. R., T. R. Coleman, A. Kumagai, and W. G. Dunphy. 1995. Myt1: a membrane-associated inhibitory kinase that phosphorylates Cdc2 on both threonine-14 and tyrosine-15. Science 270:86-90.
56. Parker, L. L., and H. Piwnica-Worms. 1992. Inactivation of the p34cdc2-cyclin B complex by the human WEE1 tyrosine kinase. Science 257:1955-1957.
57. Sebastian, B., A. Kakizuka, and T. Hunter. 1993. Cdc25M2 activation of cyclin-dependent kinases by dephosphorylation of threonine-14 and tyrosine-15. Proc Natl Acad Sci U S A 90:3521-3524.
58. Villa-Moruzzi, E. 1993. Activation of the cdc25C phosphatase in mitotic HeLa cells. Biochem Biophys Res Commun 196:1248-1254.
59. Sherr, C. J., and J. M. Roberts. 1995. Inhibitors of mammalian G1 cyclin-dependent kinases. Genes Dev 9:1149-1163.
60. Carnero, A., and G. J. Hannon. 1998. The INK4 family of CDK inhibitors. Curr Top Microbiol Immunol 227:43-55.
61. Hengst, L., and S. I. Reed. 1998. Inhibitors of the Cip/Kip family. Curr Top Microbiol Immunol 227:25-41.
62. Pan, Z. Q., J. T. Reardon, L. Li, H. Flores-Rozas, R. Legerski, A. Sancar, and J. Hurwitz. 1995. Inhibition of nucleotide excision repair by the cyclin-dependent kinase inhibitor p21. J Biol Chem 270:22008-22016.
63. el-Deiry, W. S., T. Tokino, V. E. Velculescu, D. B. Levy, R. Parsons, J. M. Trent, D. Lin, W. E. Mercer, K. W. Kinzler, and B. Vogelstein. 1993. WAF1, a potential mediator of p53 tumor suppression. Cell 75:817-825.
64. Zhang, H., G. J. Hannon, and D. Beach. 1994. p21-containing cyclin kinases exist in both active and inactive states. Genes Dev 8:1750-1758.

65. Hannon, G. J., and D. Beach. 1994. p15INK4B is a potential effector of TGF-beta-induced cell cycle arrest. Nature 371:257-261.
66. Reynisdottir, I., K. Polyak, A. Iavarone, and J. Massague. 1995. Kip/Cip and Ink4 Cdk inhibitors cooperate to induce cell cycle arrest in response to TGF-beta. Genes Dev 9:1831-1845.
67. Reynisdottir, I., and J. Massague. 1997. The subcellular locations of p15(Ink4b) and p27(Kip1) coordinate their inhibitory interactions with cdk4 and cdk2. Genes Dev 11:492-503.
68. Pardee, A. B. 1974. A restriction point for control of normal animal cell proliferation. Proc Natl Acad Sci U S A 71:1286-1290.
69. Motokura, T., T. Bloom, H. G. Kim, H. Juppner, J. V. Ruderman, H. M. Kronenberg, and A. Arnold. 1991. A novel cyclin encoded by a bcl1-linked candidate oncogene. Nature 350:512-515.
70. Weisenburger, D. D., W. G. Sanger, J. O. Armitage, and D. T. Purtilo. 1987. Intermediate lymphocytic lymphoma: immunophenotypic and cytogenetic findings. Blood 69:1617-1621.
71. Hall, M., and G. Peters. 1996. Genetic alterations of cyclins, cyclin-dependent kinases, and Cdk inhibitors in human cancer. Adv Cancer Res 68:67-108.
72. Dobashi, Y., M. Shoji, S. X. Jiang, M. Kobayashi, Y. Kawakubo, and T. Kameya. 1998. Active cyclin A-CDK2 complex, a possible critical factor for cell proliferation in human primary lung carcinomas. Am J Pathol 153:963-972.
73. Wolfel, T., M. Hauer, J. Schneider, M. Serrano, C. Wolfel, E. Klehmann-Hieb, E. De Plaen, T. Hankeln, K. H. Meyer zum Buschenfelde, and D. Beach. 1995. A p16INK4a-insensitive CDK4 mutant targeted by cytolytic T lymphocytes in a human melanoma. Science 269:1281-1284.
74. Yamamoto, H., T. Monden, H. Miyoshi, H. Izawa, K. Ikeda, M. Tsujie, T. Ohnishi, M. Sekimoto, N. Tomita, and M. Monden. 1998. Cdk2/cdc2 expression in colon carcinogenesis and effects of cdk2/cdc2 inhibitor in colon cancer cells. Int J Oncol 13:233-239.

75. Kim, J. H., M. J. Kang, C. U. Park, H. J. Kwak, Y. Hwang, and G. Y. Koh. 1999. Amplified CDK2 and cdc2 activities in primary colorectal carcinoma. Cancer 85:546-553.
76. Easton, J., T. Wei, J. M. Lahti, and V. J. Kidd. 1998. Disruption of the cyclin D/cyclin-dependent kinase/INK4/retinoblastoma protein regulatory pathway in human neuroblastoma. Cancer Res 58:2624-2632.
77. Harper, J. W., and S. J. Elledge. 1996. Cdk inhibitors in development and cancer. Curr Opin Genet Dev 6:56-64.
78. Kamb, A. 1998. Cyclin-dependent kinase inhibitors and human cancer. Curr Top Microbiol Immunol 227:139-148.
79. King, R. W., R. J. Deshaies, J. M. Peters, and M. W. Kirschner. 1996. How proteolysis drives the cell cycle. Science 274:1652-1659.
80. Pagano, M. 1997. Cell cycle regulation by the ubiquitin pathway. Faseb J 11:1067-1075.
81. Shi, Y., M. Zou, N. R. Farid, and S. T. al-Sedairy. 1996. Evidence of gene deletion of p21 (WAF1/CIP1), a cyclin-dependent protein kinase inhibitor, in thyroid carcinomas. Br J Cancer 74:1336-1341.
82. Knudson, A. G., Jr. 1971. Mutation and cancer: statistical study of retinoblastoma. Proc Natl Acad Sci U S A 68:820-823.
83. Gage, J. R., C. Meyers, and F. O. Wettstein. 1990. The E7 proteins of the nononcogenic human papillomavirus type 6b (HPV-6b) and of the oncogenic HPV-16 differ in retinoblastoma protein binding and other properties. J Virol 64:723-730.
84. Chellappan, S., V. B. Kraus, B. Kroger, K. Munger, P. M. Howley, W. C. Phelps, and J. R. Nevins. 1992. Adenovirus E1A, simian virus 40 tumor antigen, and human papillomavirus E7 protein share the capacity to disrupt the interaction between transcription factor E2F and the retinoblastoma gene product. Proc Natl Acad Sci U S A 89:4549-4553.
85. Moran, E. 1993. Interaction of adenoviral proteins with pRB and p53. Faseb J 7:880-885.

86. Mudrak, I., E. Ogris, H. Rotheneder, and E. Wintersberger. 1994. Coordinated trans activation of DNA synthesis- and precursor-producing enzymes by polyomavirus large T antigen through interaction with the retinoblastoma protein. Mol Cell Biol 14:1886-1892.
87. Beijersbergen, R. L., R. M. Kerkhoven, L. Zhu, L. Carlee, P. M. Voorhoeve, and R. Bernards. 1994. E2F-4, a new member of the E2F gene family, has oncogenic activity and associates with p107 in vivo. Genes Dev 8:2680-2690.
88. Johnson, D. G., W. D. Cress, L. Jakoi, and J. R. Nevins. 1994. Oncogenic capacity of the E2F1 gene. Proc Natl Acad Sci U S A 91:12823-12827.
89. Pierce, A. M., I. B. Gimenez-Conti, R. Schneider-Broussard, L. A. Martinez, C. J. Conti, and D. G. Johnson. 1998. Increased E2F1 activity induces skin tumors in mice heterozygous and nullizygous for p53. Proc Natl Acad Sci U S A 95:8858-8863.
90. Weiss, A., A. Herzig, H. Jacobs, and C. F. Lehner. 1998. Continuous Cyclin E expression inhibits progression through endoreduplication cycles in Drosophila. Curr Biol 8:239-242.
91. Follette, P. J., R. J. Duronio, and P. H. O'Farrell. 1998. Fluctuations in cyclin E levels are required for multiple rounds of endocycle S phase in Drosophila. Curr Biol 8:235-238.
92. Coverley, D., C. Pelizon, S. Trewick, and R. A. Laskey. 2000. Chromatin-bound Cdc6 persists in S and G2 phases in human cells, while soluble Cdc6 is destroyed in a cyclin A-cdk2 dependent process. J Cell Sci 113 (Pt 11):1929-1938.
93. Yu, Q., Y. Geng, and P. Sicinski. 2001. Specific protection against breast cancers by cyclin D1 ablation. Nature 411:1017-1021.
94. Ortega, S., I. Prieto, J. Odajima, A. Martin, P. Dubus, R. Sotillo, J. L. Barbero, M. Malumbres, and M. Barbacid. 2003. Cyclin-dependent kinase 2 is essential for meiosis but not for mitotic cell division in mice. Nat Genet 35:25-31.

95. Berthet, C., E. Aleem, V. Coppola, L. Tessarollo, and P. Kaldis. 2003. Cdk2 knockout mice are viable. Curr Biol 13:1775-1785.
96. Ye, X., C. Zhu, and J. W. Harper. 2001. A premature-termination mutation in the Mus musculus cyclin-dependent kinase 3 gene. Proc Natl Acad Sci U S A 98:1682-1686.
97. Geisen, C., and T. Moroy. 2002. The oncogenic activity of cyclin E is not confined to Cdk2 activation alone but relies on several other, distinct functions of the protein. J Biol Chem 277:39909-39918.
98. Matsumoto, Y., and J. L. Maller. 2004. A centrosomal localization signal in cyclin E required for Cdk2-independent S phase entry. Science 306:885-888.
99. Ohtsubo, M., and J. M. Roberts. 1993. Cyclin-dependent regulation of G1 in mammalian fibroblasts. Science 259:1908-1912.
100. Resnitzky, D., M. Gossen, H. Bujard, and S. I. Reed. 1994. Acceleration of the G1/S phase transition by expression of cyclins D1 and E with an inducible system. Mol Cell Biol 14:1669-1679.
101. Tsai, L. H., E. Lees, B. Faha, E. Harlow, and K. Riabowol. 1993. The cdk2 kinase is required for the G1-to-S transition in mammalian cells. Oncogene 8:1593-1602.
102. van den Heuvel, S., and E. Harlow. 1993. Distinct roles for cyclin-dependent kinases in cell cycle control. Science 262:2050-2054.
103. Geng, Y., W. Whoriskey, M. Y. Park, R. T. Bronson, R. H. Medema, T. Li, R. A. Weinberg, and P. Sicinski. 1999. Rescue of cyclin D1 deficiency by knockin cyclin E. Cell 97:767-777.
104. Adams, P. D., W. R. Sellers, S. K. Sharma, A. D. Wu, C. M. Nalin, and W. G. Kaelin, Jr. 1996. Identification of a cyclin-cdk2 recognition motif present in substrates and p21-like cyclin-dependent kinase inhibitors. Mol Cell Biol 16:6623-6633.
105. Chen, J., P. Saha, S. Kornbluth, B. D. Dynlacht, and A. Dutta. 1996. Cyclin-binding motifs are essential for the function of p21CIP1. Mol Cell Biol 16:4673-4682.

106. Schulman, B. A., D. L. Lindstrom, and E. Harlow. 1998. Substrate recruitment to cyclin-dependent kinase 2 by a multipurpose docking site on cyclin A. Proc Natl Acad Sci U S A 95:10453-10458.
107. Dowdy, S. F., P. W. Hinds, K. Louie, S. I. Reed, A. Arnold, and R. A. Weinberg. 1993. Physical interaction of the retinoblastoma protein with human D cyclins. Cell 73:499-511.
108. Vlach, J., S. Hennecke, K. Alevizopoulos, D. Conti, and B. Amati. 1996. Growth arrest by the cyclin-dependent kinase inhibitor p27Kip1 is abrogated by c-Myc. Embo J 15:6595-6604.
109. Carrano, A. C., E. Eytan, A. Hershko, and M. Pagano. 1999. SKP2 is required for ubiquitin-mediated degradation of the CDK inhibitor p27. Nat Cell Biol 1:193-199.
110. Zhao, J., B. K. Kennedy, B. D. Lawrence, D. A. Barbie, A. G. Matera, J. A. Fletcher, and E. Harlow. 2000. NPAT links cyclin E-Cdk2 to the regulation of replication-dependent histone gene transcription. Genes Dev 14:2283-2297.
111. Ma, T., B. A. Van Tine, Y. Wei, M. D. Garrett, D. Nelson, P. D. Adams, J. Wang, J. Qin, L. T. Chow, and J. W. Harper. 2000. Cell cycle-regulated phosphorylation of p220(NPAT) by cyclin E/Cdk2 in Cajal bodies promotes histone gene transcription. Genes Dev 14:2298-2313.
112. Ait-Si-Ali, S., S. Ramirez, F. X. Barre, F. Dkhissi, L. Magnaghi-Jaulin, J. A. Girault, P. Robin, M. Knibiehler, L. L. Pritchard, B. Ducommun, D. Trouche, and A. Harel-Bellan. 1998. Histone acetyltransferase activity of CBP is controlled by cycle-dependent kinases and oncoprotein E1A. Nature 396:184-186.
113. Bradbury, E. M., R. J. Inglis, and H. R. Matthews. 1974. Control of cell division by very lysine rich histone (F1) phosphorylation. Nature 247:257-261.
114. Rao, H., and B. Stillman. 1995. The origin recognition complex interacts with a bipartite DNA binding site within yeast replicators. Proc Natl Acad Sci U S A 92:2224-2228.

115. Furstenthal, L., B. K. Kaiser, C. Swanson, and P. K. Jackson. 2001. Cyclin E uses Cdc6 as a chromatin-associated receptor required for DNA replication. J Cell Biol 152:1267-1278.
116. Coverley, D., H. Laman, and R. A. Laskey. 2002. Distinct roles for cyclins E and A during DNA replication complex assembly and activation. Nat Cell Biol 4:523-528.
117. Chen, Z., V. B. Indjeian, M. McManus, L. Wang, and B. D. Dynlacht. 2002. CP110, a cell cycle-dependent CDK substrate, regulates centrosome duplication in human cells. Dev Cell 3:339-350.
118. Okuda, M., H. F. Horn, P. Tarapore, Y. Tokuyama, A. G. Smulian, P. K. Chan, E. S. Knudsen, I. A. Hofmann, J. D. Snyder, K. E. Bove, and K. Fukasawa. 2000. Nucleophosmin/B23 is a target of CDK2/cyclin E in centrosome duplication. Cell 103:127-140.
119. Fisk, H. A., and M. Winey. 2001. The mouse Mps1p-like kinase regulates centrosome duplication. Cell 106:95-104.
120. Mussman, J. G., H. F. Horn, P. E. Carroll, M. Okuda, P. Tarapore, L. A. Donehower, and K. Fukasawa. 2000. Synergistic induction of centrosome hyperamplification by loss of p53 and cyclin E overexpression. Oncogene 19:1635-1646.
121. Murre, C., P. S. McCaw, H. Vaessin, M. Caudy, L. Y. Jan, Y. N. Jan, C. V. Cabrera, J. N. Buskin, S. D. Hauschka, A. B. Lassar, and et al. 1989. Interactions between heterologous helix-loop-helix proteins generate complexes that bind specifically to a common DNA sequence. Cell 58:537-544.
122. Prabhu, S., A. Ignatova, S. T. Park, and X. H. Sun. 1997. Regulation of the expression of cyclin-dependent kinase inhibitor p21 by E2A and Id proteins. Mol Cell Biol 17:5888-5896.
123. Peverali, F. A., T. Ramqvist, R. Saffrich, R. Pepperkok, M. V. Barone, and L. Philipson. 1994. Regulation of G1 progression by E2A and Id helix-loop-helix proteins. Embo J 13:4291-4301.

124. Choi, J., M. L. Costa, C. S. Mermelstein, C. Chagas, S. Holtzer, and H. Holtzer. 1990. MyoD converts primary dermal fibroblasts, chondroblasts, smooth muscle, and retinal pigmented epithelial cells into striated mononucleated myoblasts and multinucleated myotubes. Proc Natl Acad Sci U S A 87:7988-7992.
125. Hara, E., M. Hall, and G. Peters. 1997. Cdk2-dependent phosphorylation of Id2 modulates activity of E2A-related transcription factors. Embo J 16:332-342.
126. Deed, R. W., E. Hara, G. T. Atherton, G. Peters, and J. D. Norton. 1997. Regulation of Id3 cell cycle function by Cdk-2-dependent phosphorylation. Mol Cell Biol 17:6815-6821.
127. Roberts, A. B., and L. M. Wakefield. 2003. The two faces of transforming growth factor beta in carcinogenesis. Proc Natl Acad Sci U S A 100:8621-8623.
128. Liu, F. 2003. Receptor-regulated Smads in TGF-beta signaling. Front Biosci 8:s1280-1303.
129. Moustakas, A., and D. Kardassis. 1998. Regulation of the human p21/WAF1/Cip1 promoter in hepatic cells by functional interactions between Sp1 and Smad family members. Proc Natl Acad Sci U S A 95:6733-6738.
130. Yagi, K., M. Furuhashi, H. Aoki, D. Goto, H. Kuwano, K. Sugamura, K. Miyazono, and M. Kato. 2002. c-myc is a downstream target of the Smad pathway. J Biol Chem 277:854-861.
131. Kang, Y., C. R. Chen, and J. Massague. 2003. A self-enabling TGFbeta response coupled to stress signaling: Smad engages stress response factor ATF3 for Id1 repression in epithelial cells. Mol Cell 11:915-926.
132. Matsuura, I., N. G. Denissova, G. Wang, D. He, J. Long, and F. Liu. 2004. Cyclin-dependent kinases regulate the antiproliferative function of Smads. Nature 430:226-231.
133. Cooley, A., S. Zelivianski, and J. S. Jeruss. 2010. Impact of cyclin E overexpression on Smad3 activity in breast cancer cell lines. Cell Cycle 9:4900-4907.

134. Sherr, C. J. 1993. Mammalian G1 cyclins. Cell 73:1059-1065.
135. Clurman, B. E., R. J. Sheaff, K. Thress, M. Groudine, and J. M. Roberts. 1996. Turnover of cyclin E by the ubiquitin-proteasome pathway is regulated by cdk2 binding and cyclin phosphorylation. Genes Dev 10:1979-1990.
136. Singer, J. D., M. Gurian-West, B. Clurman, and J. M. Roberts. 1999. Cullin-3 targets cyclin E for ubiquitination and controls S phase in mammalian cells. Genes Dev 13:2375-2387.
137. Nakayama, K., H. Nagahama, Y. A. Minamishima, M. Matsumoto, I. Nakamichi, K. Kitagawa, M. Shirane, R. Tsunematsu, T. Tsukiyama, N. Ishida, M. Kitagawa, K. Nakayama, and S. Hatakeyama. 2000. Targeted disruption of Skp2 results in accumulation of cyclin E and p27(Kip1), polyploidy and centrosome overduplication. Embo J 19:2069-2081.
138. Bai, C., P. Sen, K. Hofmann, L. Ma, M. Goebl, J. W. Harper, and S. J. Elledge. 1996. SKP1 connects cell cycle regulators to the ubiquitin proteolysis machinery through a novel motif, the F-box. Cell 86:263-274.
139. Winston, J. T., D. M. Koepp, C. Zhu, S. J. Elledge, and J. W. Harper. 1999. A family of mammalian F-box proteins. Curr Biol 9:1180-1182.
140. Koepp, D. M., L. K. Schaefer, X. Ye, K. Keyomarsi, C. Chu, J. W. Harper, and S. J. Elledge. 2001. Phosphorylation-dependent ubiquitination of cyclin E by the SCFFbw7 ubiquitin ligase. Science 294:173-177.
141. Strohmaier, H., C. H. Spruck, P. Kaiser, K. A. Won, O. Sangfelt, and S. I. Reed. 2001. Human F-box protein hCdc4 targets cyclin E for proteolysis and is mutated in a breast cancer cell line. Nature 413:316-322.
142. Ye, X., G. Nalepa, M. Welcker, B. M. Kessler, E. Spooner, J. Qin, S. J. Elledge, B. E. Clurman, and J. W. Harper. 2004. Recognition of phosphodegron motifs in human cyclin E by the SCF(Fbw7) ubiquitin ligase. J Biol Chem 279:50110-50119.
143. Won, K. A., and S. I. Reed. 1996. Activation of cyclin E/CDK2 is coupled to site-specific autophosphorylation and ubiquitin-dependent degradation of cyclin E. Embo J 15:4182-4193.

144. Keyomarsi, K., and A. B. Pardee. 1993. Redundant cyclin overexpression and gene amplification in breast cancer cells. Proc Natl Acad Sci U S A 90:1112-1116.
145. Fukuse, T., T. Hirata, H. Naiki, S. Hitomi, and H. Wada. 2000. Prognostic significance of cyclin E overexpression in resected non-small cell lung cancer. Cancer Res 60:242-244.
146. Leach, F. S., S. J. Elledge, C. J. Sherr, J. K. Willson, S. Markowitz, K. W. Kinzler, and B. Vogelstein. 1993. Amplification of cyclin genes in colorectal carcinomas. Cancer Res 53:1986-1989.
147. Muller-Tidow, C., R. Metzger, K. Kugler, S. Diederichs, G. Idos, M. Thomas, B. Dockhorn-Dworniczak, P. M. Schneider, H. P. Koeffler, W. E. Berdel, and H. Serve. 2001. Cyclin E is the only cyclin-dependent kinase 2-associated cyclin that predicts metastasis and survival in early stage non-small cell lung cancer. Cancer Res 61:647-653.
148. Erlanson, M., and G. Landberg. 2001. Prognostic implications of p27 and cyclin E protein contents in malignant lymphomas. Leuk Lymphoma 40:461-470.
149. Iida, H., M. Towatari, M. Tanimoto, Y. Morishita, Y. Kodera, and H. Saito. 1997. Overexpression of cyclin E in acute myelogenous leukemia. Blood 90:3707-3713.
150. Yasui, W., Y. Akama, H. Kuniyasu, H. Yokozaki, S. Semba, F. Shimamoto, and E. Tahara. 1996. Expression of cyclin E in human gastric adenomas and adenocarcinomas: correlation with proliferative activity and p53 status. J Exp Ther Oncol 1:88-94.
151. Akama, Y., W. Yasui, H. Yokozaki, H. Kuniyasu, K. Kitahara, T. Ishikawa, and E. Tahara. 1995. Frequent amplification of the cyclin E gene in human gastric carcinomas. Jpn J Cancer Res 86:617-621.
152. Molendini, L., M. S. Benassi, G. Magagnoli, M. Merli, M. R. Sollazzo, P. Ragazzini, G. Gamberi, C. Ferrari, A. Balladelli, P. Bacchini, and P. Picci. 1998. Prognostic significance of cyclin expression in human osteosarcoma. Int J Oncol 12:1007-1011.

153. Schraml, P., C. Bucher, H. Bissig, A. Nocito, P. Haas, K. Wilber, S. Seelig, J. Kononen, M. J. Mihatsch, S. Dirnhofer, and G. Sauter. 2003. Cyclin E overexpression and amplification in human tumours. J Pathol 200:375-382.
154. Martin, L. G., G. W. Demers, and D. A. Galloway. 1998. Disruption of the G1/S transition in human papillomavirus type 16 E7-expressing human cells is associated with altered regulation of cyclin E. J Virol 72:975-985.
155. Moberg, K. H., D. W. Bell, D. C. Wahrer, D. A. Haber, and I. K. Hariharan. 2001. Archipelago regulates Cyclin E levels in Drosophila and is mutated in human cancer cell lines. Nature 413:311-316.
156. Calhoun, E. S., J. B. Jones, R. Ashfaq, V. Adsay, S. J. Baker, V. Valentine, P. M. Hempen, W. Hilgers, C. J. Yeo, R. H. Hruban, and S. E. Kern. 2003. BRAF and FBXW7 (CDC4, FBW7, AGO, SEL10) mutations in distinct subsets of pancreatic cancer: potential therapeutic targets. Am J Pathol 163:1255-1260.
157. Keyomarsi, K., D. Conte, Jr., W. Toyofuku, and M. P. Fox. 1995. Deregulation of cyclin E in breast cancer. Oncogene 11:941-950.
158. Buckley, M. F., K. J. Sweeney, J. A. Hamilton, R. L. Sini, D. L. Manning, R. I. Nicholson, A. deFazio, C. K. Watts, E. A. Musgrove, and R. L. Sutherland. 1993. Expression and amplification of cyclin genes in human breast cancer. Oncogene 8:2127-2133.
159. Courjal, F., G. Louason, P. Speiser, D. Katsaros, R. Zeillinger, and C. Theillet. 1996. Cyclin gene amplification and overexpression in breast and ovarian cancers: evidence for the selection of cyclin D1 in breast and cyclin E in ovarian tumors. Int J Cancer 69:247-253.
160. Keyomarsi, K., S. L. Tucker, T. A. Buchholz, M. Callister, Y. Ding, G. N. Hortobagyi, I. Bedrosian, C. Knickerbocker, W. Toyofuku, M. Lowe, T. W. Herliczek, and S. S. Bacus. 2002. Cyclin E and survival in patients with breast cancer. N Engl J Med 347:1566-1575.
161. Bortner, D. M., and M. P. Rosenberg. 1997. Induction of mammary gland hyperplasia and carcinomas in transgenic mice expressing human cyclin E. Mol Cell Biol 17:453-459.

162. Hinchcliffe, E. H., C. Li, E. A. Thompson, J. L. Maller, and G. Sluder. 1999. Requirement of Cdk2-cyclin E activity for repeated centrosome reproduction in Xenopus egg extracts. Science 283:851-854.
163. Spruck, C. H., K. A. Won, and S. I. Reed. 1999. Deregulated cyclin E induces chromosome instability. Nature 401:297-300.
164. Sutter, T., T. Dansranjavin, J. Lubinski, T. Debniak, J. Giannakudis, C. Hoang-Vu, and H. Dralle. 2002. Overexpression of cyclin E protein is closely related to the mutator phenotype of colorectal carcinoma. Int J Colorectal Dis 17:374-380.
165. Porter, D. C., N. Zhang, C. Danes, M. J. McGahren, R. M. Harwell, S. Faruki, and K. Keyomarsi. 2001. Tumor-specific proteolytic processing of cyclin E generates hyperactive lower-molecular-weight forms. Mol Cell Biol 21:6254-6269.
166. Mull, B. B., J. Cox, T. Bui, and K. Keyomarsi. 2009. Post-translational modification and stability of low molecular weight cyclin E. Oncogene 28:3167-3176.
167. Moore, J. D., J. Yang, R. Truant, and S. Kornbluth. 1999. Nuclear import of Cdk/cyclin complexes: identification of distinct mechanisms for import of Cdk2/cyclin E and Cdc2/cyclin B1. J Cell Biol 144:213-224.
168. Moore, J. D., S. Kornbluth, and T. Hunt. 2002. Identification of the nuclear localization signal in Xenopus cyclin E and analysis of its role in replication and mitosis. Mol Biol Cell 13:4388-4400.
169. Delk, N. A., K. K. Hunt, and K. Keyomarsi. 2009. Altered subcellular localization of tumor-specific cyclin E isoforms affects cyclin-dependent kinase 2 complex formation and proteasomal regulation. Cancer Res 69:2817-2825.
170. Akli, S., P. J. Zheng, A. S. Multani, H. F. Wingate, S. Pathak, N. Zhang, S. L. Tucker, S. Chang, and K. Keyomarsi. 2004. Tumor-specific low molecular weight forms of cyclin E induce genomic instability and resistance to p21, p27, and antiestrogens in breast cancer. Cancer Res 64:3198-3208.

171. Bagheri-Yarmand, R., A. Biernacka, K. K. Hunt, and K. Keyomarsi. 2010. Low molecular weight cyclin E overexpression shortens mitosis, leading to chromosome missegregation and centrosome amplification. Cancer Res 70:5074-5084.
172. Hanahan, D., and R. A. Weinberg. 2000. The hallmarks of cancer. Cell 100:57-70.
173. Mittendorf, E. A., Y. Liu, S. L. Tucker, T. McKenzie, N. Qiao, S. Akli, A. Biernacka, Y. Liu, L. Meijer, K. Keyomarsi, and K. K. Hunt. 2010. A novel interaction between HER2/neu and cyclin E in breast cancer. Oncogene 29:3896-3907.
174. Scaltriti, M., P. J. Eichhorn, J. Cortes, L. Prudkin, C. Aura, J. Jimenez, S. Chandarlapaty, V. Serra, A. Prat, Y. H. Ibrahim, M. Guzman, M. Gili, O. Rodriguez, S. Rodriguez, J. Perez, S. R. Green, S. Mai, N. Rosen, C. Hudis, and J. Baselga. 2011. Cyclin E amplification/overexpression is a mechanism of trastuzumab resistance in HER2+ breast cancer patients. Proc Natl Acad Sci U S A 108:3761-3766.
175. Wingate, H., N. Zhang, M. J. McGarhen, I. Bedrosian, J. W. Harper, and K. Keyomarsi. 2005. The tumor-specific hyperactive forms of cyclin E are resistant to inhibition by p21 and p27. J Biol Chem 280:15148-15157.
176. Wingate, H., I. Bedrosian, S. Akli, and K. Keyomarsi. 2003. The low molecular weight (LMW) isoforms of cyclin E deregulate the cell cycle of mammary epithelial cells. Cell Cycle 2:461-466.
177. Span, P. N., V. C. Tjan-Heijnen, P. Manders, L. V. Beex, and C. G. Sweep. 2003. Cyclin-E is a strong predictor of endocrine therapy failure in human breast cancer. Oncogene 22:4898-4904.
178. Akli, S., T. Bui, H. Wingate, A. Biernacka, S. Moulder, S. L. Tucker, K. K. Hunt, and K. Keyomarsi. 2010. Low-molecular-weight cyclin E can bypass letrozole-induced G1 arrest in human breast cancer cells and tumors. Clin Cancer Res 16:1179-1190.
179. Bales, E., L. Mills, N. Milam, M. McGahren-Murray, D. Bandyopadhyay, D. Chen, J. A. Reed, N. Timchenko, J. J. van den Oord, M. Bar-Eli, K.

Keyomarsi, and E. E. Medrano. 2005. The low molecular weight cyclin E isoforms augment angiogenesis and metastasis of human melanoma cells in vivo. Cancer Res 65:692-697.

180. Akli, S., C. S. Van Pelt, T. Bui, A. S. Multani, S. Chang, D. Johnson, S. Tucker, and K. Keyomarsi. 2007. Overexpression of the low molecular weight cyclin E in transgenic mice induces metastatic mammary carcinomas through the disruption of the ARF-p53 pathway. Cancer Res 67:7212-7222.
181. Roberts, J. J., and A. J. Thomson. 1979. The mechanism of action of antitumor platinum compounds. Prog Nucleic Acid Res Mol Biol 22:71-133.
182. Kerr, J. F., A. H. Wyllie, and A. R. Currie. 1972. Apoptosis: a basic biological phenomenon with wide-ranging implications in tissue kinetics. Br J Cancer 26:239-257.
183. Giaccia, A. J., and M. B. Kastan. 1998. The complexity of p53 modulation: emerging patterns from divergent signals. Genes Dev 12:2973-2983.
184. Shapiro, G. I., C. D. Edwards, M. E. Ewen, and B. J. Rollins. 1998. p16INK4A participates in a G1 arrest checkpoint in response to DNA damage. Mol Cell Biol 18:378-387.
185. Fornari, F. A., J. K. Randolph, J. C. Yalowich, M. K. Ritke, and D. A. Gewirtz. 1994. Interference by doxorubicin with DNA unwinding in MCF-7 breast tumor cells. Mol Pharmacol 45:649-656.
186. Cross, S. M., C. A. Sanchez, C. A. Morgan, M. K. Schimke, S. Ramel, R. L. Idzerda, W. H. Raskind, and B. J. Reid. 1995. A p53-dependent mouse spindle checkpoint. Science 267:1353-1356.
187. Tishler, R. B., P. B. Schiff, C. R. Geard, and E. J. Hall. 1992. Taxol: a novel radiation sensitizer. Int J Radiat Oncol Biol Phys 22:613-617.
188. Liebmann, J., J. A. Cook, J. Fisher, D. Teague, and J. B. Mitchell. 1994. In vitro studies of Taxol as a radiation sensitizer in human tumor cells. J Natl Cancer Inst 86:441-446.
189. Meijer, L. 1996. Chemical inhibitors of cyclin-dependent kinases. Trends Cell Biol 6:393-397.

190. Vesely, J., L. Havlicek, M. Strnad, J. J. Blow, A. Donella-Deana, L. Pinna, D. S. Letham, J. Kato, L. Detivaud, S. Leclerc, and et al. 1994. Inhibition of cyclin-dependent kinases by purine analogues. Eur J Biochem 224:771-786.
191. De Azevedo, W. F., S. Leclerc, L. Meijer, L. Havlicek, M. Strnad, and S. H. Kim. 1997. Inhibition of cyclin-dependent kinases by purine analogues: crystal structure of human cdk2 complexed with roscovitine. Eur J Biochem 243:518-526.
192. Meijer, L., A. Borgne, O. Mulner, J. P. Chong, J. J. Blow, N. Inagaki, M. Inagaki, J. G. Delcros, and J. P. Moulinoux. 1997. Biochemical and cellular effects of roscovitine, a potent and selective inhibitor of the cyclin-dependent kinases cdc2, cdk2 and cdk5. Eur J Biochem 243:527-536.
193. Tamaoki, T. 1991. Use and specificity of staurosporine, UCN-01, and calphostin C as protein kinase inhibitors. Methods Enzymol 201:340-347.
194. Takahashi, I., Y. Saitoh, M. Yoshida, H. Sano, H. Nakano, M. Morimoto, and T. Tamaoki. 1989. UCN-01 and UCN-02, new selective inhibitors of protein kinase C. II. Purification, physico-chemical properties, structural determination and biological activities. J Antibiot (Tokyo) 42:571-576.
195. Wang, Q., P. J. Worland, J. L. Clark, B. A. Carlson, and E. A. Sausville. 1995. Apoptosis in 7-hydroxystaurosporine-treated T lymphoblasts correlates with activation of cyclin-dependent kinases 1 and 2. Cell Growth Differ 6:927-936.
196. Bedrosian, I., C. Lee, S. L. Tucker, S. L. Palla, K. Lu, and K. Keyomarsi. 2007. Cyclin E-associated kinase activity predicts response to platinum-based chemotherapy. Clin Cancer Res 13:4800-4806.
197. Akli, S., C. S. Van Pelt, T. Bui, L. Meijer, and K. Keyomarsi. 2011. Cdk2 is required for breast cancer mediated by the low-molecular-weight isoform of cyclin E. Cancer Res 71:3377-3386.
198. Lambert, L. A., N. Qiao, K. K. Hunt, D. H. Lambert, G. B. Mills, L. Meijer, and K. Keyomarsi. 2008. Autophagy: a novel mechanism of synergistic cytotoxicity between doxorubicin and roscovitine in a sarcoma model. Cancer Res 68:7966-7974.

199. Benson, C., J. White, J. De Bono, A. O'Donnell, F. Raynaud, C. Cruickshank, H. McGrath, M. Walton, P. Workman, S. Kaye, J. Cassidy, A. Gianella-Borradori, I. Judson, and C. Twelves. 2007. A phase I trial of the selective oral cyclin-dependent kinase inhibitor seliciclib (CYC202; R-Roscovitine), administered twice daily for 7 days every 21 days. Br J Cancer 96:29-37.
200. Hsieh, W. S., R. Soo, B. K. Peh, T. Loh, D. Dong, D. Soh, L. S. Wong, S. Green, J. Chiao, C. Y. Cui, Y. F. Lai, S. C. Lee, B. Mow, R. Soong, M. Salto-Tellez, and B. C. Goh. 2009. Pharmacodynamic effects of seliciclib, an orally administered cell cycle modulator, in undifferentiated nasopharyngeal cancer. Clin Cancer Res 15:1435-1442.
201. Akli, S., and K. Keyomarsi. 2003. Cyclin E and its low molecular weight forms in human cancer and as targets for cancer therapy. Cancer Biol Ther 2:S38-47.
202. Inada, M., J. Yamashita, and M. Ogawa. 1997. Neutrophil elastase inhibitor (ONO-5046-Na) inhibits the growth of human lung cancer cell lines transplanted into severe combined immunodeficiency (scid) mice. Res Commun Mol Pathol Pharmacol 97:229-232.
203. Inada, M., J. Yamashita, S. Nakano, and M. Ogawa. 1998. Complete inhibition of spontaneous pulmonary metastasis of human lung carcinoma cell line EBC-1 by a neutrophil elastase inhibitor (ONO-5046.Na). Anticancer Res 18:885-890.
204. Nguyen, H. H., I. Aronchik, G. A. Brar, D. H. Nguyen, L. F. Bjeldanes, and G. L. Firestone. 2008. The dietary phytochemical indole-3-carbinol is a natural elastase enzymatic inhibitor that disrupts cyclin E protein processing. Proc Natl Acad Sci U S A 105:19750-19755.
205. Sato, T., S. Takahashi, T. Mizumoto, M. Harao, M. Akizuki, M. Takasugi, T. Fukutomi, and J. Yamashita. 2006. Neutrophil elastase and cancer. Surg Oncol 15:217-222.
206. Foekens, J. A., C. Ries, M. P. Look, C. Gippner-Steppert, J. G. Klijn, and M. Jochum. 2003. Elevated expression of polymorphonuclear leukocyte

elastase in breast cancer tissue is associated with tamoxifen failure in patients with advanced disease. Br J Cancer 88:1084-1090.

207. Foekens, J. A., C. Ries, M. P. Look, C. Gippner-Steppert, J. G. Klijn, and M. Jochum. 2003. The prognostic value of polymorphonuclear leukocyte elastase in patients with primary breast cancer. Cancer Res 63:337-341.

208. Desmedt, C., F. E. Ouriaghli, V. Durbecq, A. Soree, M. A. Colozza, E. Azambuja, M. Paesmans, D. Larsimont, M. Buyse, A. Harris, M. Piccart, P. Martiat, and C. Sotiriou. 2006. Impact of cyclins E, neutrophil elastase and proteinase 3 expression levels on clinical outcome in primary breast cancer patients. Int J Cancer 119:2539-2545.

209. Akizuki, M., T. Fukutomi, M. Takasugi, S. Takahashi, T. Sato, M. Harao, T. Mizumoto, and J. Yamashita. 2007. Prognostic significance of immunoreactive neutrophil elastase in human breast cancer: long-term follow-up results in 313 patients. Neoplasia 9:260-264.

210. Yokota, T., T. Bui, Y. Liu, M. Yi, K. K. Hunt, and K. Keyomarsi. 2007. Differential regulation of elafin in normal and tumor-derived mammary epithelial cells is mediated by CCAAT/enhancer binding protein beta. Cancer Res 67:11272-11283.

211. Caruso, J. A., K. K. Hunt, and K. Keyomarsi. 2010. The neutrophil elastase inhibitor elafin triggers rb-mediated growth arrest and caspase-dependent apoptosis in breast cancer. Cancer Res 70:7125-7136.

212. Koff, A., A. Giordano, D. Desai, K. Yamashita, J. W. Harper, S. Elledge, T. Nishimoto, D. O. Morgan, B. R. Franza, and J. M. Roberts. 1992. Formation and activation of a cyclin E-cdk2 complex during the G1 phase of the human cell cycle. Science 257:1689-1694.

213. Draetta, G. F. 1994. Mammalian G1 cyclins. Curr Opin Cell Biol 6:842-846.

214. Bresnahan, W. A., I. Boldogh, T. Ma, T. Albrecht, and E. A. Thompson. 1996. Cyclin E/Cdk2 activity is controlled by different mechanisms in the G0 and G1 phases of the cell cycle. Cell Growth Differ 7:1283-1290.

215. Keyomarsi, K., and T. W. Herliczek. 1997. The role of cyclin E in cell proliferation, development and cancer. Prog Cell Cycle Res 3:171-191.

216. Bito, T., M. Ueda, A. Ito, and M. Ichihashi. 1997. Less expression of cyclin E in cutaneous squamous cell carcinomas than in benign and premalignant keratinocytic lesions. J Cutan Pathol 24:305-308.
217. Dutta, A., R. Chandra, L. M. Leiter, and S. Lester. 1995. Cyclins as markers of tumor proliferation: immunocytochemical studies in breast cancer. Proc Natl Acad Sci U S A 92:5386-5390.
218. Erlanson, M., C. Portin, B. Linderholm, J. Lindh, G. Roos, and G. Landberg. 1998. Expression of cyclin E and the cyclin-dependent kinase inhibitor p27 in malignant lymphomas-prognostic implications. Blood 92:770-777.
219. Sakaguchi, T., A. Watanabe, H. Sawada, Y. Yamada, J. Yamashita, M. Matsuda, M. Nakajima, T. Miwa, T. Hirao, and H. Nakano. 1998. Prognostic value of cyclin E and p53 expression in gastric carcinoma. Cancer 82:1238-1243.
220. Harwell, R. M., D. C. Porter, C. Danes, and K. Keyomarsi. 2000. Processing of cyclin E differs between normal and tumor breast cells. Cancer Res 60:481-489.
221. Porter, D. C., and K. Keyomarsi. 2000. Novel splice variants of cyclin E with altered substrate specificity. Nucleic Acids Res 28:E101.
222. Emerman, J. T., J. Enami, D. R. Pitelka, and S. Nandi. 1977. Hormonal effects on intracellular and secreted casein in cultures of mouse mammary epithelial cells on floating collagen membranes. Proc Natl Acad Sci U S A 74:4466-4470.
223. Barcellos-Hoff, M. H., J. Aggeler, T. G. Ram, and M. J. Bissell. 1989. Functional differentiation and alveolar morphogenesis of primary mammary cultures on reconstituted basement membrane. Development 105:223-235.
224. Petersen, O. W., L. Ronnov-Jessen, A. R. Howlett, and M. J. Bissell. 1992. Interaction with basement membrane serves to rapidly distinguish growth and differentiation pattern of normal and malignant human breast epithelial cells. Proc Natl Acad Sci U S A 89:9064-9068.

225. Weaver, V. M., and M. J. Bissell. 1999. Functional culture models to study mechanisms governing apoptosis in normal and malignant mammary epithelial cells. J Mammary Gland Biol Neoplasia 4:193-201.
226. Schmeichel, K. L., and M. J. Bissell. 2003. Modeling tissue-specific signaling and organ function in three dimensions. J Cell Sci 116:2377-2388.
227. Weaver, V. M., S. Lelievre, J. N. Lakins, M. A. Chrenek, J. C. Jones, F. Giancotti, Z. Werb, and M. J. Bissell. 2002. beta4 integrin-dependent formation of polarized three-dimensional architecture confers resistance to apoptosis in normal and malignant mammary epithelium. Cancer Cell 2:205-216.
228. Gudjonsson, T., L. Ronnov-Jessen, R. Villadsen, F. Rank, M. J. Bissell, and O. W. Petersen. 2002. Normal and tumor-derived myoepithelial cells differ in their ability to interact with luminal breast epithelial cells for polarity and basement membrane deposition. J Cell Sci 115:39-50.
229. Fournier, M. V., K. J. Martin, P. A. Kenny, K. Xhaja, I. Bosch, P. Yaswen, and M. J. Bissell. 2006. Gene expression signature in organized and growth-arrested mammary acini predicts good outcome in breast cancer. Cancer Res 66:7095-7102.
230. Band, V., and R. Sager. 1989. Distinctive traits of normal and tumor-derived human mammary epithelial cells expressed in a medium that supports long-term growth of both cell types. Proc Natl Acad Sci U S A 86:1249-1253.
231. Gray-Bablin, J., J. Zalvide, M. P. Fox, C. J. Knickerbocker, J. A. DeCaprio, and K. Keyomarsi. 1996. Cyclin E, a redundant cyclin in breast cancer. Proc Natl Acad Sci U S A 93:15215-15220.
232. Muthuswamy, S. K., D. Li, S. Lelievre, M. J. Bissell, and J. S. Brugge. 2001. ErbB2, but not ErbB1, reinitiates proliferation and induces luminal repopulation in epithelial acini. Nat Cell Biol 3:785-792.
233. Debnath, J., S. K. Muthuswamy, and J. S. Brugge. 2003. Morphogenesis and oncogenesis of MCF-10A mammary epithelial acini grown in three-dimensional basement membrane cultures. Methods 30:256-268.

234. Tibes, R., Y. Qiu, Y. Lu, B. Hennessy, M. Andreeff, G. B. Mills, and S. M. Kornblau. 2006. Reverse phase protein array: validation of a novel proteomic technology and utility for analysis of primary leukemia specimens and hematopoietic stem cells. Mol Cancer Ther 5:2512-2521.
235. Kaplan, E. P., and P. Meier. 1958. Nonparametric estimation of incomplete observatons. J Am Stat Assoc 53:457-481.
236. Cox, D. R. 1972. Regression models and life-tables. J R Stat Soc 34:187-220.
237. Band, V., D. Zajchowski, V. Kulesa, and R. Sager. 1990. Human papilloma virus DNAs immortalize normal human mammary epithelial cells and reduce their growth factor requirements. Proc Natl Acad Sci U S A 87:463-467.
238. Soule, H. D., T. M. Maloney, S. R. Wolman, W. D. Peterson, Jr., R. Brenz, C. M. McGrath, J. Russo, R. J. Pauley, R. F. Jones, and S. C. Brooks. 1990. Isolation and characterization of a spontaneously immortalized human breast epithelial cell line, MCF-10. Cancer Res 50:6075-6086.
239. Debnath, J., K. R. Mills, N. L. Collins, M. J. Reginato, S. K. Muthuswamy, and J. S. Brugge. 2002. The role of apoptosis in creating and maintaining luminal space within normal and oncogene-expressing mammary acini. Cell 111:29-40.
240. Schalkwijk, J., C. de Roo, and G. J. de Jongh. 1991. Skin-derived antileukoproteinase (SKALP), an elastase inhibitor from human keratinocytes. Purification and biochemical properties. Biochim Biophys Acta 1096:148-154.
241. Alkemade, H. A., I. M. van Vlijmen-Willems, U. J. van Haelst, P. C. van de Kerkhof, and J. Schalkwijk. 1994. Demonstration of skin-derived antileukoproteinase (SKALP) and its target enzyme human leukocyte elastase in squamous cell carcinoma. J Pathol 174:121-129.
242. Lindahl, T., G. Landberg, J. Ahlgren, H. Nordgren, T. Norberg, S. Klaar, L. Holmberg, and J. Bergh. 2004. Overexpression of cyclin E protein is associated with specific mutation types in the p53 gene and poor survival in human breast cancer. Carcinogenesis 25:375-380.

243. Reginato, M. J., K. R. Mills, E. B. Becker, D. K. Lynch, A. Bonni, S. K. Muthuswamy, and J. S. Brugge. 2005. Bim regulation of lumen formation in cultured mammary epithelial acini is targeted by oncogenes. Mol Cell Biol 25:4591-4601.
244. Kornblau, S. M., R. Tibes, Y. H. Qiu, W. Chen, H. M. Kantarjian, M. Andreeff, K. R. Coombes, and G. B. Mills. 2009. Functional proteomic profiling of AML predicts response and survival. Blood 113:154-164.
245. Weaver, V. M., O. W. Petersen, F. Wang, C. A. Larabell, P. Briand, C. Damsky, and M. J. Bissell. 1997. Reversion of the malignant phenotype of human breast cells in three-dimensional culture and in vivo by integrin blocking antibodies. J Cell Biol 137:231-245.
246. Harris, S. L., and A. J. Levine. 2005. The p53 pathway: positive and negative feedback loops. Oncogene 24:2899-2908.
247. Mueller, M. M., W. Peter, M. Mappes, A. Huelsen, H. Steinbauer, P. Boukamp, M. Vaccariello, J. Garlick, and N. E. Fusenig. 2001. Tumor progression of skin carcinoma cells in vivo promoted by clonal selection, mutagenesis, and autocrine growth regulation by granulocyte colony-stimulating factor and granulocyte-macrophage colony-stimulating factor. Am J Pathol 159:1567-1579.
248. MacCallum, D. E., J. Melville, S. Frame, K. Watt, S. Anderson, A. Gianella-Borradori, D. P. Lane, and S. R. Green. 2005. Seliciclib (CYC202, R-Roscovitine) induces cell death in multiple myeloma cells by inhibition of RNA polymerase II-dependent transcription and down-regulation of Mcl-1. Cancer Res 65:5399-5407.
249. Foell, J. L., D. Max, C. Giersberg, D. Korholz, and M. S. Staege. 2008. Sensitivity of Hodgkin's lymphoma cell lines to the cell cycle inhibitor roscovitine. Anticancer Res 28:887-894.
250. Pampaloni, F., E. G. Reynaud, and E. H. Stelzer. 2007. The third dimension bridges the gap between cell culture and live tissue. Nat Rev Mol Cell Biol 8:839-845.

251. Martin, K. J., D. R. Patrick, M. J. Bissell, and M. V. Fournier. 2008. Prognostic breast cancer signature identified from 3D culture model accurately predicts clinical outcome across independent datasets. PLoS One 3:e2994.
252. Steelman, L. S., S. C. Pohnert, J. G. Shelton, R. A. Franklin, F. E. Bertrand, and J. A. McCubrey. 2004. JAK/STAT, Raf/MEK/ERK, PI3K/Akt and BCR-ABL in cell cycle progression and leukemogenesis. Leukemia 18:189-218.
253. Hoyle, P. E., P. W. Moye, L. S. Steelman, W. L. Blalock, R. A. Franklin, M. Pearce, H. Cherwinski, E. Bosch, M. McMahon, and J. A. McCubrey. 2000. Differential abilities of the Raf family of protein kinases to abrogate cytokine dependency and prevent apoptosis in murine hematopoietic cells by a MEK1-dependent mechanism. Leukemia 14:642-656.
254. Woods, D., D. Parry, H. Cherwinski, E. Bosch, E. Lees, and M. McMahon. 1997. Raf-induced proliferation or cell cycle arrest is determined by the level of Raf activity with arrest mediated by p21Cip1. Mol Cell Biol 17:5598-5611.
255. Aisenberg, A. C., D. M. Finkelstein, K. P. Doppke, F. C. Koerner, J. F. Boivin, and C. G. Willett. 1997. High risk of breast carcinoma after irradiation of young women with Hodgkin's disease. Cancer 79:1203-1210.
256. Tokunaga, M., J. E. Norman, Jr., M. Asano, S. Tokuoka, H. Ezaki, I. Nishimori, and Y. Tsuji. 1979. Malignant breast tumors among atomic bomb survivors, Hiroshima and Nagasaki, 1950-74. J Natl Cancer Inst 62:1347-1359.
257. Reya, T., S. J. Morrison, M. F. Clarke, and I. L. Weissman. 2001. Stem cells, cancer, and cancer stem cells. Nature 414:105-111.
258. Dick, J. E. 2003. Breast cancer stem cells revealed. Proc Natl Acad Sci U S A 100:3547-3549.
259. Lapidot, T., C. Sirard, J. Vormoor, B. Murdoch, T. Hoang, J. Caceres-Cortes, M. Minden, B. Paterson, M. A. Caligiuri, and J. E. Dick. 1994. A cell initiating human acute myeloid leukaemia after transplantation into SCID mice. Nature 367:645-648.

260. Bonnet, D., and J. E. Dick. 1997. Human acute myeloid leukemia is organized as a hierarchy that originates from a primitive hematopoietic cell. Nat Med 3:730-737.
261. Sutherland, H. J., A. Blair, and R. W. Zapf. 1996. Characterization of a hierarchy in human acute myeloid leukemia progenitor cells. Blood 87:4754-4761.
262. Bruce, W. R., and H. Van Der Gaag. 1963. A Quantitative Assay for the Number of Murine Lymphoma Cells Capable of Proliferation in Vivo. Nature 199:79-80.
263. Al-Hajj, M., M. S. Wicha, A. Benito-Hernandez, S. J. Morrison, and M. F. Clarke. 2003. Prospective identification of tumorigenic breast cancer cells. Proc Natl Acad Sci U S A 100:3983-3988.
264. Singh, S. K., C. Hawkins, I. D. Clarke, J. A. Squire, J. Bayani, T. Hide, R. M. Henkelman, M. D. Cusimano, and P. B. Dirks. 2004. Identification of human brain tumour initiating cells. Nature 432:396-401.
265. Bao, S., Q. Wu, S. Sathornsumetee, Y. Hao, Z. Li, A. B. Hjelmeland, Q. Shi, R. E. McLendon, D. D. Bigner, and J. N. Rich. 2006. Stem cell-like glioma cells promote tumor angiogenesis through vascular endothelial growth factor. Cancer Res 66:7843-7848.
266. Beier, D., P. Hau, M. Proescholdt, A. Lohmeier, J. Wischhusen, P. J. Oefner, L. Aigner, A. Brawanski, U. Bogdahn, and C. P. Beier. 2007. CD133(+) and CD133(-) glioblastoma-derived cancer stem cells show differential growth characteristics and molecular profiles. Cancer Res 67:4010-4015.
267. Taylor, M. D., H. Poppleton, C. Fuller, X. Su, Y. Liu, P. Jensen, S. Magdaleno, J. Dalton, C. Calabrese, J. Board, T. Macdonald, J. Rutka, A. Guha, A. Gajjar, T. Curran, and R. J. Gilbertson. 2005. Radial glia cells are candidate stem cells of ependymoma. Cancer Cell 8:323-335.
268. Bao, S., Q. Wu, R. E. McLendon, Y. Hao, Q. Shi, A. B. Hjelmeland, M. W. Dewhirst, D. D. Bigner, and J. N. Rich. 2006. Glioma stem cells promote radioresistance by preferential activation of the DNA damage response. Nature 444:756-760.

269. Piccirillo, S. G., B. A. Reynolds, N. Zanetti, G. Lamorte, E. Binda, G. Broggi, H. Brem, A. Olivi, F. Dimeco, and A. L. Vescovi. 2006. Bone morphogenetic proteins inhibit the tumorigenic potential of human brain tumour-initiating cells. Nature 444:761-765.
270. Morrison, S. J., and I. L. Weissman. 1994. The long-term repopulating subset of hematopoietic stem cells is deterministic and isolatable by phenotype. Immunity 1:661-673.
271. Morrison, S. J., A. M. Wandycz, H. D. Hemmati, D. E. Wright, and I. L. Weissman. 1997. Identification of a lineage of multipotent hematopoietic progenitors. Development 124:1929-1939.
272. Wright, M. H., A. M. Calcagno, C. D. Salcido, M. D. Carlson, S. V. Ambudkar, and L. Varticovski. 2008. Brca1 breast tumors contain distinct CD44+/CD24- and CD133+ cells with cancer stem cell characteristics. Breast Cancer Res 10:R10.
273. Fidler, I. J., and I. R. Hart. 1982. Biological diversity in metastatic neoplasms: origins and implications. Science 217:998-1003.
274. Heppner, G. H. 1984. Tumor heterogeneity. Cancer Res 44:2259-2265.
275. Visvader, J. E., and G. J. Lindeman. 2008. Cancer stem cells in solid tumours: accumulating evidence and unresolved questions. Nat Rev Cancer 8:755-768.
276. Nowell, P. C. 1976. The clonal evolution of tumor cell populations. Science 194:23-28.
277. Dontu, G., W. M. Abdallah, J. M. Foley, K. W. Jackson, M. F. Clarke, M. J. Kawamura, and M. S. Wicha. 2003. In vitro propagation and transcriptional profiling of human mammary stem/progenitor cells. Genes Dev 17:1253-1270.
278. Ginestier, C., M. H. Hur, E. Charafe-Jauffret, F. Monville, J. Dutcher, M. Brown, J. Jacquemier, P. Viens, C. G. Kleer, S. Liu, A. Schott, D. Hayes, D. Birnbaum, M. S. Wicha, and G. Dontu. 2007. ALDH1 is a marker of normal and malignant human mammary stem cells and a predictor of poor clinical outcome. Cell Stem Cell 1:555-567.

279. Ponti, D., A. Costa, N. Zaffaroni, G. Pratesi, G. Petrangolini, D. Coradini, S. Pilotti, M. A. Pierotti, and M. G. Daidone. 2005. Isolation and in vitro propagation of tumorigenic breast cancer cells with stem/progenitor cell properties. Cancer Res 65:5506-5511.
280. Rappa, G., and A. Lorico. 2010. Phenotypic characterization of mammosphere-forming cells from the human MA-11 breast carcinoma cell line. Exp Cell Res 316:1576-1586.
281. Rappa, G., J. Mercapide, F. Anzanello, L. Prasmickaite, Y. Xi, J. Ju, O. Fodstad, and A. Lorico. 2008. Growth of cancer cell lines under stem cell-like conditions has the potential to unveil therapeutic targets. Exp Cell Res 314:2110-2122.
282. Chute, J. P., G. G. Muramoto, J. Whitesides, M. Colvin, R. Safi, N. J. Chao, and D. P. McDonnell. 2006. Inhibition of aldehyde dehydrogenase and retinoid signaling induces the expansion of human hematopoietic stem cells. Proc Natl Acad Sci U S A 103:11707-11712.
283. Sladek, N. E. 2003. Human aldehyde dehydrogenases: potential pathological, pharmacological, and toxicological impact. J Biochem Mol Toxicol 17:7-23.
284. Morimoto, K., S. J. Kim, T. Tanei, K. Shimazu, Y. Tanji, T. Taguchi, Y. Tamaki, N. Terada, and S. Noguchi. 2009. Stem cell marker aldehyde dehydrogenase 1-positive breast cancers are characterized by negative estrogen receptor, positive human epidermal growth factor receptor type 2, and high Ki67 expression. Cancer Sci 100:1062-1068.
285. Mani, S. A., W. Guo, M. J. Liao, E. N. Eaton, A. Ayyanan, A. Y. Zhou, M. Brooks, F. Reinhard, C. C. Zhang, M. Shipitsin, L. L. Campbell, K. Polyak, C. Brisken, J. Yang, and R. A. Weinberg. 2008. The epithelial-mesenchymal transition generates cells with properties of stem cells. Cell 133:704-715.
286. Sheridan, C., H. Kishimoto, R. K. Fuchs, S. Mehrotra, P. Bhat-Nakshatri, C. H. Turner, R. Goulet, Jr., S. Badve, and H. Nakshatri. 2006. CD44+/CD24- breast cancer cells exhibit enhanced invasive properties: an early step necessary for metastasis. Breast Cancer Res 8:R59.

287. Hay, E. D. 1995. An overview of epithelio-mesenchymal transformation. Acta Anat (Basel) 154:8-20.
288. Thiery, J. P. 2003. Epithelial-mesenchymal transitions in development and pathologies. Curr Opin Cell Biol 15:740-746.
289. Honeth, G., P. O. Bendahl, M. Ringner, L. H. Saal, S. K. Gruvberger-Saal, K. Lovgren, D. Grabau, M. Ferno, A. Borg, and C. Hegardt. 2008. The CD44+/CD24- phenotype is enriched in basal-like breast tumors. Breast Cancer Res 10:R53.
290. Sorlie, T., C. M. Perou, R. Tibshirani, T. Aas, S. Geisler, H. Johnsen, T. Hastie, M. B. Eisen, M. van de Rijn, S. S. Jeffrey, T. Thorsen, H. Quist, J. C. Matese, P. O. Brown, D. Botstein, P. Eystein Lonning, and A. L. Borresen-Dale. 2001. Gene expression patterns of breast carcinomas distinguish tumor subclasses with clinical implications. Proc Natl Acad Sci U S A 98:10869-10874.
291. Li, Y., W. P. Hively, and H. E. Varmus. 2000. Use of MMTV-Wnt-1 transgenic mice for studying the genetic basis of breast cancer. Oncogene 19:1002-1009.
292. Rosner, A., K. Miyoshi, E. Landesman-Bollag, X. Xu, D. C. Seldin, A. R. Moser, C. L. MacLeod, G. Shyamala, A. E. Gillgrass, and R. D. Cardiff. 2002. Pathway pathology: histological differences between ErbB/Ras and Wnt pathway transgenic mammary tumors. Am J Pathol 161:1087-1097.
293. Fillmore, C. M., and C. Kuperwasser. 2008. Human breast cancer cell lines contain stem-like cells that self-renew, give rise to phenotypically diverse progeny and survive chemotherapy. Breast Cancer Res 10:R25.
294. Phillips, T. M., W. H. McBride, and F. Pajonk. 2006. The response of CD24(-/low)/CD44+ breast cancer-initiating cells to radiation. J Natl Cancer Inst 98:1777-1785.
295. Li, X., M. T. Lewis, J. Huang, C. Gutierrez, C. K. Osborne, M. F. Wu, S. G. Hilsenbeck, A. Pavlick, X. Zhang, G. C. Chamness, H. Wong, J. Rosen, and J. C. Chang. 2008. Intrinsic resistance of tumorigenic breast cancer cells to chemotherapy. J Natl Cancer Inst 100:672-679.

296. Donnenberg, V. S., and A. D. Donnenberg. 2005. Multiple drug resistance in cancer revisited: the cancer stem cell hypothesis. J Clin Pharmacol 45:872-877.
297. Gupta, P. B., T. T. Onder, G. Jiang, K. Tao, C. Kuperwasser, R. A. Weinberg, and E. S. Lander. 2009. Identification of selective inhibitors of cancer stem cells by high-throughput screening. Cell 138:645-659.
298. Liotta, L. A. 1986. Tumor invasion and metastases--role of the extracellular matrix: Rhoads Memorial Award lecture. Cancer Res 46:1-7.
299. Derksen, P. W., X. Liu, F. Saridin, H. van der Gulden, J. Zevenhoven, B. Evers, J. R. van Beijnum, A. W. Griffioen, J. Vink, P. Krimpenfort, J. L. Peterse, R. D. Cardiff, A. Berns, and J. Jonkers. 2006. Somatic inactivation of E-cadherin and p53 in mice leads to metastatic lobular mammary carcinoma through induction of anoikis resistance and angiogenesis. Cancer Cell 10:437-449.
300. Vleminckx, K., L. Vakaet, Jr., M. Mareel, W. Fiers, and F. van Roy. 1991. Genetic manipulation of E-cadherin expression by epithelial tumor cells reveals an invasion suppressor role. Cell 66:107-119.
301. Pajalunga, D., and M. Crescenzi. 2004. Regulation of cyclin E protein levels through E2F-mediated inhibition of degradation. Cell Cycle 3:1572-1578.
302. Geng, Y., E. N. Eaton, M. Picon, J. M. Roberts, A. S. Lundberg, A. Gifford, C. Sardet, and R. A. Weinberg. 1996. Regulation of cyclin E transcription by E2Fs and retinoblastoma protein. Oncogene 12:1173-1180.
303. Fillmore, C., and C. Kuperwasser. 2007. Human breast cancer stem cell markers CD44 and CD24: enriching for cells with functional properties in mice or in man? Breast Cancer Res 9:303.
304. Balicki, D. 2007. Moving Forward in Human Mammary Stem Cell Biology and Breast Cancer Prognostication Using ALDH1. Cell Stem Cell 1:485-487.
305. Blethrow, J. D., J. S. Glavy, D. O. Morgan, and K. M. Shokat. 2008. Covalent capture of kinase-specific phosphopeptides reveals Cdk1-cyclin B substrates. Proc Natl Acad Sci U S A 105:1442-1447.

306. Iizuka, M., and B. Stillman. 1999. Histone acetyltransferase HBO1 interacts with the ORC1 subunit of the human initiator protein. J Biol Chem 274:23027-23034.
307. Iizuka, M., O. F. Sarmento, T. Sekiya, H. Scrable, C. D. Allis, and M. M. Smith. 2008. Hbo1 Links p53-dependent stress signaling to DNA replication licensing. Mol Cell Biol 28:140-153.
308. Sharma, M., M. Zarnegar, X. Li, B. Lim, and Z. Sun. 2000. Androgen receptor interacts with a novel MYST protein, HBO1. J Biol Chem 275:35200-35208.
309. Contzler, R., A. Regamey, B. Favre, T. Roger, D. Hohl, and M. Huber. 2006. Histone acetyltransferase HBO1 inhibits NF-kappaB activity by coactivator sequestration. Biochem Biophys Res Commun 350:208-213.
310. Georgiakaki, M., N. Chabbert-Buffet, B. Dasen, G. Meduri, S. Wenk, L. Rajhi, L. Amazit, A. Chauchereau, C. W. Burger, L. J. Blok, E. Milgrom, M. Lombes, A. Guiochon-Mantel, and H. Loosfelt. 2006. Ligand-controlled interaction of histone acetyltransferase binding to ORC-1 (HBO1) with the N-terminal transactivating domain of progesterone receptor induces steroid receptor coactivator 1-dependent coactivation of transcription. Mol Endocrinol 20:2122-2140.
311. Burke, T. W., J. G. Cook, M. Asano, and J. R. Nevins. 2001. Replication factors MCM2 and ORC1 interact with the histone acetyltransferase HBO1. J Biol Chem 276:15397-15408.
312. Aggarwal, B. D., and B. R. Calvi. 2004. Chromatin regulates origin activity in Drosophila follicle cells. Nature 430:372-376.
313. Iizuka, M., T. Matsui, H. Takisawa, and M. M. Smith. 2006. Regulation of replication licensing by acetyltransferase Hbo1. Mol Cell Biol 26:1098-1108.
314. Suzuki, T., H. Shen, K. Akagi, H. C. Morse, J. D. Malley, D. Q. Naiman, N. A. Jenkins, and N. G. Copeland. 2002. New genes involved in cancer identified by retroviral tagging. Nat Genet 32:166-174.
315. Hu, X., H. M. Stern, L. Ge, C. O'Brien, L. Haydu, C. D. Honchell, P. M. Haverty, B. A. Peters, T. D. Wu, L. C. Amler, J. Chant, D. Stokoe, M. R.

Lackner, and G. Cavet. 2009. Genetic alterations and oncogenic pathways associated with breast cancer subtypes. Mol Cancer Res 7:511-522.

316. Doyon, Y., C. Cayrou, M. Ullah, A. J. Landry, V. Cote, W. Selleck, W. S. Lane, S. Tan, X. J. Yang, and J. Cote. 2006. ING tumor suppressor proteins are critical regulators of chromatin acetylation required for genome expression and perpetuation. Mol Cell 21:51-64.
317. Wang, W. Z., H. O. Liu, Y. H. Wu, Y. Hong, J. W. Yang, Y. H. Liu, W. B. Wu, L. Zhou, L. L. Sun, J. J. Xu, X. J. Yun, and J. X. Gu. 2010. Estrogen receptor alpha (ERalpha) mediates 17beta-estradiol (E2)-activated expression of HBO1. J Exp Clin Cancer Res 29:140.
318. Zong, H., Z. Li, L. Liu, Y. Hong, X. Yun, J. Jiang, Y. Chi, H. Wang, X. Shen, Y. Hu, Z. Niu, and J. Gu. 2005. Cyclin-dependent kinase 11(p58) interacts with HBO1 and enhances its histone acetyltransferase activity. FEBS Lett 579:3579-3588.
319. Wu, Z. Q., and X. Liu. 2008. Role for Plk1 phosphorylation of Hbo1 in regulation of replication licensing. Proc Natl Acad Sci U S A 105:1919-1924.
320. Kim, J. H., M. Chae, W. K. Kim, Y. J. Kim, H. S. Kang, H. S. Kim, and S. Yoon. 2011. Salinomycin sensitizes cancer cells to the effects of doxorubicin and etoposide treatment by increasing DNA damage and reducing p21 protein. Br J Pharmacol 162:773-784.
321. Singal, P. K., and N. Iliskovic. 1998. Doxorubicin-induced cardiomyopathy. N Engl J Med 339:900-905.
322. Gharib, M. I., and A. K. Burnett. 2002. Chemotherapy-induced cardiotoxicity: current practice and prospects of prophylaxis. Eur J Heart Fail 4:235-242.
323. Jasencakova, Z., A. Meister, J. Walter, B. M. Turner, and I. Schubert. 2000. Histone H4 acetylation of euchromatin and heterochromatin is cell cycle dependent and correlated with replication rather than with transcription. Plant Cell 12:2087-2100.
324. Kueh, A. J., M. P. Dixon, A. K. Voss, and T. Thomas. 2011. HBO1 is required for H3K14 acetylation and normal transcriptional activity during embryonic development. Mol Cell Biol 31:845-860.

325. Ayer, D. E., C. D. Laherty, Q. A. Lawrence, A. P. Armstrong, and R. N. Eisenman. 1996. Mad proteins contain a dominant transcription repression domain. Mol Cell Biol 16:5772-5781.
326. Kasten, M. M., D. E. Ayer, and D. J. Stillman. 1996. SIN3-dependent transcriptional repression by interaction with the Mad1 DNA-binding protein. Mol Cell Biol 16:4215-4221.
327. Burdette-Radoux, S., R. G. Tozer, R. C. Lohmann, I. Quirt, D. S. Ernst, W. Walsh, N. Wainman, A. D. Colevas, and E. A. Eisenhauer. 2004. Phase II trial of flavopiridol, a cyclin dependent kinase inhibitor, in untreated metastatic malignant melanoma. Invest New Drugs 22:315-322.
328. Grendys, E. C., Jr., J. A. Blessing, R. Burger, and J. Hoffman. 2005. A phase II evaluation of flavopiridol as second-line chemotherapy of endometrial carcinoma: a Gynecologic Oncology Group study. Gynecol Oncol 98:249-253.
329. Pan, M. H., W. L. Chang, S. Y. Lin-Shiau, C. T. Ho, and J. K. Lin. 2001. Induction of apoptosis by garcinol and curcumin through cytochrome c release and activation of caspases in human leukemia HL-60 cells. J Agric Food Chem 49:1464-1474.
330. Sun, Y., X. Jiang, S. Chen, and B. D. Price. 2006. Inhibition of histone acetyltransferase activity by anacardic acid sensitizes tumor cells to ionizing radiation. FEBS Lett 580:4353-4356.
331. Lau, O. D., T. K. Kundu, R. E. Soccio, S. Ait-Si-Ali, E. M. Khalil, A. Vassilev, A. P. Wolffe, Y. Nakatani, R. G. Roeder, and P. A. Cole. 2000. HATs off: selective synthetic inhibitors of the histone acetyltransferases p300 and PCAF. Mol Cell 5:589-595.

VITA

MyLinh Thi Duong was born in Tam Quang, Vietnam on August 17, 1983 to her parents Binh Duong and Ta Thi Dang. Her family immigrated to the United States of America in 1995 and settled down in Houston, Texas. After earning her high school diploma from Northbrook High School in 2002, she began her collegiate studies at Rice University in Houston, Texas. She graduated Magna Cum Laude with a degree of Bachelor of Science in biochemistry from Rice in May 2006. Three months later, she enrolled in the University of Texas Health Science Center at Houston Graduate School of Biomedical Sciences in pursuance of a doctor of philosophy degree in cancer biology. In 2007, she and Chun Huai Yau tied the knots and they are expecting a baby girl in December 2011.

Permanent address:
3317 Clearview Circle
Houston, Texas 77025